Exploring the roles of the C-terminal of Pol2, the catalytic subunit of DNA Polymerase ε, in replication and checkpoint response

by Nicholas Sillett

A Thesis Submitted
To the University of Warwick
In Partial Fulfilment for the
Degree of Doctor of Philosophy in
Interdisciplinary Biomedical Research

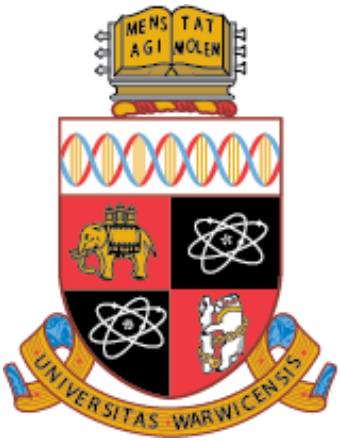

University of Warwick
Warwick Medical School

29th March 2019

Table of Contents

Table of Figures

Table of Tables

Acknowledgements

First of all, I would like to thank the Medical Research Council for my funding throughout the four years of my Masters and PhD. I would like to extend my deepest thanks to Andrew McAinsh and Jonathan Millar who, as course directors for the MRC DTP, have been a constant source of support during my time here at Warwick, as well as Sally Blakeman who has always been there to help, however big or small the problem. I am also grateful to Joe van de Wiel, for the many kilograms of cashews he has given me over the years as well as sharing the joys of frisbee and going to Westwood. He has always been available to talk when things have not gone to plan, so I would just like to say thanks.

Secondly, being a part of the De Piccoli lab has been a wonderful experience and it has been a pleasure to work with all the members past and present over the years. Giacomo has been a brilliant mentor and I am very grateful for the opportunity to work alongside him. As a supervisor, he has provided continuous support and encouragement, and I owe a lot of my personal development over the last three years to him. The GDP lab has often felt like a second family, and I would like to thank all of them simply for being great: Ed Miller, for teaching me many of the techniques that I am still using now; Alicja Winczura for being an impressive source of knowledge whenever I have encountered problems, as well as available for a quick chat about anything; Rowin Appanah who has served as a regular reminder that I could be working harder and is a fantastic person to bounce ideas with, including the non-scientific; Katy Stokes for helping whenever I needed a hand and for being good fun; and finally Emma Lones, who I never thought I would forgive for usurping my position as the baby PhD student of the lab but quickly won me over.

Lastly, I would like to extend my deepest gratitude to my parents, Caroline and Peter, who have always supported me through every decision I have made. Probably for the best I chose not to do that A Level in English Literature. My brothers, Andrew and Richard, have always set standards of excellence which I have never thought I could possibly emulate. However, their constant encouragement has helped me achieve things I thought were beyond me and they have never stopped having faith in my ability. I also want to thank Sheila Burgess for her unwavering belief in me. She has read every bit of work I have submitted and will most likely struggle through

this entire thing for little reward. Finally, I must recognise that I could not have completed this without Susie Sillett, my wife. For the past three years, she has done everything she can to support me over the course of my PhD, from driving me in at 5am for a long day of experiments to helping me proof-read my submissions. The love and kindness she has shown me has carried me through the highs and lows, and I cannot overstate how important she has been in my successes, even if she does not quite agree.

Declaration

This thesis is submitted to the University of Warwick in support of my application for the degree of Doctor of Philosophy in Interdisciplinary Biomedical Research. It has been composed by myself and has not been submitted in any previous application for any degree.

The work presented (including data generated and data analysis) was carried out by the author.

Abstract

During DNA duplication, the eukaryotic replisome functionally and physically links the unwinding of the template DNA with the synthesis of the novel strand. In *Saccharomyces cerevisiae, the* latter task is performed by three DNA polymerases, namely Pol α and Pol δ synthesizing the lagging strand, and Pol ε the leading strand. Uniquely among the polymerases, Pol ε is also involved in origin firing and is associated with activation of the S-phase checkpoint.

Pol2, its catalytic subunit, is characterized by an N-terminus that contains exonuclease and polymerase domains, and an essential C-terminus. C-terminal mutants have been shown to have a range of phenotypes, including defects in origin firing, replication, DNA damage repair and checkpoint activation. However, it is unclear if all these defects arise from its origin firing deficiency or whether the C-terminus has a multi-faceted role in the functioning and maintenance of the replisome.

In the work I will present, I have observed that expression of the last 236 residues of Pol2 was sufficient to partially suppress the defects in origin firing, fork progression and checkpoint signaling inherent to a truncation mutant, *pol2-11*. Furthermore, I identified conserved residues essential for suppressive effects of the C-terminal fragment, possibly indicating their importance in the unique versatility of this polymerase. Finally, I observed that, independently of origin firing, Pol2 appears to play a crucial role in signaling the DNA damage checkpoint.

Chapter 1: Introduction

1.1 Preamble

When a mitotic cell commits to dividing, it must first replicate its entire genome during the S phase of the cell cycle. This process is highly complex and tightly controlled, ensuring that each of the many millions or billions of bases in the genome is duplicated totally faithfully and only once. In eukaryotic cells, the large, dynamic and conserved machinery responsible for this is known as the replisome. A key component of this machine are the DNA polymerase complexes, which are responsible for the catalysis of dNTPs into the nascent strands of DNA. In all known eukaryotic cells, three complexes carry out this function: polymerases α, δ and ε. Amongst these, DNA polymerase ε is somewhat unique for its established roles in functions outside of DNA synthesis, including recruiting components to origins required for origin firing and the signalling of fork stalling and defects in DNA replication, mediated through the activation of the S phase checkpoint (see below for details) (Navas et al., 1995, Lou et al., 2008, Sengupta et al., 2013). Strikingly, in *Saccharomyces cerevisiae* and *Drosophila melanogaster,* these non-catalytic functions are so pronounced that the polymerase and exonuclease domains within the N-terminal domain of the main subunit of DNA polymerase ε, have been shown not to be essential for cell viability (Kesti et al., 1999, Suyari et al., 2012). The non-catalytic C-terminus, therefore, plays an essential role in origin firing and checkpoint signalling (Sengupta et al., 2013). This thesis has focused on further understanding how the C-terminus functions throughout replication as well as assessing if these two aforementioned functions of Pol ε are in fact independent of each other.

This introduction will initially outline the eukaryotic cell cycle, focusing on the processes that occur for DNA replication to take place. First, how replication starts with origin licensing, as the inactive form of the helicase motor is loaded onto the DNA at origins; following from this, how origins of replication fire and subsequently the way in which replisome machinery at replication forks carry out the synthesis of DNA; lastly, I will elucidate how

the replisome is disassembled as fully replicated DNA strands converge. Many obstacles, however, interfere with the process of DNA replication and I will explore how cells cope with the numerous factors that can impede genome duplication, termed replication stresses, by signalling the S phase and DNA damage checkpoints. In addition, I will focus on how DNA polymerase ε has been implicated in this. Finally, I will thoroughly examine the functions, including the individual roles of its subunits, and structure of DNA Polymerase ε, and how these are conserved through from fission yeast to higher eukaryotes and humans.

1.2 Using *Saccharomyces cerevisiae* as a model organism.

In this study, I have used *Saccharomyces cerevisiae*, as a model organism to study eukaryotic replication. This organism is colloquially known as budding yeast, due to the nature of its replication where daughter cells form as a bud from the mother cell, slowly increasing in size before their eventual abscission, in a process that takes roughly 90 minutes in optimal conditions (Herskowitz, 1988). Compared to the doubling time of 23h for HeLa cells, this allows cell cycle experiments to be carried out within a day, as opposed to the week when working with human cells. Most importantly, proteins involved in DNA replication and repair show a significant level of evolutionary conservation. Each of the replisome components, for example, has a single orthologue in all eukaryotic cells studied thus far. These features make budding yeast a powerful tool to understand key conserved processes of genome duplication. This organism has a genome comprised of 16 chromosomes which was the first to be fully sequenced and shares many pathways with human cells, ensuring that discoveries are transferable (Goffeau et al., 1996). Budding yeast are also highly genetically tractable. It is very easy to stably insert, mutate or delete genes within the genome by exploiting their homologous recombination systems and co-transform these constructs with marker genes (Compton et al., 1982). This organism can either exist as a diploid or haploid, the latter of which exist as two mating types: MATa and MATα. Haploid budding yeast can be exploited experimentally by the use of mating pheromones named according to either of the two mating types that produce them, A and α factor, which arrest the

cells of the opposite mating type in G1, permitting the synchronisation of cells prior to a release into S phase. These cells also provide a very simple method of generating new strains, as two haploid strains with the desired genotypes can be mated together before the resulting diploid is forced to undergo meiosis and the resulting haploids can be selected for the desired genotype.

1.3 From 1 to 2: The Fundamentals of DNA Replication

1.3.1 The Cell Cycle

Eukaryotic cells, from single-celled organisms to complex multicellular eukaryota, follow a pre-defined sequence of events as they replicate known as the cell cycle, detailed in figure 1.1. While the time this takes to complete varies between organisms, these cycles all follow the path of an interphase, comprised of an initial growth phase (G_1), followed by the replication of DNA (S phase), before a second growth phase (G_2). After this comes the second distinct phase of the cell cycle, the mitotic phase, during which the newly replicated chromosomes are segregated between the mother and daughter cell and they physically divide. Once the cell commits to dividing and passes what is known as the restriction point in higher eukaryotes and ‘Start’ in yeast, which occurs in G_1 prior to S phase, it will proceed through each phase of the cell cycle irrespective of changes to the stimuli that induced the division. When cells are not committing to dividing, for example somatic cells in multicellular organisms, they exist in a temporary (quiescent) or permanent (senescent) state, termed G_0 when related to the cell cycle. Permanent replicative senescence is also occasionally induced as a response to stresses like DNA damage. In order to protect the dividing cells from irreversibly committing to the next phase of the cell cycle before all the necessary steps in the previous one have been concluded, cells have evolved a series of checkpoints that block the cell cycle until the appropriate time. The checkpoint monitors different aspects of cell biology, from monitoring their size and metabolic activity, which occurs prior to committing to S or M phase to ensure cells are large enough to divide, to monitoring the integrity of the DNA, like in the DNA damage and intra-S checkpoints that

prevent mitotic entry in response to stalling forks or DNA damage (Barnum and O'Connell, 2014). Additionally, these can monitor the orientation and attachment of the mitotic spindle to the chromosomes, the mitotic spindle checkpoint, to ensure timely and accurate segregation of chromosomes to the daughter cells (Barnum and O'Connell, 2014). Additionally, to ensure the smooth and unidirectional progression of the cell duplication process, each phase of the cell cycle is tightly regulated by a careful interplay of expression and degradation of various proteins that regulate the processes that define each stage, a mechanism that is conserved through eukaryota.

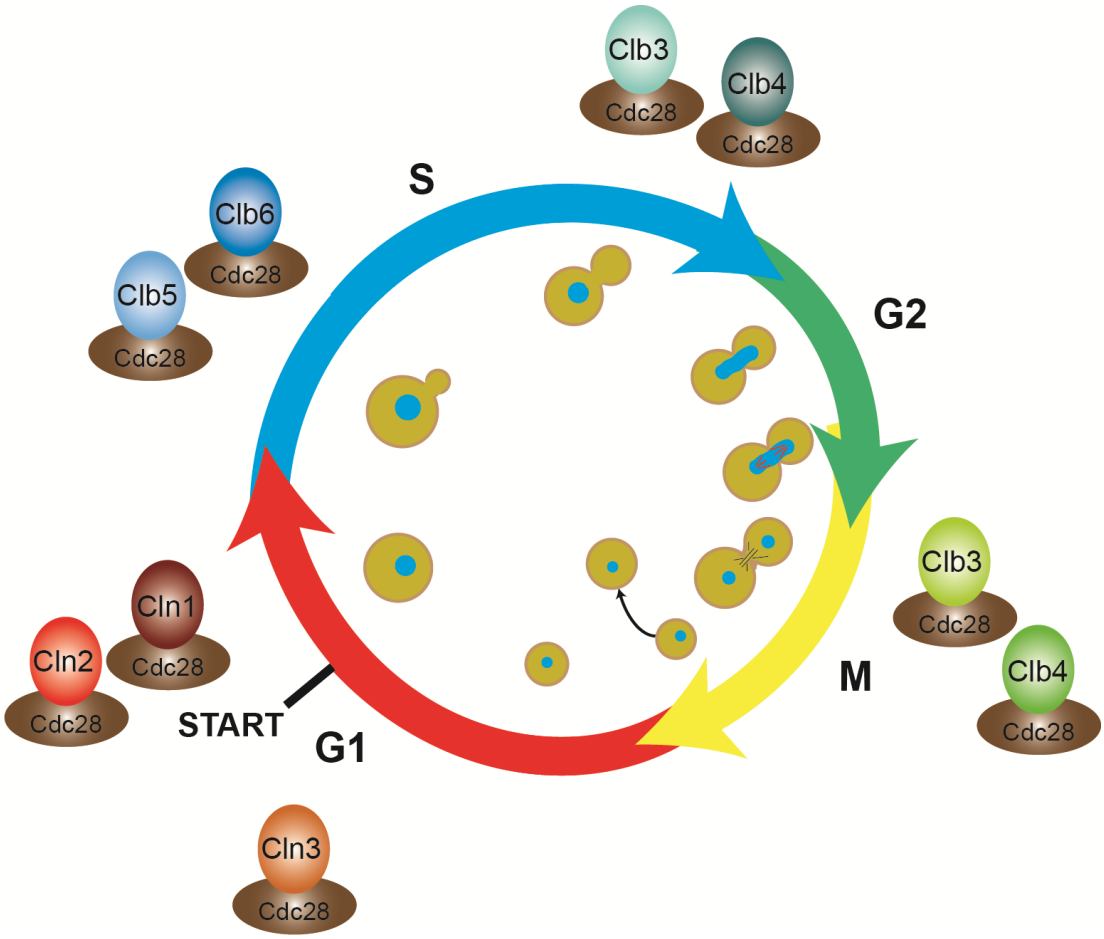

Figure 1.1: A schematic diagram of the cell cycle of *Saccharomyces cerevisiae*. Depicted are each stage of the mitotic cell cycle, with the length of each arrow representative of the time it takes. On the outside are the CDK complexes active at each phase, while on the inside is a depiction of the cell morphology as it divides.

In *S. cerevisiae*, also known as budding yeast, the chief regulator of the cell cycle is the cyclin family of proteins, which are co-factors for the essential cyclin-dependent kinase (CDK) termed Cdc28, and, in complex, effect the numerous cellular processes that define each phase of the cell cycle. There are nine cyclins that bind to Cdc28 which can be classified by the phase during which they are present and function into three separate groups: those that act at in G_1 and at the G_1-S transition (Cln1-3), during S phase (Clb5 and -6) and at mitosis (Clb1-4) (Andrews and Measday, 1998). In yeast cells, the presence of nutrients like sugars and a nitrogen source is sufficient to initiate the cell cycle by increasing the levels of Cln3 (Parviz and Heideman, 1998). While its expression and protein levels are present throughout the cell cycle, *CLN3* transcription peaks early in G_1 and, in complex with Cdc28, crucially functions to push the cell beyond 'Start' to commit it to dividing (McInerny et al., 1997). This is achieved in concert with the MBF (MluI Cell Cycle Box Binding Factor) and SBF (Swi4–Swi6 cell cycle box Binding Factor) transcription factors, which upregulate expression of G_1 specific genes that have the MluI Cell Cycle Box (MCB) or Swi4–Swi6 cell cycle box (SCB) elements in their promoters. Ordinarily, SBF is bound to Whi5, causing this to exist as a repression complex bound to SCB-containing promoters. The Cln3-CDK phosphorylates this inhibitory subunit, promoting its dissociation, thus allowing SBF to promote transcription of its target genes (de Bruin et al., 2004). The modified expression patterns allow the cell to increase in size to that required for replication, pheromone resistance and increased concentrations of S phase-related proteins, including the other G1 (*CLN1* and *CLN2*) and DNA replication (*CLB5* and *CLB6*) cyclins, therefore being fully prepared to replicate DNA (Tyers et al., 1993, McInerny et al., 1997). Clb5/6-CDK, however, is kept in an inactive state outside of S phase by the binding of the inhibitor Sic1 (Schwob et al., 1994).

The Cln1- and Cln2-CDK complexes are able to increase their own transcription, which peak in late G_1, via a positive feedback loop, and further the transcriptional programme initiated by Cln3 to express several proteins required for DNA replication. In addition, Cln1/2-Cdc28 crucially phosphorylates Sic1, thereby targeting it for destruction (Nishizawa et al.,

1998). This inhibition does not occur by a single phosphorylation event, but is triggered by multiple phosphorylations of Sic1; a graduated increase in kinase of CDK activity is therefore necessary until a threshold is reached, whereupon sudden degradation is induced. Currently, it is believed that this occurs by an initial phosphorylation by Cln2-CDK, which provides a docking site for itself to then phosphorylate the protein at multiple sites (Koivomagi et al., 2011). The phosphorylations at these degron sites trigger an initial inefficient Sic1 degradation, thus releasing a small amount of Clb5-CDK. This emerging kinase swiftly phosphorylates Sic1 at other degron sites, which efficiently promotes its recognition and destruction by the Cdc4 subunit of the Skp-Cullin-F-box (SCF) ubiquitin ligase and providing a switch to allow the Clb5- and Clb6-CDKs to predominate (Koivomagi et al., 2011). These Clb5/Clb6-Cdc28 complexes are then able to allow early origin firing and initiation of replication (detailed below). They also inhibit new origin licensing by targeting Cdc6 for destruction, Orc2 for inhibition, as well as Cdt1 and Mcm2-7 complexes not on the DNA for nuclear export. Additionally, S phase CDK promotes centrosome duplication and budding, although these are somewhat redundant with the other Clb family members (Donaldson, 2000). Moreover, the early S CDK complexes phosphorylate the Cdh1 adapter of the anaphase promoting complex (APC/C), inhibiting their association and possibly targeting it for nuclear export (Jaquenoud et al., 2002). This complex is crucial in the maintenance of G_1 by, among other functions, ensuring the degradation of mitotic cyclins (Irniger and Nasmyth, 1997). Cln1 and -2 are degraded in S phase by SCF^{Cdc4} and SCF^{Grr1}, which targets them for ubiquitin-mediated degradation following their phosphorylation by CDK, although it is unclear what signal drives their depletion (Quilis and Igual, 2017).

Protein levels of Clb3 and -4 are raised from early S phase to mitosis, and their kinase complexes function in regulating S phase with a certain amount of redundancy with Clb5 and -6, but also in early mitotic processes like spindle formation, pole separation and activation of condensin, which promotes chromosome condensation (St-Pierre et al., 2009) (Grandin and Reed, 1993, Segal et al., 2000). The protein levels of Clb1 and Clb2 peak

towards late G_2 and have been implicated in bipolar spindle formation as well as their elongation, but more significantly in activation of the APC/C^{Cdc20} (Rahal and Amon, 2008, Kuczera et al., 2010). APC/C^{Cdc20} has two known essential functions: degrading the Clb5/6 family of cyclins and as an inhibitor of separase, securin, a protease that cleaves the cohesin proteins that hold sister chromatids together before anaphase onset (Peters, 2002, Thornton and Toczyski, 2003). Beyond these essential roles, it also functions in cell cycle regulation through degradation of spindle-associated proteins as well as kinases that regulate both DNA replication and mitosis, such as Dbf4 and Cdc6 in the case of the former, and the Aurora family in the latter (Vodermaier, 2004). The inhibition of securin promotes the release of the Cdc14 phosphatase, which functions to reverse many of the mitotic CDK phosphorylations to promote mitotic exit, although recently it has been postulated that this is most likely to occur in concert with other phosphatases (Visintin et al., 1998, Powers and Hall, 2017). Targets of Cdc14 include Sic1 and Cdh1, which promote its reassociation with APC/C, allowing the inhibition and degradation of mitotic cyclins (Visintin et al., 1998). This allows the separation of the daughter cell by telophase and cytokinesis, and the complete shutdown of CDK activity, by virtue of the cyclin degradation, permits the licensing of origins in preparation for the next round of replication (Hatano et al., 2016).

While timely expression of proteins that can complex with kinases and induce reversible phosphorylations is crucial to promote the onset of various phases of the cell cycle, equally important is the irreversible degradation of these same factors in order to transition from the previous one to the next and prevent backtracking. As has been previously established, while rates of transcription of these cyclin genes vary throughout the cell cycle, their resultant protein levels are also subjected to control by ubiquitylation and degradation by the 26S proteasome. In budding yeast, this is primarily carried out by APC/C and SCF, which broadly control the mitotic and interphase progressions, respectively, although with far-reaching effects throughout and beyond the cell cycle (Peters, 1998). As mentioned, SCF refers to a family of E3 ligases linked by their shared subunits that comprise

their name, as a result, they have more roles outside regulating the cell cycle, like regulating the Wnt and inflammation signalling pathways through targeting β–catenin and IκB for degradation, respectively (Fuchs et al., 1999). In the cell cycle, these ubiquitin ligases target the G_1 cyclins Cln1 and -2 for degradation, as well as the Sic1, the inhibitor of DNA replication CDK complexes, following its phosphorylation by the aforementioned Cln1- and Cln2-CDK complexes (Verma et al., 1997). The intensive role of these enzymes that target destruction of many disparate proteins throughout both interphase and mitosis underlines the importance of the proteasome and degradation machinery in a healthy cell cycle progression.

1.3.2 Origin Licensing

With its smaller genomes and ten-fold faster DNA replication rate, prokaryotic replication starts at a single origin of replication and finishes at a pre-defined termination site. In *E. coli,* replication of the whole 4.6Mbps genome takes about 40 minutes, while in the early replications of a fertilized *Xenopus laevis* embryo, duplicating the over 3000 Mbps of DNA takes only 30 minutes (Kermi et al., 2017). This is due to the fact that, in eukaryotes replication starts, or ‘fires’, from many origins across each chromosome and seemingly only finishes when two forks converge. In order to begin replication, these origins are sequentially loaded with an inactive form of the motor helicase in a process known as origin licensing and shown in figure 1.2. Each step of loading and subsequently firing the origin is tightly temporally localized to stages of the cell cycle, thus ensuring they are only able to fire once. Cells can only license origins in the absence of S phase/ mitotic CDK activity, while origin firing must occur in their presence. Uniquely for eukaryotes, budding yeast origins are defined by an 11 base pair specific AT-rich consensus sequence, known as an autonomously replicating sequence (ARS).

In higher eukaryotes, one example of particular initiation sites that can be pinpointed to regions spanning a few kilobases is known to occur in the β-globin gene locus in erythroid cells. In this example, origin firing is known to occur between the δ- and β-globin genes, and deletions of sequences both at these sites and those further than 50kb away have been shown to disrupt

the initiation event that occurs from here (Cimbora et al., 2000). However, with this latter point in mind, transplanting an 8kb region containing the initiation site to another genetic locus was still sufficient to fire origins at this new site (Aladjem et al., 1998). Despite the significant difference in what defines an origin in these eukarya, whether it's simply a consensus sequence or an intricate interplay of disparate genetic elements, many aspects of how components are loaded onto these to form a functioning replisome are well conserved. Throughout the cell cycle, origin recognition complexes (ORC), formed of ORC1-6, recognize and bind to conserved ARS sequences across the genome in an ATP-dependent manner (Shackleton and Peltier, 1992). In higher eukaryotes, the binding of ORC is also the critical factor deciding origin licensing. The binding of ORC is affected by several factors and seems to prefer regions with high GC content, CpG islands and sequences that are liable to form secondary structures like G quadruplexes (Cayrou et al., 2011).

Upon G_1 entry and in low levels of CDK activation, Cdc6, whose transcription is limited to this phase, binds and subsequently acts as a scaffold and opens up a binding interface on ORC6 for seemingly two rounds of loading Cdt1-Mcm2-7 complexes to bind, thus forming the pre-recognition complex (Pre-RC) (Randell et al., 2006, Takara and Bell, 2011, Ticau et al., 2015). At this point, the motors that drive each of the helicases of the resultant forks, the AAA+ ATPase Mcm2-7 complexes, are now present at origins as head-to-head double hexamers, but yet to be activated. While there is no consensus on exactly how the Mcm2-7 double hexamer is loaded, it is hypothesised that Cdt1 disrupts the interface between Mcm2 and -5, thus holding it open and pliable to be loaded onto DNA (Remus et al., 2009, Evrin et al., 2009). Following its biding to ORC-Cdc6 at origins, the complex is proposed to remodel in an ATP-dependent manner and close around the DNA, while expelling Cdt1 (Frigola et al., 2017). It is important to note here that the Cln2-CDK activation in late G_1 phosphorylates Cdc6 to target it for degradation and promotes the nuclear export of Mcm2-7, thus preventing further origin licensing (Nguyen et al., 2001).

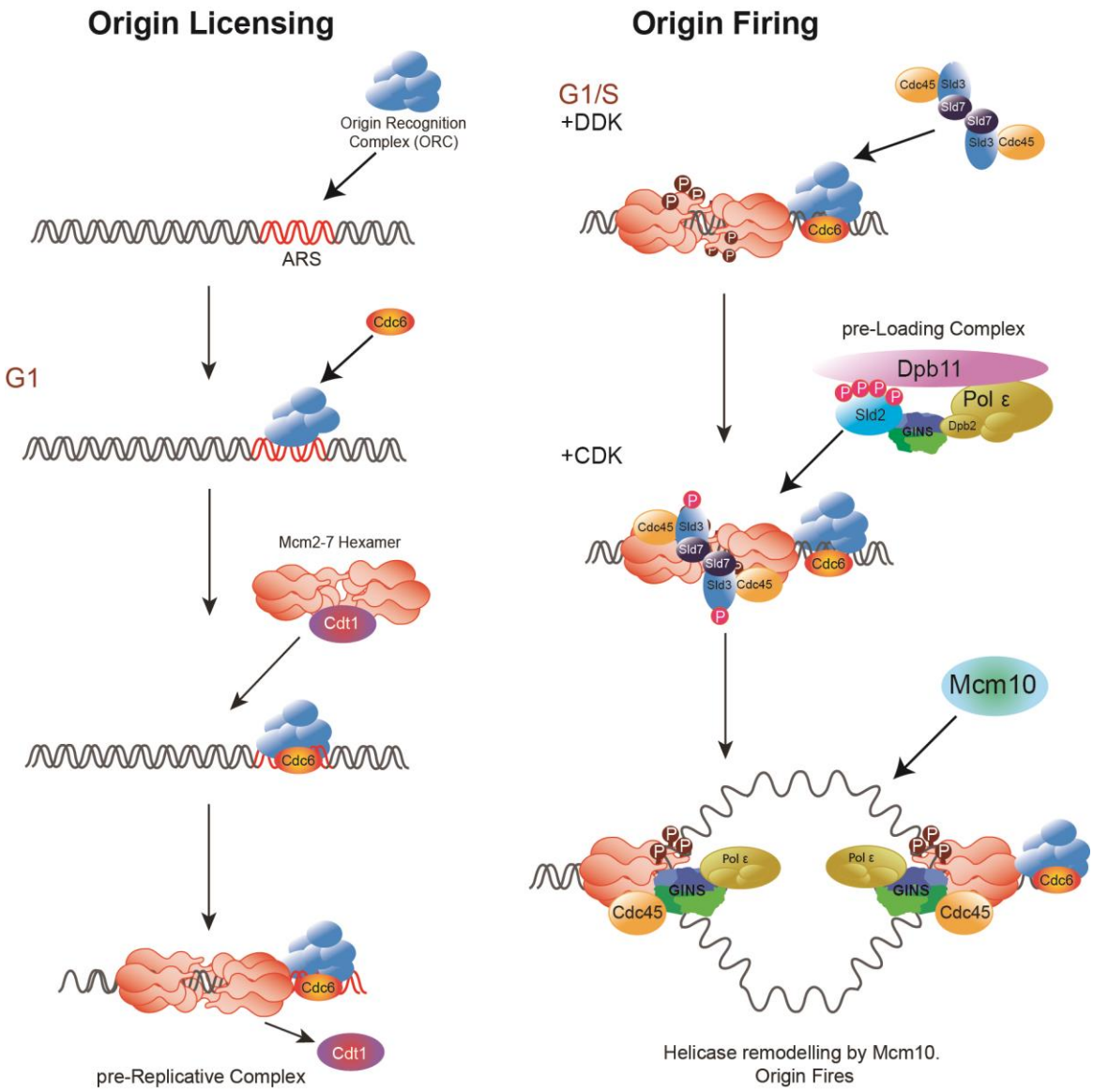

Figure 1.2: A cartoon depicting the processes of origin licensing and firing during DNA replication. Throughout the cell cycle, ORC binds the autonomously replicating sequences (ARS) across the genome. In G_1, the Mcm hexamers has bound to the ORCs at origins of replication through the concerted action of Cdc6 and Cdt1. This process is known as origin licensing. During the transition to S phase, two kinases become active, Cyclin- and Dbf4-dependent kinases (CDK and DDK, respectively) and they function to activate the loaded helicases at origins to fire them. DDK phosphorylates residues on the Mcm hexamer, and provide a binding interface for Sld7, which brings a component of the helicase, Cdc45 and Sld3. Independently of this, CDK-phosphorylated Sld2, Dpb11, Pol ε and GINS form a fragile complex known as the pre-Loading Complex (pre-LC). Pol ε is bound to this through its Dpb2 subunit's N-terminus binding to the Psf1 subunit of GINS. When Sld3 at the origin is phosphorylated by CDK, the pre-LC is able to bind to the origin. Mcm10 binds to the origin and activates the helicase in a remodelling step to promote the initial stages of elongation and generate a bubble from which replication can begin. Finally, Sld2, -3 and -7 leave and other accessory factors, like the other polymerases bind and replication begins.

1.3.3 Origin Firing

Across each chromosome, origins have unique temporal properties, allowing them to fire early, late or remain dormant in the S phase, which in higher eukaryota generally correspond to the accessibility provided by the chromatin structure (Tabancay and Forsburg, 2006). The early temporal control is regulated by the forkhead box transcription factors Fkh1 and Fkh2, whose binding sites are enriched at early firing origins (Knott et al., 2012). The activity of Fkh1/2 at origins appears distinct from its transcription factor activity and they appear to function by preferentially recruiting Dbf4, further facilitating the recruitment of the helicase subunit, Cdc45 (Fang et al., 2017). Concentrations of firing factors are limiting in the cell and it is believed that this property could engender the temporal nature of origin firing, as Cdc45 is required by replisomes for the entirety of replication, so their completion and disassembly would be required for further origins to fire (Tanaka et al., 2011). Meanwhile, chromatin configuration also appears to be a large determinant of timing, with the histone deacetylase, Rpd3, being heavily implicated in generating a more closed state at late firing origins, although the further implications of this are yet to be elucidated (Knott et al., 2009). The definitions are far more complex and somewhat looser in other multicellular organisms, where initiation appears to occur within larger regions that have no sequence specificity, although they have been linked to DNA features like GC content, or chromatin features, but still abide by a similar temporal programme of firing timings (Rhind et al., 2010).

A growing theory is linking these regions of replication origin to topologically associated domains (TADs). This localises origins of replication in the context of areas of the genome nearby specific clusters of genes that are differentially regulated in cells, dictated by the chromatin states of these regions and their resulting placement within the nucleus. The more accessible regions are located towards the centre of the nucleus, presumably where protein concentrations of firing-associated factors would be rich, whereas the more heterochromatic areas are placed more in the periphery (Pope et al., 2014). This somewhat strengthens the notion of origin firing remaining a technically stochastic process, but still one where, on a

genome-wide level, specific origins are able to consistently fire following specified temporal programmes in specific cell types, due to some simply being more probable to fire earlier or later in replication (Rhind et al., 2010). Interestingly, despite the much smaller, more compact chromosomes of budding yeast, TADs have also been identified, but although this conserved genomic architecture has been observed, the link to replication timing has not (Eser et al., 2017).

The mechanistic understanding of origin firing has been greatly helped by the *in vitro* studies performed by the Diffley and Speck groups, in which replication initiation in budding yeast has been able to be reconstituted through the use of purified proteins (Yeeles et al., 2015). From these experiments, it has been shown that through the expression of 12 firing factors, a stable CMG helicase (termed due to its composition of the Cdc45-Mcm2-7-GINS complexes) coupled to DNA Polymerase ε could be loaded onto the DNA and begin unwinding it, although replication itself could not be initiated (Yeeles et al., 2015). In addition to the 4 complexes mentioned, purified ORC, Cdt1, Cdc6, Sld2 (also known as Drc1), Sld3/7, Dpb11, Mcm10 and the Clb5 cyclin- and Db4-dependent kinase (S-CDK and DDK, respectively) were also expressed; the roles these factors play in origin firing will be elucidated here and have been broadly outlined in figure 1.2 (Yeeles et al., 2015).

At the G_1/S transition, both the S phase-CDK and DDK become active and immediately phosphorylate their target proteins. DDK phosphorylates MCMs 2, 4 and 6, during late G_1, the latter two resulting in the creation of two binding interfaces for the Sld3-Sld7 complex, which allows the arrival of the another subunit of the helicase, Cdc45, to be brought to the replisome hexamers (Deegan et al., 2016). In this heterotrimer, Sld3 is bound to Cdc45 through its central domain Cdc45 and to Sld7 through its N-terminus (Tanaka et al., 2011). Interestingly, Sld7 actually reduces Sld3's binding affinity for Cdc45, which is believed to allow it to be removed from the origin before it fires (Tanaka et al., 2011). Clb5/6-complexed CDK subsequently phosphorylates Sld3 and Sld2, which are able to bind to the BRCA1 C Terminus (BRCT) domains at the N-terminal and C-terminal of

Dpb11, respectively (Tanaka et al., 2007). Current research suggests that a transient pre-loading complex (pre-LC) is formed away from the origin, comprising of at least Pol ε, GINS (formed of the Sld5-Psf1, Psf2 and Psf3 subunits), Sld2, and Dpb11 (Muramatsu et al., 2010). The association of Pol ε with the pre-LC is dependent on binding through its B-subunit, Dpb2, and this has been elucidated by yeast-2-hybrid (Y2H) assays, immunoprecipitations and single-particle electron microscopy, showing its N-terminus binding to the Psf1 subunit of GINS, and its C-terminus to Pol2's C-terminal zinc finger (Sengupta et al., 2013, Sun et al., 2015, Isoz et al., 2012, Dua et al., 1998). The expression of the N-terminus of Dpb2 was sufficient to assemble the CMG on its own, however this resulted in a replisome with Pol2 being absent and the resultant replication was extremely slow and cell proliferation was affected (Sengupta et al., 2013). This work neatly illustrates Pol ε's essential roles beyond DNA synthesis, in its assembling of the active helicase at the origin, but also its provision of a physical link between the two. Parallel work in fission yeast has shown that this appears to be a conserved function, where it was demonstrated that Pol ε is required for the assembly of the CMG complex at origins and that the C-terminus of Pol2 is critical in initiating the progression of the helicase (Handa et al., 2012).

Upon CDK's phosphorylations, the Dpb11 within is able to bind to the origin through Sld3 and thus bring the final component of the helicase, GINS, to activate it (Zegerman and Diffley, 2010, Muramatsu et al., 2010). For the origin to be able to fire and two replication forks to emerge bi-directionally from it, the helicase must first be activated. This process is still not well understood but leads to a remodelling of the Mcm2-7 double hexamer leading to the incorporation of Cdc45 and GINS. The formation of the CMG, however, does not allow the initiation of DNA unwinding per se. A key role in the final remodelling to the active form of the CMG is played by Mcm10. It is speculated that, with its ability to bind single strand DNA (ssDNA), Mcm10 is essential in this process and has been implicated in remodelling the closed double hexamer to the open single hexamer present at forks and possibly even bring polymerase α to the active fork and allowing replication to begin (van Deursen et al., 2012, Zhu et al., 2007). This remodelling process has

been hypothesised to occur through Mcm10 inducing a conformational shift in the Mcm2 subunit of the helicase, revealing an Mcm10-binding motif, allowing the CMG to activate and begin replication (Looke et al., 2017). Additionally, cryo-EM structural analysis elucidated the dynamics of an activating helicase, where it showed that after an initial unwinding of DNA by 0.6-0.7 turns by the helicase, the activation step mediated by Mcm10 is distinct and requiring ATP hydrolysis, whereupon the DNA is unwound an extra turn (Douglas et al., 2018). Finally, initiation of the helicase activity, as seen *in vitro*, requires the activity of DNA topoisomerase and RPA, as the former is required for resolving supercoils to allow unwinding of the DNA and the latter to coat the ssDNA as it emerges from the helicase to prevent re-annealing (Yeeles et al., 2015, Douglas et al., 2018).

1.3.4 DNA Synthesis at the Replisome

After the origins have fired, two replication forks emerge bi-directionally and begin the process of synthesising new strands of DNA. This is carried out specifically by the replisome, and is made up of the CMG helicase, three DNA polymerases, as well as several other factors which physically and functionally coordinate the activity of unwinding and DNA synthesis, which is shown in figure 1.3. At the fork, the CMG helicase functions to unwind the double stranded DNA (dsDNA), while DNA polymerase α generates small RNA primers with its primase activity, from which the two more processive polymerases, ε and δ, take over. On the leading strand, replication is carried out continuously by Pol ε, while on the lagging strand, due to the 5'-3' directionality required by the polymerase, the DNA is replicated in roughly 200bp stretches, termed Okazaki fragments, by Pol δ with the assistance of the proliferating cell nuclear antigen (PCNA) sliding clamp, which greatly improves its processivity (Langston and O'Donnell, 2008). As previously mentioned, *in vitro* work with the 16 factors that allowed origin firing also allowed elongation to occur, in which the CMG was activated but the replication that subsequently occurred was unable to progress beyond extremely slow rates (Yeeles et al., 2015). In these experiments, the addition of the Pol α complex, Ctf4, a topoisomerase (Topo II) and RPA, was required for the subsequent replication (Yeeles et al.,

2015). *In vivo* replication rates were recapitulated, however, when proteins from the conserved fork protection complex (Mrc1, Csm3 and Tof1), together with DNA polymerase ε, were added (Yeeles et al., 2017).

The fork protection complex functions to stabilise the replisome when it pauses in response to replication stresses and, in doing so, keeps it intact for it to restart when the impediment has been removed. In addition to this, Tof1 is known to interact with TopI, a topoisomerase that resolves supercoils through nicking and closing the DNA to allow fork progression (Park and Sternglanz, 1999). Tof1 and Csm3 form a tight complex together and this has long been known to associate in a mutually dependent manner with forks

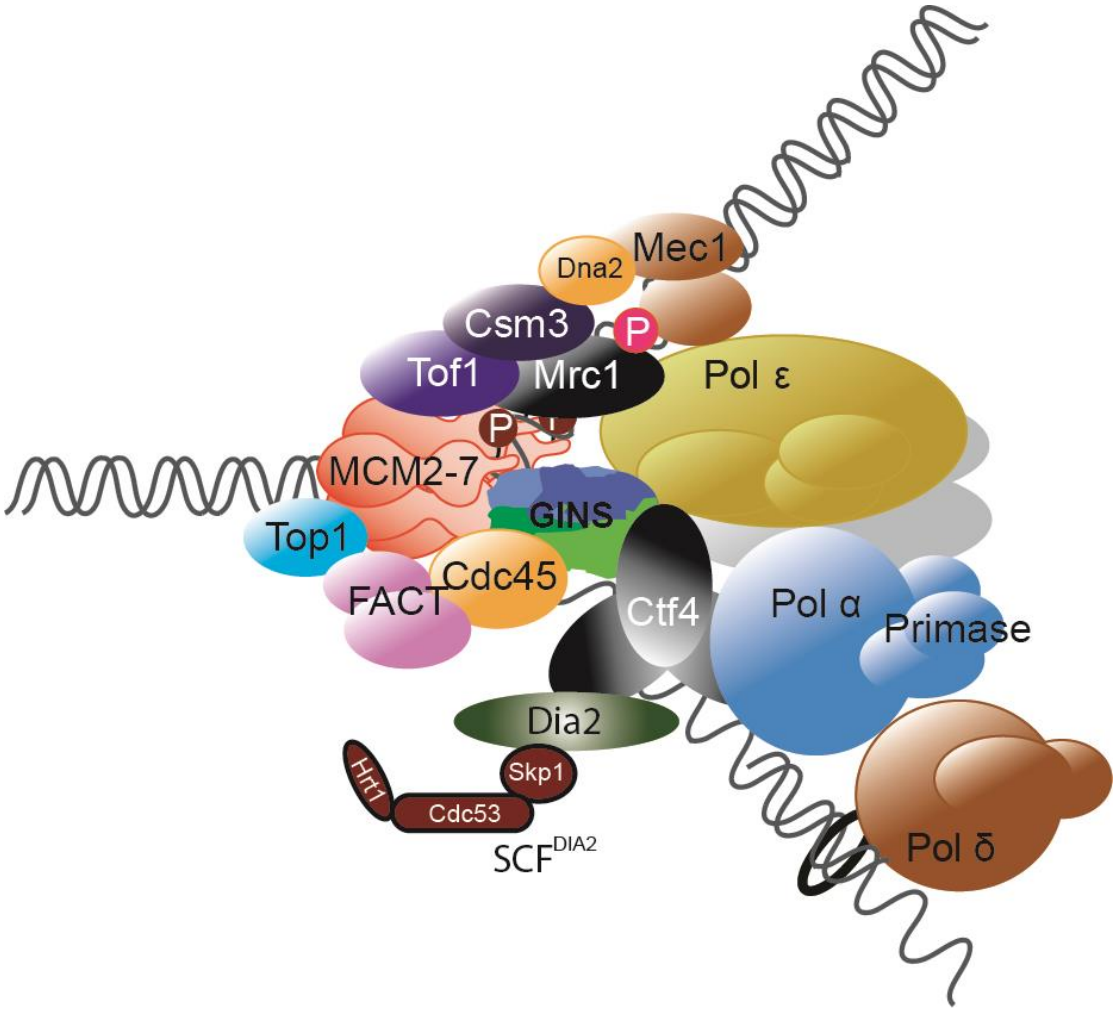

Figure 1.3: A simplified depiction of the Eukaryotic replisome as it replicates DNA. Important subunits are the 3 polymerases: α, ε and δ responsible for DNA synthesis and the components of the CMG helicase: Mcm2-7, Cdc45 and GINS. This model is predicated on the assumption that Pol ε is providing leading strand synthesis and Pol δ synthesising the lagging strand with the help of its clamp, PCNA (black circle)

exclusively during S phase (Bando et al., 2009). This complex is essential for regulating forks as they encounter protein barriers that prevent further progression in programmed fork arrest and, while the mechanism is not fully understood, it is believed to function by antagonising the Rrm3 helicase and is regulated by DDK (Bastia et al., 2016). Mrc1's association with the replisome is also still not fully understood, while partly dependent on the Tof1/Csm3 complex, it is also likely driven by its strong interactions with Pol2 and Mcm6 (Komata et al., 2009, Lou et al., 2008). Mrc1 is a known mediator of the S phase checkpoint (see below) but, in addition to this function, it also contributes to the high processivity of forks which has been hypothesised to be due to coupling the processes of the helicase unwinding through its Mcm6 binding to the DNA synthesis carried out by its other binding partner, Pol2 (Lou et al., 2008).

As mentioned, DNA polymerase α has a key role in DNA synthesis whereby it kickstarts the process. This complex is a heterotetramer, made out of 2 primase domains (Pri1 and Pri2), its polymerase domain Pol1 and its Pol12 B subunit. Its activity begins with the polymerase generating a short 10nt RNA primer through its primase activity, followed by its elongation with a 20nt stretch of DNA from which the processive polymerases, ε and δ, can take over, the latter of which is dependent on the loading of PCNA first (Nick McElhinny et al., 2008). Crystallography data provided the rationale for the low processivity of Pol α, since its substrate binding thumb domain preferentially binds DNA/RNA hybrids, thus favouring the hand-over between primase and DNA polymerase, which results in its limited synthesis (Perera et al., 2013). This occurs each time replication must restart on each strand which, occurs infrequently on the leading strand due to the continuous nature of its replication, while this is not the case on the lagging, where this must take place roughly every 200nt after each Okazaki fragment is elongated to the next (Nick McElhinny et al., 2008). Pol α is tethered to the replisome through its Pol1 subunit to Ctf4, a trimeric hub protein that also binds numerous other components, including Pol ε through Dpb2 and GINS through Sld5, among many others (Villa et al., 2016).

The two more processive polymerases, δ and ε, carry out the bulk of DNA replication as the genome is replicated. As mentioned previously, Pol ε is comprised of Pol2, Dpb2, Dpb3 and Dpb4, while Pol δ is a heterotrimer comprised of its catalytic subunit Pol3 and its accessory subunits Pol31 and Pol32 and, in its active form, a dimer of these heterotrimers. Both of these holoenzymes, in contrast to Pol α, also possess 3'-5' exonuclease activity, which allows them to proof-read DNA and ensure the fidelity of replication,

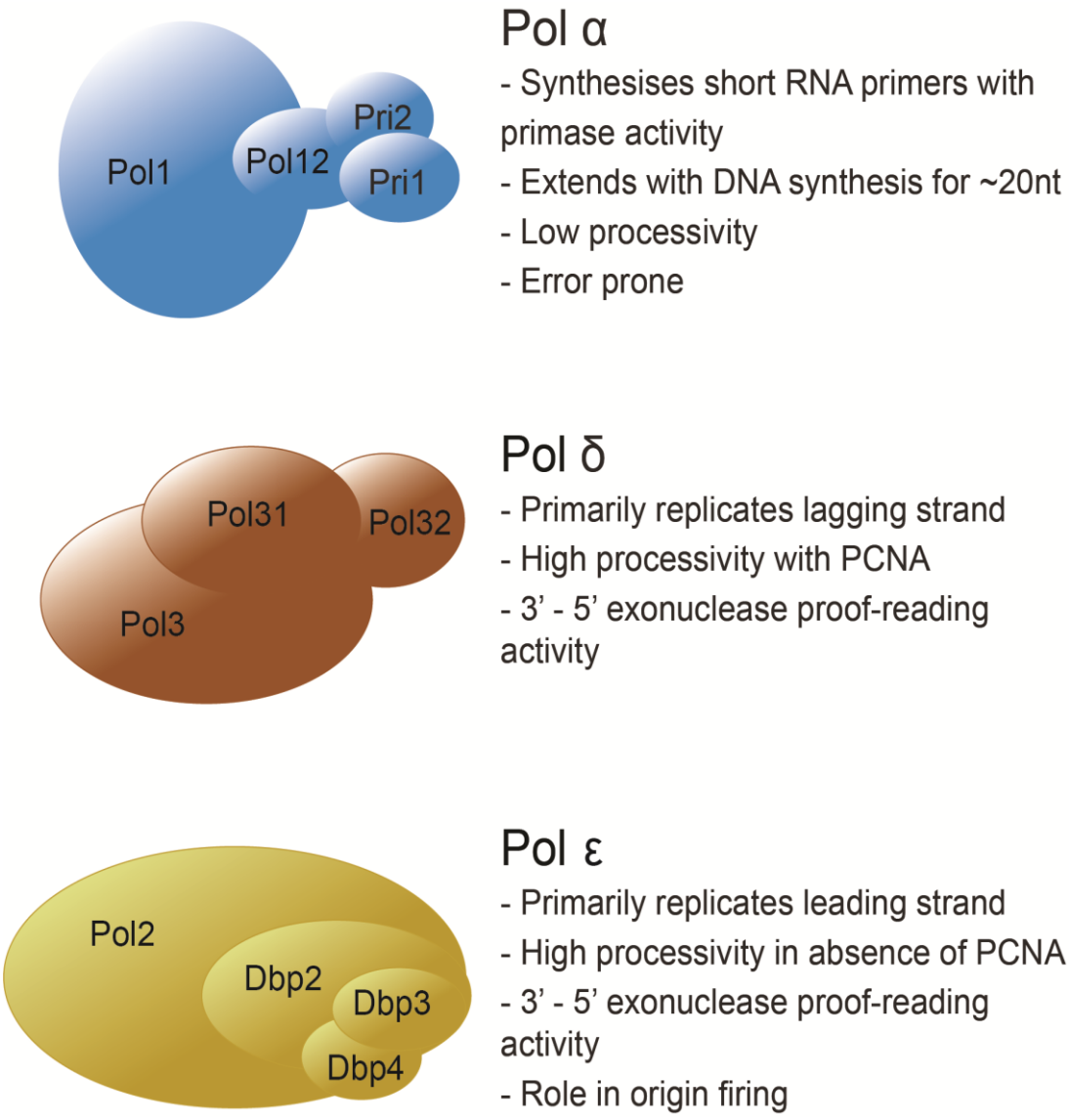

Figure 1.4: A summary of the structures and roles played by the three main DNA polymerases. This diagram shows the composition of the holoenzymes of the three DNA polymerases responsible for DNA synthesis at the fork. Their individual subunits have been labelled and their characteristics are listed to the right.

contributing importantly in maintaining genome stability (Morrison and Sugino, 1993).

These polymerases are known to interact with the sliding clamp PCNA, loaded by the replication factor C (RFC) complex, formed of its main subunit Rfc1 together with the Rfc2-5, however, of the two, Pol δ's affinity for PCNA, as measured by surface plasmon resonance, is much higher and this is best explained by PIP motifs (PCNA interacting peptide) present in all 3 subunits, with possibly each binding a member of the processivity factor's homotrimer (Acharya et al., 2011). In the context of Pol δ, this interaction with PCNA could go well beyond the enhanced processivity it provides and assist it in the process of Okazaki fragment maturation, in which the completed sequences on the lagging strand must be removed of their RNA primers and ligated together. It is believed Pol δ displaces the RNA strand by continuing DNA synthesis and the growing 5' flap is then cleaved by the flap endonuclease Rad27 (FEN1), although whether this flap is formed and excised at once or incrementally is still debated (Garg et al., 2004, Liu et al., 2004). Unfortunately, the nature of the flap to be processed is not well understood and a second pathway has been postulated for a larger flap which could bind RPA and, as a result, occlude its degradation by FEN1. By necessity, this would initially be degraded by the action of the helicase/nuclease Dna2 to produce a small fragment that would be processed by FEN1 (Bae et al., 2001).

It has also been hypothesised that RNase H acts in concert with FEN1 in an alternative, non-flap processing pathway, in which the former digests the DNA-annealed RNA primer until the last base, which is presumably removed with the 5' exonuclease activity of FEN1 (Turchi et al., 1994). Interestingly, PIP boxes have been identified in both DNA ligase, Rad27 and RNase H Rnh201, which would allow them to maintain their presence at the lagging strand and quickly allow the maturation of Okazaki fragments (Karanja and Livingston, 2009, Nguyen et al., 2011). Furthermore, recent *in vitro* work has illustrated an important role chromatin appears to play in the dynamics of Pol δ elongation. This work suggests that the synthesis of Pol δ is in fact only constrained by encounters with chromatin and that it continues

strand displacement until it comes into contact with a nucleosome, thereby suggesting that Okazaki fragment length is dictated solely by chromatin rather than a property inherent to Pol δ (Devbhandari et al., 2017, Smith and Whitehouse, 2012). Additionally, this would appear to result in the removal of the entirety of the DNA synthesised by Pol α, which is presumably evolutionarily beneficial due to its higher error rate thereby ensuring genome integrity (Kunkel, 2004). Disputing this is the fact that error-prone mutants of Pol1 have been known to have increased mutation rates in the resultant cells, and it has been hypothesised that Pol δ functions to proof-read these (Pavlov et al., 2006).

As has been mentioned, it is clear that the role of Pol ε goes far beyond that of simply replicating DNA. The essential non-catalytic role of Pol ε was originally studied through the use of Pol2 alleles containing deletions, one of which was the *pol2-16 allele* containing a deletion of the exonuclease and catalytic domains that remained viable, albeit with a reduced replication rate, indicating that there is a certain redundancy in the DNA synthesis of Pol ε, (Kesti et al., 1999). Additionally, *in vitro* work has demonstrated that the presence of Pol ε with the helicase greatly increased the latter's processivity, which was not the case with either of the other two polymerases (Kang et al., 2012). Despite the DNA synthesis activity being seemingly redundant, Pol ε is commonly accepted to be responsible for replicating the leading strand. This was elegantly shown by Pursell *et al.*, which utilised a mutant Pol2 that frequently mismatched T-dTMPs and a *URA3* reporter gene, within which two hotspots exist for misincorporation of T-dTMP, to assess the mutagenic rates. Through experimenting in orienting the *URA3* around an origin so that these hotspots would be present on the leading or lagging strands, it was shown that the high mutagenesis occurred when these hotspots were present on the leading strand, the A to T transversions occurred over 20 times more frequently on the leading strand than lagging, elegantly illustrating the strand specificity of Pol ε (Pursell et al., 2007).

Recently, even the idea that Pol ε is responsible for leading strand synthesis has been debated, as work done by Johnson *et al.* put forward the possibility that in fact Pol δ is responsible for both strands' syntheses

(Johnson et al., 2015). This work is predicated upon the use of two error-prone mutants of Pol2 and Pol3 and observing the frequency of their signature mutations within each strand. Their data showed that the characteristic errors of the Pol3 enzyme were present on both leading and lagging strands, whereas the Pol2 mutant's errors lay mostly on the leading strand (Johnson et al., 2015). It was proposed that the main role of Pol ε is to initiate DNA synthesis and then proofreading and correcting errors made by Pol δ. These findings however have been disputed, and it has been suggested that this study could simply be overstating the role that Pol δ is known to play in synthesising the leading strand. Despite this, it is perhaps more likely that there is a less obvious division of labour, and that the choice of polymerase is far more fluid than previously thought. ε and δ could interchange depending on the situation, thus allowing replication to still occur even without the polymerase activity of Pol ε. Additionally, from the EM study of the eukaryotic replisome, the calculated position of Pol ε was at the 'top', with no obvious path for the DNA to get to the catalytic domain of the enzyme, perhaps indicating this less prominent role in replication (Sun et al., 2015). Further to this, as part of the *in vitro* replication reactions mentioned previously, the presence of a non-catalytic Pol ε complex that was able to carry out its essential initiation functions allowed Pol δ to carry out leading strand synthesis. However, the rates of DNA synthesis were much reduced compared to those observed in the presence of Pol ε, a phenotype exacerbated by the additional absence of Mrc1. These experiments appeared to show that while perhaps not involved in the long-term synthesis of the leading strand, Pol δ does function to establish it initially. It is then out-competed by Pol ε for this specific synthetic role, to the extent that even a 20-fold excess in the former's concentration is not able to significantly impact its presence at the leading strand (Yeeles et al., 2017). Previous work has observed that the stabilisation of Pol ε binding by CMG is not replicated with Pol δ (Georgescu et al., 2014). It has been hypothesised that Pol δ is possibly cycling on and off the template strand, as it would on the discontinuous lagging strand. This possibly gives an opportunity for Pol ε to begin replicating the leading strand, however the nature of this dynamic occurring on the lagging strand has yet to be explored. The concept of Pol δ

initiating leading strand replication has also been strengthened by recent work observing ribonucleotide inclusion on the leading strand *in vivo* using both wild type and catalytic dead *POL2* alleles. The results of these experiments illustrated that signatures of Pol δ replication were present in the immediacy of origins, but this appeared to switch to a Pol ε signature after the length of roughly one Okazaki fragment (Garbacz et al., 2018). Furthermore, in a catalytic dead Pol2 mutant, Pol δ was confirmed to take over synthesis of both strands at the fork, although with low efficiency and resulting genome instability (Garbacz et al., 2018).

During DNA replication, epigenetic as well as genetic information must be passed from the mother to the daughter cell. As a large protein complex bound to DNA, nucleosomes provide a significant blockage for replication forks as they carry out replication and as a result, the replisome has developed mechanisms to disassemble and reassemble them while preserving their heterochromatic configuration. While the exact mechanisms of the process of recycling histones from parental to daughter DNA is not well understood, many proteins have been identified as being involved in the process. The nucleosomes encountered by the replisome are believed to be destabilised prior to their disassembly and this function has been associated with the Ino80 and Iswi2 proteins, which are believed to disrupt the nucleosome-DNA contacts while allowing them to be recycled at the fork (Prado and Maya, 2017). Perhaps best known amongst the chromatin recycling proteins is the essential histone chaperone FACT complex, which is believed to work in concert with Mcm2 to bind disassembled H3-H4 tetramers from oncoming nucleosomes, where they then deposit them behind the fork on completed DNA, preserving their epigenetic markings (Foltman et al., 2013). Recently, the non-essential accessory subunits of Pol ε, Dpb3 and -4, have been implicated in recycling these nucleosomes preferentially onto the leading strand possibly with the Asf1 chaperone in concert with a whole host of other proteins, thereby indicating that the establishment of these imprints on the lagging strand is carried out by a separate pathway (Yu et al., 2018). Ctf4 also appears to be central in this process, as it is known to bind Mms22, a subunit of the Rtt101 ubiquitin

ligase complex that ubiquitylates the FACT complex and promotes its association to the helicase, as well as being implicated with Asf1 in the transfer of the H3K56ac modification (Luciano et al., 2015).

1.3.5 Replication Termination

Interestingly, while great strides have been made in delineating the step-wise assembly and gradual progression to origin firing, the understanding of how replication terminates beyond two forks converging and the replisomes disassembling is comparatively less. A well-regulated termination mechanism is vital in maintaining genome stability through the prevention of re-replication. This process is much more difficult to study than other aspects of replication as it does not occur at a specific stage of the cell cycle, unlike origin firing and DNA synthesis, but instead as single events that are specific to the stretches of DNA being replicated and cannot be simply induced. In spite of this, various aspects of this process have been studied in eukaryotes, mainly through work performed in budding yeast, *X. laevis* egg extracts and *Caenorhabditis elegans*. This process was originally studied in *Escherichia coli* and in mammalian systems SV40 virus plasmid, which is replicated with eukaryotic factors except for encoding its own helicase (Sowd and Fanning, 2012). However, these do not provide good models for eukaryotic systems as their DNA is circular and their replication ends in a termination zone, which is genetically defined in *E. coli* but is positioned dynamically according to the site of the origin of replication in the SV40 system (Weaver et al., 1985).

In *E. coli*, this is dictated by termination zones made up of ten *ter* sites, which each bind the Tus protein and stall the two forks after they have passed through the first five of these they encounter. Currently, the mechanism of termination after the two forks encounter each other is hypothesised to involve the two helicases passing each other after supercoil removal until they collide with the leading strand generated by the other replisome. At this point, it is believed that the helicase can then be unloaded by being substituted by a RecQ helicase, with the 3’ flap from the encountered leading strand removed, resected and ligated together (Wendel et al., 2014). The mechanism of how the bacterial replisome is removed from

the DNA is still unknown, but phenotypes of Pol I mutants have implicated its role in the process (Markovitz, 2005).

In eukaryotic systems, this process is much more reminiscent of that observed in SV40 replication, as termination sites have been shown to be sequence nonspecific. In budding yeast, although early research focused on finding specific *Ter* sites, which provided moderate success in finding certain loci that possess fork pausing elements to assist fork convergence, the use of Okazaki fragment deep sequencing has identified many more sites that frequently occur midway between origins whose defining properties are the firing programme timings of the surrounding origins (McGuffee et al., 2013). This finding has also been confirmed in higher eukaryotes and is easily reconciled with our understanding of the less prescriptive nature of origin firing compared to prokaryotic systems therefore necessitating the nature of fork convergence to be more dynamic (Petryk et al., 2016). Due to this more stochastic nature of fork convergence in these organisms, much of the research focus has been on the mechanism of the replisome disassembly and removal that occurs. Once forks converge, it is believed that the oncoming helicases bypass each other, which could be permitted as their helicases are translocating on the two opposite leading strands, and displacing each replisome onto the oncoming fork's lagging strand (Fu et al., 2011). From here, it is unclear how the gaps between each replisome and the last Okazaki fragment of the lagging strand are then resolved by the polymerase machinery, as it is known that while this would take place on the de facto leading strand, Pol ε is unable to perform the strand displacement required for maturation, possibly meaning Pol δ could be reloaded to perform this sole function. Once these gaps are filled and ligated though, the replisome is removed by a disassembly pathway newly discovered in eukaryotes, with no known correspondence to prokaryotic or SV40 systems.

Highly conserved fork disassembly pathways have been identified in both budding yeast and higher eukarya. Here, upon finishing replication, Mcm7 is polyubiquitinated (at lysine 27 in budding yeast, unknown in other organisms) by the SCF E3 ubiquitin ligase coupled with the specific substrate receptor Dia2 (SCF^{Dia2}) in budding yeast, and $CRL2^{Lrr1}$ in frog and worms

(Moreno et al., 2014, Maric et al., 2014, Maric et al., 2017). This is then recognised by a segregase complex known as Cdc48 in yeast (p97 and CDC-48 in *X. laevis* and *C. elegans*, respectively), which disassembles the replisome from the DNA through the ATPase activity of its titular subunit (Maric et al., 2014, Moreno et al., 2014). Interestingly, *C. elegans* possesses a backup pathway of replisomal removal that occurs in the early stage of mitosis. Although its exact mechanism and whether it is present in other higher eukaryotes is not known. In this process, the CDC-48 segregase is assisted with a different co-factor, UBXN-3, and acts independently of $CLR2^{LRR1}$ with regulation provided by a small ubiquitin-like modifier (SUMO) protease, possibly indicating a role for SUMO in place of the ubiquitinylation (Sonneville et al., 2017).

1.3 Checkpoint Signalling During Replication in Yeast

1.4.1 Cell Cycle Checkpoints in Yeast

As a cell divides, there are numerous factors, both endogenous and exogenous, that can disrupt this process and, if unchecked, could lead to widespread genome instability. These can range from physical insults, such as to the backbone of the DNA causing a blockage, to a scarcity of dNTPs with which to carry out synthesis, encountering transcription machinery or even single and double strand DNA breaks (DSBs). Despite referring to a huge range of possible impediments, collectively these are termed replication stresses and the cell has developed highly conserved pathways that enable it to recognise them, arrest the cell cycle and remove the source of stress before allowing restart. The recognition of these stresses is what allows them to be defined by a singular term, as they all cause an accumulation of ssDNA, which is recognised and used to signal the appropriate checkpoint. Without recognising these stresses, the ramifications for the cell can be catastrophic. Widespread genome instability can be noted from the results of mutants with disrupted checkpoint pathway sensors, and even transient exposure to replication stress leads to severe lethality. In this piece of work, this will be addressed but, for the sake of clarity, I will be focusing mainly on the checkpoint pathways as they occur during S phase.

During DNA replication, stalled forks and damaged DNA can be detected and elicit the checkpoint response either at the replication fork (S phase checkpoint), which is signalled by the replisome itself as it stalls at forks due to a physical blockage or an inability to continue replication, or behind the replication fork (DNA damage checkpoint), which is signalled by mediators away from replication forks. Importantly, both of these signalling cascades are dependent on DNA replication for their activation, but can be distinguished in their genetic dependency (Tercero et al., 2003). In budding yeast, these two parallel pathways share a common mechanism of action: they both allow the transduction of signal from a sensor kinase Mec1 (ortholog of ATR in humans) to the effector kinase Rad53 (ortholog of Chk2 in human cells, but functionally behaving like Chk1), leading to its full activation and autophosphorylation. There is a certain level of redundancy

between these two pathways, as deleting either of the two mediators produces cells that are viable and exhibit delayed but sustained checkpoint activation in response to replication stress, however double mutants prove to be non-viable (Alcasabas et al., 2001). These pathways can be studied experimentally through a range of drugs which can simulate these precisely. The S phase checkpoint can be activated by addition of the chemotherapy drug hydroxyurea (HU), which reduces the free radical site within the active site of the ribonucleotide reductase (RNR) enzyme (Singh and Xu, 2016). Inhibition of RNR prevents dNTP biosynthesis, thus depriving the replication machinery of its ability to carry out DNA synthesis. This causes fork stalling, causing ssDNA to build up at the fork, which is then coated by RPA and recognised by the checkpoint machinery. This is often a preferred method of studying the S phase checkpoint as a whole as its addition arrests all replication forks, instead of relying on a subset to encounter a specific induced damage (Slater, 1973). Meanwhile, the DNA damage checkpoint can be targeted through use of the alkylating agent, methyl methanesulfonate (MMS). This methylates DNA bases, which must be removed through base excision repair, leaving stretches of ssDNA throughout the genome, which activate the DNA damage repair machinery. Additionally, MMS has been suggested to directly induce the formation of abasic sites in the genome, which are also required to be removed by base excision repair (Xiao et al., 2001). The accumulation of ssDNA that results from the presence of this drug causes activation of Mec1 and the beginning of the checkpoint signalling cascade.

One finding that has complicated a lot of the study of checkpoint proteins that form part of the replisome is the understanding of a threshold regulating an effective checkpoint activation. This was discovered through use of a mutant allele of an *ORC* subunit, which lowered rates of origin firing and therefore the numbers of active replication forks during an S phase (Shimada et al., 2002). This allele had been previously noted to possess checkpoint defects through an inability to inhibit late firing origins in response to hydroxyurea and a significant loss of viability when exposed to MMS (Shirahige et al., 1998, Weinberger et al., 1999). Through further study of this

allele by using dosage compensation, it was found that the number of forks present in the cell was directly proportional to the levels of S phase checkpoint response. It was concluded that there existed a 'threshold value' of replication forks that was to be met before a robust checkpoint that would protect the cell from the genomic instability induced by the replication stress if gone unchecked (Shimada et al., 2002). This has confused the designation of many proteins identified in replication initiation that have also been implicated in signalling the S phase checkpoint, as any mutant that would negatively affect the former would also be faulty in activating the latter and so proteins could erroneously be assessed of forming part of the checkpoint network.

1.4.2 The Activators and Downstream Targets of the Checkpoint

Before exploring in further detail the difference between the two pathways of checkpoint activation at forks, I will first define the common elements and the two conserved kinases at the heart of it. Moreover, I will illustrate the downstream response triggered by the checkpoint activation during DNA replication. Mec1 is constitutively a weak kinase and member of the phosphoinositide 3-kinase-related kinases (PIKK) family. This signalling cascade is shown in figure 1.5, in which I have highlighted a subset of the downstream targets of the checkpoint. Mec1 exists in a homodimer with Ddc2 (ATRIP in humans) and this allows its localisation to RPA-bound ssDNA and, furthermore, deletions of either of these results in lethality for the cell, underlining their interdependent function (Paciotti et al., 2000). Structurally, Ddc2 appears to bind to the Rfa1 subunit of RPA and homodimerizes with other locally bound molecules through its N-terminus, and this promotes the recruitment of multiple Mec1 subunits to these ssDNA sites (Zou and Elledge, 2003). The localization of Mec1 to ssDNA, however, is not sufficient for its activation, and this is carried out by other checkpoint mediators unique to the pathway being activated, including Dpb11, 9-1-1 and Dna2, in events further characterised below. The nature of its activation ensures that Mec1 remains functional only at a local level and, in order to transduce the checkpoint signal, its substrates must be recruited to these sites through adapter proteins. In the case of DNA damage signalling,

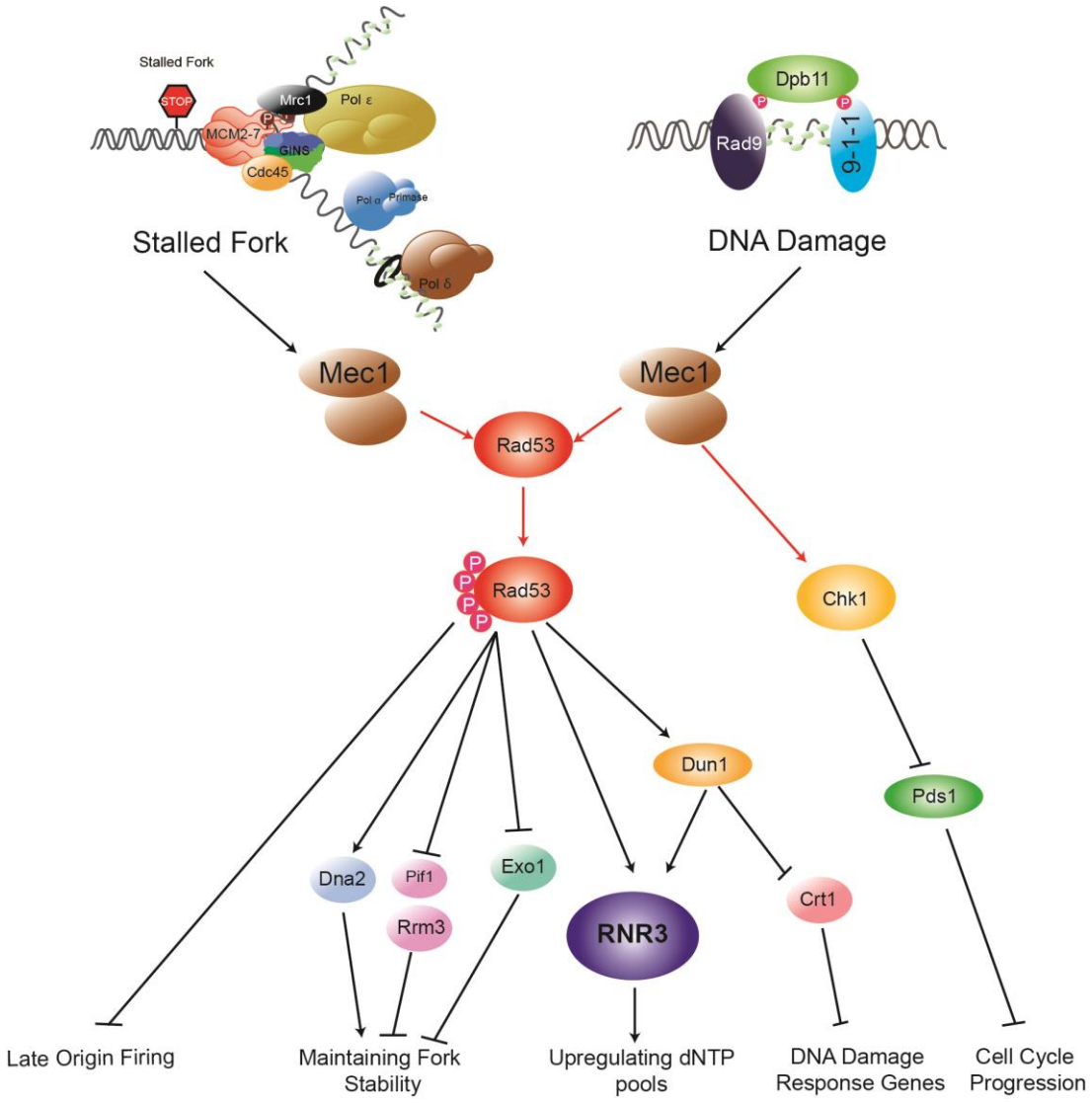

Figure 1.5: A depiction of the downstream signalling cascade of S phase and DNA damage checkpoint signalling. When replication stress is detected either at or away from the replication fork, the S phase and DNA damage checkpoints are signalled, respectively. These both culminate in the activation of Mec1 and Rad53, two serine-threonine kinases that effect cellular changes to respond to the replication stress. Some of these pathways are shown in this diagram, although this is just a subset of the many interactions that take place in this signalling cascade.

histone markers of DNA damage are able to recruit these mediators and one of the most prominent, ɣ-H2A, is phosphorylated in a Mec1-dependent manner (Downs et al., 2000). Mec1 phosphorylates over 100 targets on S/T-Q motifs in response to its activation, including the effector kinases Chk1 and Rad53, however it is the activation of the latter that is crucial in effecting the widespread cellular events required for a robust checkpoint response

(Bastos de Oliveira et al., 2015). In addition to this role in checkpoint, Mec1 is also crucial during the normal functioning of DNA replication, where its activity rates are as high as in its response to stress (Bastos de Oliveira et al., 2015). It appears that Mec1 functions at forks and prevents the formation of chromosomal rearrangements during ordinary replication in a manner independent from its Rad53 activation activity (Lanz et al., 2018). This process is believed to act in some redundancy with another PIKK member, Tel1 (human ATM), which is primarily involved in the signalling of DSBs and is activated by the Mre11/Rad50/Xrs2 (MRX) complex that recognises these lesions (Nakada et al., 2003, Lanz et al., 2018).

The main effector kinase, Rad53, is structurally characterised by its two forkhead-associated domains (FHA), which recognise phospho-threonine residues, and these flank its serine/threonine kinase region (Durocher et al., 1999). Rad53 exists as an inactive homodimer that is ordinarily bound to chromatin, however, upon detection of stress, it is transiently localised at sites of damage by mediators through associations with its FHA domains. In the presence of activated Mec1, it is phosphorylated at multiple sites within a region dense in SQ/TQ motifs close to its N-terminus (Chen et al., 2014). This allows Rad53 to extensively autophosphorylate *in trans* and this, specifically through modification of threonine-354, removes a self-inhibitory loop that fully exposes its catalytic site (Wybenga-Groot et al., 2014). This extensive autophosphorylation allows an efficient amplification of a localised checkpoint signal, allowing it to effect the processes across the nucleus required to respond to replication stresses recruited to chromatin. Chk1 is another effector kinase activated in parallel with Rad53, although its roles in checkpoint signalling are comparatively minor and appear partially redundant, unlike in higher eukaryotes where it has an essential function (Liu et al., 2000). The mode of Chk1 activation is also mediated by Mec1 and recruited in a Rad9-dependent manner (Chen et al., 2009).

From here and together with Mec1, Rad53 functions to immediately halt further DNA synthesis through **inhibiting late origin** firing as well as preventing progression in the cell cycle. The former occurs by the inhibitory

phosphorylation of the firing factors Sld3 and Dbf4 by Rad53, which prevents further origin firing, therefore reducing the risk of either damaged DNA being replicated as well as preserving an origin complement ready to be fired when replication resumes (Lopez-Mosqueda et al., 2010, Zegerman and Diffley, 2010). This mechanism is conserved in higher eukaryotes, as the human and *Xenopus* Sld3 ortholog, Treslin, has been found to be inhibitorily phosphorylated by Chk1, preventing further Cdc45 loading at origins (Guo et al., 2015). Cells are also prevented from entering mitosis with a damaged or unduplicated genome through another kinase, Chk1, that is activated downstream of Mec1 in a parallel pathway to Rad53 (Sanchez et al., 1999). This kinase functions to prevent the APC/C-mediated degradation of Pds1, a securin that ensures sister chromatid cohesion through the inhibition of the separase Esp1 (Agarwal et al., 2003). In addition to this, phosphorylation profiles of Rad53 in response to activators of the S phase and DNA damage checkpoints have revealed many members of the mitotic exit network (Zhou et al., 2016). In *Sz. pombe* and higher eukaryotes, this mitotic arrest is induced by the inhibition of the Cdc25 phosphatase through phosphorylation by Chk1 and this ensures the Cdc2 (CDK) remains inactive due to its inhibition by Wee1 (Sanchez et al., 1997, Furnari et al., 1997).

Following the progression to the next phase of the cell cycle, many genes encoding proteins required in S phase are inhibited in this transition, however, upon activation of either checkpoint, transcription is in fact turned back on and, analogous to a known pathway in fission yeast, which is theorised to be due to the inactivation of the transcriptional co-repressor Nrm1 (Bruin, 2009). When specifically activated by the DNA damage checkpoint, the signal transduced by the pathway causes the upregulation of over 200 transcripts and while the mechanisms surrounding activation of most of these are yet unknown, a fraction are DNA damage response genes that are induced through inactivation of the transcriptional repressor, Crt1, by the a downstream kinase of Rad53, Dun1. (Huang et al., 1998, Bruin, 2009). Furthermore, Rad53 has been shown to directly phosphorylate Nrm1, preventing its binding to MBF targets, which are differentiated from those of SBF by their S phase checkpoint-induced expression (Travesa et al., 2013).

Further to this, in order to assist in the eventual replication restart, dNTP pools are increased through controlling gene expression and more directly through its kinase cascade. Transcriptionally, the inactivation of Crt1 by Dun1 inactivates this repressor that acts at the promoters of *RNR* genes, thus upregulating their expression and increasing dNTP production (Huang et al., 1998). In addition, Rad53 is also believed to indirectly increase *RNR1* expression through its regulation of histone levels, which allows the upregulation of the transcription activator, Ixr1 (Tsaponina et al., 2011). Dun1 also exerts effects at the protein level through targeting for degradation two inhibitors of the RNR complex, Dif1 and Sml1, allowing cytoplasmic localisation in the case of the former and preventing its direct inhibition in the latter (Lee et al., 2008, Zhao and Rothstein, 2002). This has also been shown to be a conserved feature in humans, as it has been demonstrated that sustained transcription in the presence of replication stress is necessary to protect the cell against DNA damage, as many mammalian checkpoint mediators have short half-lives (Bertoli et al., 2013, Bertoli et al., 2016). Many of these mediators are controlled by the E2F transcription factor family, and one characterised mechanism has shown Chk1 is able to inhibitory phosphorylate the E2F6 transcriptional repressor, thereby increasing the expression of its targets (Bertoli et al., 2016).

The key function of the S phase checkpoint is believed to be to maintain the capability of replication forks to restart DNA replication following the recovery from replication stress. The importance of this can be seen in the response in checkpoint mutants, where even short exposures to replication stresses can lead to lethality. It appears that the forks in these cells are more likely to collapse upon fork stalling, resulting in them being unable to restart replication, even after the stress has been removed (Tercero and Diffley, 2001). At collapsed forks, Rad53 also plays a key role in inhibiting the helicases Pif1 and Rrm3, which ordinarily assist the replisome in bypassing potential stalling elements. At stalled forks though, they can potentially continue to unwind the nascent lagging strand, allowing it to form secondary structures that would cause catastrophe, therefore their inhibition allows the fork to remain in a position to restart replication (Rossi et

al., 2015). The S phase checkpoint also inhibits nucleases; exonuclease regulation appears to play a crucial role in this process, as Exo1 and Dna2 have both been shown to be modulated by Rad53 and important in fork stability following arrest. Dna2 is phosphorylated by Rad53 and through its nucleolytic activity is believed to degrade nascent DNA strands to prevent their annealing, which could cause fork reversal and be deleterious for the cell (Hu et al., 2012). In response to DNA damage specifically, Exo1 appears to be inhibited by Rad53 thus preventing it from targeting the fork, which, through an unknown mechanism, has been shown to negatively impact upon its integrity (Segurado and Diffley, 2008). Additionally, this inhibition has also been implicated in preventing unwanted nucleolytic processing away from the fork at sites of DNA damage, thus preventing a further build-up of ssDNA and therefore modulating the checkpoint response (Morin et al., 2008). This collapse could emerge due to an inability of checkpoint mediators to slow replication in periods of stress, as it has been noted in Rad53 and Mec1 mutants that fork progression remains high (De Piccoli et al., 2012, Szyjka et al., 2008). Additionally, in human cells, it has been shown that in ATR mutants, depletion of RPA occurs in periods of stress, as stably stalled forks continue to generate ssDNA to an excess and this eventually results in widespread breakage and catastrophe (Toledo et al., 2013). There is currently debate in the field as to whether the checkpoint plays a role in regulating the stability of the fork in order to prevent collapse, or whether this is a function carried out independently by the replisome and instead the checkpoint solely functions to induce restart once the stress has been removed (Cortez, 2015). While previous work stated that the abundance of many replisome components, especially polymerase subunits, were reduced in *mec1Δ* and *rad53Δ* mutants, this was disputed as an artefact of the fact that this was only analysed at early origins as, when forks were examined genome-wide, loss of interactions of replisome components were not noted (Cobb et al., 2005, Lucca et al., 2004, De Piccoli et al., 2012). Considering there are many replisomal subunits that are phosphorylated in response to replication stress by Mec1 and Rad53, it is reasonable to consider that the checkpoint must play a role at forks, although whether this is to stabilise

them or to prime them for restart is unclear and subject to further research (De Piccoli et al., 2012, Chen et al., 2010, Smolka et al., 2007).

1.4.3 The S Phase Checkpoint

As previously mentioned, the S phase checkpoint is activated at forks in response to specific replication stresses that somehow cause forks to stall and accumulate ssDNA and this pathway is shown in figure 1.6. These can be endogenous factors, such as fluctuations in the dNTPs pool or oxidation of the DNA template (Giannattasio and Branzei, 2017). Exogenously, this could be due DNA damage caused by UV light, exposure to genotoxic chemicals that attack the DNA or to inhibitors of the replication machinery such as the polymerase and topoisomerase complexes by aphidocolin and camptothecin, respectively (Giannattasio and Branzei, 2017). Interestingly, DNA damage can cause different effects depending on the strand they effect, as bulky adducts on the leading strand can stall the replisome due to their tight association, whereas if occurring on the lagging strand, its discontinuous nature enables it to skip over a potential blockage and leave it for the DNA damage checkpoint to deal with (Fu et al., 2011). Upon encountering a blockage, the fork protection complex stabilises the replisome to form a pausing complex, thus preventing the uncoupling of the replisome and the fork, a function underpinned by Mrc1's direct binding to Mcm6 and its Tof1-mediated interaction with Cdc45, both of which are subunits of the helicase (Katou et al., 2003, Komata et al., 2009). As a result and through Ddc2, Mec1 is recruited to the fork (Deshpande et al., 2017). This Mec1 is then believed to phosphorylate and activate Mrc1, which transduces this signal to Rad53 (Alcasabas et al., 2001). In some cases, it is believed that even greater amounts of ssDNA can build up through the constant re-priming and extension activity of polymerases α and δ, therefore generating a larger lagging strand and then members of the classical DNA damage pathway, such as the heterotrimeric Rad17-Mec3-Ddc1 (9-1-1) clamp, can bind here and further accentuate the signal generated (Majka et al., 2006). This generates a stronger Mec1

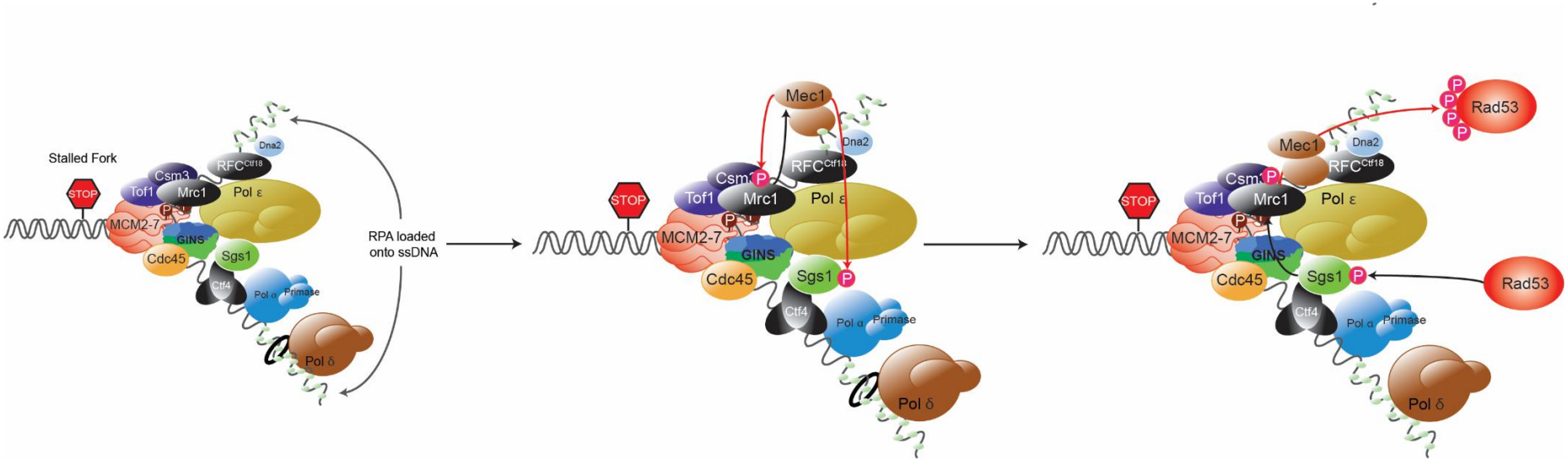

Figure 1.6: A model for S phase checkpoint activation at the fork. When the replication fork stalls either due to a physical blockage or a lack of dNTPs with which to carry out DNA synthesis, it will signal the S phase checkpoint. This starts with the coating of excess ssDNA present at the fork with RPA. This is recognised by Ddc2-Mec1 and this complex is recruited to the fork, where it phosphorylates and activates Mrc1. Mrc1 then positively regulates the stabilisation of activated Mec1 at the fork. Mec1 also phosphorylates Sgs1, allowing it to bind Rad53. Rad53 then binds to Mrc1, which promotes its phosphorylation by Mec1. Rad53 then autophosphorylates to amplify the checkpoint signal and proceeds to effect multiple cellular changes to respond to the replication stress.

activation and resultant checkpoint response, but this mechanism can be considered an accessory for the S phase checkpoint and will be discussed further in ‘The DNA Damage Checkpoint’ section. The redundancy of this system can be observed by the fact that deletion of the 9-1-1 complex or its loader has little effect on the timely activation of Rad53 in response to HU (Bjergbaek et al., 2005).

Despite playing a crucial role in ensuring high levels of fork progression during replication, Mrc1 is also the key mediator of activating the S phase checkpoint at forks following phosphorylation by Mec1. Comparative analysis of a mutant with potential Mec1 phosphorylation sites mutated (*mrc1-AQ*) and a deletion showed a separation of function between the fork progression and checkpoint roles of Mrc1 (Osborn and Elledge, 2003, Szyjka et al., 2005). Upon its phosphorylation and activation by Mec1, it has been suggested that Mrc1 then creates a positive feedback loop, although the nature of this stabilization activity remains unclear, through which it can accumulate Mec1 at the fork to provide a sustained checkpoint response until the replication stress has been removed (Naylor et al., 2009). Mrc1 has been shown to be bound by the FHA1 domain of Rad53 after exposure to replication stress, and this would provide the basis by which Rad53 can be activated, thus leading to its autophosphorylation and amplification of the checkpoint signal (Smolka et al., 2006). This process of recruiting Rad53 to the forks for its subsequent Mrc1-mediated activation is carried out together by two complexes: the Ctf18-Dcc1-Ctf8-Rfc2-4 and Sgs1.

Ctf18-RFC is a clamp loader complex and member of the RFC family of proteins. RFC complexes are formed of a ‘core’ of Rfc2-4 subunits but have different main subunits that dictate their function. While the complex commonly referred to as RFC (Rfc1-RFC in longform) has Rfc1 as its main subunit that confers its ability to load the PCNA clamp on DNA, Ctf18 is the large protein that dictates the checkpoint role of its RFC complex (Majka and Burgers, 2004). However, unlike other RFC complexes, Ctf18-RFC additionally requires the association of the Ctf8-Dcc1 dimer, through association with its Ctf18 subunit, to carry out its dual function (Mayer et al., 2001). This binding module provided by the dimer allows it to bind Pol2,

which appears to have a role in signalling the checkpoint, in a manner that is conserved from yeast to humans (Garcia-Rodriguez et al., 2015). When this specific interaction was disrupted through mutation of *CTF18*, checkpoint activation was severely diminished, and seemingly only possible through activation by the DNA damage pathway, a phenotype similar to *ctf18Δ* strains (Garcia-Rodriguez et al., 2015). Outside of checkpoint signalling, this complex has been implicated in establishing sister chromatid cohesion as well as, typically for the RFC family, the loading and unloading of PCNA (Lengronne et al., 2006, Bylund and Burgers, 2005). The role Ctf18-RFC plays in S phase checkpoint signalling remains poorly understood although has been pinpointed to be downstream of Mec1 activation and this research remains ongoing (Garcia-Rodriguez et al., 2015).

Sgs1 is a RecQ helicase that is known to track with the replisome as it progresses and recently has been further and further implicated in activating the S phase checkpoint (Cobb et al., 2003). It is believed to be recruited to the fork through its two SUMO-interacting motifs (SIMs), which recognise the SUMOylated SMC complex (Bermudez-Lopez et al., 2016). RecQ helicases unwind DNA in the 3'-5' direction and are integral in maintaining genomic stability in numerous organisms (Seki et al., 2006). In the S phase checkpoint, Sgs1 would appear to a central player as it has been shown to change conformation upon phosphorylation Mec1 in response to fork stalling, which allows it to bind the FHA1 domain of Rad53 (Hegnauer et al., 2012). As this interaction with Rad53 occurs at the same binding site as Mrc1, it is possible that Sgs1 could operate as 'handing over' Rad53 to Mrc1 for it to be phosphorylated, as this activation pathway is known to be shared by the two proteins (Bjergbaek et al., 2005). More recently, another helicase, the CMG, has also been implicated in propagating the signal from the mediator kinase to Rad53. An *MCM2* mutant has been experimentally characterised that, in response to fork stalling, Mrc1 kinetics remained normal while simultaneously being insufficient to transduce this signal to hyperphosphorlate Rad53, indicating a possible role in the Mcm2-7 subunits possibly dynamically restructuring in order for the replisome to respond to periods of replication stress (Tsai et al., 2015). Together, the activities of

these proteins in activating and propagating the S phase checkpoint illustrate a very dynamic replisome and complex signalling network between its constituent parts, and further research in this area will certainly prove fruitful in extending our understanding of this process.

1.4.4 The DNA Damage Checkpoint

Because DNA damage can occur at any point of the cell cycle, the cell must possess mechanisms that are able to detect and repair it at any point, all while delaying the cell cycle before this process is complete. In relation to the S phase of the cell, these pathways must be able to recognise regions of single or double strand breaks behind replication forks and signal these for repair. This is carried out by a convergence of two pathways governed by Rad24-RFC (shortened to Rad24) and Rad9, which activate Mec1 at these sites of DNA damage and activate Rad53 to generate the checkpoint response, both of which are shown in figure 1.7 (de la Torre-Ruiz et al., 1998). Rad24 is a member of the RFC complex family, and with its titular main subunit has a much decreased affinity for PCNA, although retaining its ability to unload it, and instead loads the alternative DNA damage sensing clamp, 9-1-1, onto DNA (Yao et al., 2006).

Meanwhile, Rad9 is a sensor of DNA damage that is able to bind two variants of post-translationally modified chromatin. The first of these modifications is the Dot1-mediated methylation of lysine 79 on histone H3, which is bound through the TUDOR domain of Rad9, although evidence is lacking that this is a direct response to DNA damage as it is present across the genome (Grenon et al., 2007). The second is the phosphorylation serine-129 of H2A (ɣ-H2AX), a well characterised chromatin modification that arises in large domains around sites of DSBs in a Mec1-dependent manner, that Rad9 binds through its BRCT domains (Hammet et al., 2007). Interestingly, both of these modifications are restricted to the G_1/S phase of the cell cycle when eliciting activation of the Rad9-mediated checkpoint pathway, although the H3K29 methylation is an important step in the actual DNA repair pathway in G_2 (Grenon et al., 2007). Abolishing the binding of Rad9 to these chromatin modifications through mutation of its TUDOR domain eliminates the checkpoint arrest in G_1 in response to DNA damage (Wysocki et al.,

2005). In G_2, the activity of Rad9 is modulated by its phosphorylation carried out by CDK, which allows it to synergise with the Rad24/9-1-1 pathway of DNA damage signalling (Pfander and Diffley, 2011). Concurrently, in a manner similar to how RFC is able to load PCNA around dsDNA, it is assumed that Rad24 scans across the genome and recognises ssDNA-dsDNA junctions, at which it is able to load the 9-1-1 complex throughout the cell cycle (Kondo et al., 2001). Once the 9-1-1 complex is loaded upon this same site of DNA damage, its Ddc1 subunit activates Mec1 and is subsequently phosphorylated by it at Thr602, which provides a binding site for Dpb11 (Puddu et al., 2008). In addition to its central role in origin firing, Dpb11 is equally crucial in activating both pathways of the DNA damage checkpoint, where it is known to bind to and activate the Mec1-Ddc2 complex through its C-terminus (Navadgi-Patil and Burgers, 2008). This allows Mec1 activation at sites of damage, which then activates Rad53 to propagate the checkpoint signal

It is at this point that this pathway can also converge with the Rad9-mediated pathway. Upon its phosphorylation by CDK, Rad9 is able to bind Dpb11, whose recruitment of Mec1 could allow the latter's stabilisation at these sites of damage and, as a ternary complex with Rad9, the sensor kinase would be able to phosphorylate Rad9 and thus provide a scaffold for Rad53 trans-activation (Pfander and Diffley, 2011). Rad9 can be phosphorylated at multiple sites by Mec1, which appears to facilitate the former to recruit Rad53 through both of its FHA1 and FHA2 to these sites, thus allowing its subsequent hyperphosphorylation and activation by Mec1 (Schwartz et al., 2002).

1.4.5 Terminating the Checkpoint Signal

While signalling the DNA damage is vitally important for cells so that this can be repaired before progressing in the cell cycle, once the original stress ceases to exist, it is necessary for the checkpoint to be turned off. Considering the ability of Rad53 to autophosphorylate, this cannot be a passive process relying on the removal of the original signal alone, so it is actively turned off by phosphatase-dependent and -independent systems. When components of both systems are deleted, continued hyperactivation of

Rad53 is noted in response to MMS, causing DNA damage to go unrepaired and consequently causing acute sensitivity to the drug (Jablonowski et al., 2015). The recently discovered phosphatase-independent pathway is achieved by the specific disruption of the Rad9 scaffold used for DNA damage signalling through the concerted actions of the Rtt107-Slx4 complex (Ohouo et al., 2013). These two proteins constitutively form a dimer and are recruited to ɣ-H2AX DNA damage sites through recognition by the Rtt107 subunit (Balint et al., 2015). Further to this, Slx4 is phosphorylated at multiple positions by Mec1 and CDK, which provides a binding interface for Dpb11 in a mutually exclusive manner (Ohouo et al., 2013). This essentially allows the Rtt107-Slx4 complex to supplant Rad9 both from binding to DNA and signalling through Dpb11 (which can be seen by higher Rad9 recruitment to damage sites in *slx4Δ* cells), therefore preventing the transduction of signal from Mec1 to Rad53 and thus preventing further checkpoint activation (Dibitetto et al., 2016).

The abrogation of Rad53 signal is also mediated by the dynamic action of a number of phosphatases and protein degradation that is vital in switching off the checkpoint and resuming cell cycle progression. Current research suggests that the phosphatase-directed deactivation of Rad53 – both by targeting the upstream activation pathway or reversing Rad53 phosphorylations – is specific to the stress encountered by the cell, with PP1 being linked to HU-related recovery, PP2C (Ptc2/Ptc3) to DSBs and PP4 (Psy2-Pph3) to MMS (Bazzi et al., 2010, Leroy et al., 2003, Szyjka et al., 2008). PP4 has been shown to be crucial in removing the DNA damage signals generated by genotoxic agents like MMS, as it can target dephosphorylate ɣ-H2AX as well as forming a complex with Mec1-Ddc2 through which it can oppose many of its functions (Hustedt et al., 2015). Further to this, PP4 has been implicated in simultaneously functioning with the checkpoint dampening mechanism of Rtt107-Slx4. Through its ability to dephosphorylate Rad53 in conditions of widespread DNA damage as seen in MMS, PP4 is hypothesised to deactivate the global pools of hyperphosphorylated Rad53 activated by the response to the initial stress, while the Rtt107-Slx4 complex works at the local level of removing the

signals themselves (Jablonowski et al., 2015). Together, this allows the steady removal of the damage checkpoint, allowing cells to begin DNA repair and cell cycle progression. Mrc1 has also been linked with replication restart following replication stress, although this is achieved by its degradation (Chaudhury and Koepp, 2017). This degradation is carried out by SCF^{Dia2} and is mediated by Sgs1 which then promotes fork restart (Chaudhury and Koepp, 2017). While the loss of Mrc1 would presumably prevent further activation of Rad53, leading to attenuation of the checkpoint signal, it is not understood whether it dynamically reattaches to replisomes after the fork starts synthesis, as it is well documented how important Mrc1 is in progression. Additionally, this appears to be conserved in human cells as similar observations have been made regarding the degradation of Claspin in downregulating Chk1 to promote recovery from replication stress (Mailand et al., 2006).

1.4.6 DNA Polymerase ε and the S Phase Checkpoint

DNA Polymerase ε has also been linked many times in checkpoint signalling, but the mechanism remains elusive. Much of the early evidence of this role emerged from research into various C-terminal mutants of its catalytic subunit, Pol2, (Navas et al., 1995). When mutants targeting this C-terminus were characterised, many had very sick phenotypes including temperature sensitivity, the severe sensitivity to genotoxic agents and the lack of induction of Rnr3 in response to replication stress, a hallmark in defects in checkpoint activation (Navas et al., 1995). Strikingly, the extreme C-terminal sequence of Pol2 binds Dpb2 and through this to GINS (Dua et al., 1998, Sengupta et al., 2013). While the checkpoint defects observed in Pol2 mutants would provide a natural conclusion to be drawn about its role in stress signalling, this picture was elucidated before the role of DNA polymerase epsilon in origin firing was discovered (Muramatsu et al., 2010). In light of this discovery, some of the checkpoint defects observed might be an indirect consequence of a defect in origin firing, since lowering the concentration of replication forks during replication impacts the cell's ability reach the threshold activation required to generate a robust response to replication stress (Shimada et al., 2002).

More recently, more concrete implications of checkpoint function have been made through the discovery of many interactions with checkpoint related proteins present at the replisome. In fact, Pol2 binds directly with Mrc1, which has been found to have two separate binding domains with Pol2: one at the N-terminus and the other in the C-terminus (Lou et al., 2008). Mrc1 appeared to play two distinct roles, one being in DNA replication, where it appears to stabilize Pol ε, so much so that it can suppress the temperature sensitivity of a C-terminal truncation, *pol2-11*, while its deletion coupled with this allele was lethal, indicating its importance in replication. It is also suggested that this interaction plays a role in signalling the checkpoint, due to its ability to suppress the HU and MMS sensitivity of *pol2-11*. On a more molecular level, it was found that the phosphorylation of Mrc1 in response to checkpoint activation, the binding interface between Mrc1 and Pol2's N-termini is lost, potentially allowing it to interact with other proteins to effect the checkpoint. From other research involving Ctf18-RFC, which was shown to bind to the Pol2 N-terminus upon checkpoint activation, this could neatly dovetail with the loss of Mrc1, potentially allowing a conformational change that permits Polymerase ε to effect the S phase checkpoint (Lou et al., 2008, Garcia-Rodriguez et al., 2015). Further work involving double mutants of *pol2-11* coupled with *sgs1Δ* appeared to be in one epistasis group, as replication times quantified by FACS analysis did not differ between their single and double mutants, which could possibly implicate Pol ε in recruiting and stabilising Sgs1, thus allowing it to bind Rad53 following its phosphorylation by Mec1, although this hypothesis is speculative (Frei and Gasser, 2000, Hegnauer et al., 2012). The binding of Pol ε with Dpb11 and with Sld2 has also led some to speculate that this could be the potential source of its involvement in checkpoint signalling in response to fork stalling, a hypothesis derived from the identical phenotype noted in double mutants in a *ddc1Δ* background between *dpb4Δ, dpb11-1* and *drc1-1* (a mutant of Sld2), indicating their presence in a single epistatic group (Puddu et al., 2011). The hypothesis suggests that a Pol ε-Dpb11 (with or without Sld2) complex was assembled on the leading strand in response to fork stalling, and this could then induce Mec1 activation to signal the S phase checkpoint.

More recently, work carried out on a Dpb2 mutant has implicated it in signalling a specific pathway of the S phase checkpoint, the Nrm1 branch which oversees activation of the MBF transcription factor (Dmowski et al., 2017). This controls the expression of many G1/S-related “switch genes”, so-called because they are assumed to be required for stress response but must be able to be switched off in order for the cell cycle to progress (Smolka et al., 2012). The Dpb2 mutant possesses reduced Pol2 and Psf1 interactions and therefore, it can be assumed, a reduced rate of origin firing and so checkpoint signalling would theoretically be affected (Dmowski et al., 2017). Notably in this experiment though, one aspect specifically of the checkpoint response is affected, rather than something as general as Rad53 activation, so a genuine role of Dpb2 in signalling this is possible, although the mechanism this could occur through is not clear (Dmowski et al., 2017). Nevertheless, since much is known about the regulation of transcription in response to replication stress, it’s still not clear how this pathway, downstream of Rad53 and Dun1 activation, might be singularly affected by a Dpb2 mutant. Unfortunately, many of the associations of Pol ε functioning in checkpoint signalling remain circumstantial, with as of yet no direct involvement in any known pathway pinpointed, however, the evidence remains persuasive that this polymerase complex plays some role in this cellular process.

While in the previous chapters I have presented the broader context of DNA replication and checkpoint response, I will now focus in more detail on the subject of this thesis, namely Pol ε. In the remaining chapters, I will describe its composition, biochemical features, evolutionary conservation and the mutations associated with the disease in humans.

1.5 DNA Polymerase ε in *Saccharomyces cerevisiae*

DNA Polymerase ε is one of the two processive polymerase complexes in budding yeast and is widely thought to carry out the DNA replication on the leading strand at the fork, although for reasons mentioned previously, this might occur in combination with DNA polymerase delta. It has essential roles in replication initiation through forming the pre-loading complex and is hypothesised to have an as yet unknown role in signalling the

S phase checkpoint due to its many known associations with checkpoint-mediating proteins. Pol ε is a heterotetramer of a catalytic subunit, Pol2, an essential B subunit, Dpb2 and two non-essential subunits, Dpb3 and -4.

1.5.1 The Catalytic Subunit, Pol2

Pol2 is made of two distinct sections: a catalytic N-terminus, and a largely non-conserved, unstructured C-terminal half. This can be understood from an evolutionary perspective as it believed to have originated from a fusion of the catalytic N-terminus of an archaeal type 2 polymerase with that of a catalytic-dead C-terminus of a protobacterial or bacteriophage polymerase (Tahirov et al., 2009). Within the N-terminal half lies the polymerase and exonuclease domains, which provide its 5'-3' DNA synthesis 3'-5' proof-reading activities, respectively (Dua et al., 1998). Distinct from Pol δ, which requires binding to PCNA to anchor it to the DNA and ensure its processivity, Pol ε remains highly processive in its absence and has a far reduced affinity for the sliding clamp, compared to Pol δ. While a putative PIP box has been predicted in Pol2, little is known of the function of such a sequence and mutating it had little effect on replication (Chilkova et al., 2007). This could be due to the fact that Pol ε is able to anchor itself to the DNA and, from its crystal structure, the presence of its unique P domain could explain this (Hogg et al., 2014). This P domain is part of Pol ε's larger palm region and appears to generate greater contacts with the emerging dsDNA from the active site, therefore possibly substituting for the anchor effect of PCNA (Hogg et al., 2014). Further, it has also been hypothesised that the physical interaction of Pol ε with the CMG, the ring structure of the Mcm hexamer is able to effectively function as a PCNA-like clamp for the polymerase's processivity (Langston et al., 2014). Underlining the inherent nature of Pol2's superior catalytic activity comes from recent *in vitro* studies that illustrate even without other subunits of its holoenzyme, it was able to achieve comparable rates of synthesis (Ganai et al., 2015). Interestingly, the catalytic activity of Pol2 was only compromised compared to that of Pol ε during the incorporation of the first dNTP, where it was noted to be considerably slower (Ganai et al., 2015). Additional *in vitro* work has also underlined the importance of Pol ε in stimulating the CMG helicase, the

presence of the former greatly increased the latter's processivity, which was not the case with either of the other two polymerases (Kang et al., 2012).

As previously mentioned, this entire N-terminus is not essential for the viability of the cell and survival is possible when this is entirely deleted, as it is in the *pol2-16* allele (Kesti et al., 1999). In these cells, the lagging strand polymerase δ is able to take over leading strand replicative duties, although this results in slower replication times and rising genetic instability (Garbacz et al., 2018). This phenotype is not present in a catalytic dead *POL2* allele, which is instead lethal for the cell, presumably as it sterically occludes Pol δ from the leading strand and prevents any synthesis taking place (Dua et al., 1999). This idea is consistent with the developing theory of Pol ε displacing Pol δ early into elongation from the origin, at which it stays until the end of replication (Garbacz et al., 2018, Yeeles et al., 2017).

The essential nature of the Pol2 C-terminus was of great interest during early research into the Pol ε complex. Structurally, for the most part it was largely non-conserved with few structural elements, except at the very end where, within its last 100 residues lie two zinc fingers characteristic of a catalytic polymerase subunit (Dua et al., 1998). Interestingly, in other polymerases these zinc finger domains are normally placed close to the catalytic domains, but within Pol2 these are separated by over a thousand residues, possibly due to the fusion event of the archaeal and protobacterial polymerase domains being an insertion of the latter into this separating region (Tahirov et al., 2009). C-terminal truncations of *POL2*, including the 36 C-terminal residue truncation in *pol2-11*, typically exhibited severe sensitivities to both temperature and genotoxic agents (Navas et al., 1995). Many of these experiments illustrated the essential nature of the C-terminus, as larger deletions of C-terminal regions proved to be inviable, while C-terminal fragments could be expressed under the expression of a galactose-inducible promoter which were able to compensate the lethality of *pol2Δ* (Kesti et al., 1999). The essential nature of the C-terminus and the phenotypes exhibited by mutants affecting these regions led to the assumption that the Pol ε complex must play a role in checkpoint signalling as well as an unspecified non-catalytic function during DNA replication. Much

like the zinc fingers within other catalytic polymerase subunits, these were found to be responsible for binding its B subunit, Dpb2 (Sanchez Garcia et al., 2004, Dua et al., 1998). Recently, it was discovered that Dpb2 provides a physical link between Pol ε and the CMG helicase, while forming part of the pre-LC during the process of origin firing, therefore partially explaining the essential importance of the Pol2 C-terminus in DNA replication (Sengupta et al., 2013). In retrospect, research that showed high-copy numbers of *DPB2* and *DPB11* were able to suppress the temperature sensitivity of *pol2-11*, perfectly explains the nature of the role of the C-terminus in origin firing, as increasing the protein levels of the other pre-LC members was sufficient to remedy what presumably became a less stable interaction on Pol2's end at high temperatures (Araki et al., 1995). It appears Dpb2 is the basis of the essential nature of Pol2's C-terminus within DNA replication and through disrupting the process of origin firing could certainly affect its checkpoint response. However, it is still widely believed that Pol2 has some additional role in S phase checkpoint signalling independent of this interaction, while the mechanism remains elusive.

This depiction of Pol2 as a protein of two distinct halves is somewhat consistent with what it known about Pol ε structural dynamics as a whole, in which it appears as a bilobed structure with the catalytic and non-catalytic N- and C-termini located spatially apart, with the intervening residues providing a flexible linker (Zhou et al., 2017). This bilobed structure gives Pol2 a flexibility that has allowed it to be captured in two different structural states by electron microscopy, and this could point to two functional states, one of which must be its positioning during DNA synthesis at the leading strand while the other could be its structure before it establishes itself synthesising DNA on the leading strand or, more speculatively, even a restructured role when the S phase checkpoint is signalled at forks (Zhou et al., 2017). Uniquely, Pol ε is so far the only polymerase complex whose processivity rates have been observed to be dependent on a physical, stable interaction to the CMG, as removing Pol α's interaction through deletion of Ctf4 has little effect, at least *in vitro,* while a stable association between Pol δ and the helicase is yet to be observed (Yeeles et al., 2017). Current understanding of

the structure of these polymerases at the fork through electron microscopy appears to suggest that Pol ε is tightly associated with the CMG, which is understandable as it is directly bound via its Dpb2 subunit, and placed ahead of the helicase, which could implicate it playing roles in interacting either with the parental DNA or in fact with the chromatin that must be removed before local DNA can be replicated (Pellegrini and Costa, 2016). This is further exemplified by data obtained from cross-linking mass spectrometry and electron microscopy that showed the Pol2 C-terminus to also bind the CMG at its Mcm2 and -6 subunits, which is consistent with the observation that Pol ε uniquely stimulates helicase activity (Sun et al., 2015). However, what is not clear is whether its catalytic subunit is placed at the 'front' or the 'rear' of the helicase, resulting either in the nascent DNA having to loop round to reach the polymerase or if being fed straight into it, respectively (Sun et al., 2015, Pellegrini and Costa, 2016).

1.5.2 The Essential B Subunit, Dpb2

Dpb2, like the B subunits of Pol α and δ, Pol12 and Pol31 respectively, is a highly conserved, essential member of its polymerase complex, although its function had long remained elusive. Neither of Pol31 or Pol12 have a demonstrated enzymatic role in DNA replication, but fulfil essential structural roles of binding its other polymerase subunits, although the latter has been implicated in the elongation and capping of telomeres (Burgers and Gerik, 1998, Grossi et al., 2004). Mutational analysis had shown that alleles conferring temperature sensitivity induced high mutation rates following replication and this appeared to be caused by a disrupted interaction with the C-terminus of Pol2 (Jaszczur et al., 2009). This interaction was further characterised through the use of a lethal allele of *DPB2* containing two mutations in its C-terminus, *dpb2-200 (*a point and a nonsense mutation which truncated its last 5 residues). This revealed an uncharacterised binding motif within its C-terminus that resulted in the disruption of its interaction with Pol2's second Zn finger and that this was essential for viability (Isoz et al., 2012). The essential function of Dpb2 in DNA replication was found not long afterwards through study of its N-terminal domain. The work analysed this region, which had previously been

shown to bind Dpb11 and GINS subunit Psf1 by yeast-2-hybrid assays and implicated in origin firing, but especially focused on a highly conserved domain unique to the Pol ε B subunit contained within (Takayama et al., 2003). The interaction between Psf1 and Dpb2 was confirmed through immunoprecipitation and localised to the C-terminus of Psf1 and the N-terminal unique motif of Dpb2, and this was shown to be crucial in the formation of GINS but had no effect on Pol ε assembly (Sengupta et al., 2013). This underlined the importance of Dpb2 in forming the pre-LC that Pol ε forms a part of alongside Dpb11, Sld2 and GINS that is so crucial in the final step of CMG assembly at the origin (Muramatsu et al., 2010). The neat delineation of the N- and C-terminal binding domains was shown by the fact that the N-terminus alone was sufficient to form the CMG helicase at origins at levels similar to full-length Dpb2, however the replisomes that resulted did not have Pol ε integrated at the fork (Sengupta et al., 2013). Together, these results showed an essential role for Dpb2 in forming the replisome at forks during the process of origin firing through the actions of its N-terminus Additionally, it elucidated a crucial role for the C-terminus in bringing the leading strand polymerase to the fork and then maintaining this association as replication forks begin chromosome duplication (Sengupta et al., 2013).

While this role of Dpb2 in origin firing is very much clear, much like with Pol2 there are many other roles in the cell cycle it has been implicated in but with little understanding of possible mechanistic underpinnings. Connected with this is the phosphorylation of Dpb2 at the hands of both the G_1 and S phase CDK, which has also been the subject of research into a possible role in the regulation of the G1/S transition. It has been noted that mutating these phosphorylation sites, while not lethal in and of themselves, in conjunction with the *pol2-11* allele results in cell death (Kesti et al., 2004). While the simplest conclusion is that this phosphorylation could be an event that allows remodelling of the complex for it to potentiate efficient DNA synthesis, it has also been hypothesised that the fact these phosphorylation events are cell cycle specific, it could be involved in the Dpb2 signalling of the G_1/S-specific MBF transcription ‘switch‘ (Dmowski and Fijalkowska, 2017).

1.5.3 The Non-Essential Subunits: Dpb3 and Dpb4

The Dpb3 and -4 subunits of DNA polymerase ε are probably the least understood with regards to their function in replication, but, uniquely, they form parts of other protein complexes involved in DNA replication. Both of these proteins contain histone fold motifs and form a tightly bound heterodimer, binding to the C-terminus of Pol2 (Dua et al., 2000, Sun et al., 2015). When these are deleted *in vitro* little effect is noticed in the replication in mutation rates or fork progression, while *in vivo*, there is a significant increase in the mutation rates, to the extent that it resembles an exonuclease-null *POL2* mutant (Aksenova et al., 2010). A possible cause of this phenotype is that these subunits appear to stabilise the interaction between Pol ε and the template DNA; in their absence, Pol ε might show ineffective synthesis that leaves gaps behind forks as it replicates and reduced proof-reading by the holoenzyme (Aksenova et al., 2010). The subsequent filling in of these gaps by Pol ζ or Pol δ, is presumably error prone while functioning on the leading strand, therefore mis-incorporating DNA bases at these sites and giving rise to the increased mutation rates noticed in these mutants. Furthering the notion of the importance of these subunits in promoting the stability of Pol ε is the difference in phenotypes observed between *dpb4Δ* alone and its presence with mutants of other replisome component. Loss of Dpb4 engendered a slight temperature sensitivity as well as a mild growth defect of a slightly prolonged S phase (Ohya et al., 2000). However, in a genetic background of two separate Pol2 C-terminal mutants, *pol2-11* and *pol2-12,* this deletion proved lethal (Ohya et al., 2000). It can be concluded that Dpb4 could stabilise many of the interactions of Pol2 at its C-terminus, possibly including that with Dpb2, and what is being observed in these double mutants is a loss of interaction between the catalytic and B subunits in Pol ε.

Another widely held belief about these proteins is in their supposed roles in regulating chromatin during DNA replication, presumably through their aforementioned histone fold motifs that, predictably, are characterised by their ability to bind histones (Caretti et al., 1999). This characteristic of Dpb3 and -4 has implicated it in the inheritance of chromatin configurations

after replication (Iida and Araki, 2004). This work studied genes areas of chromatin proximal to telomeres that were prone to switching between euchromatic to heterochromatic states as these epigenetics were inherited after replication and the mechanisms through which cells dictated these switch events (Iida and Araki, 2004). Two separate complexes were found to work antagonistically in switching these chromatin regions to expressed and silenced states, and these were ISW2/yCHRAC and Pol ε, respectively. ISW2/yCHRAC contained a Dpb3-like subunit as well as Dpb4 and as a result, deletions of either of the non-essential subunits caused either more switching to euchromatic states in *dpb3Δ*, or increased occurrences of both switch events in *dpb4Δ* (Iida and Araki, 2004). While it is not unique for polymerase accessory subunits to function in other complexes, notably Pol δ's to fulfil essential roles in polymerase ζ, it is unusual for these to exist in ones that are so functionally distinct (Johnson et al., 2012). Notably, this effect on chromatin states was only present at the specific regions proximal to telomeres, so it is unclear how much of a role, if any, Dpb3 and -4 have at impacting epigenetics at the other heterochromatic sites like rDNA or mating type loci. Furthermore, Dpb3 and -4 have also been implicated in the deposition of recycling and deposition of nucleosomes at the fork during replication. Here, it appears that Dpb3-Dpb4 bind nucleosomes encountered at the fork and bias their recycling onto the leading, rather than lagging strand, therefore setting up heterochromatic transmission (Yu et al., 2018).

1.6 DNA Polymerase ε in other organisms

1.6.1 *Schizosaccharomyces pombe* Pol ε

The DNA polymerase ε complex found in fission yeast is structurally very similar to that seen in *S. cerevisiae*, formed from a heterotetrameric structure containing a catalytic subunit, Cdc20, an essential non-catalytic B subunit and two non-catalytic accessory subunits, the latter three of which are named identically to their orthologs in budding yeast. The structure of Cdc20 is also highly conserved from its budding yeast counterpart, as it contains the same N-terminal catalytic domain containing polymerase and

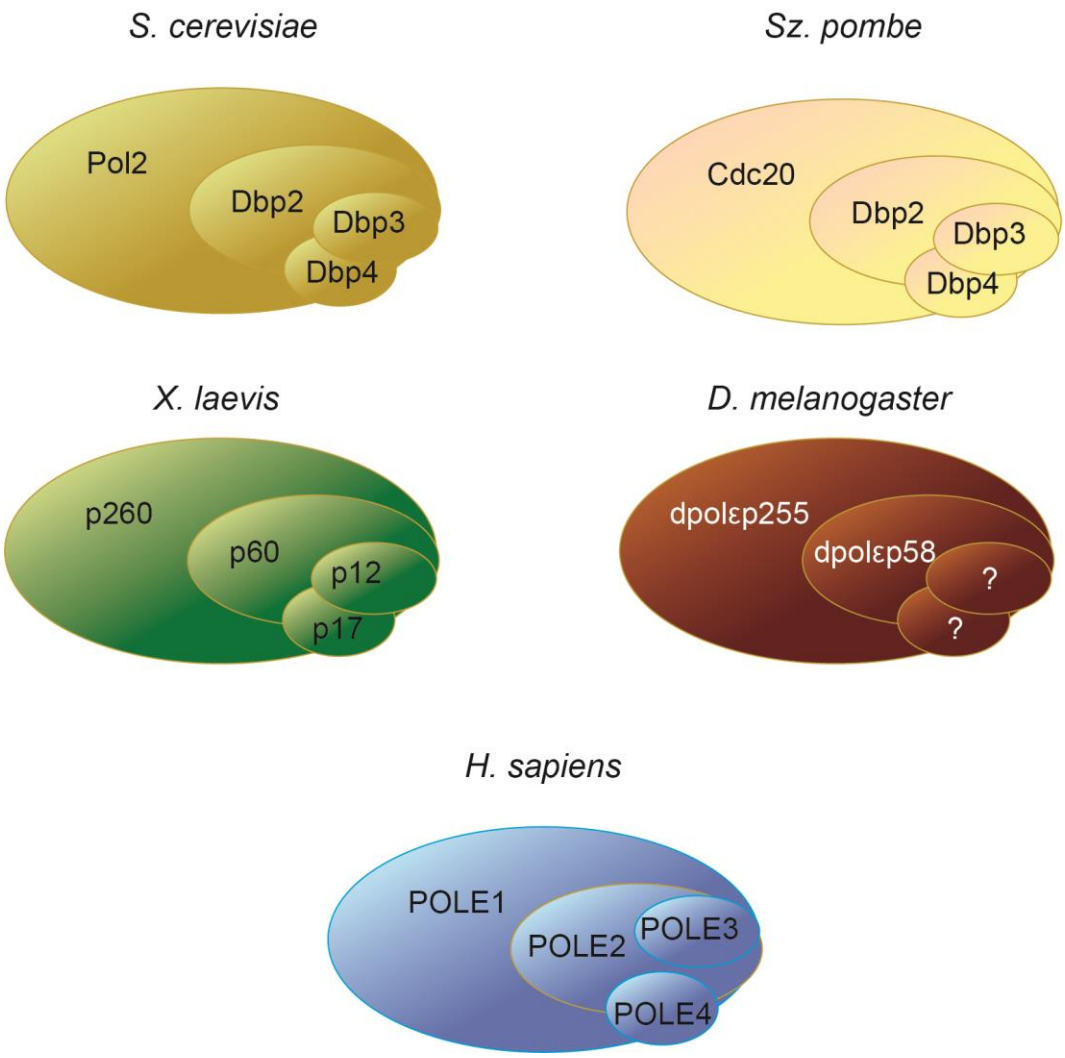

Figure 1.8: The structures of the DNA Polymerase ε complexes in *Saccharomyces cerevisiae*, *Schizosaccharomyces pombe*, *Xenopus laevis*, *Drosophila melanogaster* and *Homo sapiens*. For each holoenzyme, each subunit is labelled with its name, except for the *Drosophila* Pol ε complex. As yet, the small accessory subunits have not been identified, but it isn't believed that this is due to a different subunit configuration.

exonuclease domains coupled with the non-catalytic, zinc finger-containing C-terminus. Similar too is the disposable nature of the catalytic region of Cdc20, however, these cells do accumulate large amounts of DNA damage during replication and are dependent on the presence of this checkpoint for their repair and viability (Feng and D'Urso, 2001). Pol ε is also widely accepted to be the leading strand polymerase in the fission yeast replisome, and recent work mapping polymerase usage sequencing genome wide has

not only confirmed this but also the notion of Pol δ occasionally initiating this synthesis before being switched out by Pol ε (Daigaku et al., 2015).

Cdc20's C-terminus has been shown to be the essential part for its role in DNA replication, and this appears to be the conserved function in origin firing as identified in *S. cerevisiae*. In the same manner as budding yeast, the C-terminus of Cdc20 binds Dpb2 and this promotes the formation of the CMG at origins directly through GINS during DNA initiation (Handa et al., 2012). In addition to this, Pol ε appears to also have a direct role in stimulating the activity of the helicase, giving it a non-catalytic role in DNA replication as well, similar to what has been observed *in vitro* with the coupling of human Pol ε to a CMG helicase (Kang et al., 2012, Handa et al., 2012). While these C-terminal functions appear very similar to those observed in budding yeast, the main difference between the functions of these two polymerases is in their involvement in checkpoint signalling. In fission yeast, when various mutants of *CDC20* were generated, temperature sensitivity phenotypes were noted but the S phase checkpoint defects that are hallmarks of the *POL2* alleles were not exhibited (D'Urso and Nurse, 1997). Interestingly, when C-terminal mutations in loci corresponding to *pol2-11*, this proved lethal. It is worth noting, however, that while a checkpoint signalling function for a DNA polymerase is conserved, this instead appears to be a separate function carried out by Pol α (D'Urso et al., 1995).

Unusually in fission yeast Cdc20, Dpb2 and Dpb3 are all essential for viability, while Dpb4 remains dispensable (Spiga and D'Urso, 2004). When Dpb3 was removed, cells accumulated in S phase, possibly indicating an important role in fork progression (Spiga and D'Urso, 2004). The function of Dpb3 and Dpb4 have been studied and, similar to budding yeast, have also been shown to have roles in the maintenance of chromatin states after replication. Pol ε has long been implicated in the establishment of heterochromatin, which is found in centromeres, telomeres and mating type loci in fission yeast, as Cdc20 has been found to bind the CLCR complex during fork progression, which is responsible for the deposition of H3K9 methylation and histone hypoacetylation specifically at centromeric regions (Li et al., 2011). The histone fold motif observed in budding yeast is

conserved in *Sz. pombe* and through analysis of their crystal structure, these two proteins form a heterodimer resembling the H2A-H2B structures found in nucleosomes (He et al., 2017). Disruption of the formation of this heterodimer causes a loss of heterochromatin silencing throughout the many regions of the genome, instead of just at telomeres, as seen in budding yeast (He et al., 2017). Whether these findings of Pol ε's role in establishing silencing can be translated to higher eukaryotes, where chromatin states are used to differentiate gene expression between cell types is yet to be seen.

1.6.2 Pol ε in Higher Eukaryotes

In metazoa, less work has been carried out with respect to the exact functions and dynamics of Pol ε, owing to the increased complexity of their systems. In *X. laevis* and *Drosophila melanogaster*, however, important observations have been carried out that closely illustrates the high degree of conservation of function that exists between yeast and higher eukarya. In both of these organisms, these complexes are again heterotetramers formed of catalytic, B and accessory subunits (p260, p60, p12 and p17 in *Xenopus*, dpolεp255, dpolεp58, accessory subunits still uncharacterised in *Drosophila*) (Shikata et al., 2006). In *Xenopus*, the catalytic p260 subunit also has the conserved structure of a catalytic N-terminus with C-terminal zinc fingers and it serves as the hub upon which the other subunits bind, with p60 binding to the C-terminal motifs and p12 and p17 closer to the N-terminus (Shikata et al., 2006). As *Xenopus* studies are carried out in cell free environments, this means that instead of viability being used to assess the importance of a replication protein, instead its loss can be assessed by the effects upon replication dynamics. Here, limited replication can occur without Pol ε but with synthesis rates being enormously impacted as well as the accumulation of replication intermediates, this led to the hypothesis that possibly due to the larger genomes of higher eukaryotes, Pol δ was not simply able to fill in the role of, presumably, leading strand synthesis (Waga et al., 2001). This could explain why, when using this system, a catalytic dead mutant (either by deletion or point mutation) of p260 was unable to achieve replication rates that could sustain viability for a cell, meaning that its catalytic activity becomes essential in *Xenopus* (Shikata et al., 2006).

Tentative initial experiments have also sought to interrogate whether the division of labour of the processive polymerases at the fork is conserved in *Xenopus.* These experiments separately depleted Pol ε and δ and analysed how elongation was affected (Fukui et al., 2004). The results showed that elongation defects were far more pronounced in the absence of Pol δ, which is consistent with what is observed in other organisms that lagging strand synthesis is unable to be compensated by the presence of Pol ε (Fukui et al., 2004). It was also observed that initiation was unaffected by depletion of either polymerase, although this was measured by protein depletion, leaving open the possibility that low amount of Pol ε might allow origin firing in these cell extracts (Fukui et al., 2004). The conservation of this interaction illustrates the similarity of *Xenopus* Pol ε to those found in yeast, and gives little reason to assume that it is not also primarily the leading strand polymerase in this enzyme.

In *Drosophila*, while even less progress has been made in understanding this complex as a whole, some interesting discoveries have been made about the catalytic and B subunits that lead us to believe that many of the complex's features in yeast are conserved in multicellular eukaryotes. Most strikingly is the essential nature of the non-catalytic C-terminus of dpolεp255, which was illustrated in a knockdown experiment in the eye disc. Illustrating once again the high level of conservation of Pol2, dpolεp255 too contains a catalytic N-terminus with exonuclease and polymerase domains as well as a C-terminus with two zinc fingers although with an ATPase or ATP binding site just upstream of these (Suyari et al., 2012). In an experiment isolated to the cells present in the eye disc, the endogenous dpolεp255 was knocked down via RNAi followed by expression of the C-terminus of the catalytic subunit and measured the formation of clusters of cells in the eye disc (Suyari et al., 2012). Remarkably, expression of the C-terminus near fully restored the loss of viability and rescued the replication defects that occurred from the knockdown (Suyari et al., 2012). Interestingly, this finding was not universal for somatic cells in the fly when this same experiment was carried out in cells within the salivary gland. It is believed that the higher levels of endoreplication, that is multiple S phases

without cell division, within these cells meant that the Pol δ was simply not able to compensate its absence (Suyari et al., 2012). Genetic interactions were also detected with dpolεp255, with many of these pointing to associations with both chromatin remodelling and replication initiation, both of which are well known and characterised associations noted in Pol ε in fission and budding yeast, respectively, although little follow-up work has been completed on this front (Suyari et al., 2012). dpolεp58 was also the subject of study, due to little being known about the function of the polymerase B subunit within a multicellular organism. This was found to be essential in either S phase initiation and progression and also had a genetic interaction with ORC2 (Sahashi et al., 2013). It was suggested that this could have been analogous to the Pol ε-GINS interaction in yeast during origin firing, although this seems to be speculative.

1.6.3 Human Pol ε

The human DNA polymerase ε complex is also a heterotetramer comprised of the PolE1 (also known as p261) catalytic subunit, p59 B subunit and p12 and p17 accessory subunits. Conventionally, the catalytic N-terminus and structural C-terminus is conserved in human PolE1 too, with its B-subunit also binding to the zinc finger motifs present at its very periphery, while p12 and p17 heterodimer bind somewhat more centrally in the protein like in *Xenopus* (Tahirov et al., 2009). Unfortunately, because the less prescriptive nature of origins in humans makes the study of DNA initiation difficult, it is not clear whether PolE1 plays the same conserved role in origin firing. However, it has been shown to interact and be stimulated by the CMG component GINS, which could indicate a conservation of the Psf1-Dpb2 interaction that is so crucial in the essential origin firing activity of Pol ε in budding yeast (Bermudez et al., 2011). While crystal structures have been solved for PolE1-p59 interaction, it is still unknown what its N-terminal binding partner is (Baranovskiy et al., 2017). Interestingly, the EM structure of human GINS overlaps remarkably well with that seen in budding yeast, including the flexibility of the Psf1 subunit, indicating its interaction with another replisome component (Sun et al., 2015).

PolE1 also has a strong resemblance to the budding yeast Pol ε complex, as it has been implicated in DNA repair (Moiseeva et al., 2016). Two separate, very early *in vitro* studies illustrated first that Pol ε co-purified as part of a larger complex that mediated homologous recombination in response to double strand breaks, and then that it was proficient in performing the gap-filling synthesis required after nucleotide excision repair alongside RPA, RFC, PCNA and DNA ligase (Jessberger et al., 1993, Shivji et al., 1995). Furthermore, the PolE1 C-terminus has also been found to interact with, and be stimulated *in vitro* by*,* Mdm2, the E3 ubiquitin ligase that targets the main tumour suppressor p53, and therefore being responsible for cell cycle regulation as well as DNA repair (Asahara et al., 2003). It is hypothesised that Mdm2 could function to aid the transition of Pol ε reconfiguring from a replicative complex to one that repairs DNA, which could involve remodelling the protein composition at this site (Asahara et al., 2003). More recently, it was demonstrated that PolE1 undergoes phosphorylation in its C-terminus in response to DNA damage, which was found to disrupt the binding of it to MMS19, a protein involved in Fe/S cluster assembly (Moiseeva et al., 2016). While the modification of PolE1 in response to damage is no doubt interesting, it is very unclear what this phosphorylation could signify, as its abrogation does not entail greater sensitivities to DNA damaging agents, and neither is it understood what the relevance of an assembly of an iron sulphur complex at the polymerase could be (Moiseeva et al., 2016). Interestingly, while the C-terminus of PolE1 shares the same B subunit binding activities seen in other eukarya, its expression is not able to suppress the deletion of the whole gene (Bermudez et al., 2011). This could indicate a greater need for the full catalytic activity of Pol ε in maintaining cell viability due to the size of the genome.

Owing to its essential nature as one of the major processive polymerase, genetic disorders arising from mutations in PolE1 are extremely rare, although they do exist, as frequently, genetic disruptions simply would result in death. Two diseases have been linked to haploinsufficiencies of the PolE1 subunit, but each of these present with rather different phenotypes. One of these was discovered in 11 relatives, all of whom exhibited mild facial

dysmorphism, immunodeficiency, livedo, and short stature (known as FILS syndrome) which was pinpointed to a homozygous single nucleotide polymorphism in the intron of *POLE1*, which causes an alternative splice product that results in 90% of the resulting transcripts to be missing exon 34 (Pachlopnik Schmid et al., 2012). Interestingly, the sufferers of this syndrome did not report higher levels of cancer susceptibility, but their *POLE1* insufficiency restricted the ability of numerous cell types to enter S phase and begin proliferation, which appeared to specifically affect the lymphocytes and osteoblasts, which would explain the immunodeficiency and problems relating to stature (Pachlopnik Schmid et al., 2012). Interestingly, another patient outside of this initial family case study was also diagnosed with the exact same causative mutation, albeit with much more severe phenotypes (Thiffault et al., 2015). This variability in symptom preservation was assumed to be the result of possible interactions between this haploinsufficiency with a pre-existing fault in the mismatch repair pathway, thus creating a much more severe phenotype (Thiffault et al., 2015). Moreover, a parallel study in mice and humans illustrated that knockout of the Dpb4 ortholog in mice destabilised the entirety of the complex and this caused growth defects as well as defective B and T cell maturation, similar to those noted in FILS and related syndromes (Bellelli et al., 2018). Furthermore, at a cellular level, this loss of Pol ε caused defects in origin firing, replicative damage and genetic instability and remarkably, many of these were found to also be present in patient cells containing PolE1 mutations (Bellelli et al., 2018). This work simultaneously illustrates the heightened structural importance of the smaller accessory subunits in the mammalian Pol ε complex as well as hinting that the checkpoint and origin firing activities observed in budding yeast possibly being conserved through to humans.

Mutations in PolE1 have also been identified as germline mutations which can give rise to many cancer predispositions, including colorectal tumours (Palles et al., 2013). These mutations are localised to the exonuclease ‘proof-reading’ domain in the N-terminus of PolE1, which is consistent with the necessity of inherent genome instability that is crucial in

the survival and evolution of cancer cells (Palles et al., 2013). More recently, mutations targeted in this exonuclease domain have also been characterised as an early feature of carcinogenesis in somatic endometrial and colorectal tumours (Temko et al., 2018). These mutations appeared before the tumours had become malignant, but their presence appeared to induce the genetic instability that then allowed subsequent driver mutations to arise, with many of these appearing to arise as a direct result of this impaired proof-reading mechanism (Temko et al., 2018). Furthermore, genetic screenings of PolE1 in colorectal cancer cell lines has identified that proof-reading mutations appear to emerge as a result an independent defect in mismatch repair, and together these produce high levels of genome instability for transformation (Yoshida et al., 2011). Another study sought to characterise several exonuclease mutants, and assess how these mutations affected tumourigenesis (Barbari et al., 2018). Interestingly, many of these mutants exhibited stronger mutator phenotypes than those observed in cells where the exonuclease domain has been removed completely, indicating that in order to drive the genome instability to push tumourigenesis, the function of PolE1 is affected in additional, unknown ways to this defective proof-reading (Barbari et al., 2018). Very few, if any mutations appear to have been mapped to the C-terminus of PolE1, but having seen its conserved importance throughout many eukaryotic organisms, this is unsurprising as disrupting this region would more than likely inhibit replication initiation in the cell and be lethal as a result.

1.7 Aims for the Thesis

My aims for this thesis are to broaden our understanding of the multi-faceted role of Pol ε in DNA replication and in order to do this I have sought to answer two questions. The first of these was to further characterise the nature of the essential C-terminus of Pol2. While this has already been well characterised in its ability to bind Dpb2 and therefore assist in fulfilling Pol ε's essential role in origin firing, I seek to find out if this also has a wider role during replication. I have therefore generated constructs of a short 236 residue Pol2 C-terminal fragment which contains the two proximal zinc

fingers. I will express this alongside a truncation mutant, *pol2-11*, which contains many of the characteristic C-terminal defects and observe whether these can be suppressed by the expression of the fragment. Through this work, I seek to try to pinpoint the feature or features that underpin the essential function of the Pol2 C-terminus.

Another aspect of this project has been to focus on the proposed role Pol ε plays in checkpoint signalling. While Pol2 is a known interactor with many mediators of the S phase checkpoint, some of the best evidence for this function has been provided by the severe checkpoint defects exhibited by its C-terminal mutants. However, with the knowledge that this same region of the protein is important in origin firing, this presents the possibility that the observed checkpoint defects are in fact due to reduced numbers of replication forks. I have therefore coupled *pol2-11* with a system that significantly increases the levels of origin firing in the cell. By doing so, I will be able to delineate any checkpoint defect present in *pol2-11* from one in origin firing and therefore gain a better understanding of the protein's role in checkpoint signalling.

Chapter 2: Materials and Methods

2.1 Yeast Culturing Methods

2.1.1 Media Preparation for Cell Culturing

Yeast cells can either be grown in liquid or solid medium, which are constituted of the same material, save for the addition of agar in the latter. Strains were stored at -80°C a 25% glycerol solution in a 2mL cryogenic vial (Corning) and stored until needed. Cultures were initiated by streaking a small amount of this mixture on a solid medium and grown in an incubator at 24°C. From their growth on agar plates, these colonies could then be inoculated in liquid medium for use in transformations, cell cycle experiments, genomic extraction or harvesting of cells for an immunoprecipitation. Because cells were derived from W303-1a, they contained the alleles: *ade2-1, ura3-1, his3-11,15 trp1-1, leu2-3,112, can1-100* and *rad5*-535. This allowed the transformation of DNA substrates conjugated to reporter genes that repaired the amino acid producing alleles inherent to the strain. This rendered the transformants prototrophic for biosynthesis of these amino acids and could be grown in amino acid-deficient selective media where this was excluded. Transformation constructs could also be conjugated to *hphNT* or *kanMX* cassettes, which permitted growth in selective yeast extract peptone dextrose (YPD) media containing either HygromycinB ((Hygromycin B Gold™, InvivoGen) or Geneticin (Invitrogen). Rapid sporulation medium (RSM) plates were used as media for diploid cells, inducing meiosis and allowing tetrad dissection to obtain haploids.

Table 2.1: A table containing the composition of the various media used for cell culturing in this study

Media	Recipe
YPD	1% (w/v) yeast extract (Bacto) 2% (w/v) peptone (Oxoid) 2% (w/v) glucose (can be raffinose or galactose) (Can be optionally supplemented with 25-200mM HU (Sigma) or 0.005-0.033% MMS (Sigma)) For solid agar medium: 2% (w/v) Formedium agar For selectivity, can be supplemented with 0.2 mg/ml Geneticin (G418) (Invitrogen) or 0.3 mg/ml HygromycinB (Hygromycin B Gold, InvivoGen)
Amino Acid-Deficient Selective Medium	0.17% (w/v) yeast nitrogen base (Difco) 0.5% (w/v) NH_4SO_4 0.2% (w/v) glucose 0.2% (w/v) Kaiser SC single Drop-out (Formedium) For solid agar medium: 2% (w/v) Formedium agar
RSM Medium	0.25% (w/v) yeast extract (Bacto) 1.5% (w/v) K(C2H3CO2) 0.1% (w/v) glucose (can be raffinose or galactose) 2.5% (v/v) amino acid mix
Lysogeny broth (LB)	1% (w/v) bacto-tryptone 0.5% (w/v) yeast extract (Bacto) 1% (w/) NaCl pH 7.0 For solid agar medium: 2% (w/v) agar (Formedium) For selectivity, can be supplemented with 100 µg/ml ampicillin or 50 µg/ml kanamycin.
SOC Medium	2% (w/v) tryptone 0.5% (w/v) yeast extract 10 mM NaCl 2.5 mM KCl 10 mM MgCl2 10 mm MgSO4 pH 6.8-7.0 20 mM glucose (added prior to use)

Amino Acid Mix	0.4% (w/v) adenine 0.2% (w/v) arginine 0.4% (w/v) histidine 0.2% (w/v) leucine 0.2% (w/v) lysine 0.2% (w/v) methionine 1% (w/v) phenylalanine 0.2% (w/w) tryptophan 0.08% (w/w) tyrosine

2.1.2 Mating Type Checking of Haploids and Storage of Yeast Strains

The mating type of budding yeast is a crucial tool in the study of the cell cycle. When haploid strains are exposed to a mating pheromone of the opposite mating type, get ready to mate by arresting in G_1 and undergoing morphological changes which manifests as a protrusion known as a ‘shmoo’. Haploid yeast can be one of two mating types: mate A (MATa) or mate α (MATα), and each produce to their own mating pheromone, termed A and α factor. The use of these mating factors in a cell cycle experiment permits us to arrest a whole population of haploid cells in G_1, thus allowing them to be released in a synchronised manner into S phase and beyond. In order to check the mating type of haploid strains, cells were inoculated overnight in 5mL YPD in a shaking incubator at 24°C. The following day, 200µL was diluted to 1.2mL with fresh YPD and α factor was added to a final concentration of 7.5µg/mL and left shaking for at least 3 hours. After this time had elapsed, these cultures were viewed under a microscope to check their morphology. If cells presented with long protusions (termed ‘shmoos’), they were typed as MATa, whereas if they were unaffected, as MATα.

2.1.3 Yeast Crossing

To cross yeast cells of differing genotype, two haploid strains are required of opposite mating type. In advance of crossing, they must be streaked onto YPD agar plates 2-3 days in advance from their 25% glycerol stocks stored at -80°C. 2-3 colonies of the strain with the fewest markers was resuspended in 250µL sterile water, followed by the addition of a fraction of

that amount of the other strain. These were vortexed vigorously for several seconds, before 100µL was spotted on a YPD plate and left to dry, then to grow at 24°C overnight. The following day, this spot was then streaked onto a medium selective for one of the markers present in the minority strain and not in the majority in order to select for diploids and left overnight to grow at 24°C. Individual colonies on the selective medium was then streaked onto an RSM plate to sporulate for 3-5 days at 30°C. When enough asci were visible from the streaks on the RSM plate, they were treated with β-glucoronidase from *Helix pomatia* (Sigma) for 30 minutes to digest the ascus, followed by tetrad dissection on a YPD plate using a Singer MSM400. Desired strains were then selected for by replica plating onto the various selective media.

2.1.4 Transformation of Yeast Strains

Strains to be transformed were inoculated in liquid YPD medium the night before the transformation. The following day they were counted and diluted to $0.5x10^7$ in a volume calculated from which 10^8 cells could be collected for each transformation. These were left to grow for 2 hours to reach a cell density of $1x10^7$. These were then washed in sterile water and resuspended in a solution of 0.1M lithium acetate and 1M Tris-HCl (both pH 7.5) to a final cell density of $2x10^9$. 50µL of this cell suspension (10^8 cells) was then added to a 10µL volume containing 1-2µg of the chosen DNA sample to be transformed (this could be a digested plasmid or integrating PCR product) with 500µg of freshly denatured carrier ssDNA (extracted from salmon sperm) and mixed via tapping and vortexing. 40% PEG 4000 in 0.1 M lithium acetate (pH 7.5) 1 M Tris-HCl (pH 7.5) was added to a final concentration of 33.3% (w/v) PEG and vortexed vigorously to mix. This was then incubated for 40 minutes at 24°C on a rotating wheel before adding sterile DMSO to a final concentration of 10% and heat-shocking at 42°C for 15 minutes. Immediately after this, the tubes were quickly placed on ice for 2 minutes, followed by centrifugation and supernatant removal. If the marker of the transformation product was autotrophic, the pellet was resuspended in sterile TE pH7.5 and plated in appropriate volumes to generate separate, single colonies on the required selective media. If the transformation involves markers antibiotic resistance, like *kanMX* or *hphNT*, then the pellet is

resuspended in non-selective YPD and incubated on a rotating wheel at 24°C for at least 3 hours to allow expression of the antibiotic resistance gene, prior to being plated on appropriate selective plates.

2.1.5 Dilution Spotting

Strains to be used were streaked onto YPD plates from their 25% glycerol suspensions stored at -80°C three days before being used in this experiment and left at 24°C to grow. YP agar plates of different compositions, including the type of sugar used as well as the presence of any genotoxic compounds like MMS or HU, were poured into square 100mm plates (Sterilin). Cells were then resuspended in 1mL sterile water and counted. These suspensions were then diluted to concentrations of $0.5x10^6$, $0.5x10^5$, $0.5x10^4$ and $0.5x10^3$ in sterile water. 10µL of each resuspension from each strain was then spotted onto the plates in a line and plates were left to dry before being left to grow in an incubator at different temperatures. After 48 hours and every 24 hours subsequently, plates were scanned at 800dpi in 8-bit greyscale using an Epson V700 scanner and saved as a TIFF.

2.1.6 Generation of Yeast Cultures for Subsequent FACS/TCA Sample Preparation

For these experiments, colonies were inoculated in YP media and left to grow overnight in a shaking incubator at 24°C. On the day of the experiment, cells were diluted to the required volume of the experiment at a final cell density of $0.3\text{-}0.4x10^7$, depending on the fitness of the cells. These cells were left to grow for 90-120 minutes until a cell density of $0.7\text{-}0.9x10^7$ cells/mL was reached. Samples taken here are asynchronous and following this, α factor was added to a final concentration of 7.5µg/mL for at least 3 hours. The addition of α factor arrests MATa haploids in G_1, thus synchronizing the culture. In experiments where galactose-inducible expression of proteins were used, cells were inoculated overnight in YP supplemented with raffinose, while they were switched to galactose-supplemented medium for 40 minutes still in the presence of α factor after they were arrested in G_1. The rest of the experiment was performed with

galactose-supplemented media. If an S phase was being studied, cells were centrifuged at 3000rpm for 3 minutes and washed three times, each with a quarter of the original volume of fresh medium, followed by resuspension in fresh media. If the cultures were to be exposed to HU or MMS first, the cells were washed, as before, 3 times in fresh media before being resuspended in YP containing 0.2M HU or 0.033% MMS. Following this exposure, if samples were required to analyse the ensuing S phase, cells were washed as before and resuspended in fresh media. If cells were required to be arrested in G_2, DMSO-resuspended benomyl was added to YP at a concentration of 10µg/mL and boiled. When the solution had cooled to room temperature, nocodazole was added to 15µg/mL. When cells reached the logarithmic growth phase, they were centrifuged and resuspended in this media and left to arrest for at least 3 hours.

For fluorescence activated cell sorting (FACS) analysis, aliquots of 1mL (containing roughly 10^7 cells) were taken at the required timepoint and spun down. The supernatant was then removed and the cells were resuspended and fixed in 70% ethanol. At this point the samples were stored at 4°C until needed for processing. For samples to be prepared for trichloroacetic acid (TCA) protein precipitation, 10mL of sample was taken at the required timepoint and centrifuged for 3 minutes at 3000rpm at 4°C. The supernatant was removed and the pellet washed once with 1mL of cold, sterile water. The cells spun down at 20,000*g* for 1 minute, with the supernatant removed and the pellet resuspended in 300µL 20% TCA and stored at -20°C until their preparation.

2.1.7 Preparation of Yeast Cultures for Immunoprecipitation

A pre-inoculum was generated the day before the cell harvesting takes place, where several colonies of cells from each strain used were resuspended in a quarter the volume of YP media that used in the next day's experiment and left in a shaking incubator at 24°C overnight. For immunoprecipitation experiments, YP media is supplemented with 2.5µg/mL adenine. On the day of experiment, this pre-inoculum was counted and cells were diluted to a volume required for the experiment (250mL per sample for

dilute popcorn, 1L for concentrated) at a final cell density of 0.3-0.4x10^7, depending on the sickness of the cells. They were then left to grow for two hours and counted until a cell density of 0.7-0.9x10^7 cells/mL was reached. For S phase samples, cells were arrested with α factor, at a concentration of 7.5μg/ml, and then harvested 30 minutes after releasing from G_1. While for HU samples, arrested cells were resuspended and washed three times with fresh medium, before being released into media supplemented with 0.2M HU, before samples being taken at timepoints into this exposure that are stated in each experiment. If proteins under the control of galactose-inducible promoters were used and samples were required at specific stages of the cell cycle, cultures were grown overnight and in the initial stages of the experiments in YP supplemented with raffinose, and after the G_1 arrest, cells were switched to galactose-supplemented media for 40 minutes still in the presence of α factor. Galactose-supplemented media was then used for each stage for the rest of the experiment. In the GST-6His immunoprecipitation experiments, asynchronous samples were required with expression of the galactose-induced protein, so cells were switched to galactose-supplemented media after reaching the logarithmic growth phase and left a further 4 hours to ensure maximum recovery of the protein.

To harvest cells used for immunoprecipitation of TAP- or FLAG-tagged proteins, cultures were pelleted by a centrifugation of 3000rpm for 3 minutes and washed twice with 20mM HEPES-KOH pH7.9, followed by a wash of 100mM HEPES-KOH ph7.9, 100mM KOAc, 10mM MgOAc, 2mM EDTA. For dilute popcorn samples, after centrifugation the pellet was resuspended in a volume three times its mass with 100mM HEPES-KOH ph7.9, 100mM KOAc, 10mM MgOAc, 2mM EDTA supplemented with 2 mM glycerophosphate (Johnson Matthey), 2 mM NaF (Fisher), 1 mM DTT, 1% (v/v) Sigma protease inhibitor cocktail (for fungal and yeast extracts, Sigma) and 0.24% (w/v) EDTA-free Complete Protease Inhibitor Cocktail (Roche). For concentrated samples, the pellet is instead resuspended in a volume a quarter of its mass with 100mM HEPES-KOH ph7.9, 100mM KOAc, 10mM MgOAc, 2mM EDTA supplemented with 8 mM glycerophosphate, 8 mM NaF, 1 mM DTT, 4% (v/v) Sigma protease inhibitor cocktail (for fungal and yeast

extracts) and 0.48% (w/v) EDTA-free Complete Protease Inhibitor Cocktail. These suspensions were then snap-frozen by being pipetted drop-wise into liquid nitrogen. After evaporation of the liquid nitrogen, this 'popcorn' was stored at -80°C until needed for the immunoprecipitation. If samples were to be used in immunoprecipitations at different stringencies, the KOAc concentration in these buffers was altered to those stated in that experiment.

To harvest cells used for immunoprecipitation of GST-6His-tagged proteins, cultures were pelleted by a centrifugation of 3000rpm for 3 minutes and washed twice with 20mM Tris-HCl pH8.0, followed by a wash of 50mM Tris-HCl ph8.0, 50mM NaCl, 10mM $MgCl_2$, 2mM EDTA, 20mM Imidazole and 5mM β-mercaptoethanol. The pellet was then weighed and resuspended in in a volume a quarter of its mass with 50mM Tris-HCl ph8.0, 50mM NaCl, 10mM $MgCl_2$, 2mM EDTA, 20mM Imidazole and 5mM β-mercaptoethanol supplemented with 8 mM glycerophosphate, 8 mM NaF, 4% (v/v) Sigma protease inhibitor cocktail (for fungal and yeast extracts) and 0.48% (w/v) EDTA-free Complete Protease Inhibitor Cocktail. These suspensions were then snap-frozen by being pipetted drop-wise into liquid nitrogen. After evaporation of the liquid nitrogen, this 'popcorn' was stored at -80°C until needed for the immunoprecipitation.

2.1.8 List of Strains Used in this Study

Table 2.2: A table containing the yeast strains used in this study. This is ordered by strain number and each's genotype is listed, including their mating type, denoted by 'MAT'. All strains are derived from W303-1a, which contains the alleles: *ade2-1, ura3-1, his3-11,15 trp1-1, leu2-3,112, can1-100 and rad5-535*.

STRAIN NO.	GENOTYPE	SOURCE
CS 1	*MATa*	Lab Collection
CS 6	*MATα*	Lab Collection
CS 74	*MATa, pep4Δ::ADE2*	Lab Collection
CS 699	*MATa, Mms21-5FLAG (hphNT), pep4Δ::ADE2, Gal-TAP-NLS (URA3)*	Lab Collection
CS 700	*MATa, Mms21-5FLAG (hphNT), pep4Δ::ADE2, Gal-TAP-NLS-Pol2 (1986-2222) (URA3)*	Lab Collection

CS 722	*MATa, rad24Δ (hphNT)*	Lab Collection
CS 1159	*MATa, pol2-11, ufd4Δ::URA3CP*	Lab Collection
CS 1160	*MATα, pol2-11, ufd4Δ::URA3CP*	Lab Collection
CS 1162	*MATa, pol2-11, Mcm4-5FLAG-9his (hphNT), ufd4Δ::URA3CP, pep4Δ::ADE2*	Lab Collection
CS 1164	*MATa, Mcm4-5FLAG-9his (hphNT), ufd4Δ::URA3CP, pep4Δ::ADE2*	Lab Collection
CS 1166	*MATa, Mcm4-5FLAG-9his (hphNT), pep4Δ::ADE2*	Lab Collection
CS 1167	*MATα, mrc1Δ (hphNT)*	Lab Collection
CS 1213	*MATa, rad9Δ (HIS3)*	Lab Collection
CS 1214	*MATα, rad9Δ (HIS3)*	Lab Collection
CS 1463	*MATa, pol2-11, ufd4Δ::URA3CP, Gal-TAP-NLS (URA3)*	Lab Collection
CS 1465	*MATa, pol2-11, ufd4Δ::URA3CP, Gal-TAP-NLS-Pol2 (1986-2222) (URA3)*	Lab Collection
CS 1467	*MATa, dpb3Δ (kanMX), dpb4Δ (kanMX)*	Lab Collection
CS 1476	*MATa, pol2-11, ufd4Δ::URA3CP, pep4Δ::ADE2, Gal-TAP-NLS (URA3)*	Lab Collection
CS 1478	*MATa, pol2-11, ufd4Δ::URA3CP, pep4Δ::ADE2, Gal-TAP-NLS-Pol2 (1986-2222) (URA3)*	Lab Collection
CS 1922	*MATa, pol2-11, ufd4Δ::URA3CP, Gal-TAP-NLS-Pol3(1-999)/Pol2(1986-2222) (URA3)*	This study
CS 2099	*MATa, pol2-11, ufd4Δ::URA3CP, GAL-TAP-Pol2 (2103-2222) (Leu)*	This study
CS 2101	*MATa, pol2-11, ufd4Δ::URA3CP, GAL-TAP-Pol2 (2162-2222) (Leu)*	This study
CS 2105	*MATa, pol2-11, ufd4Δ::URA3CP, GAL-TAP-Pol2 (2103-2222) (Mutant B: C2164S, C2167S) (Leu)*	This study
CS 2111	*MATa, pol2-11, ufd4Δ::URA3CP, GAL-TAP-Pol2 (2103-2222) (Mutant B C2164S C2167S) (Leu)*	This study
CS 2126	*MATa, trp1::Sld2-PGAL1-10-Dpb11::TRP1, ura3::Sld3-PGAL1-10-Dbf4::URA3, leu2::Sld7-PGAL1-10-Cdc45::LEU2*	Zegerman Lab
CS 2166	*MATa, pol2-11, ufd4Δ::URA3CP, Gal-TAP-NLS-PolE1 (2082-2286) (Leu)*	This study
CS 2168	*MATa, pol2-11, ufd4Δ::URA3CP, Gal-TAP-NLS-PolE1 (2153-2286) (Leu)*	This study

CS 2178	*MATa sld3-7 (KanMX), pol2-11, ufd4Δ::URA3CP, GAL-UBR1 (His), GAL-TAP-NLS (Ura) mms21-5FLAG (hphNT)*	This study
CS 2179	*MATa sld3-7 (KanMX), pol2-11, ufd4Δ::URA3CP, GAL-UBR1 (His), GAL-TAP-NLS-Pol2(1986-2222) (Ura) mms21-5FLAG (hphNT)*	This study
CS 2180	*MATa, pol2-11, ufd4Δ::URA3CP, GAL-UBR1 (His), GAL-TAP-NLS (Ura) mms21-5FLAG (hphNT)*	This study
CS 2181	*MATa, pol2-11, ufd4Δ::URA3CP, GAL-UBR1 (His), GAL-TAP-NLS-Pol2(1986-2222) (Ura) mms21-5FLAG (hphNT)*	This study
CS 2182	*MATa sld3-7 (KanMX), ufd4Δ::URA3CP, GAL-UBR1 (His), GAL-TAP-NLS (Ura) mms21-5FLAG (hphNT)*	This study
CS 2183	*MATa sld3-7 (KanMX), ufd4Δ::URA3CP, GAL-UBR1 (His), GAL-TAP-NLS-Pol2(1986-2222) (Ura) mms21-5FLAG (hphNT)*	This study
CS 2189	*MATa, Mcm4-5FLAG (hphNT), pol2-11, ufd4Δ::URA3CP, pep4Δ::ADE2, GAL-3HA-NLS (Trp)*	This study
CS 2191	*MATa, Mcm4-5FLAG (hphNT), pol2-11, ufd4Δ::URA3CP, pep4Δ::ADE2, GAL-3HA-NLS-Pol2(1986-2222) (Trp)*	This study
CS 2308	*pol2 mutant E (L2198A, F2201A, V2204A, L2213A, I2217A) (KanMX)*	This study
CS 2343	*MATa, pol2 mutant E (KanMX), mrc1Δ (hphNT)*	This study
CS 2345	*MATa, pol2 mutant E (KanMX), Mcm4-5FLAG (hphNT), pep4Δ::ADE2*	This study
CS 2347	*MATa, pol2 mutant E (KanMX), rad9Δ (his3MX)*	This study
CS 2379	*MATa, pol2-11, mms21-5FLAG (hphnt), ufd4Δ::URA3CP, Rad9Δ (HIS), GAL-TAP-NLS (URA)*	This study
CS 2381	*MATa, pol2-11, mms21-5FLAG (hphnt), ufd4Δ::URA3CP, Rad9Δ (HIS), GAL-TAP-NLS-Pol2(1986-2222) (URA)*	This study
CS 2485	*MATa, pol2-11, Mcm4-5FLAG (hphNT), , Sdl2::GAL::Dpb11 (Trp), Sld3::GAL::Dbf4 (Ura3), Sld7::GAL::Cdc45 (Leu2), ufd4Δ::URA3CP, pep4Δ::ADE2*	This study
CS 2555	*MATa, Mcm4-5FLAG (hphNT), , Sdl2::GAL::Dpb11 (Trp), Sld3::GAL::Dbf4 (Ura3), Sld7::GAL::Cdc45 (Leu2), ufd4Δ::URA3CP, pep4Δ::ADE2*	This study
CS 2742	*MATa, sld2Δ (Leu2), sld2-6 (Trp)*	Araki Lab
CS 2724	*MATa, pol2 mutant E (KanMX), cdc7-1*	This study
CS 2725	*MATa, pol2 mutant E (KanMX), dpb11-1*	This study
CS 2748	*MATa, GAL-GST-6His-Pol2(1986-2222), pep4Δ::ADE2*	This study

CS 2750	*MATa, pol2 mutant E (KanMX), sld3-5*	This study
CS 2752	*MATa, sld2Δ (Leu2), sld2-6 (Trp), pol2 mutant E (KanMX)*	This study
CS 2942	*MATa, mcm10-1 (KanMX), GAL-UBR1 (His3)*	This study
CS 2943	*MATa, mcm10-1 (KanMX), GAL-UBR1 (His3), pol2 mutant E (KanMX)*	This study
CS 2944	*MATa, GAL-GST-6His, pep4Δ::ADE2*	This study
CS 3037	*MATa, Mcm3-TAP (KanMX), GAL-UBR1 (His3), pep4Δ::ADE2*	This study
CS 3039	*MATa, Mcm3-TAP (KanMX), GAL-UBR1 (His3), mcm10-1 (KanMX), pep4Δ::ADE2*	This study
CS 3041	*MATa, Mcm3-TAP (KanMX), GAL-UBR1 (His3), pol2 mutant E (KanMX), pep4Δ::ADE2*	This study
CS 3043	*MATa, Mcm3-TAP (KanMX), GAL-UBR1 (His3), mcm10-1 (KanMX), pol2 mutant E (KanMX), pep4Δ::ADE2*	This study
CS 3192	*pol2 mutant E(E) (L2198E, F2201E, V2204E, L2213E, I2217E) (KanMX)*	This study
CS 3261	*MATa, pol2 mutant E(E) (KanMX), mrc1Δ (hphNT)*	This study
CS 3263	*MATa, pol2 mutant E(E) (KanMX), radΔ (his3MX)*	This study
CS 3265	*MATa, pol2 mutant E(E) (KanMX), mcm10-1 (KanMX), GAL-UBR1 (His3)*	This study
CS 3279	*MATa, trp1::Sld2-PGAL1-10-Dpb11::TRP1, ura3::Sld3-PGAL1-10-Dbf4::URA3, leu2::Sld7-PGAL1-10-Cdc45::LEU2, ctf18Δ (Trp)*	This study
CS 3324	*MATa, Dpb3-TAP (KanMX), pep4Δ::ADE2*	This study
CS 3326	*MATa, Dpb3-TAP (KanMX), pol2-11, ufd4Δ::URA3CP, pep4Δ::ADE2*	This study
CS 3328	*MATa, Dpb3-TAP (KanMX), pol2 mutant E (KanMX), pep4Δ::ADE2*	This study
CS 3330	*MATa, Dpb3-TAP (KanMX), pol2 mutant E(E) (KanMX), pep4Δ::ADE2*	This study
CS 3332	*MATa, Mcm4-5FLAG (hphNT), pol2 mutant E(E) (KanMX), pep4Δ::ADE2*	This study
CS 3468	*MATa, trp1::Sld2-PGAL1-10-Dpb11::TRP1, ura3::Sld3-PGAL1-10-Dbf4::URA3, leu2::Sld7-PGAL1-10-Cdc45::LEU2, rad24Δ (hphNT)*	This study
CS 3557	*MATa, trp1::Sld2-PGAL1-10-Dpb11::TRP1, ura3::Sld3-PGAL1-10-Dbf4::URA3, leu2::Sld7-PGAL1-10-Cdc45::LEU2, dpb2-1*	This study

CS 3559	*MATa, trp1::Sld2-PGAL1-10-Dpb11::TRP1, ura3::Sld3-PGAL1-10-Dbf4::URA3, leu2::Sld7-PGAL1-10-Cdc45::LEU2, pol2 mutant E(E) (KanMX)*	This study
CS 3624	*MATa, trp1::Sld2-PGAL1-10-Dpb11::TRP1, ura3::Sld3-PGAL1-10-Dbf4::URA3, leu2::Sld7-PGAL1-10-Cdc45::LEU2, psf1-1*	This study
CS 3626	*MATa, trp1::Sld2-PGAL1-10-Dpb11::TRP1, ura3::Sld3-PGAL1-10-Dbf4::URA3, leu2::Sld7-PGAL1-10-Cdc45::LEU2, sgs1Δ (Ura)*	This study
CS 3630	*MATa, trp1::Sld2-PGAL1-10-Dpb11::TRP1, ura3::Sld3-PGAL1-10-Dbf4::URA3, leu2::Sld7-PGAL1-10-Cdc45::LEU2 mrc1Δ (hphNT)*	This study
CS 3696	*MATa, trp1::Sld2-PGAL1-10-Dpb11::TRP1, ura3::Sld3-PGAL1-10-Dbf4::URA3, leu2::Sld7-PGAL1-10-Cdc45::LEU2, rad9Δ (his3MX)*	This study
CS 3775	*MATa, trp1::Sld2-PGAL1-10-Dpb11::TRP1, ura3::Sld3-PGAL1-10-Dbf4::URA3, leu2::Sld7-PGAL1-10-Cdc45::LEU2, pol2-11, ufd4Δ::URA3CP*	This study
CS 3777	*MATa, trp1::Sld2-PGAL1-10-Dpb11::TRP1, ura3::Sld3-PGAL1-10-Dbf4::URA3, leu2::Sld7-PGAL1-10-Cdc45::LEU2, pol2-11, ufd4Δ::URA3CP, rad24Δ (hphNT)*	This study

2.2 *Escherichia coli* Culturing Methods

2.2.1 Harvesting of Competent Cells for Transformation

Stocks of DH5α stored at -80°C in 25% glycerol suspensions were streaked onto LB agar plates and grown at 37°C overnight. The following day, 20-30 colonies were used to inoculate 277.5 mL SOC media and grown in a shaking incubator for 22-24 hours at 25°C. Once the OD_{600} had reached 0.6, the cells were placed in ice for 10 minutes (herein, each subsequent step took place at 4°C), followed by centrifugation at 1200 *g* in a high speed centrifuge. All subsequent centrifugations were carried out at this speed. The supernatant was removed and the cells were resuspended in 80mL TB buffer (10mM PIPES pH7.9, 15mM CaCl2, 250mM KCl, 55mM MnCl2, final pH adjusted to 6.7) and left on ice for a further 10 minutes. This was centrifuged once again, resuspended in 10mL TB buffer and had DMSO added to a final concentration of 7%. After a further 10 minute incubation, the solution was aliquoted into fresh Eppendorfs and snap frozen in liquid nitrogen. The competent cells were then stored at -80°C until required.

2.2.2 *E. coli* Transformation

Aliquots of chemically competent cells were thawed on ice and then 100µL was aliquoted into Eppendorf tubes containing the plasmid DNA or ligation products to be transformed. The solution was then mixed by tapping and pipetting and then left for 30 minutes on ice. Cells were then heat-shocked at 42°C for 90 seconds and then cooled back on ice for a further 2 minutes. These were then diluted in 900µL LB pre-warmed to 37°C and then grown at 37°C with shaking for an hour. Cells were then plated on LB agar plates supplemented with the appropriate antibiotic for the selection marker of the plasmid and grown for roughly 16 hours at 37°C.

2.3 Molecular Cloning Techniques

2.3.1 Detection of Genotype by PCR

In order to confirm the presence of a transformed product at the correct loci, a colony or genomic sample-based PCR strategy was used, whose use depended on the required size of the PCR products. For this, oligonucleotides were designed specific for the construct that was being experimented with, and these were created to align both within the transformed DNA as well as the flanking genomic sequence. These resultant PCR reactions would be tested by running on an 0.8% agarose gel to see if they were the correct length according to the predicted sizes of the bands.

2.3.2 List of Plasmids Used in this Study

Table 2.3 A list of the plasmids used in this study. Here, plasmids are ordered by their number and their genotypes, including their backbones and insert, as well as a description of what they were used for.

Plasmid No.	Insert	Backbone	Description	Source
pCS15	GAL-TAP-NLS-Pol3(1-999)	pRS305	A plasmid to integrate GAL-TAP-NLS-Pol3(1-999) into the genome at the *LEU2* locus	This study

pCS16	GAL-TAP-NLS-Pol3(1-1097)	pRS305	A plasmid to integrate GAL-TAP-NLS-Pol3(1-1097) into the genome at the *LEU2* locus	This study
pCS17	GAL-TAP-NLS-Pol3(1-999)/Pol2(1986-2222)	pRS305	A plasmid to integrate GAL-TAP-NLS-Pol3(1-999)/Pol2(1986-2222) into the genome at the *LEU2* locus	This study
pCS34	GAL-3HA-NLS-Pol3(1-999)	pRS305	A plasmid to integrate GAL-3HA-NLS-Pol3(1-999) into the genome at the *LEU2* locus	This study
pCS35	GAL-3HA-NLS-Pol3(1-1097)	pRS305	A plasmid to integrate GAL-3HA-NLS-Pol3(1-1097) into the genome at the *LEU2* locus	This study
pCS36	GAL-3HA-NLS-Pol3(1-999)/Pol2(1986-2222)	pRS305	A plasmid to integrate GAL-3HA-NLS-Pol3(1-999)/Pol2(1986-2222) into the genome at the *LEU2* locus	This study
pCS45	GAL-3HA-NLS	pRS304	A plasmid to integrate GAL-3HA-NLS into the genome at the *TRP* locus	This study
pCS46	GAL-3HA-NLS-Pol2(1986-2222)	pRS304	A plasmid to integrate GAL-3HA-NLS-Pol2(1986-2222) into the genome at the *TRP* locus	This study
pCS199	GAL-TAP-NLS-Pol2(2103-2222)	pRS306	A plasmid to integrate GAL-TAP-NLS-Pol2(2103-2222) into the genome at the *URA3* locus	This study
pCS200	GAL-TAP-NLS-Pol2(2162-2222)	pRS305	A plasmid to integrate GAL-TAP-NLS-Pol2(2162-2222) into the genome at the *LEU2* locus	This study
pCS201	GAL-TAP-NLS-Pol2(2103-2222) MutB (C2164S C2167S)	pRS305	A plasmid to integrate GAL-TAP-NLS-Pol2(2103-2222) MutB into the genome at the *LEU2* locus	This study
pCS202	GAL-TAP-NLS-Pol2(2103-2222) MutE (L2198A F2201A V2204A L2213A I2217A)	pRS305	A plasmid to integrate GAL-TAP-NLS-Pol2(2103-2222) MutE into the genome at the *LEU2* locus	This study

pCS203	GAL-TAP-NLS-Pol2(1986-2222) MutE (L2198A F2201A V2204A L2213A I2217A)	pRS305	A plasmid to integrate GAL-TAP-NLS-Pol2(1986-2222) MutE into the genome at the *LEU2* locus	This study
pCS204	GAL-GST-6His	pRS306	A plasmid to integrate GAL-GST-6His into the genome at the *URA* locus	This study
pCS205	GAL-GST-His-Pol2(1986-2222)	pRS306	A plasmid to integrate GAL-GST-6His-Pol2(1986-2222) into the genome at the *URA* locus	This study

2.4 Biochemical techniques

2.4.1 Protein Detection by Immunoblotting

SDS-PAGE gels of an appropriate percentage were prepared depending on the protein being visualised - in this study, this ranged between 6-14% polyacrylamide (National Diagnostics). When set, the protein samples to be run were thawed at 37°C and thoroughly resuspended. After the wells had been washed out with running buffer, the samples, along with 2-3µl of protein ladder were each pipetted into each lane and the gel was run in a 1X Tris/glycine running buffer at 110V until the desired resolution between bands was achieved. Gels were semi-dry transferred, with the gel and nitrocellulose membrane used to be soaked for at least 15 minutes in room temperature transfer buffer beforehand. Within the transfer cassette, 3 layers of chromatography paper soaked in transfer buffer were placed, followed by the nitrocellulose membrane. The gel was placed followed by three more layers of chromatography paper. Each layer was rolled over lightly to ensure there were no bubbles between them, thus giving a clean transfer. Before the cassette was closed, the stack was dried as much as possible, ensuring minimal transfer buffer residue was left. This was transferred at 13V for 90 minutes. When the transfer was finished, the membrane was removed and immediately stained in 0.1% (v/w) Ponceau S in 5% (v/v) acetic acid solution to act as a loading control and after sufficient washes with sterile water was scanned. It was subsequently blocked with 5% milk dissolved in TBS-T

shaking for one hour at 25°C. After this, the membrane underwent three 10 minute washes in TBS-T. It was then incubated with a solution containing the primary antibody dissolved in the milk blocking solution at 4ºC overnight on a shaker. The membrane was washed 3 more times in TBS-T and then incubated for one hour with the secondary antibody, all of which were dissolved in 5% milk. The membranes were washed three more times with TBS-T, followed by a 90 second incubation with ECL solution (GE Healthcare), after which it was blotted dry, sealed in plastic and placed in a film cassette. Membranes were exposed onto Amersham Hyperfilm ECL films (GE Healthcare) in the cassette and developed in a dark room and for differing lengths of time. Resultant films were scanned at 300dpi in 8-bit greyscale using an Epson V700 scanner and saved in the TIFF format.

Table 2.4: A table of the primary antibodies used for immunoblotting in this study

Antibody	Host	Concentration Used	Source
anti-Pol2	Sheep	1:1000	Lab
anti-Pol1	Sheep	1:1000	Gift from Karim Labib
anti-Mrc1	Sheep	1:1000	Gift from Karim Labib
anti-Ctf4	Sheep	1:15000	Gift from Karim Labib
anti-Cdc45	Sheep	1:1500	Gift from Karim Labib
anti-Dpb2	Sheep	1:1000	Gift from Karim Labib
anti-Rad53	Mouse	1:1500	Abcam (EL7.E1)
anti-Csm3	Sheep	1:1000	Gift from Karim Labib
anti-Psf1	Sheep	1:250	Gift from Karim Labib
anti-PCNA	Mouse	1:5000	CRUK antibodies
anti-ɣH2AX	Rabbit	1:1000	Abcam (ab15083)
anti-TAP-HRP (PAP)	Rabbit	1:100,000-1:10,000	Sigma (1291)
anti-FLAG M2	Mouse	1:50,000-1:5000	Sigma (F1804)
anti-GST	Mouse	1:5000	Merck (71097)

Table 2.5: A table of the secondary antibodies used in this study.

Antibody	Host	Concentration Used	Source
anti-Rabbit IgG-HRP	Mouse	1:1,000	Rockland (18-8816-33)
anti-Rabbit IgG-HRP	Goat	1:10,000	Cell Signalling Technology (#7074)
anti-Mouse IgG-HRP	Horse	1:10,000	Cell Signalling Technology (#7076)
anti-Sheep IgG-HRP	Donkey	1:5000- 1:10,000	Sigma (A3415)

2.4.2 Protein Detection by Coomassie Staining

In order to examine the presence or relative concentrations of proteins obtained from immunoprecipitated samples, Coomassie staining of gels was used. Samples were loaded into pre-cast Novex Wedgewell 4-12% Tris-Glycine polyacrylamide gels and ran at 240V in the supplied Tris-glycine buffer. When the desired separation of bands has been achieved, the gels were then removed from their cassettes and washed three times in distilled water for 5 minutes each. Following this, the gel was stained with roughly 25mL SimplyBlue SafeStain (ThermoFisher) for 1 hour at 25°C with gentle agitation. The stain was then removed and the gel washed with water for up to 3 hours, followed by a second wash to obtain a clear background. Gels were then scanned at 300dpi in 48-bit colour using an Epson V700 scanner.

2.4.3 TCA Protein Preparation of Yeast Samples

The TCA sample was thoroughly resuspended, followed by adding an equal volume of 0.5mm micro glass beads (Thistle Scientific) and vortexing vigorously for 5 minutes. The solution was then quickly pelleted and resuspended in 300µL 5% TCA and transferred to a new tube. After spinning for ten minutes, the supernatant was then removed and the pellet resuspended and boiled for 5 minutes in 1x Laemmli buffer supplemented with 150mM Tris. After another 10 minute spin at 3000*g*, the supernatant was extracted and frozen at -20°C until needed.

2.4.4 Genomic Extraction from Yeast Cells

Genomic samples were extracted from yeast by inoculating the desired strain overnight in 5mL of YPD at 24°C the day before. This sample was then pelleted, the supernatant removed, and washed once with sterile water before being transferred to a screwcap Eppendorf. The pellet was resuspended in 200µL of yeast lysis buffer (100mM NaCl, 10 mM Tris-HCl (pH 8.0), 1 mM EDTA, 1% SDS, 2% Triton), 200µL TE pH 8.0, and 200µL Phenol/Chloroform/Isoamyl alcohol (25:24:1, pH 8.0) (Acronis Organics) and mixed with a ~200µL aliquot of 0.5mm micro glass beads (Thistle Scientific) and mixed vigorously for 10 minutes. The tubes were then centrifuged at 12,000*g* for 2 minutes and 380µL of the clear supernatant was transferred to a fresh Eppendorf and mixed with 760µL 100% ethanol. The precipitated DNA was then pelleted and washed in 70% ethanol in order to remove residual phenol contamination. This ethanol was removed and the pellet left to dry at 37°C, before being resuspended in 50µL TE pH 8.0 supplemented with 50µg/mL RNAse A and incubated at 37°C for at least an hour. This sample could be used immediately or stored at -20°C until required.

2.4.5 Preparation of Yeast Cells for FACS Analysis

For processing, the solution was thoroughly resuspended and a 200µL sample was taken. This sample was then mixed in 50mM Na citrate buffer and spun down at 3000*g* for 3 minutes. The cell pellet was washed once more with Na citrate and centrifuged once again. The supernatant was removed and the pellet was resuspended in 50mM Na citrate with 0.1mg/mL RNase A, at which point it was incubated for at least 2 hours at 37°C. The solutions were then pelleted again, whereupon the supernatant was removed and the pellet was resuspended in 50mM HCl with 5mg/mL pepsin. This was incubated at 37°C again for 30 minutes. Finally, the solution was spun down with the supernatant removed, and the pellet was resuspended in 50mM Na citrate with 2µg/ml propidium iodide. The cells were kept in the dark to prevent the reagent's degradation. Before being passed through the Becton Dickinson FACScan flow cytometer, the cells were sonicated for 5 seconds at 8 microns and vortexed to ensure sample homogeneity.

2.4.6 Immunoprecipitation of TAP or FLAG-tagged Proteins

Before the immunoprecipitation (IP) experiment takes place, first the antibody-conjugated beads must be prepared. First, an aliquot of Dynabeads M-270 Epoxy (Invitrogen) resuspended in dimethyl formide was taken and washed twice with 0.1M sodium phosphate (pH 7.4). The beads are then left in 0.1M sodium phosphate, 1M ammonium sulphate (pH7.4) with approximately 300µg of anti-sheep IgG (Sigma S1265) or anti-FLAG M2 (Sigma F1804) for TAP or FLAG-tag IPs, respectively, and left for 3 days at 4°C on a rotating wheel. Before their incubation with the cell extract in experiment, these beads were washed four times with PBS, followed by a wash with PBS/0.5% NP-40, then 4 washes with PBS with 5mg/mL BSA (Sigma).

For the IP, the popcorn was grinded to a powder using a 6870 FreezerMill (SPEX SamplePrep) in the presence of liquid nitrogen. This involved 6 separate 1 minute long rounds of 14 cycles per second, with a minute's cool down in between each one. In concentrated popcorn samples, the resulting powder was thawed at room temperature, and then mixed with a volume of 50% (v/v) glycerol, 100 mM HEPES-KOH (pH 7.9), 100 mM KOAc, 50 mM MgOAc, 0.5% Igepal CA-630 (Sigma), 2mM EDTA supplemented with 2 mM glycerophosphate, 2 mM NaF, 1 mM DTT, 1% (v/v) Sigma protease inhibitor cocktail and 0.24% (w/v) EDTA-free Complete Protease Inhibitor Cocktail buffer a quarter of its mass as well as 1mL of a solution of 10% (v/v) glycerol, 100 mM HEPES-KOH (pH 7.9) 100 mM KOAc, 50 mM MgOAc, 0.1% (v/v) Igepal® CA-630, 2mM EDTA supplemented with 2 mM glycerophosphate, 2 mM NaF, 1 mM DTT, 1% (v/v) Sigma protease inhibitor cocktail and 0.24% (w/v) EDTA-free Complete Protease Inhibitor Cocktail. This solution was then incubated for one hour with Pierce™ Universal Nuclease for Cell Lysis (ThermoFisher) at an 800 units/µL concentration at 4°C on a rotating wheel. For dilute samples, the thawed sample was mixed with a volume plus 50µL of 50% (v/v) glycerol, 100 mM HEPES-KOH (pH 7.9), 100 mM KOAc, 50 mM MgOAc, 0.5% Igepal CA-630, 2mM EDTA supplemented with 2 mM glycerophosphate, 2 mM NaF, 1 mM DTT, 1% (v/v) Sigma protease inhibitor cocktail and 0.24% (w/v) EDTA-free

Complete Protease Inhibitor Cocktail buffer equal to a quarter of its volume, followed by an incubation with 400U/µL nuclease. Once incubated for an hour to degrade the DNA, the extract was centrifuged for 30 minutes at 25,129 *g* in a high speed centrifuge at 4°C, after which the resulting supernatant was transferred to an ultracentrifuge tube. The extracts were centrifuged again, this time at 100,*000 g* at 4°C for 1 hour in an ultracentrifuge.

This supernatant contained the whole cell extract of which a small sample was taken and boiled with Laemmli buffer for subsequent analysis of the experiment. The rest was incubated for two hours at 4°C with the prepared beads, with a maximum 0.7mL WCE to each tube of 100µL beads. The supernatant was removed from the beads, a sample of which was taken and boiled with Laemmli buffer, while the beads were washed four times with a solution of 100 mM HEPES-KOH (pH 7.9), 100 mM KOAc, 50 mM MgOAc, 2 mM EDTA, 0.1% (v/v) Igepal® CA-630, once with 2 mM glycerophosphate, 2 mM NaF, 1 mM DTT, 1% (v/v) Sigma protease inhibitor cocktail and 0.24% (w/v) EDTAfree Complete Protease Inhibitor Cocktail and three times without. Each aliquot of beads was then boiled in the presence of 50µL of Laemmli buffer, which was then removed and snap-frozen. In experiments taking place with different wash stringencies, the concentration of KOAc in all of the buffers was adjusted to the volume stated in the experiment.

2.4.7 2-Step Immunoprecipitation of GST-6His-Tagged Proteins

Prior to the IP, the two sets of resins that are used for each step must be prepared. For the first step, Glutathione-Sepharose 4B resin (GE Healthcare) was used, where the required amount of resin/ethanol slurry was transferred to a fresh tube after thorough resuspension. The gel was sedimented via centrifugation and washed once with 10 x the resin volume in cold PBS. This was followed by another wash in cold PBS, but using the same volume as the resin. Following this were three washes with a 50mM Tris-HCl ph8.0, 50mM NaCl, 10mM $MgCl_2$, 2mM EDTA, 20mM Imidazole and 5mM β-mercaptoethanol solution, before being resuspended in an aliquot of this solution and stored at 4°C until required. For the second 6His purification

step, a HisPur Cobalt Resin (ThermoFisher) was used and prepared in the same manner as the GST resin, with the exception of being washed instead with 10% (v/v) glycerol, 50 mM Tris-HCl (pH 8.0), 50 mM NaCl, 10 mM $MgCl_2$, 0.1% Igepal CA-630, 20mM Imidazole, 5mM β-mercaptoethanol.

For the IP, the popcorn was grinded using a 6870 FreezerMill. This involved 6 separate 1 minute long rounds of 14 cycles per second, with a minute's cool down in between each one. The resulting powder was thawed at room temperature, and then mixed with a volume of 50% (v/v) glycerol, 50 mM Tris-HCl (pH 8.0), 50 mM NaCl, 10 mM $MgCl_2$, 0.5% Igepal CA-630, 20mM Imidazole, 5mM β-mercaptoethanol, supplemented with 2 mM glycerophosphate, 2 mM NaF, 1 mM DTT, 1% (v/v) Sigma protease inhibitor cocktail and 0.24% (w/v) EDTA-free Complete Protease Inhibitor Cocktail buffer a quarter of its mass as well as 1mL of a 1 ml of a solution of 10% (v/v) glycerol, 50 mM Tris-HCl (pH 8.0), 50 mM NaCl, 10 mM $MgCl_2$, 0.1% Igepal CA-630, 20mM Imidazole, 5mM β-mercaptoethanol, supplemented with 2 mM glycerophosphate, 2 mM NaF, 1% (v/v) Sigma protease inhibitor cocktail and 0.24% (w/v) EDTA-free Complete Protease Inhibitor Cocktail. This solution was then incubated for one hour with Pierce™ Universal Nuclease for Cell Lysis at an 800 units/μL concentration at 4°C on a rotating wheel. Once incubated for an hour to degrade the DNA, the extract was centrifuged for 30 minutes at 25,129 *g* in a high speed centriguge at 4°C, after which the resulting supernatant was transferred to an ultracentrifuge tube. The extracts were centrifuged again, this time at 100,*000 g* at 4°C for 1 hour in an ultracentrifuge.

This supernatant contained the whole cell extract of which a small sample was taken and boiled with Laemmli buffer for subsequent analysis of the experiment. The rest was incubated for one hour at 4°C with the prepared GST resin, with a maximum 1mL WCE to each tube of 100μL resin. The supernatant was removed from the beads, a sample of which was taken and boiled with Laemmli buffer, while the beads were washed three times with a wash buffer (10% (v/v) glycerol, 50 mM Tris-HCl (pH 8.0), 50 mM NaCl, 10 mM $MgCl_2$, 0.1% Igepal CA-630, 20mM Imidazole, 5mM β-mercaptoethanol). Following this, each aliquot of resin was incubated with

200µL of the wash buffer supplemented with 20mM Glutathione to elute the bound protein for 1 hour at 4°C. This elute was then incubated with the cobalt resin for 2 hours on a rotating wheel at 4°C, before being washed twice with the wash buffer and then incubated with the same buffer, but with the Imidazole concentration raised to 250mM, for 1 hour at 4°C. The elute was then mixed with an equal volume of cold 20% TCA and centrifuged for 15 minutes at 20300 *g*. The supernatant was removed and the pellet was resuspended in 1x Laemmli buffer supplemented with 150mM Tris.

2.4.8 Preparation of Protein Samples for Mass Spectrometry Analysis

Samples were loaded into pre-cast Novex Wedgewell 10% Tris-Glycine polyacrylamide gels and ran at 125V in the supplied MOPS buffer for 15mm. The short columns from each well were then excised and cut into 10 1.5mm slices. These slices were placed in 100µL ddH_20 and sent to MS Bioworks in the USA for Mass Spectrometric analysis. The samples were washed, reduced, alkylated and then digested by trypsin and a nanoLC/MS/MS (Waters NanoAcquity HPLC/ThermoFisher Q Exactive) was then used to analyse the reaction. The 15 most abundant ions were then selected for tandem MS. The data was then processed by comparing the spectra to those from Saccharomyces cerevisiae proteins trypsinized *in silico.*

2.5 Image Analysis and Processing

2.5.1 Image Processing

Images from films or plates were opened and processed with Adobe Photoshop CC. The images were cropped as required and then processed to remove dust and scratches and despeckled to 1 pixel. The images were adjusted for brightness and contrast and formatted to widths of 3 or 6 cm while maintaining their length:width ratio and set to 508 dpi and saved as a TIFF file format. Images were then arranged to create figures using Adobe Illustrator CC.

2.5.2 Image Acquisition of FACS Analysis

When FACS analysis was run on the BD FACScan machine, excitation was induced with a 488nm laser light and the emission was detected with a 650 nm long pass filter. For each sample, 40,000 acquisitions of populations of cells between G_1 and G_2 were accepted. When all samples were analysed, each plot underwent 5 smoothing iterations and were overlaid on each other as histogram plots of FL2-H value vs the count. The resultant graphs were then saved in the PNG format and arranged and annotated using Adobe Illustrator CC software.

2.5.3 Quantification of Band Intensities

The files generated from processing the immunoblot films were analysed using ImageJ software. In the case of Rad53 immunoblots, areas were selected for the bottom, unphosphorylated bands and the top, hyperphosphorylated bands. For immunoprecipitation immunoblots, areas were drawn around the IP sample bands. Using the Gel Analyser tool, the intensity profiles of these areas were plotted. The areas under each of the peaks was then measured to quantify the intensity of each band. For Rad53, the intensity of the top band was then divided by the total of the bottom and top band intensities and plotted on a line graph using Microsoft Excel. For immunoprecipitation samples, the intensity of each band was measured, normalised to the band of the signal of the corresponding immunoprecipitated protein and then recorded in a table to 3 decimal places.

Chapter 3: Analysis of the Essential Role of the Pol2 C-terminus in DNA Replication

3.1 Background

As one of the three DNA polymerase complexes at the replication fork, Pol ε plays an integral role by conducting processive DNA synthesis on the leading strand. Like the other two polymerases, Pol ε is essential for viability but, interestingly, this is not dependent on its catalytic activity. Remarkably, if the polymerase and exonuclease domains of Pol2, the catalytic subunit of Pol ε, are deleted, the cell is viable, albeit sicker (Kesti et al., 1999). This essential role of its C-terminus is thought to be underpinned by its interaction with the B subunit of Pol ε, Dpb2, which plays an integral part in forming the origins from which replication forks emerge (Sengupta et al., 2013).

In the work presented here, I have utilised galactose-inducible expression systems coupled with a temperature sensitive *POL2* allele, *pol2-11*, to further probe the functions of the Pol2 C-terminus during replication. In this study, I have explored numerous potentially novel roles the Pol2 C-terminus partakes in during DNA replication beyond its known function in origin firing. After analysing the conserved nature of the C-terminus, this work has raised the possibility of an important role of a stretch of hydrophobic residues within its extreme C-terminus in its essential function.

3.2 The last 236 residues of the Pol2 C-terminus is sufficient to suppress growth defects of the truncation mutant *pol2-11.*

The C-terminus of Pol2 is essential in both budding yeast and fruit flies; since the evolutionarily conserved feature is within this region, namely two zinc fingers, and the conserved primary sequence homology of the last 40 amino acids, it was decided to check if expressing this was sufficient for viability. In order to understand the critical function played by the Pol2 C-terminus in DNA replication, I used strains containing an allele of Pol2 lacking the last 31 residues, *pol2-11* (Figure 3.1A), that confers a temperature sensitive phenotype as well as checkpoint defects and DNA

damage sensitivity, including sensitivity to both HU and MMS (Navas et al., 1995, Dua et al., 1998). The defects of this truncation mutant have previously been shown to be suppressed by overexpression of either *MRC1* or *DPB11* (Lou et al., 2008, Araki et al., 1995). In my experiments, I have coupled the *pol2-11* allele with a deletion of *UFD4,* which encodes an E3 ubiquitin ligase, that we found somewhat suppressed the mutant's severe growth defects by increasing the levels of protein present in the cell (Karim Labib lab, personal communication). Coupled with this was a fragment containing the last 236 residues of Pol2 that was N-terminally TAP-tagged, with a nuclear localization sequence (NLS) from the Dia2 gene inserted between these components, shown as GAL-TAP-Pol2 (1986-2222) in Fig 3.1A. As a control, the TAP tag and subsequent NLS but without the fragment was created, referred to as GAL-TAP-NLS, to ensure any effects seen from its expression were results of the Pol2 C-terminus. These were placed under the control of a galactose-inducible promoter. The ability of the C-terminus to contribute to viability when cells were grown beyond the permissive temperature of *pol2-11* was first checked with a simple dilution spotting experiment. Cells were grown on YP raffinose and YP galactose, which would repress or induce the expression of the fragment, respectively, and at different temperatures to assess the temperature sensitivity of the *pol2-11* allele.

Observing their growth in Fig 3.1B, it is clear that the *pol2-11* allele becomes lethal at 37°C, while expression of the C-terminal fragment in the galactose plates at these temperatures is sufficient to suppress the temperature sensitivity. It is important to note that the growth is not fully restored to that of the wild type and it can be inferred that replication defects remain. Additionally, when these same fragments were expressed with the wild type *POL2* allele, there was no observable growth difference, indicating that the presence of the C-terminus does not elicit any beneficial or detrimental effects to cell growth. The replication stress sensitivity previously described in *pol2-11* can also be clearly observed here due to its impacted growth in media containing 150mM HU, which is known to activate the S phase checkpoint by depleting dNTP pools. As with the temperature sensitivity, this HU sensitivity is suppressed by expressing the C-terminus,

although close examination of the colony growth shows that, again, this suppression is only partial in restoring wild type growth. These experiments have essentially recapitulated those performed by Kesti *et al.* using *pol2-16*, in which expression of the C-terminal half of Pol2 was sufficient to suppress a deletion of the whole protein, albeit with a much smaller fragment, indicating that the essential part of Pol ε lies within (Kesti et al., 1999).

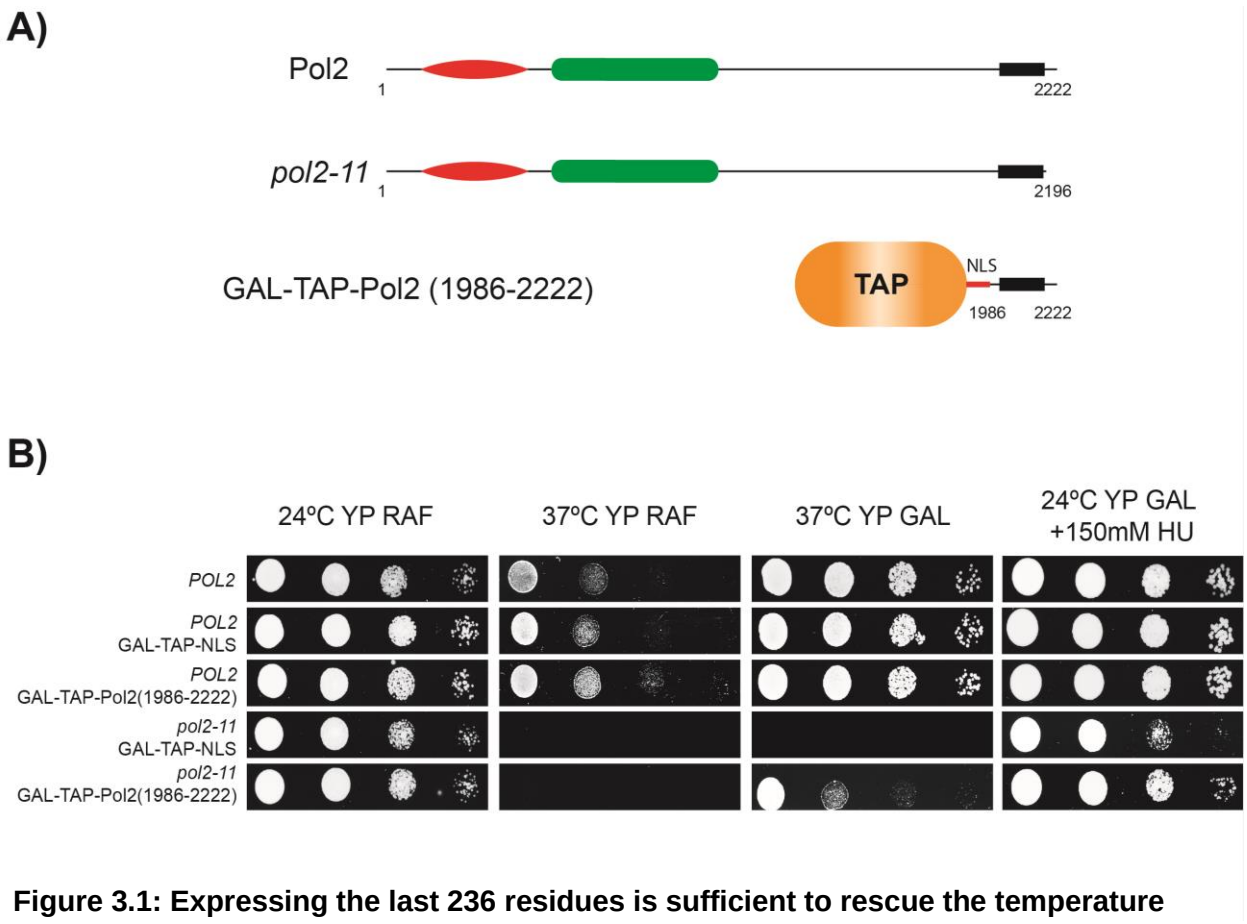

Figure 3.1: Expressing the last 236 residues is sufficient to rescue the temperature sensitivity of *pol2-11*. A) Schematic representations of wild type, the temperature sensitive *pol2-11* allele with its last 36 residues deleted and the pol2-C terminal fragment used in this experiment, in which the last 236 residues of Pol2 conjugated to an N-terminal TAP tag under the control of a GAL promoter. In the N-terminus of Pol2, the red and green blocks represent the exonuclease and polymerase domains, respectively. The black block represents the conserved C-terminal zinc-finger domain. **B)** This figure shows a dilution spotting experiment in which the strains were serially diluted 10-fold and spotted onto YP-Raf or YP-Gal plates and left to grow at 24° or 37°C with or without the presence of 150mM HU. At 37°C, beyond the restrictive temperature of *pol2-11,* cells with the fragment induction being inhibited in YP-Raf are unable to survive. However, when expression of the Pol2 fragment was induced was able to rescue the growth of the cells, although not to the same degree as wild type. Additionally, HU caused the death of *pol2-11* cells, while this phenotype was rescued by the expression of the C-terminal fragment. Data shown is representative of 6 independent experiments. Strains used in order of top to bottom: CS 1, CS 699, CS 700, CS 1463, CS 1465, and plate scans were taken 72 hours after spotting.

3.3 At the restrictive temperature of *pol2-11*, expression of the C-terminal fragment permits progression of replication.

To gain a further understanding of the replication dynamics underpinning the survival of the Pol2-expressing fragments, a FACS experiment was performed (Fig 3.2). Cells were grown to the logarithmic growth phase in raffinose-based medium and then arrested in G_1 by adding alpha factor. After which, fragment expression was induced by switching to a galactose-containing medium for 40 minutes and then the temperature was shifted to 37°C to inactivate *pol2-11*. Cells were then released from G_1, with FACS samples taken every 15 minutes for 2.5 hours.

From the FACS profiles in Fig 3.2, at 37°C, wild type replication starts almost immediately following release from G_1 and lasts between 30 and 45 minutes. Meanwhile, cells with *pol2-11* fail to start DNA replication, which would point to a defect in the origin firing process, consistent with our knowledge of Pol ε's essential role in this process (Sengupta et al., 2013). When the C- terminal fragment is expressed, replication is able to start and progress until the 2C peak can be seen. However, this process only begins 75 minutes after the release and then requires a further 75 minutes to finish replication. The delayed onset of replication would seem to indicate that with just the fragment, the ability of the cell to assemble and fire origins is reduced, but the fact it still occurs indicates that within this small fragment lies Pol ε's critical function. If the only difference in replication were a reduction of origins firing, this could explain the longer replication time, as there would be fewer forks required to replicate the entire genome. However, there are more than likely to be problems in fork progression as well, as it can be assumed Pol δ is taking over replication on the leading strand.

From these FACS analyses, it can be inferred that the complete loss of viability of these cells is due to the polymerase ε complex no longer being able to play its critical role in origin firing, as seen by the inability to move past its G_1 peak. In this case, the suppressive activity of the C-terminus could be explained by its ability to bind Dpb2 and, through that, ensure that this

can bind GINS and complete the origin firing role of Pol ε. However, as the suppression is only partial, this could indicate that this Dpb2-C-terminus binding interface is weak, thus making the pre-loading complex structurally unstable. This could result in fewer functioning complexes available to license the full complement of origins characteristic of a fully functioning firing programme.

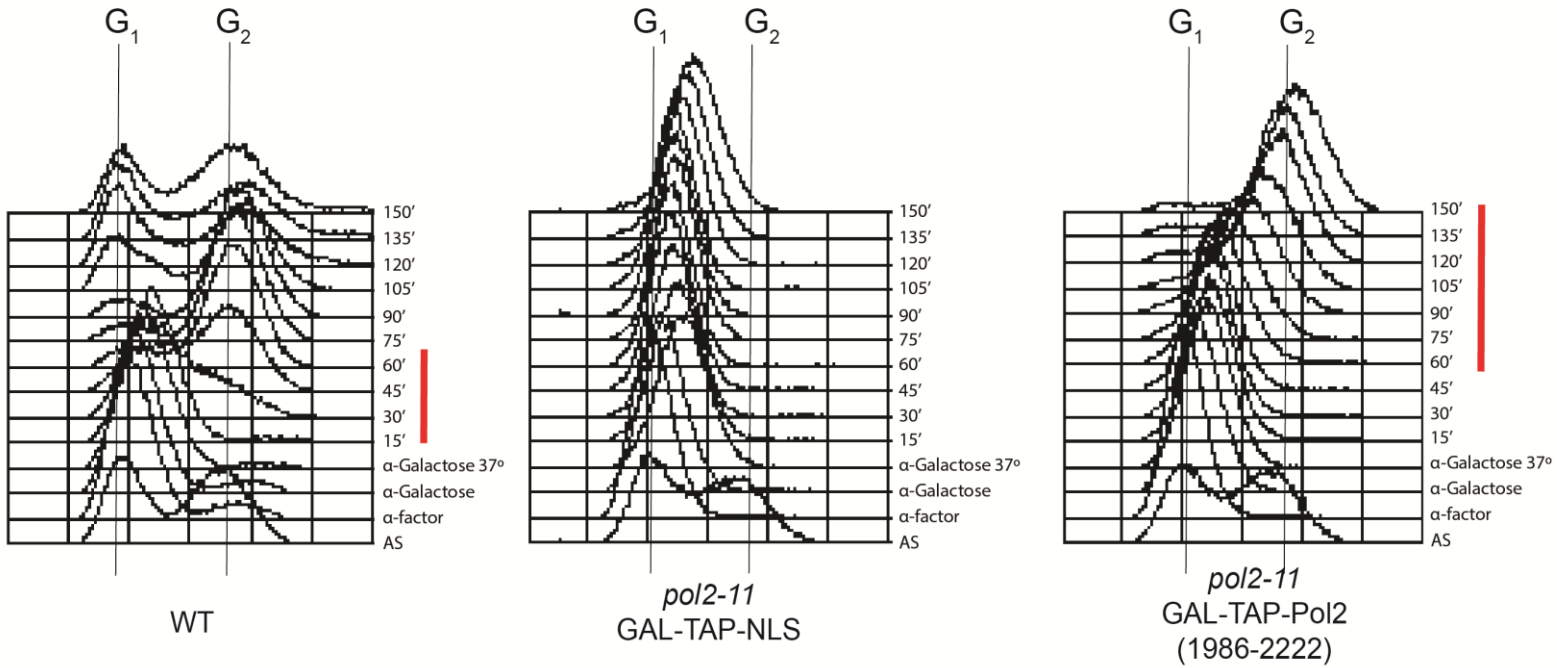

Figure 3.2: At the restrictive temperature, the inability of *pol2-11* to carry out replication is suppressed by expressing the Pol2 C-terminal fragment. FACS profiles acquired from the wild type (CS 1), *pol2-11* with the TAP-NLS (CS 1463) expressed and *pol2-11* with the TAP-Pol2 C-terminus (CS 1465) strains used in Fig 3.1. The cells were arrested in G_1 with alpha factor in YP-Raf, resuspended in YP-Gal and then shifted to the restrictive temperature of 37°C, always in the presence of alpha factor. Cells were then released from G_1 into S phase and samples were taken every 15 minutes. Black vertical lines indicate G_1 and G_2 peaks, where labeled, and the red bar shows approximate time for replication. While the Pol2 C-terminus is able to rescue viability at the restrictive temperature of *pol2-11*, the later onset of replication and increased duration of replication seems to indicate possible problems in origin firing and fork progression for these cells. Data shown is representative of 6 independent experiments.

3.4 Origin firing levels are reduced in *pol2-11* cells and this is partially suppressed by C-terminus expression.

Having seen the replication profile of this Pol2 fragment, a single-step immunoprecipitation of FLAG-tagged Mcm4 was carried out to confirm the hypothesis that diminished levels of origin firing were driving the growth defects shown in the *pol2-11* strains even at permissive temperatures. For these experiments, the strains as described before were used, except for the tag conjugated to the Pol2 fragment, which was changed to 3HA, to prevent immunoprecipitating the TAP alongside the FLAG tag. Ordinarily, TAP-tagged Mcm3 would be used for these experiments, however *pol2-11* appeared uniquely sensitive to this and this caused synthetic lethality. While this phenotype is remarkable, the reasons underpinning this have not been explored in this piece of work. Samples for immunoprecipitation were taken at 24°C during the G_1 stage of the cell cycle, where no active replisomes should be observed, and after a 90 minute arrest in HU. Having pulled down Mcm4, the protein levels of other components of an active replisome were observed through immunoblotting, as there is a direct relation between the level of origin firing and the amount of replisome formed. In this experiment, the subunits of Pol α and the CMG helicase were qualitatively analysed by immunoblotting.

As can be seen from in Fig 3.3, the replisome contents pulled down with Mcm4 vary considerably between strains. Consistent with the analysis of the FACS profiles, the ability of cells containing the *pol2-11* allele to fire origins was greatly diminished, even at its permissive temperature, so much so that the catalytic subunit of polymerase α is barely visible. When expressing the C-terminus, however, levels of origin firing appear to be somewhat alleviated, although still not to levels seen in the wild type. These observations are replicated in what was seen as an intermediate growth phenotype when expressing the Pol2 fragment.

A)

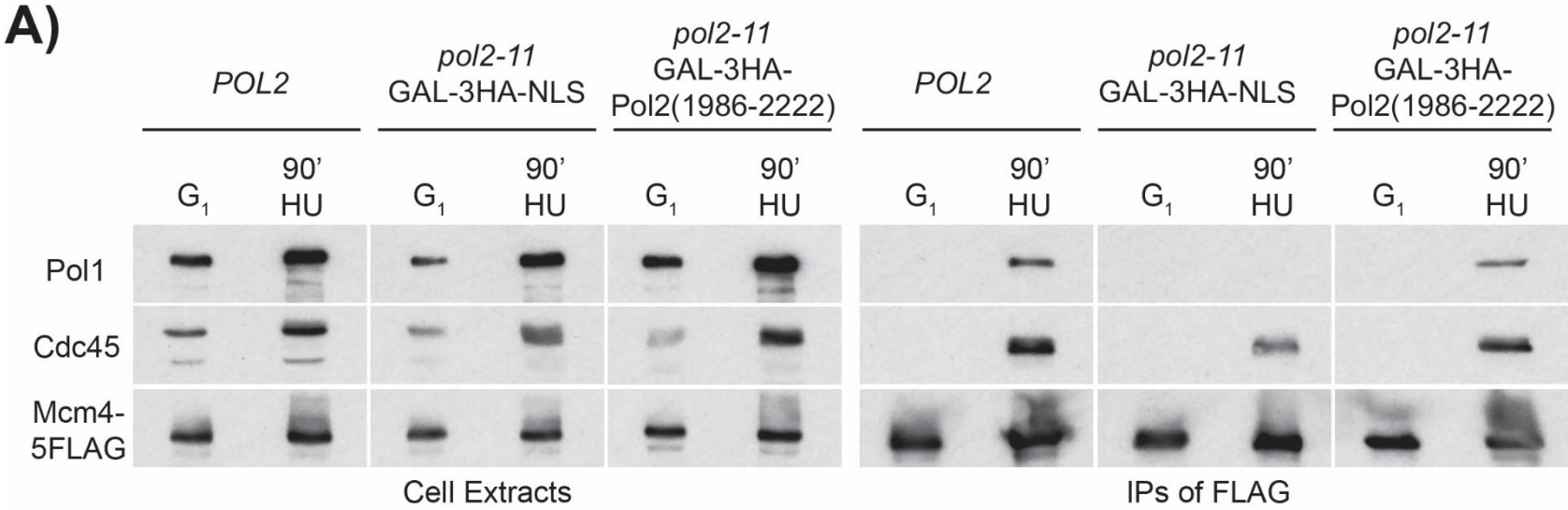

B)

	POL2	*pol2-11 GAL-3HA-NLS*	*pol2-11 GAL-3HA-Pol2 (1986-2222)*
Pol1	0.565	0.036	0.434
Cdc45	0.821	0.587	0.739

Figure 3.3: *pol2-11* contains an origin-firing defect that is only partially suppressed by expressing the 236 residues C-terminal Pol2 fragment. A) Cells carrying a FLAG-tagged version of Mcm4 (CS 1166, CS 1476, CS 1478, respectively) were arrested in alpha factor, and then released for 90' into YPD 0.2M HU at permissive tmeperature. Samples were collected and frozen at the indicated times. Following the single-step immunoprecipitation, samples were analysed by immunoblotting. Here, the C-terminal fragment was conjugated to a 3HA instead of a TAP tag. **B)** Table of quantified band intensities of the immunoprecipitated samples from the immunoblot. All values have been normalized to the intensity of the Mcm4-5FLAG band. By looking at the co-immunoprecipitated replisome proteins, it can be noted that the pol2-11 cells are far less efficient at firing origins than the wild type, while the presence of the C-terminal fragment provides an intermediate phenotype between the two.

3.5 Fusing the polymerase domain of Pol3 to the C-terminal fragment allows it to retain its suppressive effect.

Having seen only the partial suppressive effect of the Pol2 C-terminus in alleviating the temperature sensitive *pol2-11* phenotype, I hypothesized that the C-terminus, while able to suppress the defects in origin firing, might fail to suppress the defects of the loss of DNA polymerase activity on the leading strand. The physical coupling of the DNA polymerase epsilon and the helicase CMG provide in vitro a stronger directionality of the helicase, and faster progression of replication forks (Bermudez et al., 2011). Therefore, some of the defects observed in *pol2-11* with the GAL-TAP-Pol2 (1986-2222) might be due to the loss of coordination between the leading strand polymerase and the DNA helicase. To test this hypothesis, the first 999 residues containing the DNA synthesis domain of the catalytic Pol δ subunit, Pol3, were fused to the Pol2 C-terminus used in the previous experiments and placed under a galactose-inducible promoter. In addition to this, we wanted to dissect the source of the suppression mediated by Pol2-CT. To this aim, I used two differentially sized C-terminal fragments, each containing the two zinc fingers, of the human Pol2 orthologue, PolE1, which were also placed in the same expression systems. With these PolE1 fragments, it could be seen whether the presence of two zinc fingers that resemble those seen in Pol2, was sufficient to provide the suppressive effect seen with the Pol2 C-terminus, or if there were other underlying characteristics necessary for this function.

As an initial test of the effectiveness of these new constructs, dilution spotting experiments were carried out. Here, cells were plated on YP agar supplemented with either glucose (YPD) or galactose (YP GAL) to inhibit or promote expression of the fragment, respectively (shown in Fig. 3.4). These plates were then placed at different temperatures and in the presence of 150mM HU to test how well these new constructs were able to suppress the temperature sensitivity and checkpoint inherent to the *pol2-11* allele. From the experiments shown in Figure 3.4, it can be seen that the chimeric polymerase fragment appears to have a slightly greater suppressive effect at

37°C than the C-terminus alone. Working under the hypothesis that *pol2-11* could be affecting Dpb2 binding, which could entail the loss of Dpb3 and -4 as well, a *dpb3Δ*/*dpb4Δ* double mutant was used to exhibit that resulting phenotype so as to delineate it from the effects of losing Pol2 from forks. The observation that *pol2-11* GAL-Pol2-CT (1896-2222) closely resembles *dpb3*Δ *dpb4*Δ suggests that part of the partial suppression might be linked to a defect in retaining the non-essential subunits of Pol ε at forks. Nevertheless, since Dpb3 and Dpb4 have been shown to be incorporated in other complexes outside Pol ε, it's not possible to exclude that the defect observed is dependent on other defects. In addition to this, the human PolE1 fragments have no suppressive effect. However, the fusion protein is still unable to recover wild type growth levels seen with the *POL2* allele and whether the differences in growth levels between the chimera and C-terminus are significant enough is difficult to assess.

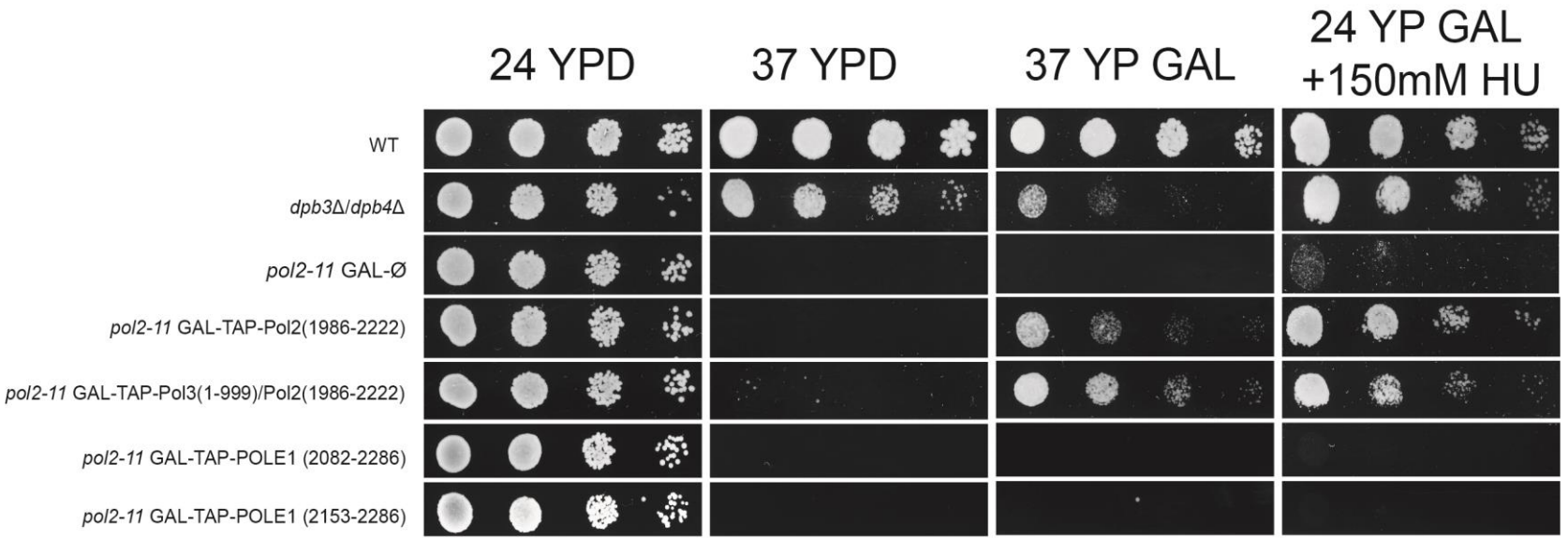

Figure 3.4: The fusion of the Pol3 polymerase domain and Pol2 C-terminus domain is able to suppress the temperature and HU sensitivity of *pol2-11* cells. Cells were serially diluted 10-fold and spotted onto YPD or YP-Gal plates and left to grow at 24° or 37°C with or without the presence of 150mM HU. In this experiment, a *dpb3Δ/dpb4Δ* was used as a control to test how much of the phenotype observed in *pol2-11* was the result of loss of Dpb3 and -4 binding to the catalytic subunit. A chimeric protein formed of the C-terminal fragment (1986-2222) used previously fused to the catalytic N-terminus of the Pol3 polymerase (1-999) was expressed to examine if the wild type function of Pol2 can be restored if DNA polymerase activity is restored to the C-terminus. This fusion protein retains the ability of the C-terminus to suppress the temperature sensitivity of the *pol2-11* activity. Two C-terminal fragments of differing lengths of the human orthologue of Pol2, POLE1, were also expressed at under the same system, however they did not have the suppressive effect of the yeast forms. Strains used in order of top to bottom: CS 1, CS 1467, CS 1463, CS 1465, CS 1922, CS 2166, CS 2168 and plate scans were taken 72 hours after spotting. The suppressive activity of the chimera has been observed in 3 independent experiments.

3.6 The Pol3/Pol2 fusion does not improve the suppressive phenotype of the C-terminus.

While the fusion of the Pol3 catalytic domain to the Pol2 C-terminal fragment appeared to retain the latter's ability to suppress the temperature sensitivity of *pol2-11*, it was unclear whether the presence of the former was having any effect of its own. In order to better understand the growth patterns observed with the Pol3/Pol2 fusion protein, a FACS experiment was performed, but with a strain containing the chimeric protein. Here, cells were grown at the logarithmic phase of growth in raffinose supplemented medium and then synchronized in G_1 by the use of alpha factor. While remaining arrested, the cells were switched to galactose to drive expression of the fragment and then, after a sufficient time, switched to the restrictive temperature of 37°C. After the medium had reached this temperature, cells were washed and released from the G_1 block to complete replication. FACS samples were taken every 15 minutes for a subsequent period of two and a half hours.

From the profile of the fusion protein, as shown in Figure 3.5, it appears that there is a slight difference between it and the Pol2 C-terminus as replication appears to take slightly longer with the fusion protein. Expression of the C-terminal fragment and the new chimeric protein both allow replication to proceed at *pol2-11*'s restrictive temperature, with the G_2 population of cells predominating by the end of the experiment. However, it is clear that the presence of a catalytic domain with this C-terminus is still not able to restore the dynamics seen in the wild type Pol2 protein, which, after two and a half hours is beginning to form a significant G_1 peak following mitosis. From this, it is likely that even after adding an active polymerase component to the C-terminus, while the origin firing activity remains, it is still unable to act as a direct replacement for Pol2. The phenotype observed in this chimeric protein could illustrate one of two things: either that the attached polymerase domain is not carrying out synthesis and replication occurs in the same way as when the Pol2 C-terminus is expressed, or that the Pol δ fragment is catalyzing DNA synthesis, but is not able to match the efficiency of a full Pol2 subunit.

This could either intimate that the connection between the C-terminal fragment and the polymerase domain is simply not able to simultaneously perform the Dpb2 binding alongside leading strand synthesis, as it is formed in such a way that it cannot be placed onto the leading strand, or that the structure of the chimeric protein is folded in a way that is intrinsically unable to perform DNA synthesis. Alternatively, this could show that that the Pol δ chimera is at forks and, being less processive, cells struggle to synthetize the DNA. Since our aim was to create a chimera with comparable activity to Pol2, we chose not to pursue this any further.

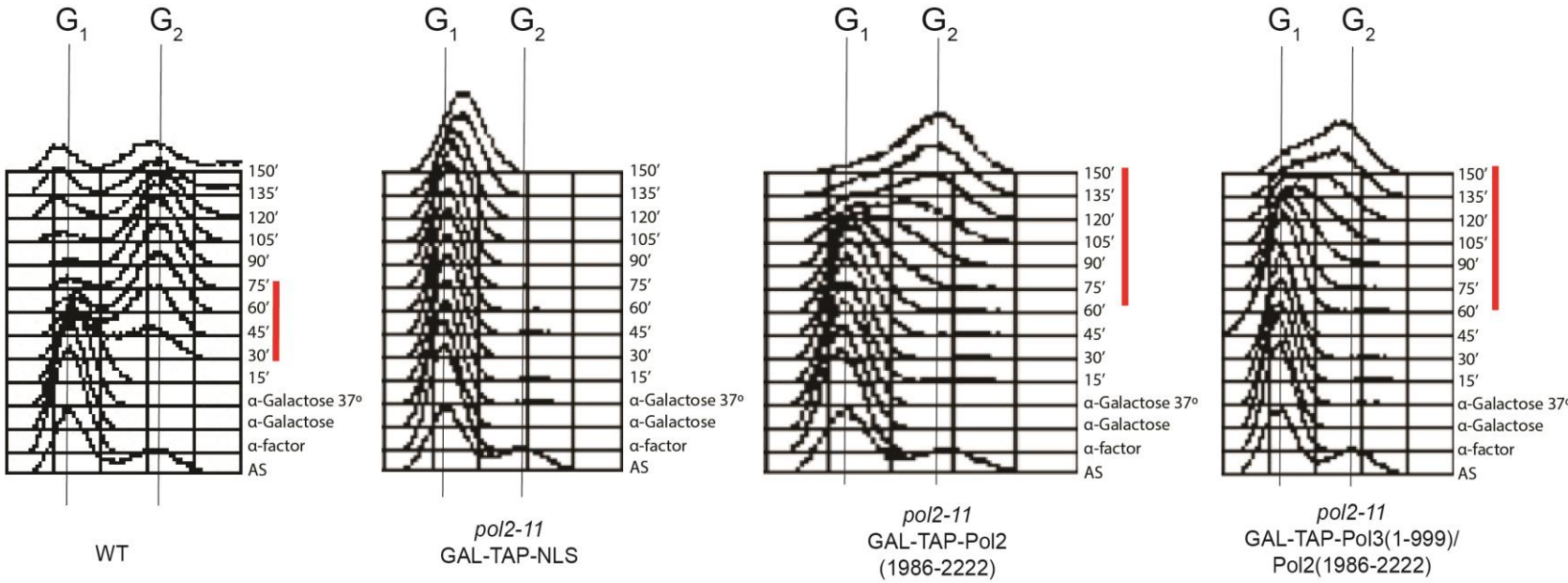

Figure 3.5: Fusing the Pol2 C-terminal fragment to an active polymerase domain is not able to recapitulate wild type replication when expressed in *pol2-11* cells. FACS profiles acquired from the wild type (CS 1), *pol2-11* with the TAP-NLS expressed (CS 1463), *pol2-11* with the TAP-Pol2 C-terminus (CS 1465) and *pol2-11* with the Pol3/Pol2 fusion (CS 1922) strains used in the dilution spotting assay above. The cells were arrested in G_1 with alpha factor in YP-Raf, before being resuspended in YP-Gal and then shifted to the restrictive temperature of 37°C and then being released from G_1 into S phase to complete replication. Black vertical lines indicate G_1 and G_2 peaks, where labelled and the red bar shows approximate time for replication. From this, it can be seen that fusing an active polymerase to the C-terminus is not able to recapitulate the wild type replication profile but instead most resembles that when the C-terminal fragment is expressed. Data shown is representative of 3 independent experiments.

3.7 The Pol2 C-terminus plays a role in fork progression.

Having seen this fragment participating in origin firing, I wanted to explore whether the fragment might play a role in fork progression as well. However, due to the lower levels origin firing observed in *pol2-11,* even with the presence of the C-terminus*,* replication time could not be used to measure this; so, we needed to first analyse the DNA replication dynamics in strains carrying a similar number of replication forks. Therefore, any difference in the time it takes to complete replication could be assigned to differences in fork progression. To accomplish this, *pol2-11* was coupled with a temperature-dependent degron conjugated to a temperature-sensitive allele of Sld3 (*sld3-7*) in order to prevent further origin firing. This heat-inducible degron is a cassette that is conjugated to the N-terminus of a target protein that encodes a ubiquitin molecule followed by a temperature sensitive dihydrofolate reductase (DHFR) complex. When the protein is translated, the ubiquitin molecule is immediately cleaved and this exposes an arginine residue that is recognized and bound by the Ubr1 E3 ligase associated with the ubiquitin-conjugating enzyme, Ubc2.When the temperature is raised to 37°C, the DHFR complex destabilizes and exposes numerous lysine residues that are polyubiquitinylated, thus targeting the protein as a whole for proteasome-mediated degradation (Dohmen et al., 1994). This system replaces the N-terminally tags Sld3 with the temperature degron cassette, termed *sld3-7*, and couples this with the E3 ubiquitin ligase, *UBR1,* under the control of a galactose-inducible promoter (Sanchez-Diaz et al., 2004). At the restrictive temperature coupled with expression of the ligase, the *sld3-7* protein is degraded and further origin licensing is blocked, however its degradation has no effect upon elongation (Kanemaki and Labib, 2006).

The experiment, outlined in Figure 3.6A, involved cells being arrested in G_1, and then released into an S phase block with HU at the permissive temperature to allow early origin firing. Cells were then switched to galactose and a temperature shift to 37°C to degrade and inactivate *sld3-7* and *pol2-11*, respectively. Here, the switch to galactose ensures the degradation of *sld3-7* as well as the expression of the TAP-tagged fragments. Cells were then released into S phase and samples taken every 10 minutes. By

analyzing the FACS profiles in Figure 3.6B, it can be seen that while replication is abated in the *sld3-7/POL2* cells, they were still able to finish replication with the reduced complement of origins. When the *sld3-7* and *pol2-11* were combined, the presence of the C- terminus allowed the cells to proceed through replication, with a 2C peak reached by the end of the experiment.

From these results, it seems the presence of the C-terminus is required in some capacity at the replication forks themselves in order for their progression. However, the nature of this function is remains to be elucidated. A possible explanation is the Pol2 C-terminal, by interacting with the replisome might stimulate the helicase activity of CMG, a function that has been given credence by a recent EM study showing the C-terminus binding both Cdc45 and, through Dpb2, the Mcm5-2 gate that promotes efficient translocation along DNA (Zhou et al., 2017). Alternatively, the presence of Pol2 C-terminal might somehow partially stabilize *pol2-11* and stimulate the role of DNA polymerase in fork progression.

A)

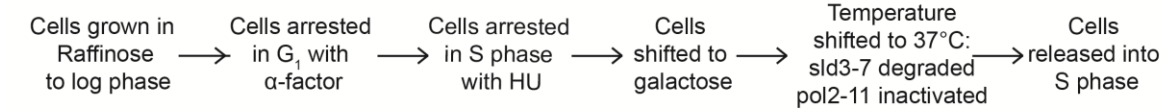
Cells grown in Raffinose to log phase
Cells arrested in G1 with α-factor
Cells arrested in S phase with HU
Cells shifted to galactose
Temperature shifted to 37°C: sld3-7 degraded pol2-11 inactivated
Cells released into S phase

B)

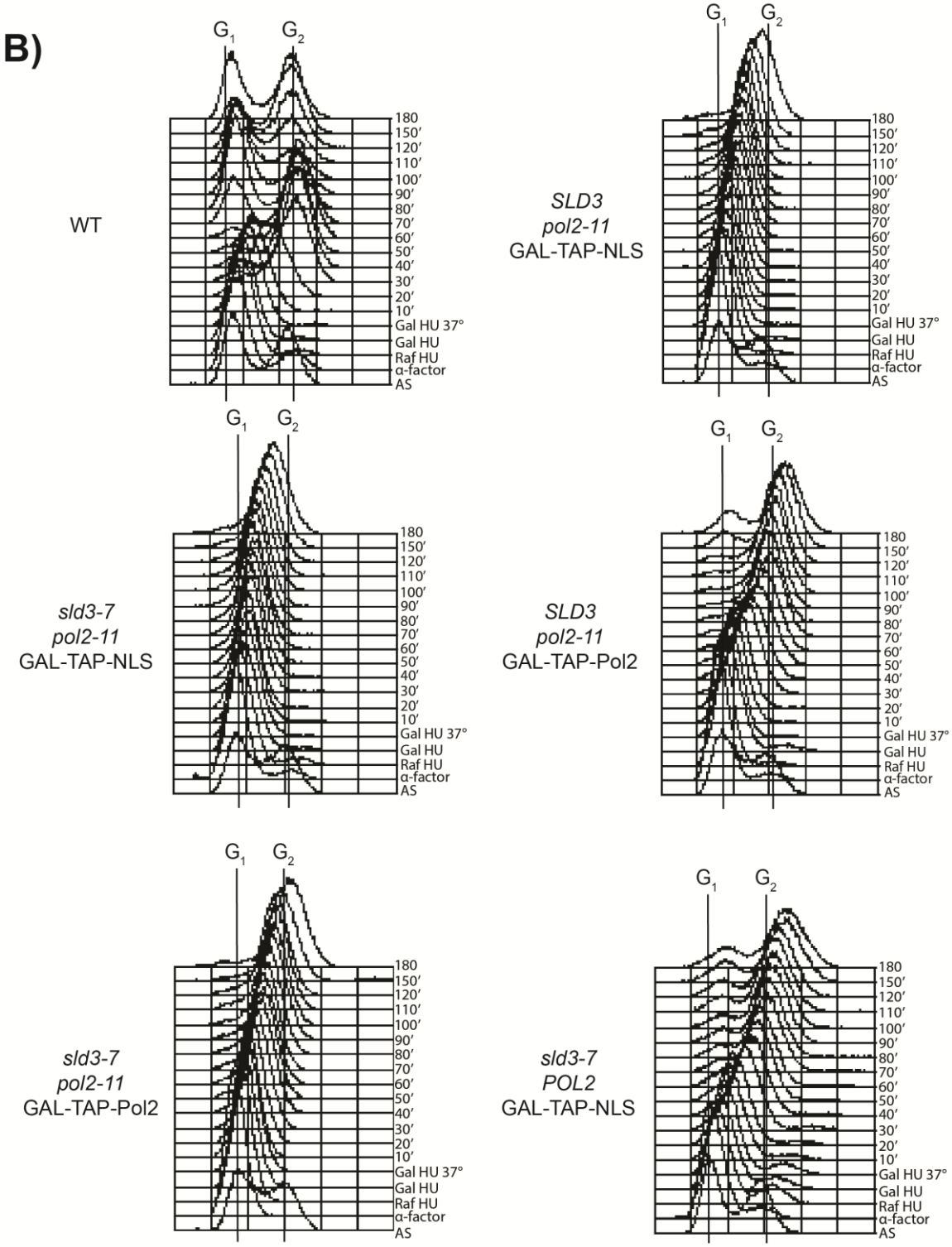
WT
SLD3 pol2-11 GAL-TAP-NLS
sld3-7 pol2-11 GAL-TAP-NLS
SLD3 pol2-11 GAL-TAP-Pol2
sld3-7 pol2-11 GAL-TAP-Pol2
sld3-7 POL2 GAL-TAP-NLS
G1
G2
180
150′
120′
110′
100′
90′
80′
70′
60′
50′
40′
30′
20′
10′
Gal HU 37°
Gal HU
Raf HU
α-factor
AS

Figure 3.6: The Pol2 C-terminus promotes fork progression in a *pol2-11* background. A) A schematic of the experiment carried out. First, cells were grown to log phase and arrested in G_1 followed by arresting in S phase in medium containing 0.2M HU so as to allow early-origin firing for 1 hour. Cells were then resuspended in YP-Gal to induce expression of the Pol2 C-terminus (1986-2222) and GAL-UBR1 for 35 minutes. Finally cells are shifted to 37°C so to degrade *sld3-7*, thus preventing further origin firing, and renders *pol2-11* non-functional for 1 hour. Cells were released in YP-Gal and samples taken every 10 minutes for 2 hours, at which point half hour samples were taken until 3 hours had elapsed. For this experiment, wild type cells (CS 1) were used alongside strains carrying wild type *SLD3* with *pol2-11* and either the empty construct or Pol2 C-terminus (CS 2180 and CS 2181, respectively). Strains with the *sld3-7* allele either had a wild type background with the empty construct (CS2182), or also possessed *pol2-11* with either the empty construct or Pol2 C-terminus (CS 2178 and CS 2179, respectively). **B)** The FACS profiles from these experiments, genotypes are shown to the left of each graph, lines indicating G_1 and G_2 peaks have been included. The *sld3-7/POL2* strain acts as a control, showing that replication can be completed with the lower numbers of origins firing, although replication is significantly slower than wild type. The profiles from *pol2-11/sld3-7* double mutants show how, with the C-terminus, replication proceeds to almost completion by the end of the time course, indicating a role for the fragment in fork progression.

3.8 Using mass spectrometry to analyse the possible interaction of Pol2 C-terminus.

In order to gain a better understanding of the role the Pol2 C-terminal fragment was playing in DNA replication, I decided to investigate its binding partners. To accomplish this, I used the experimental method shown in Figure 3.7A, in which I sought to use the C-terminus as 'bait' which I would proceed to purify by immunoprecipitation and identify the co-purified interactors through tandem mass spectrometry (MS). Initially, it was found that the TAP-tagged fragment proved extremely resistant to efficient, clean cleavage for the beads and so we decided to use a GST-6His tag instead. To purify the fragment, we performed a 2-step immunoprecipitation comprising of first pulling down the GST tag followed by the 6His. The efficiency of this reaction can be seen in the immunoblot shown in Figure 3.7B, in which a significant amount of the fragment is purified from the reaction, with comparatively little lost through inefficient binding or elution to and from the resins. However, the comparatively small amount of the Pol2 fragment being eluted compared to the control of the tag alone was a cause for concern, as large amounts of protein would be required to generate the hits on the subsequent MS screen. This is best illustrated by the Coomasie stain shown in Figure 3.7C, in which the purified Pol2 fragment is barely visible on the gel. Unfortunately, the samples sent for MS analysis were found to be extremely low in protein content and this made identification of potential interactors with the C-terminal fragment impossible. A successful screen for binding partners of the C-terminus would be a fruitful avenue as a means of understanding the function it plays in its *pol2-11* suppression, therefore it would be worthwhile exploring divergent means of accomplishing this goal, whether through the use of different tags and expression systems or even different identification methods altogether such as BioID.

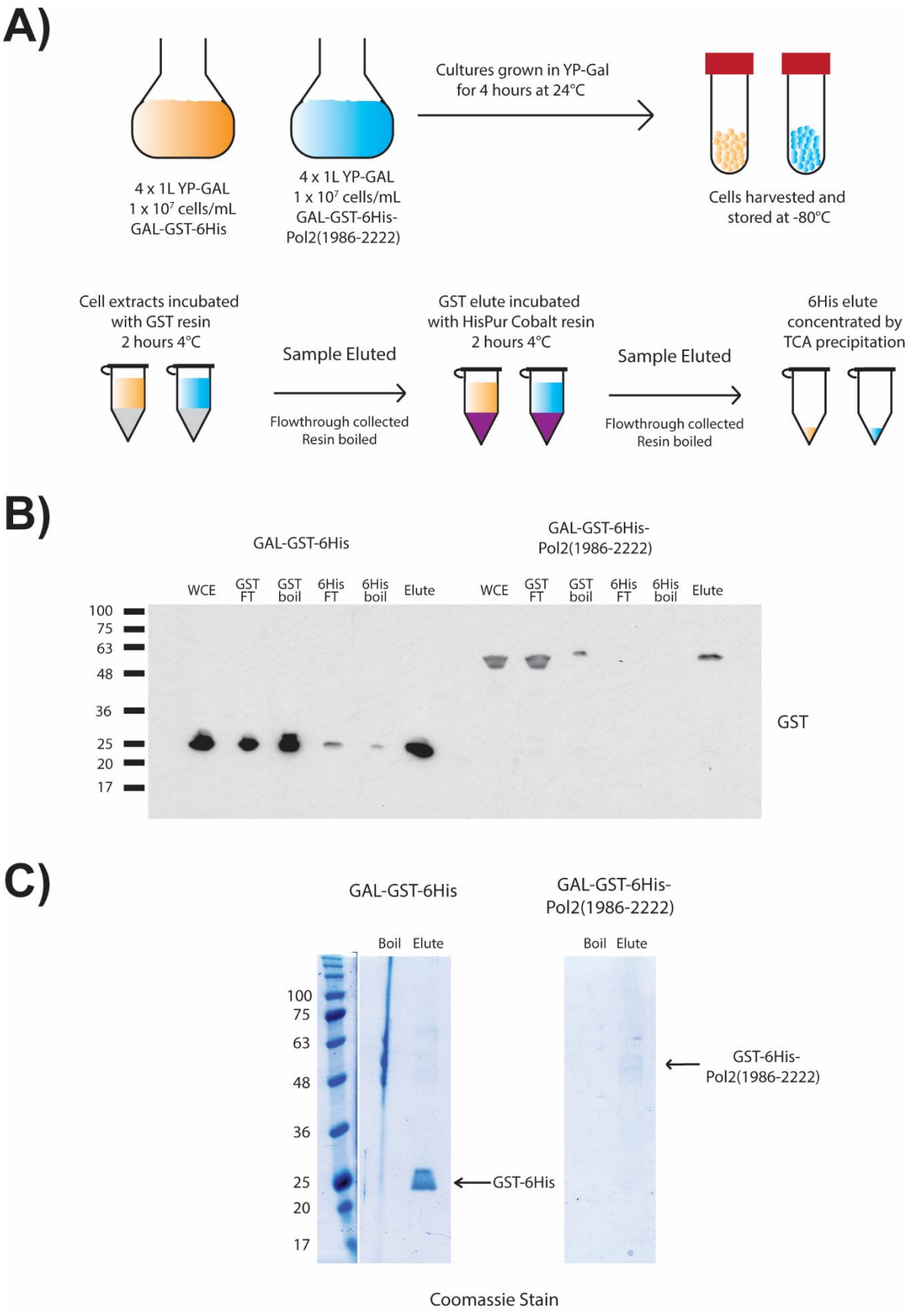
A)
4 x 1L YP-GAL
1 x 10^7 cells/mL
GAL-GST-6His
4 x 1L YP-GAL
1 x 10^7 cells/mL
GAL-GST-6His-
Pol2(1986-2222)
Cultures grown in YP-Gal
for 4 hours at 24°C
Cells harvested and
stored at -80°C
Cell extracts incubated
with GST resin
2 hours 4°C
Sample Eluted
Flowthrough collected
Resin boiled
GST elute incubated
with HisPur Cobalt resin
2 hours 4°C
Sample Eluted
Flowthrough collected
Resin boiled
6His elute
concentrated by
TCA precipitation
B)
GAL-GST-6His
GAL-GST-6His-
Pol2(1986-2222)
WCE
GST FT
GST boil
6His FT
6His boil
Elute
100
75
63
48
36
25
20
17
GST
C)
GAL-GST-6His
GAL-GST-6His-
Pol2(1986-2222)
Boil
Elute
100
75
63
48
36
25
20
17
GST-6His
GST-6His-
Pol2(1986-2222)
Coomassie Stain

Figure 3.7: Purification of the Pol2 C-terminal fragment in order to analyse its binding partners through mass spectrometry. A) A cartoon of the harvesting of yeast cells followed by the immunoprecipitation of the Pol2 fragment. The fragments that were immunoprecipitated were under a galactose-inducible promoter. As a control, one strain expressed just a GST-6His tag, while the other had this conjugated to the 236 aa Pol2 C-terminal fragment (CS 2944 and CS 2748, respectively). 4 litres of culture of each strain were grown asynchronously in YP-Raf until reaching a cell density of 1 x 10^7 cells/mL, when they were resuspended in YP-Gal. Samples were harvested after having the fragment expression induced for four hours. These samples were then used in a two-step IP in which they were first underwent a GST pulldown followed by purification with their 6His tag. The final elutions were TCA precipitated to maximise protein concentration prior to mass spectrometric analysis. Size markers are indicated by the dark horizontal lines and corresponding numbers measured in kDa. **B)** An immunoblot of GST of samples taken from various stages the 2-step IP samples. Samples were taken from whole cell extracts (WCE), flowthroughs (FT) after incubation with the resin and boiled resins (boil) to see the efficiencies of the binding and elution during each step. **C)** A Coomasie stain of the boiled and elution samples obtained from the second step of the IP to show the protein content within with expressed tagged proteins labelled.

3.9 Mutating the hydrophobic residues abrogate the suppressive effects of the Pol2 C-terminal fragment.

After having seen the ability of this C-terminal fragment to suppress the temperature sensitivity of *pol2-11*, the next step was to understand the properties of the protein that underpins this. The first step was a simple protein sequence alignment using the PRALINE service provided by Vrije Universiteit Amsterdam's Centre for Integrative Bioinformatics. Here, the alignment was carried out with the last 130 residues of the budding yeast sequence against the orthologues of *S. pombe*, *D. melanogaster*, zebrafish, mice and humans to measure their conservation. From the alignment shown in Figure 3.8A, it is clear there are certain aspects of these fragments, including the two zinc fingers and certain hydrophobic residues beyond the second zinc finger, that are well conserved between these orthologues. These latter two features were chosen to study their possible involvement in the observed phenotype. For this, four new fragments were created: two shorter fragments as well as different point mutants (here we show the *mutB* and *mutE*). The new shorter Pol2 fragments that were created were reduced from the 236 residues used previously to 119 aa and 60 aa long fragments, with the latter only containing the second zinc finger. These are represented by GAL-TAP-Pol2 (2103-2222) and GAL-TAP-Pol2 (2162-2222) in Fig 3.8, respectively. I also generated two mutants, shown below the sequence alignment and named MutB and MutE. The first targeted two cysteines within the second zinc finger, and mutated them to serine, while the latter mutated several conserved hydrophobic residues at the extreme C-terminus of Pol2 to alanine. In Fig 3.8, these are indicated by the labels GAL-TAP-Pol2 (2103-2222) Mut B and GAL-TAP-Pol2 (2103-2222) Mut E, respectively. All these new Pol2 C-terminal fragments were placed under the same expression systems with the same tags as before.

These new Pol2 fragments were used in a dilution spotting experiment in conjunction with the *pol2-11* allele to assess their ability to suppress its defects and this is shown in Figure 3.8B. Interestingly, both of the shorter fragments retained their ability to suppress the temperature sensitivity and checkpoint defects, even the shortest one containing just the second zinc

finger. Somewhat consistently with the understanding of the importance of this second zinc finger, *mut B* lost its suppressive effect although somewhat remarkably it retained its ability to restore viability in the presence of HU (Baranovskiy et al., 2017). The high conservation of the C-terminal hydrophobic residues seems to underly their importance to the function of this C-terminus, as their mutation results in a loss of its suppressive activity both at restrictive temperature and in conditions of replication stress. Fig 3.8C shows an immunoblot for TAP of cell extracts after galactose-driven expression. These results illustrate that none of the phenotypes that have been observed can be due to inefficient expression of the fragments or degradation, as their bands are all present.

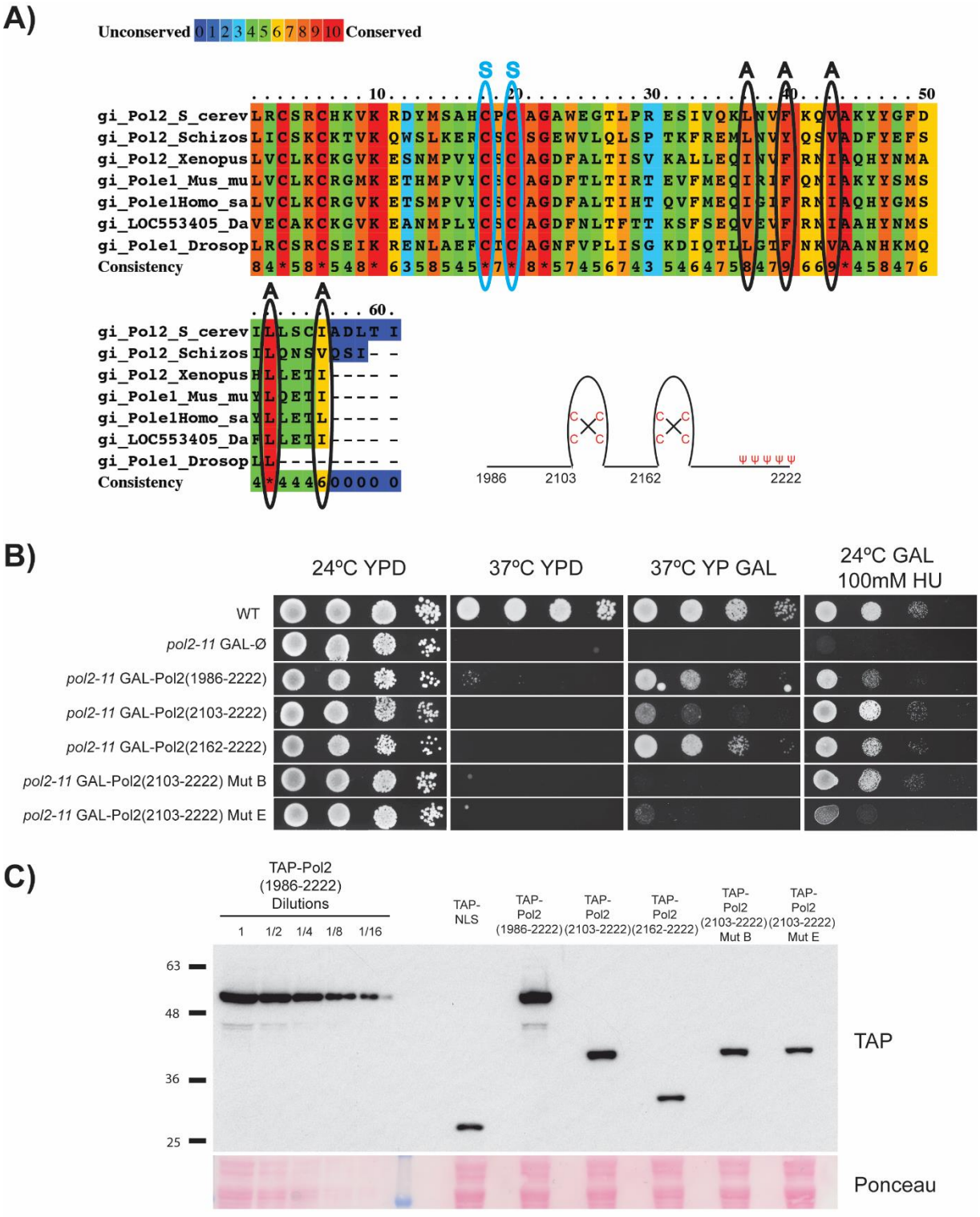
A)
Unconserved 0 1 2 3 4 5 6 7 8 9 10 Conserved
S S
A A A
10 20 30 40 50
gi_Pol2_S_cerev LRCSRCHKVK RDYMSAHCPC AGAWEGTLPR ESIVQKLNVF KQVAKYYGFD
gi_Pol2_Schizos LICSKCKTVK QWSLKERCSC SGEWVLQLSP TKFREMLNVY QSVADFYEFS
gi_Pol2_Xenopus LVCLKCKGVK ESNMPVYCSC AGDFALTISV KALLEQINVF RNIAQHYNMA
gi_Pole1_Mus_mu LVCLKCRGMK ETHMPVYCSC AGDFTLTIRT EVFMEQIRIF QNIAKYYSMS
gi_Pole1Homo_sa LVCLKCRGVK ETSMPVYCSC AGDFALTIHT QVFMEQIGIF RNIAQHYGMS
gi_LOC553405_Da VECAKCKGVK EANMPLYCSC AGDFNLTFTT KSFSEQVEVF RNIAAHYNMS
gi_Pole1_Drosop LRCSRCSEIK RENLAEFCTC AGNFVPLISG KDIQTLLGTF NKVAANHKMQ
Consistency 84*58*548* 6358545*7* 8*5745674 3 5464758479 669*458476
A A
60
gi_Pol2_S_cerev ILLSCIADLT I
gi_Pol2_Schizos ILQNSVQSI- -
gi_Pol2_Xenopus HLLETI---- -
gi_Pole1_Mus_mu YLQETI---- -
gi_Pole1Homo_sa YLLETL---- -
gi_LOC553405_Da FLLETI---- -
gi_Pole1_Drosop LL---------- -
Consistency 4*4446 0000 0
C C C C
C C C C
ψ ψ ψ ψ ψ
1986 2103 2162 2222
B)
24°C YPD
37°C YPD
37°C YP GAL
24°C GAL 100mM HU
WT
pol2-11 GAL-Ø
pol2-11 GAL-Pol2(1986-2222)
pol2-11 GAL-Pol2(2103-2222)
pol2-11 GAL-Pol2(2162-2222)
pol2-11 GAL-Pol2(2103-2222) Mut B
pol2-11 GAL-Pol2(2103-2222) Mut E
C)
TAP-Pol2 (1986-2222) Dilutions
1 1/2 1/4 1/8 1/16
TAP-NLS
TAP-Pol2 (1986-2222)
TAP-Pol2 (2103-2222)
TAP-Pol2 (2162-2222)
TAP-Pol2 (2103-2222) Mut B
TAP-Pol2 (2103-2222) Mut E
63
48
36
25
TAP
Ponceau

Figure 3.8: The conserved second zinc-finger and the hydrophobic residues at the extreme of the Pol2 C-terminus are essential for the suppressive function of *pol2-11*. A) A PRALINE alignment of the last 61 residues of Pol2 with its orthologues in *S. pombe, X. laevis, M. musculus, H. sapiens, D. rerio* and *D. melanogaster*. Colour-coded red to blue to indicate high to low levels of conservation. Blue circles were placed around the Cysteines of the second Zinc finger that were mutated to serine in Mutant B and black circles placed around the residues mutated to Alanine in Mutant E. **B)** The suppressive abilities of progressively shorter C-terminal fragments and containing mutations of conserved amino acids were tested by growth at 37°C or in the presence of 150mM HU). Mutating the second zinc finger (mutant B) unsurprisingly abrogated its suppressive effects, maybe due to its importance in Dpb2 binding. The hydrophobic residue mutant (mutant E) causes the C-terminal fragment to lose the ability to suppress the temperature and damage sensitivities of *pol2-11*, possibly indicating an essential role in the function of Pol2. Additionally, the suppressive effect of the fragment was still present in the shorter fragments used in this experiment, even when only the last 60 residues containing the last zinc finger and subsequent hydrophobic residue-rich sequence were expressed. Strains used in order of top to bottom: CS 1, CS 1463, CS 1465, CS 2099, CS 2101, CS 2105, CS 2111. Plate scans were taken 72 hours after spotting and these results have been observed two independent experiments. **C)** Immunoblots for TAP as well as a Ponceau stain used as a loading control performed on samples collected after galactose induction from the strains used in (B) to illustrate the expression of the Pol2 constructs. Also included is a serial dilution of the 1986-2222 fragment sample to show the signal linearity in relation to the protein abundance. Size markers are indicated by the dark horizontal lines and corresponding numbers measured in kDa

3.10 Mutating the hydrophobic residues of the full-length Pol2 causes synthetic defects with an *SLD2* mutant.

To this end, the five hydrophobic residues were mutated to alanine in the genomic copy of *POL2*, and the resultant strain's (*pol2 mut E*) phenotypes were initially assessed by virtue of a dilution spotting experiment, as shown in Figure 3.9. As can be seen from its full viability both at higher temperatures and in conditions of replication stress, mutating these residues appears to have little effect on the normal functioning of Pol2. However, in an attempt to probe any possible difference in function, this allele was crossed with many alleles characterised by either origin firing or checkpoint defect. One such allele was *sld2-6*, a double point mutant of *SLD2* that has been shown to be temperature sensitive, synthetically lethal with *pol2-11,* and defective in binding to Dpb11 (Kamimura et al., 1998). Notably, this allele produced synthetic defects with *pol2 mut E*, where its viability is significantly reduced at 33°C compared to the single mutant. The reason underlying this reduced growth is unclear, but it is reasonable to conclude that these hydrophobic residues could underly Pol2's binding in the pre-LC, exacerbating the already present instability inherent to the presence of *sld2-6*.

3.11 The hydrophobic mutant of Pol2, *pol2 mut E*, does not exhibit origin firing defects.

To further probe any possible defects present in the *pol2 mut E* allele that are perhaps too subtle to be observable in an experiment that just measures viability, a single-step immunoprecipitation was carried out to give a measure of its origin licensing ability. This experiment was carried out in a similar manner to the experiment in Figure 3.3, except samples here were taken at G_1, after a 30 minute release into S phase and after 90 minutes exposure to 0.2M HU. From these results, shown in Figure 3.10, very little distinction can be made between the wild type and mutant allele, indicating there is very little difference in origin firing when these hydrophobic residues are mutated, which correlates with the viability shown by the dilution spotting. This, however, does not explain why there is a synthetic defect with *sld2-6* as

it could reasonably be expected that if this was caused by these two alleles being each side of the same binding site then a moderate defect would be noticeable.

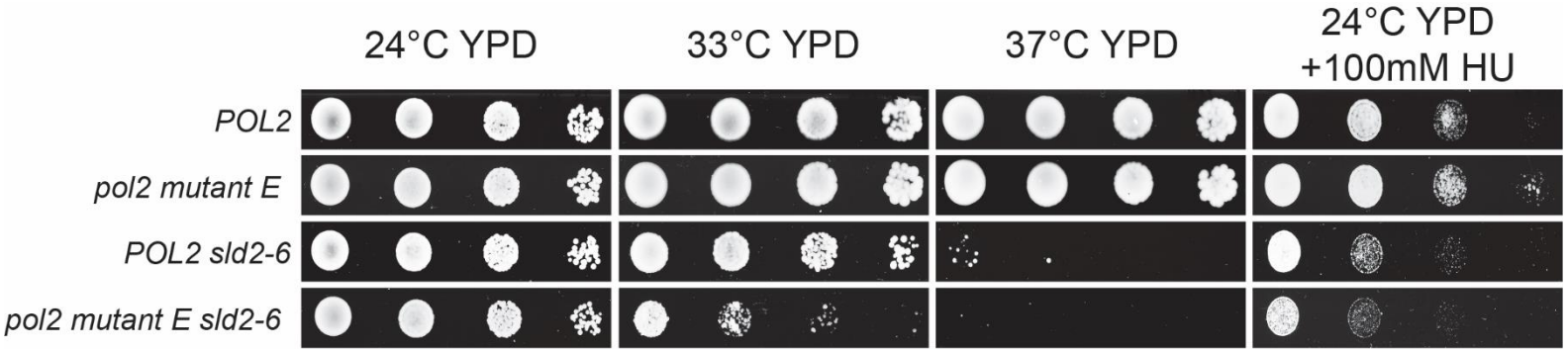

Figure 3.9: The presence of the C-terminal hydrophobic residues in a genomic copy of *POL2* is not essential for viability, but shows synthetic defects with *sld2*-6 mutations. A dilution spotting experiment was performed with strains that contained the Mutant E alanine mutations in a genomic copy of *POL2*. Alone, these provided little phenotypic difference in growth, however, in the presence of the temperature sensitive *sld2-6*, an observable loss of viability was noted at restrictive temperatures. This could indicate a possible role in mediating its binding in the pre-loading complex during origin firing. Strains used in order of top to bottom: CS 1, CS 2308, CS 2742, CS 2752. Plate scans were 72 taken hours after spotting and these results are representative of 3 independent experiments.

3.12 *pol2 mut E* shows no signs of defective Dpb2 binding.

Having hypothesised about the possibility of defective inter-complex binding being the root of the decreased vialbility of the double mutant, it was important to confirm that the binding between polymerase ε subunits was still normal, and for this another immunoprecipitation experiment was performed. Here, Dpb3 was TAP-tagged and immunoprecipitated, which was then followed by either a low (100mM) or high (700mM) stringency salt wash. The high stringency wash is not enough to separate the Pol2 and Dpb2 subunits with their wild type binding dynamics, but if their interface is disrupted then this should be shown by this experiment. Dpb2 and Pol2 were immunoblotted from the immunoprecipitated samples alongside Dpb3-TAP to assess the amounts of protein in each sample. By analysing the levels of co-precipitation of Dpb2 between the two washes can give a measure of the strength of the Pol2-Dpb2 interaction.

The results of this, displayed in Figure 3.11, show very little difference in Dpb2 levels between the low and high stringency washes, indicating that the Dpb2 binding interface with Pol2 remains strong and unaffected by the mutated hydrophobic residues. The result here is consistent with previous yeast-2-hybrid (De Piccoli, unpublished data) showing Dpb2 binding in the *pol2 mut E* C-terminal fragment as well as with the understanding that is solely the second zinc finger that is responsible for this interaction. While the Dpb2 binding remains intact in this Pol2 mutant, it could still be having effects beyond Pol ε in the wider context of a larger assembly of proteins such as the pre-loading complex, explaining the synthetic defect noted with *sld2-6.*

3.13 *pol2 mut E* shows an improved viability with a temperature sensitive mutant of *MCM10, mcm10-1.*

Having observed the importance of these hydrophobic residues in the function of the Pol2 C-terminal fragments as well as its potential role in stabilising the formation of the pre-loading complex with Sld2, it was assumed that mutating these would only cause deleterious effects for the resultant cells. Interestingly, after having screened for synthetic defects with

numerous other origin firing and checkpoint-associated proteins, including *rad9Δ*, *mrc1Δ, sld3-5, cdc7-1* and *dpb11-1*, one cross provided an increased viability. This was with a temperature sensitive mutant of *MCM10*, a protein involved in the initiation of origin licensing as well as a potentially novel role in stimulating the helicase of the replisome (van Deursen et al., 2012, Douglas et al., 2018). This point mutant with a heat-inducible degron, *mcm10-1td* (known as *mcm10-1* herein), was coupled with an E3 ubiquitin ligase, *UBR1*, expressed under a galactose-inducible promoter which assisted the degradation of the misfolded protein at restrictive temperatures. The temperature sensitivity inherent to *mcm10-1* was pinpointed to defects in origin firing, as well as fork stalling before the elongation phase of replication (Homesley et al., 2000). Interestingly, this latter defect could be suppressed with the presence of temperature sensitive mutants of the MCM2-7 complexes, *MCM5* and *MCM7*, which restored the perturbed physical interaction between the two proteins and removed both the origin firing and fork pausing defects seen in the single mutant (Homesley et al., 2000).

The improved viability of this *mcm10-1/pol2 mut E* double mutant can be seen in the dilution spotting experiment shown in Figure 3.12. Here, as the temperature the cells are grown at is increased, the viability of the cells decreases when *mcm10-1* is present, however there is a far greater drop-off in the single mutant strain. In the presence of galactose, as *UBR1* is expressed, this temperature sensitivity is much more severe as both the single and double mutant are non-viable at 33°C, presumably as the mcm10 that is present is degraded much quicker. Interestingly, there is no difference in viability between the two strains when grown in the presence of HU, even in the presence of galactose, where a difference in growth between the single and double mutants can be seen at 24°C with no replication stress.

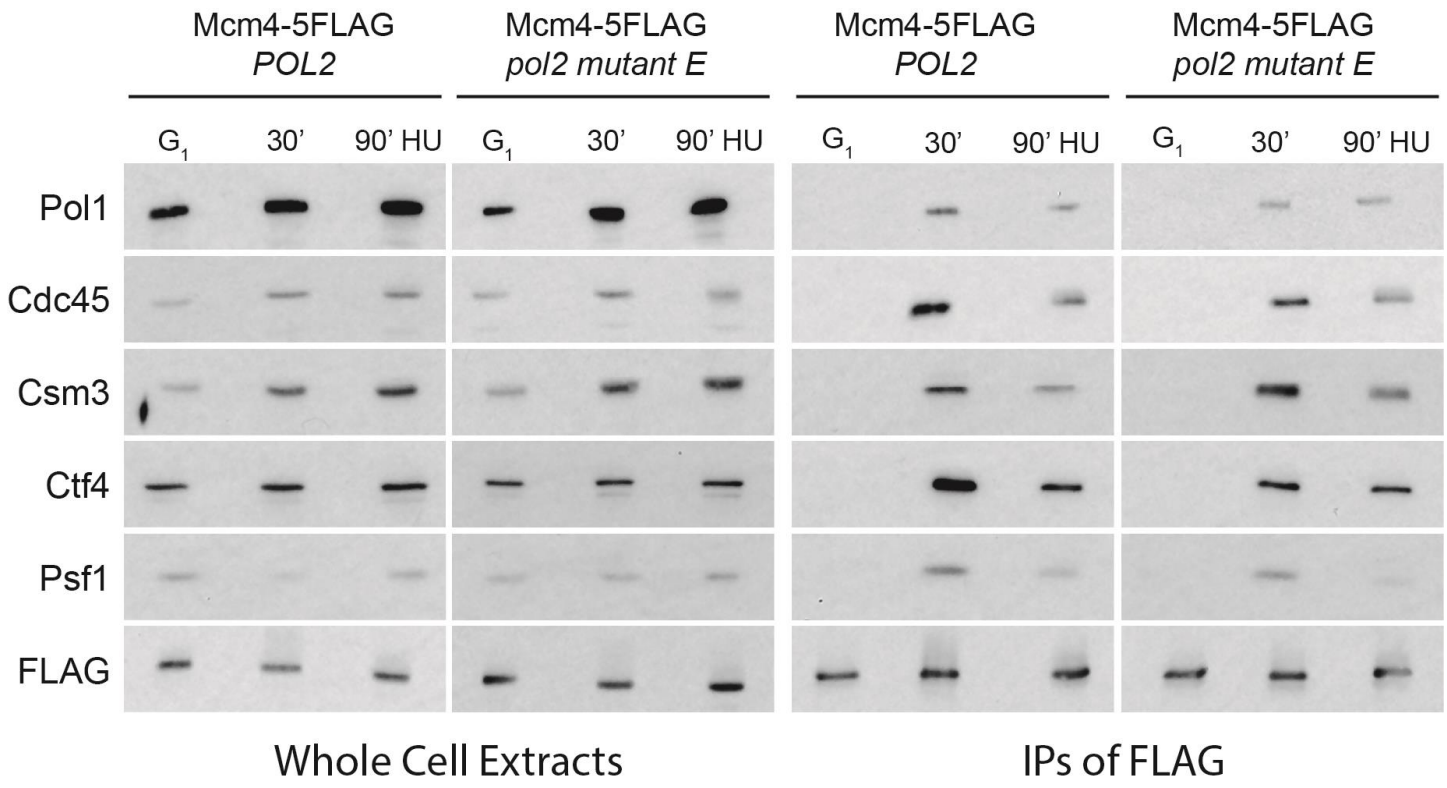

Figure 3.10: Mutating the hydrophobic residues in the Pol2 C-terminus in a genomic copy of *POL2* to alanine has no effect on origin firing. Cells carrying a FLAG-tagged version of Mcm4 in either a wild type or *pol2 mutant E* background (CS 1166 and CS 2345, respectively). These were arrested in alpha factor at 24°C, and then released either for 30' in YPD or for 90' into YPD 0.2 M HU. Samples were collected and frozen at the indicated times. Following single-step immuno-precipitation, samples were analysed by immunoblotting. Compared to the wild type Pol2, those with the fragment form similar amounts of CMG, indicating that the Mutant E allele of *POL2* is able to facilitate the process of loading and firing of origins with little impediment.

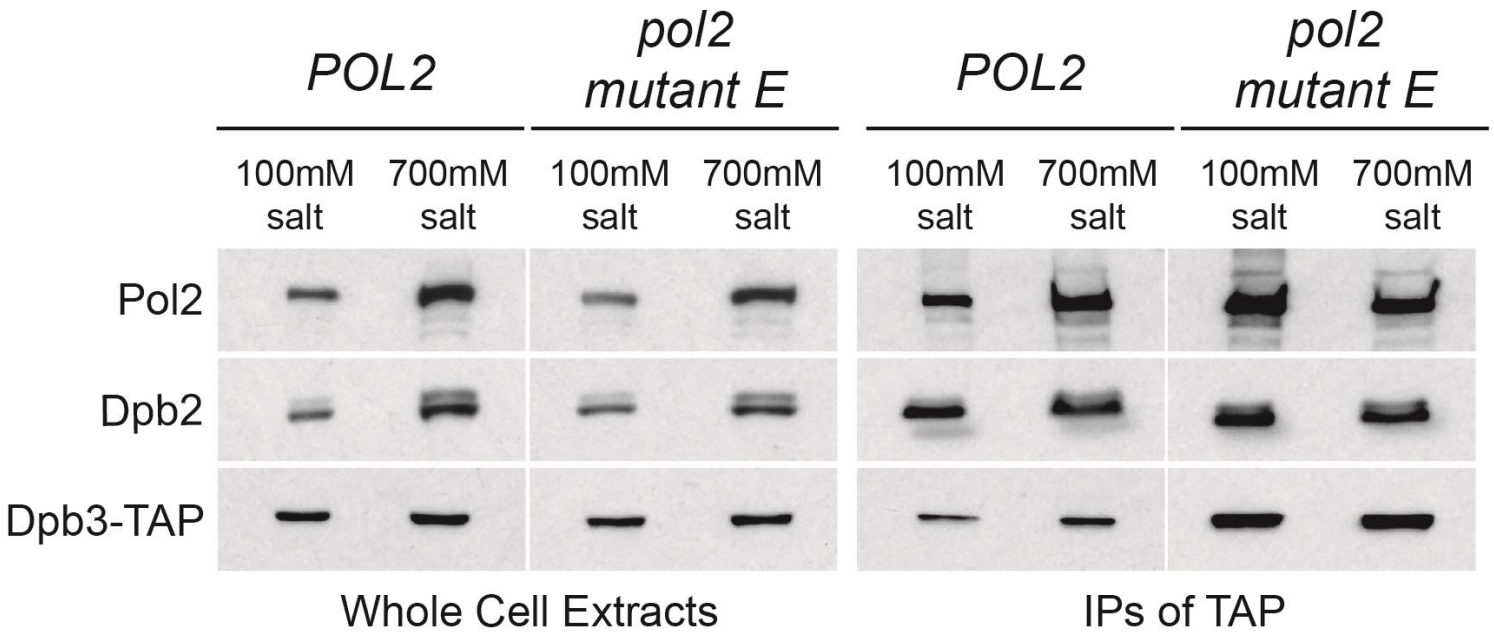

Figure 3.11: Pol2-Dpb2 binding is not affected by mutating the hydrophobic residues to alanine. Cells carrying a TAP-tagged version of Dpb3 in either a wild type or *pol2 mutant E* background (CS 3324 and CS 3328, respectively), were grown to exponential phase at 24°C. When the cells reached a density of 1-2 107 cells/ml, samples were collected and frozen. Following single-step immuno-precipitation using different salt concentrations (100mM and 700mM) to assess the stringency of the binding between Pol2 and Dpb2, samples were analysed by immunoblotting. The similar levels of Pol2 and Dpb2 between the two strains that can be observed from this experiment indicate that the presence of these mutations do not affect the Dpb2-Pol2 binding interface nor the stability of the Pol ε complex as a whole.

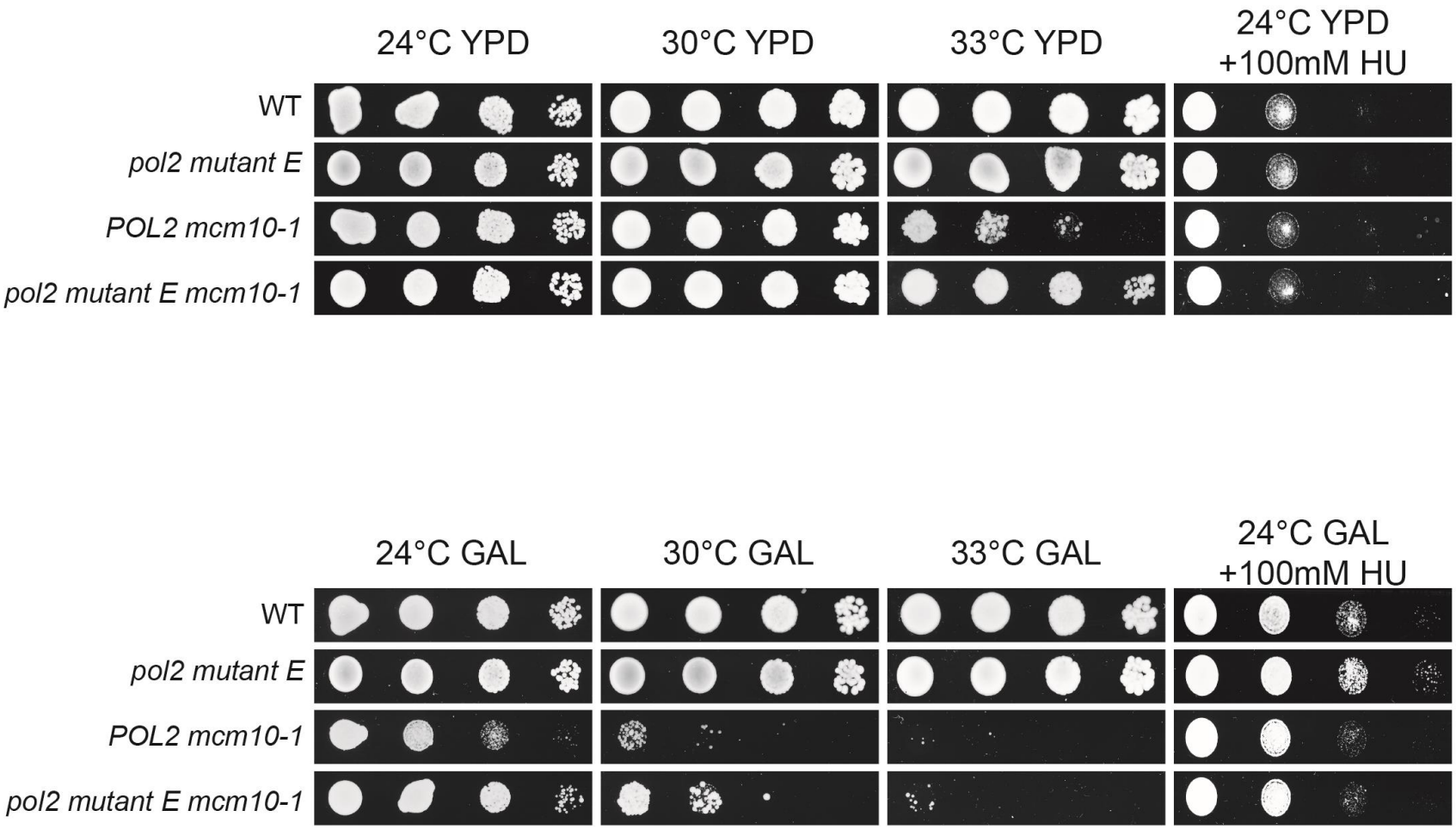
24°C YPD
30°C YPD
33°C YPD
24°C YPD
+100mM HU
WT
pol2 mutant E
POL2 mcm10-1
pol2 mutant E mcm10-1
24°C GAL
30°C GAL
33°C GAL
24°C GAL
+100mM HU
WT
pol2 mutant E
POL2 mcm10-1
pol2 mutant E mcm10-1

Figure 3.12: The presence of Pol2 Mutant E alleviates the temperature sensitivity exhibited by the *mcm10-1* allele, indicating a possible role of these conserved hydrophobic residues that is independent of origin firing efficiency. Dilution spotting experiment comparing the viabilities of strains containing *pol2 mutant E* and *mcm10-1*. The latter is temperature sensitive beyond 30°C in the presence of glucose and 28°C when grown in galactose. The temperature sensitivity phenotype is 'tighter' in the latter as this induces the expression of UBR1, a ubiquitin ligase, which aids the degradation of the mutant protein. In both cases, the double mutant has significantly improved viability, indicating some interaction between the two proteins. Strains used in order of top to bottom: CS 1, CS 2308, CS 2942, CS 2943. Plate scans were taken 72 hours after spotting and these results are representative of 3 independent experiments.

3.14 The *pol2 mut E/mcm10-1* double mutant shows no signs of impaired origin firing function.

In order to understand the observations made from this initial experiment, a single-step immunoprecipitation was carried out in order to assess the levels of origin firing between the single and double mutants of *mcm10-1* and *pol2 mut E*. Samples were collected 30 minutes after a release from G_1 in order to get the representative level of replication forks from a standard S phase. This experiment was carried out at 33°C in YPD, as this was the best illustration of the difference in viability observed from the dilution spotting experiment performed earlier. *MCM3* was TAP-tagged and this was then immunoprecipitated for the samples to be immunoblotted for other replisomal components, in this case Pol2, Cdc45 and GINS (Sld5). The presence of Csm3 was also checked to confirm the samples taken were in fact in S phase.

From the results observed in Figure 3.13, it can be seen that there is very little difference in the protein levels between any of the strains. This indicates that differences in origin firing is not what underlies the differences in viability that are seen between the single and double mutant at the restrictive temperature. Therefore, with what is known about *mcm10-1,* still leaves the possibility that it could instead be due to fork pausing before elongation occurs.

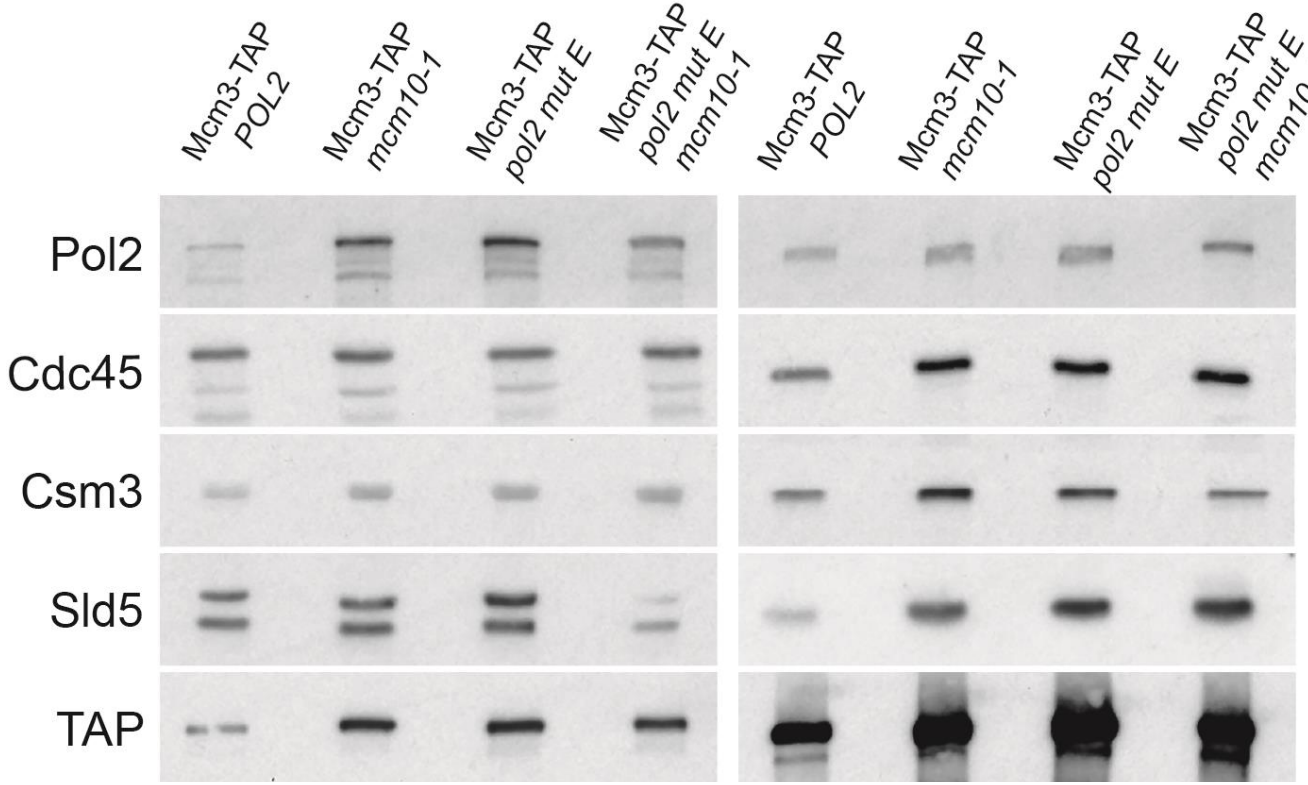

Figure 3.13: The single and double *pol2 mutant E* and *mcm10-1* mutants do not show lower levels of origin firing. Cells carrying a TAP-tagged version of Mcm3 in either a wild type (CS 3037), *mcm10-1* (CS 3039)*, pol2 mutant E (*CS 3041) or double mutant (CS 3043) background. Cells were grown to exponential phase at 24°C in YPD, were arrested in alpha factor, shifted at 33°C for 1 hour and then released for 20' in S phase. Samples were collected and frozen. Following single-step immuno-precipitation samples were analysed by immunoblotting. This Western blot shows little difference in replisome formation, indicating that origin firing efficiency is not what is underlying the improved viability noted when the *POL2* mutant is present with the *mcm10-1* allele.

3.15 The *pol2 mut E* could suppress the elongation defect of *mcm10-1* cells.

Having seen that levels of origin firing appear identical in both *mcm10-1* strains, observing replication dynamics was seen to be the best way at pinpointing the underlying issue in replication that was causing the disparity in cell growth. So, FACS experiments were carried out at 24°C in which cells were arrested in G_1, resuspended in a galactose-based medium to induce *UBR1* expression, and then released from G_1 into S phase. FACS samples were collected every 15 minutes for 3 hours and trichloroacetic acid (TCA) precipitated protein samples were taken every 30 minutes. These were then immunoblotted for Pol2 and Rad53; the former to ensure that this was not being degraded due to the presence of the ubiquitin ligase and the latter to understand if any aberrant replication was due to checkpoint activation. The FACS profiles are shown in Figure 3.14 and below each are the immunoblots from the TCA samples.

While none of the samples in these experiments fully complete one round of replication, both *MCM10* strains are able to form substantial G_2 after 3 hours and this is not seen in the single and double mutants of *mcm10-1.* In these latter strains, a clear difference can be observed between them, as the *pol2 mut E* strain is able to complete a large portion of its genome duplication even though they appear to actually start at roughly the same point (at the 90-105 minute mark). Knowing that the levels of origin firing are constant between these two strains, it is highly possible that the defect in transitioning to elongation previously noted in *mcm10-1* cells is what is underlying the slower replication in the single mutant, while the double mutant is somehow able to partially bypass this. Analysing the immunoblots shows that Pol2 levels remain constant through the experiment, while the checkpoint remains inactive in the two *MCM10* strains. However, the presence of *mcm10-1* causes a small activation at the 120 minute sample (at the beginning of replication), which would be consistent with the forks emerging from origins pausing before they transition to the elongation phase. Unfortunately, FACS analysis is not able to provide detailed enough information about the underpinnings of these differing replication profiles and for this to be

conclusively shown to be due to different levels of fork pausing after initiation another method would need to be used, such as DNA combing.

POL2

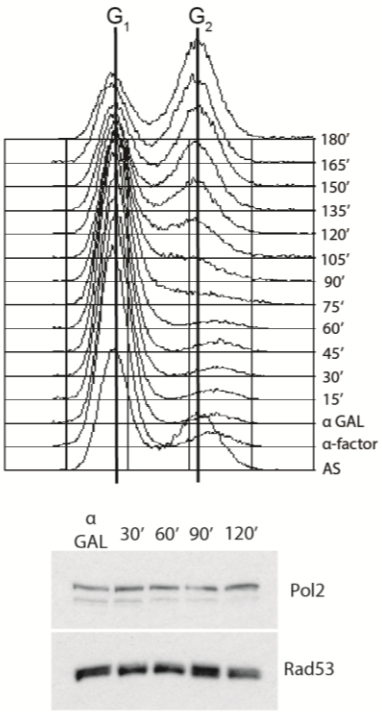

pol2 mut E

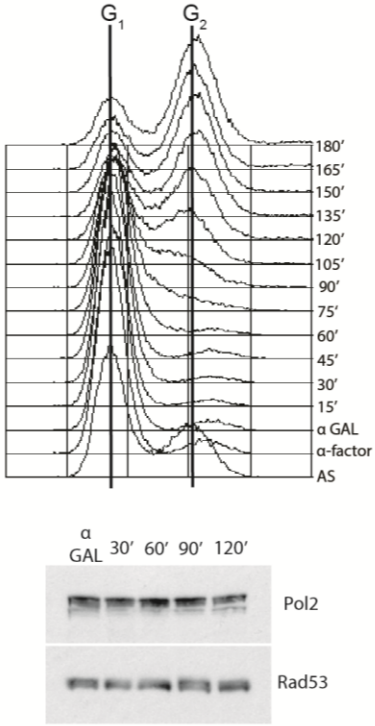

POL2
mcm10-1

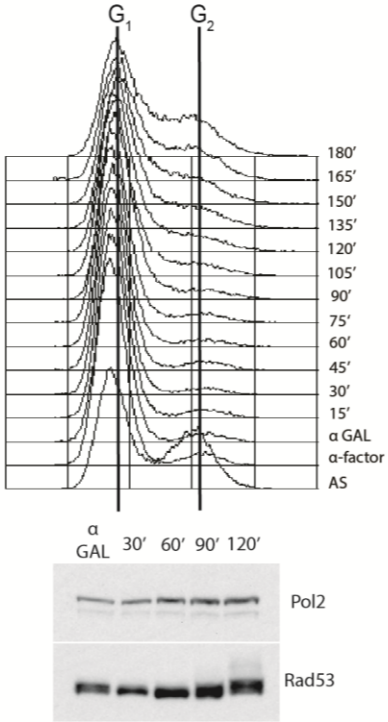

pol2 mut E
mcm10-1

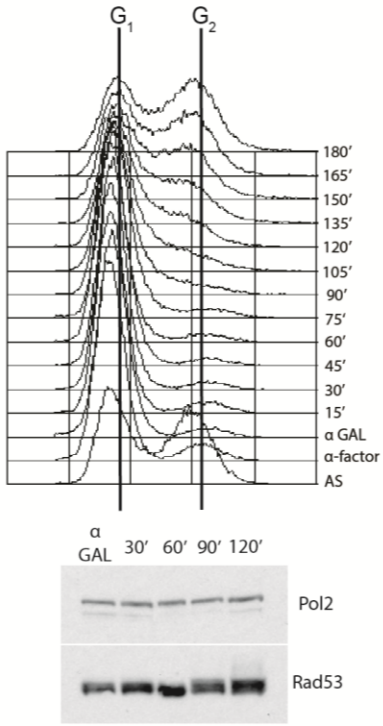

Figure 3.14: Analysis of the replication dynamics in cells with *pol2 mutant E* in the presence or absence of *mcm10-1*. FACS experiment using a wild type strain (CS 1) alongside single mutants of *pol2 mutant E* (CS 2308) and *mcm10-1* (CS 2942) as well as the double mutant (CS 2943). Cells were grown to the exponential phase, arrested in alpha factor, then shifted to the restrictive temperature of 33°C for 1 hour. Cells were then released in S phase to carry out one round of replication. Alpha factor was then added back after 90 minutes to re-arrest cells after completing replication. G_1 and G_2 peaks are labeled and the red bars indicate the length of time required for replication to complete. Immunoblots of Pol2 and Rad53 are shown below each FACS profile, with the samples taken from this experiment at 30 minute intervals for the first two hours of the release. While in *mcm10-1* cells there is little progression in S phase, in the double mutant a larger fraction of the cell population progresses and completes DNA replication. Additionally, the blots show that a weak activation in Rad53 in both *mcm10-1* strains, although with little difference between the *POL2* alleles. Additionally, it is clear Pol2 is not being degraded as its protein levels remain stable throughout. We noticed that in all of these strains, the onset replication appeared much delayed, but this effect was consistent. These FACS profiles are representative of 5 independent experiments.

3.16 Mutating the hydrophobic residues of Pol2 to glutamates produces a phenotype similar to *pol2-11.*

After the genomic *pol2 mut E* did not display as severe a phenotype alone as originally predicted, it was decided to attempt to push this system further by mutating the hydrophobic residues to hydrophilic residues instead of alanines. So, a new genomic mutant was created, called *pol2 mut E(E)*, in which the five residues were each mutated to glutamates, as shown in the new protein sequence in Figure 3.15A. The resultant strains were viable and they were first subjected to a dilution spotting experiment to analyse their growth at different temperatures as well as in the presence of HU. Additionally, this *POL2* allele was crossed with deletions of checkpoint-associated proteins as well as two other alleles with which synthetic effects were noted in the alanine *pol2 mut E*. What is immediately noticeable is the temperature sensitivity now exhibited in this new mutant. While this appears similar to the phenotype exhibited by *pol2-11*, a mutant lacking the last 26 aa, *pol2 mut E* (E) does not share the checkpoint defects, as its growth in conditions of replication stress remain similar to the wild type, indicating that these hydrophobic residues are unlikely the source of Pol2's functioning in checkpoint signalling. Interestingly, this observation points to a separation of function between the role in origin firing observed in *pol2-11* and the response to replication stress. Further to this, when crossed with the S phase and DNA damage checkpoint-associated proteins Mrc1 and Rad9, respectively, these strains are neither lethal nor possess synthetic defects, indicating that the functional underpinning of Pol2's role in checkpoint signalling is not in these residues.

Having seen the synthetic effects that occurred between the alanine mutant and *mcm10-1* and *sld2-6*, these were inserted into the new glutamate mutant to examine what the resultant phenotypes would be and whether they would be more extreme. In the case of *mcm10-1*, the results were not completely clear, but it appeared that this double mutant now had a synthetic defect. At the higher temperatures, where the alanine mutant showed improved growth over the wild type, the *pol2 mut E* (E) double mutant's growth is far worse than the single *mcm10-1* mutant. This could be explained by the fact that the

temperature sensitivities of both proteins, one dependent on defects in origin firing (*pol2 mutE(E)*) and the other to defects in replication elongation (*mcm10-1*), the mechanisms for both of which are unknown, are creating independent problems for the cell and that is reducing the viability, rather than the two defects occurring in the same pathway. However, running counter to this is the growth of the strains at the permissive temperature and the expression of *UBR1*. Here, the alanine mutant can be seen to have improved growth compared to the wild type whereas the glutamate allele has a severe growth defect. This defect might suggest that the two mutants are functioning in different pathways required for DNA replication initiation and that the double mutant has additive effects in cell growth. Therefore, a greater functional understanding of this *POL2* allele would be required before conclusions could be drawn from this. *pol2 mut E* was also seen to have a synthetic defect with *sld2-6*, and so it was checked how this would be affected by the presence of these hydrophobic mutations. As can be seen from the tetrad analysis in Figure 3.15B, these crosses were lethal. This is similar to what was observed with *pol2-11*, thus making it plausible that the temperature sensitivity defect observed in this point mutant of *POL2* could have a similar functional basis to that found in the truncation (Homesley et al., 2000).

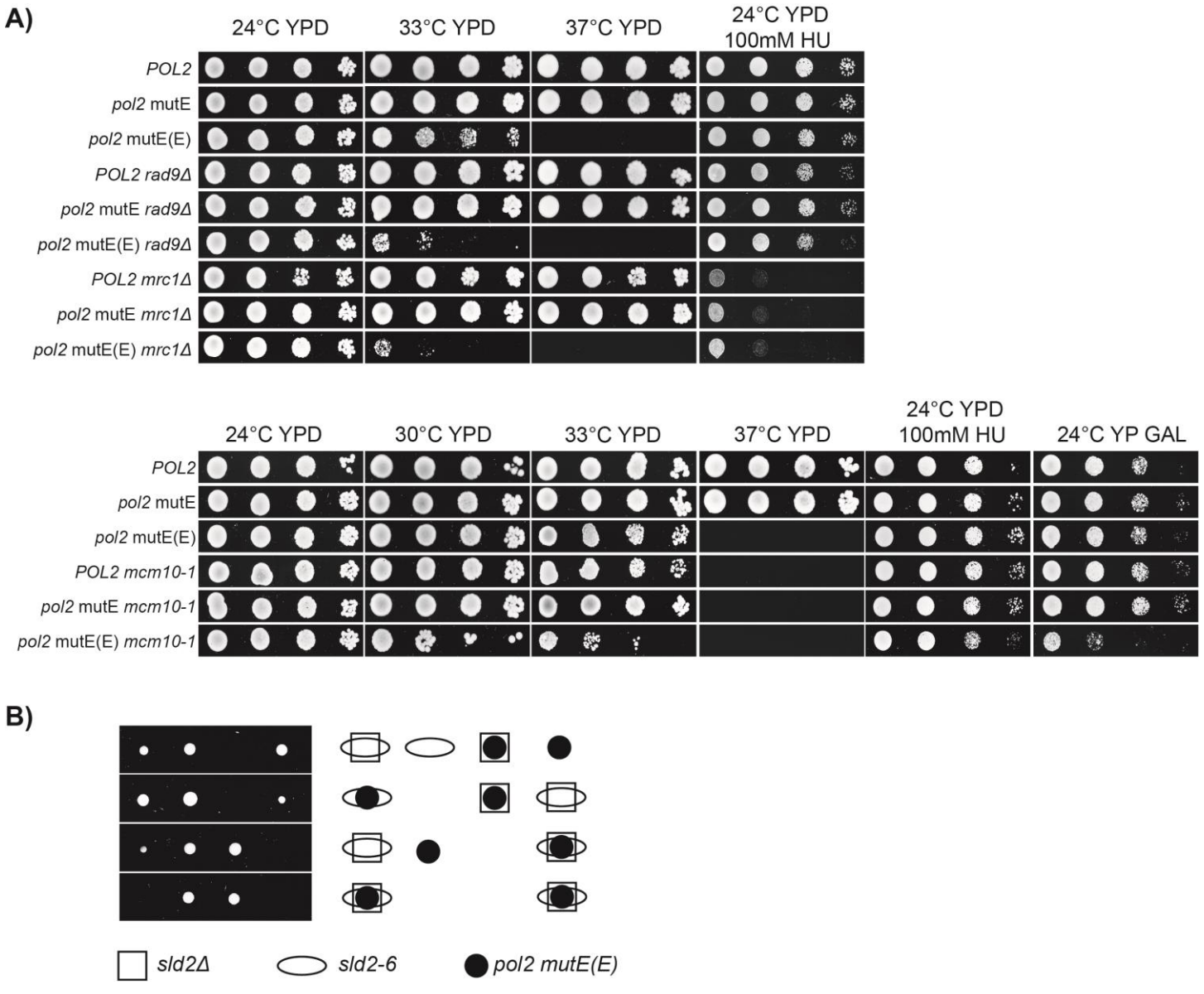
A)
24°C YPD
33°C YPD
37°C YPD
24°C YPD
100mM HU
POL2
pol2 mutE
pol2 mutE(E)
POL2 rad9Δ
pol2 mutE rad9Δ
pol2 mutE(E) rad9Δ
POL2 mrc1Δ
pol2 mutE mrc1Δ
pol2 mutE(E) mrc1Δ
24°C YPD
30°C YPD
33°C YPD
37°C YPD
24°C YPD
100mM HU
24°C YP GAL
POL2
pol2 mutE
pol2 mutE(E)
POL2 mcm10-1
pol2 mutE mcm10-1
pol2 mutE(E) mcm10-1
B)
sld2Δ
sld2-6
pol2 mutE(E)

Figure 3.15: When the hydrophobic residues at the Pol2 C-terminus are mutated to glutamate, a severe temperature sensitive phenotype can be observed. A) Dilution spotting experiments illustrating the difference in viability and genetic interaction in the wild type (*POL2*), alanine (*pol2 mutE*) and glutamate (*pol2 mutE (E)*) mutants when grown at differing temperatures and in the presence of HU. Mutating these hydrophobic residues to glutamate causes temperature sensitivity somewhat similar to *pol2-11* that is not seen with our alanine mutants. Interestingly, however, there is no visible checkpoint defect when grown in the presence of HU as there is for *pol2-11*, indicating a different cause of this phenotype. In addition, no synthetic defects can be seen from crossing with deletions of *MRC1* or *RAD9*. Additionally, the *mcm10-1* suppression previously seen when crossed with the alanine mutant is no longer present, and viability is in fact poorer in these cells. Strains used in order of top to bottom: CS 1, CS 2308, CS 3192, CS 1214, CS 2347, CS 3263, CS 1167, CS 2343, CS 3261. and plate scans were taken 96 hours after spotting. Data shown is representative of 2 independent experiments. **B)** Scans from a tetrad dissection illustrating the lethality of the *sld2-6/pol2 mutant E(E)* double mutant. The plate scans are shown on the left, where the colonies emerging from each tetrad can be seen. On the right are the genotypes each of these colonies have based upon the presence of the markers associated with each allele, with those in red indicating the assumed genotype of the dead colony.

3.17 The glutamate mutant of Pol2, *pol2 mut E(E),* exhibits a mild origin firing defect.

To further understand this new mutant and see how its phenotypes compared to those shown by *pol2-11*, a single-step immunoprecipitation of FLAG-tagged Mcm4 was carried out to assess how levels of origin firing were affected in these strains. For these experiments, samples were taken after a 30 minute release from G_1 to provide an ordinary S phase and also after a 90 minute exposure to HU, all at permissive temperature. Having immunoprecipitated these cell extracts, they were then immunoblotted for components of the CMG (Cdc45 and Psf1), polymerase complexes (Pol1) and Ctf4. Additionally, FLAG was also immunoblotted to give a measure of the amount of immunoprecipitated material in each sample.

The results from these experiments, shown in Figure 3.16, show that the amount of material pulled down at both S phase and in HU appears somewhat similar to that observed in wild type, strikingly, however, we observed a defect in checkpoint activation in the presence of *pol2-11* and *pol2 mutE(E)*, observed through the hyperphosphorylation of Psf1 (De Piccoli et al., 2012). While the alanine mutant showed no defect in origin firing or Dpb2 binding, it is possible that progressively making these mutations more disruptive could elicit a phenotype more like that observed in *pol2-11*. It is reasonable to suggest that this very C-terminal part of Pol2 with the presence of these mutations is steadily becoming more disrupted and therefore resembling the phenotype given when these residues are simply deleted.

A)

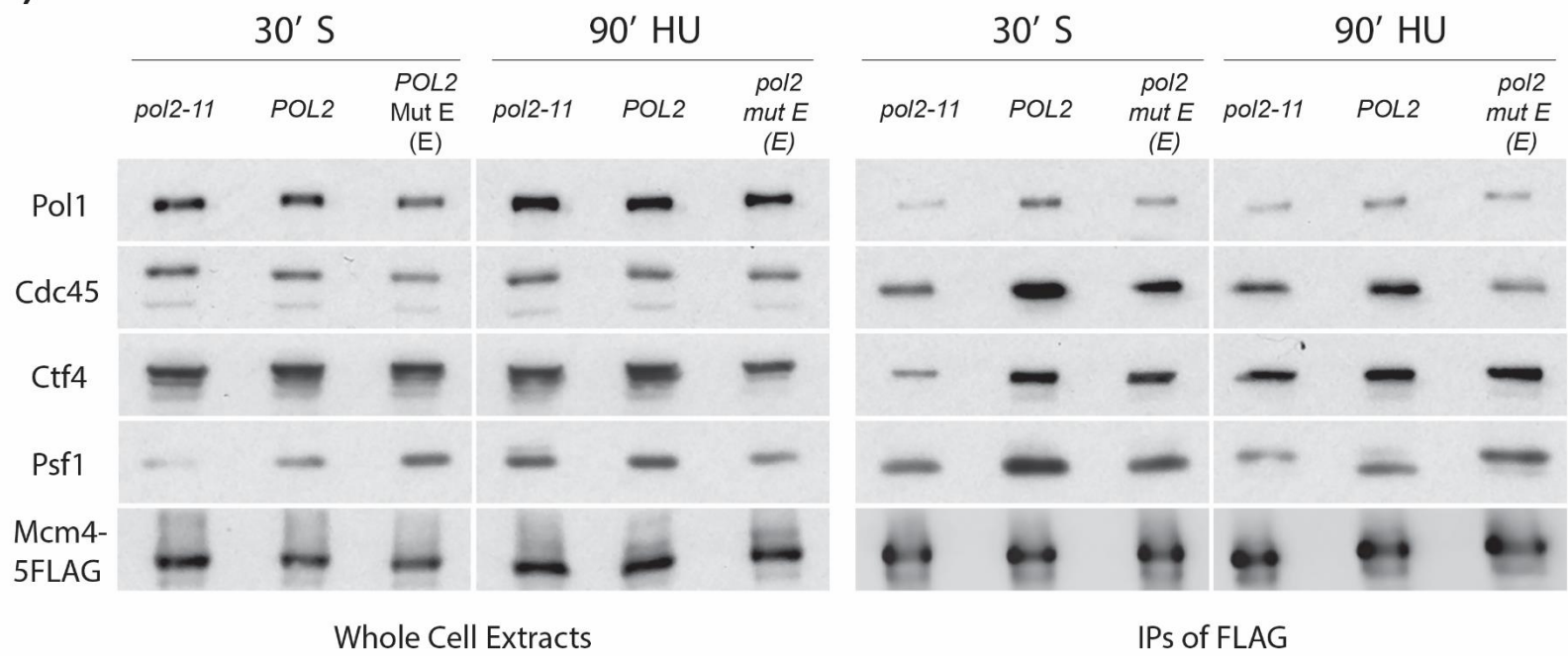

B)

	POL2		*pol2-11*		*pol2 mut E (E)*	
	30' S	**90' HU**	**30' S**	**90' HU**	**30' S**	**90' HU**
Pol1	0.633	0.441	0.145	0.189	0.323	0.232
Cdc45	1.292	0.852	0.552	0.532	0.746	0.325
Ctf4	1.016	1.016	0.247	0.638	0.725	0.921
Psf1	1.392	0.699	0.670	0.342	0.889	0.791

Figure 3.16: The glutamate-containing Pol2 hydrophobic mutant appears to show a mild origin firing defect. A) Cells carrying a FLAG-tagged version of Mcm4 in a wild type (CS 1166), *pol2-11* (CS 1162) or *pol2 mutant E(E) (*CS 3332) background. These cells were grown to exponential phase at 24°C in YPD, were arrested in alpha factor, and released and either for 30' in YPD or for 90' in YPD 0.2M HU. Samples were collected and frozen. Following single-step immuno-precipitation samples were analysed by immunoblotting. By looking at the abundance of replisome components, compared to the wild type, origin firing appeared somewhat impaired in this mutant, although not nearly as severely as observed in *pol2-11.* **B)** Table of quantified band intensities of the immunoprecipitated samples from the immunoblot. All values have been normalized to the intensity of the Mcm4-5FLAG band.

3.18 *pol2 mut E (E)* and *pol2-11* are defective in binding Dpb2.

It was hypothesized that this observed origin firing defect could be due to a loss of interaction with Dpb2 and so Dpb3 was tagged with TAP and pulled down in an immunoprecipitation. These immunoprecipitated samples were then processed in parallel; either washed with low (100mM) or high (700mM) KOAc salt washes. By subjecting these immunoprecipitations with differing salt concentrations, it can be assessed whether the binding interface between Pol2 and Dpb2 is weakened, as, while it is a stringent wash, in the wild type they would remain bound. These samples were then immunoblotted for these two components of the Pol ε complex as well as Dpb3, to assess how much of the protein sample is present.

As can be seen in Figure 3.17, while the levels of Dpb2 do not look particularly different between the two washes in any of the strains, when the levels of co-immunoprecipitation between Pol2 and Dpb2 are focused on, it is striking how little the latter is pulled down in the two *POL2* mutants. A weakened interaction could explain the reduced origin firing seen in this mutant and the temperature sensitivity, especially if the higher temperatures would further destabilize it, thus disrupting the formation of pre-loading complexes and preventing the recruitment of essential components like polymerase ε and GINS to the fork. This leads to the assumption that the defects in *pol2-11* and *pol2 mut E (E)* cells have the same root cause: a weakened interaction with their B subunits. This could indicate that the hydrophobic residues might, directly or indirectly, assist in forming the binding interface between Dpb2 and Pol2, thus underlining their importance in replication. Additionally, while the temperature sensitivity defects shown in the glutamate and *pol2-11* mutants could be pinpointed to their decreased Dpb2 binding and affected origin firing, the absence of a HU-sensitivity in *pol2 mut E (E)* might indicate an independent function in checkpoint signalling for Pol2.

A)

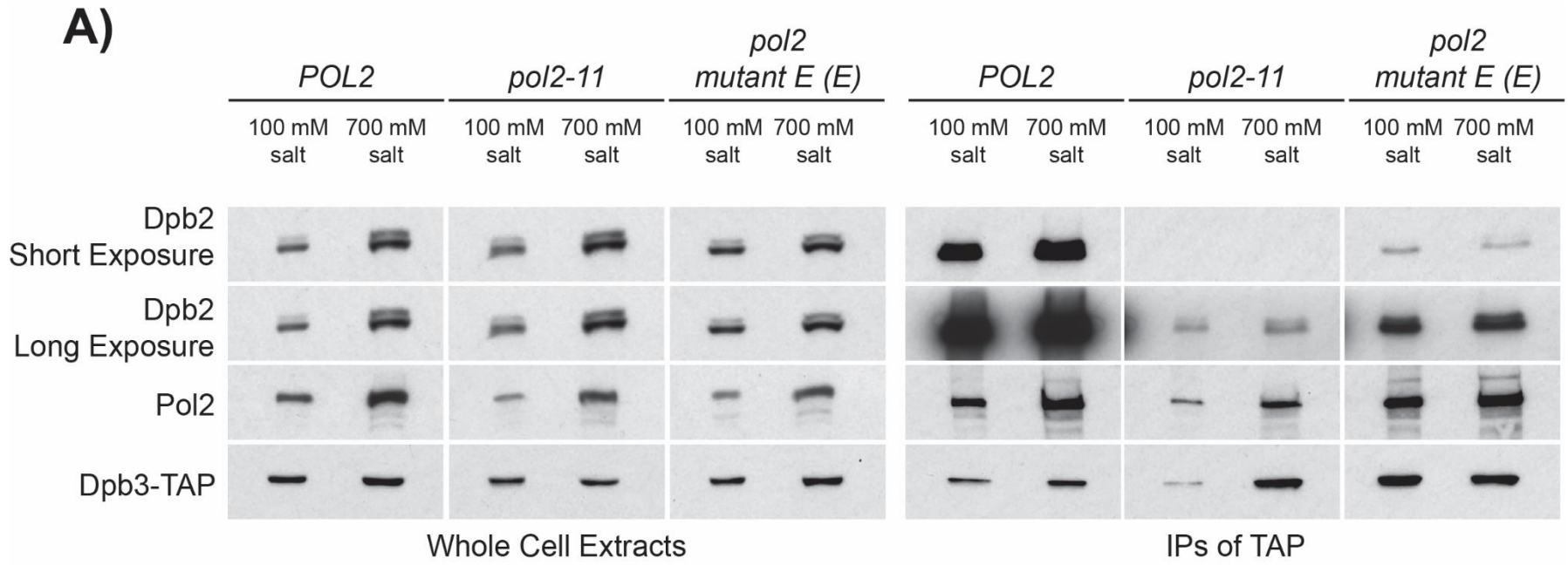

B)

	POL2		*pol2-11*		*pol2 mut E (E)*	
	100mM	**700mM**	**100mM**	**700mM**	**100mM**	**700mM**
Dpb2	1.339	1.968	1.398	0.559	0.881	1.209
Pol2	5.040	3.942	0.815	0.173	0.454	0.600

Figure 3.17: The mild origin firing defect shown in *POL2 Mutant E (E)* is due to a similar defective Dpb2 binding observed in *pol2-11* cells. A) Immunoblot from a single-step IP of Dpb3 tagged with TAP was performed with using different salt concentrations (100mM and 700mM) to assess the stringency of the binding between Pol2 and Dpb2. Strains had either a wild type, *pol2-11* or *pol2 mutant E(E)* background (CS 3324, CS 3326 and CS 3330, respectively). **B)** Table of quantified band intensities of the immunoprecipitated samples from the immunoblot. All values have been normalized to the intensity of the Dpb3-TAP band. It can be seen that the level of Dpb2 compared to that of Pol2 is reduced in the *pol2-11* cells, revealing a seeming loss of interaction that could explain its origin firing defects. A long and short exposure of Dpb2 has been used to illustrate how poor the co-immunoprecipitation of this subunit is with Pol2 in both mutants compared to the wild type. Much like the origin firing defect, this was also present in the Pol2 missense mutant, although not to the same extent. This indicates that the origin firing defects observed in both of these strains could be due to the impaired Dpb2 binding, and the degree this is disrupted could dictate how severe the defect is.

Chapter 4: Analysis of the role of Pol2 in checkpoint activation.

4.1 Background

Alongside its well characterised essential role in origin firing, DNA Polymerase ε has also long been associated with a role in signalling the S phase checkpoint, but the mechanistic understanding of this has been not been elucidated yet. Much of the evidence for Pol ε's checkpoint role primarily arises from the severe sensitivities to replication stresses exhibited by C-terminal mutants of its catalytic subunit Pol2 and the lack of induction of Rnr3 in response to replication stress (Navas et al., 1995). Additionally, Pol2 has been shown to bind to several key mediators of the checkpoint response, such as Mrc1 and Ctf18 (Lou et al., 2008, Garcia-Rodriguez et al., 2015). However, assigning a direct role in checkpoint signalling to Pol ε becomes complicated by the fact that the generation of an efficient checkpoint response is dependent on the numbers of active replication forks during S phase (Shimada et al., 2002). Therefore, with our understanding of Pol ε's essential role in origin firing, it is difficult to delineate the defective checkpoint signalling observed in the Pol2 C-terminal mutants from their known decreased levels of origin licensing.

The work presented in this chapter has attempted to understand whether the long-assumed role of Pol ε in checkpoint signalling is in fact an independent function and not simply downstream of defective origin firing programmes seen in Pol2 mutants. To this end, I have used a well-characterised C-terminal mutant of Pol2, *pol2-11*, that has been shown to have both origin firing and checkpoint defects. By using a system increasing origin firing in wild type and *pol2-11* cells to similar levels, I have shown that *pol2-11* does in fact appear to have an independent checkpoint defect. Through further probing, I have surprisingly pinpointed a possible novel role of Pol ε functioning in the same pathway as Rad9 and Rad24 in signalling the DNA damage checkpoint.

4.2 After controlling for origin firing, *pol2-11* does not have an S phase checkpoint defect.

Ever since its first uses over twenty years ago, *pol2-11* has long been noted to have numerous checkpoint defects, with its defective growth being noted in both HU and MMS (Navas et al., 1995). In order to understand the nature of these observed checkpoint defects and thus fully understand Pol2's role in checkpoint signalling, it was decided initially to confirm previously observed phenotypes. As shown before here and in the literature (Fig 3.1), *pol2-11* has a severe growth defect in HU (Navas et al., 1995). In order to gain a better understanding of the dynamics of activation of the checkpoint, a cell cycle experiment was carried out in a protocol that has been designed to favour comparison with the subsequent experiments. Here, cells were grown to the exponential phase in YP-Raf at 24°C, arrested in G_1, resuspended in YP-Gal and then released into YP-Gal containing 0.2M HU for 90 minutes. This was washed out and cells were released from the block in early S phase to complete replication, after which they were re-arrested in G_1 by addition of alpha factor. Samples were taken every 15 minutes, the protein extracts were analysed by electrophoresis and immunoblotting for Rad53, whose hyper-phosphorylated form gives a marker for activation of the checkpoint. In Figure 4.1, the wild type strain is able to fully activate the checkpoint between 30 and 45 minutes after exposure to the replication stress, and fully recover within an hour of its removal. In *pol2-11*, however, the activation is significantly delayed by almost 30 minutes and when the comparative band intensities of hyper-phosphorylated to unphosphorylated Rad53 are observed, *pol2-11* appears to be less able to fully activate the checkpoint. Additionally, the recovery time in *pol2-11* appears significantly reduced, which strengthens the observation that the checkpoint is not fully activated, as there would be less of an obstacle to recover from.

4.3 The Pol2 C-terminus does not improve checkpoint response in *pol2-11* cells, but causes a late-onset reactivation.

Having seen the delayed checkpoint activation observed in *pol2-11* cells compared to the wild type, I hypothesised that expression of the C-terminus could somewhat suppress this phenotype, as it had been shown to improve the viability of these cells when exposed to HU in dilution spotting experiments. So, the experiments from Figure 4.2A were repeated to include a *pol2-11* strain expressing the Pol2 C-terminus. The Rad53 immunoblots from this experiment are shown in Figure 4.2 and quite clearly illustrate that the C-terminus has little effect upon activation of the S phase checkpoint, as its onset remains delayed. Interestingly though, in cells expressing the C-terminus, there appears to be a reactivation of the checkpoint 90 minutes after the release from HU. This reactivation appears to have an impact on the progression of replication, as the FACS profiles in Figure 4.2B show a significant delay in the formation of the G_1 peak following mitosis. From these experiments, it would appear that the C-terminus either causes damage in *pol2-11* cells, as seen in the Rad53 activation, in opposition to the improved long-term viability shown in previous experiments in these conditions. Alternatively, this result suggests that the Pol2 C-terminal fragment allows the detection of defects not seen in its absence.

4.4 The Pol2 C-terminus checkpoint reactivation in G_2 occurs irrespective of exposure to replication stress.

In order to understand whether this reactivation of Rad53 was due to unresolved problems that arise during the response to HU, I sought to observe the effect of the C-terminus had upon checkpoint activation during an unperturbed S phase in a wild type and *pol2-11* background. In this experiment, cells were grown in YP-Raf until reaching logarithmic growth phase, whereupon they were arrested in G_1 through the addition of α factor. They were then resuspended in YP-Gal to express the C-terminal fragment before being released to complete replication. As shown by the Rad53 immunoblots in Figure 4.3A, *pol2-11* cells expressing the Pol2 C-terminus

still activate the S phase checkpoint even when not exposed to replication stress in the form of HU beforehand. It was also clear that the Pol2 C-terminus does not cause this reactivation alone, and this occurs only when expressed alongside *pol2-11*. When analysed alongside the FACS profiles shown in Figure 4.3B, this activation appears to occur during late-S or G_2 phase and causes a significant delay into mitotic entry, concurrent with an activation of the G_2/M DNA damage checkpoint.

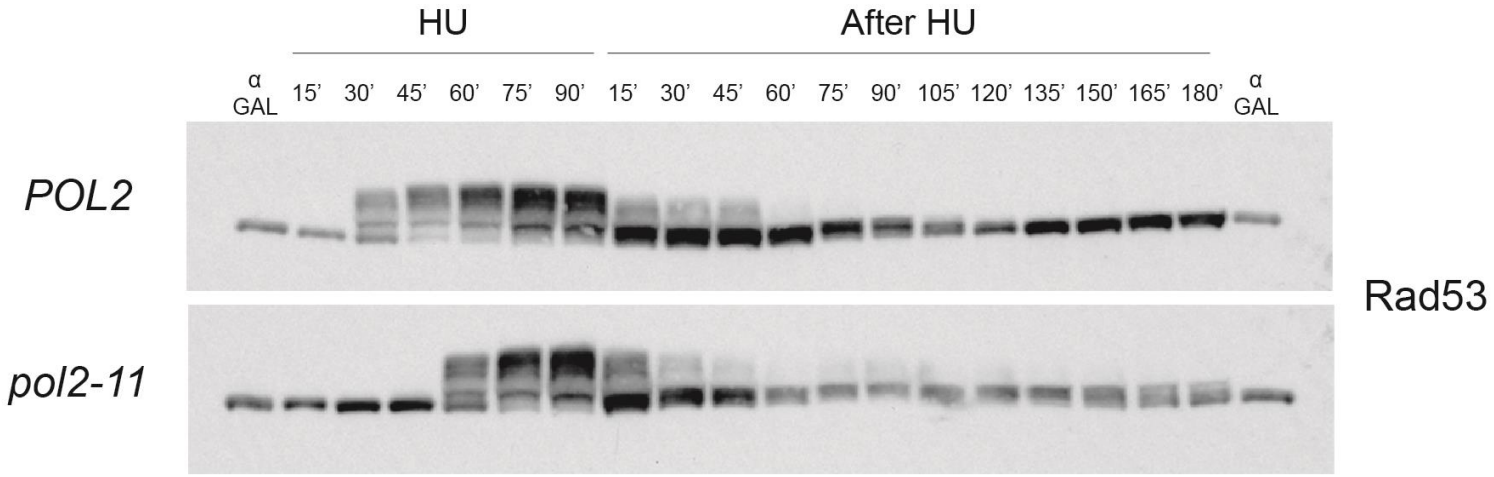

Figure 4.1: *pol2-11* cells show a checkpoint defect characterised by a delayed response to replication stress. Immunoblots of Rad53 from samples collected from a cell cycle experiment in order to check the functioning of the S phase checkpoint in cells containing the wild type *POL2* (CS 1) and *pol2-11* alleles (CS 1463). Here, cells were grown to the exponential phase in YP-Raf at 24°C, arrested in alpha factor and resuspended in YP-Gal for 35 minutes. They were then released in YP-Gal 0.2M HU for 90 minutes, after which they were washed and resuspended in YP-Gal to progress through the cell cycle for 3 hours. α factor was added back to arrest cells in G1 after the progression in S phase. TCA samples were taken every 15 minutes starting from their arrest in G_1 in YP-Gal. *pol2-11* has a clear delay in phosphorylating Rad53 compared to the wild type, indicating a checkpoint defect. Data shown is representative of 8 independent experiments.

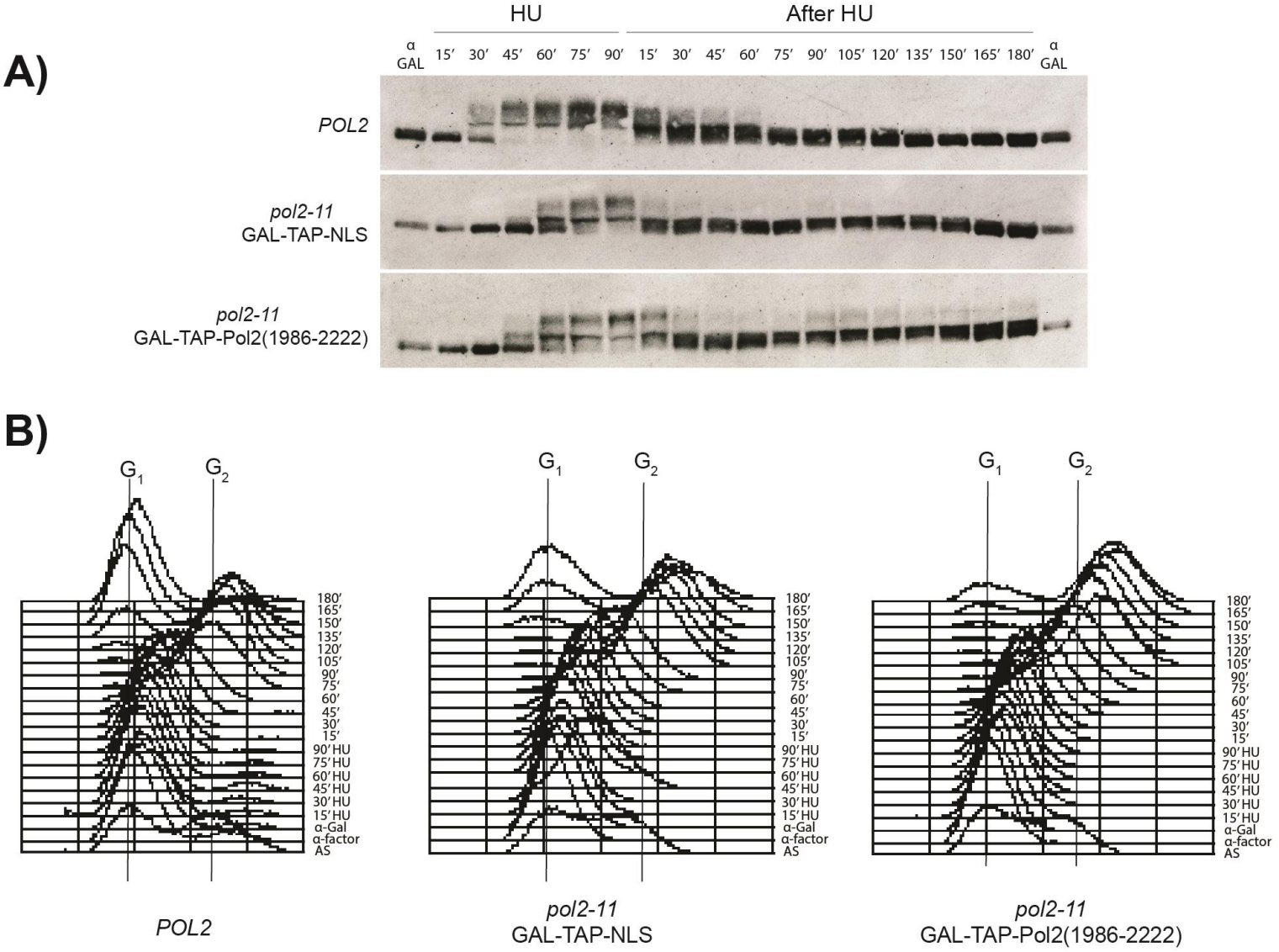
A)
HU
After HU
α GAL
15′ 30′ 45′ 60′ 75′ 90′
15′ 30′ 45′ 60′ 75′ 90′ 105′ 120′ 135′ 150′ 165′ 180′
α GAL
POL2
pol2-11
GAL-TAP-NLS
pol2-11
GAL-TAP-Pol2(1986-2222)
B)
G1
G2
180′
165′
150′
135′
120′
105′
90′
75′
60′
45′
30′
15′
90′HU
75′HU
60′HU
45′HU
30′HU
15′HU
α-Gal
α-factor
AS
POL2
pol2-11
GAL-TAP-NLS
pol2-11
GAL-TAP-Pol2(1986-2222)

Figure 4.2: While expression of the C-terminus mildly ameliorates the delayed checkpoint response of *pol2-11*, it also reactivates the checkpoint after its recovery from replications stress. A) Immunoblots of Rad53 from samples collected from a cell cycle experiment in order to check how expression of the Pol2 C-terminus affected *pol2-11*'s ability to activate the S phase checkpoint. For these experiments, a wild type strain (CS 1) and two *pol2-11* strains, one expressing a blank TAP-NLS construct and the other the Pol2 C-terminus (CS 1463 and CS 1465, respectively), were used. Here, cells were grown to the exponential phase in YP-Raf at 24°C, arrested in alpha factor and resuspended in YP-Gal for 35 minutes to express the Pol2 C-terminal fragment. They were then released in YP-Gal 0.2M HU for 90 minutes, after which they were washed and resuspended in YP-Gal to progress through the cell cycle for 3 hours. α factor was added back to arrest cells in G1 after the progression in S phase. **B)** FACS replication profiles from the experiment in (A), where G_1 and G_2 peaks are labelled. The reactivation of the checkpoint clearly prevents the *pol2-11* strain expressing the fragment from finishing replication as quickly as when expressing a just the TAP, as the cell cycle appears to stall in G_2. Data shown is representative of 6 independent experiments.

A)

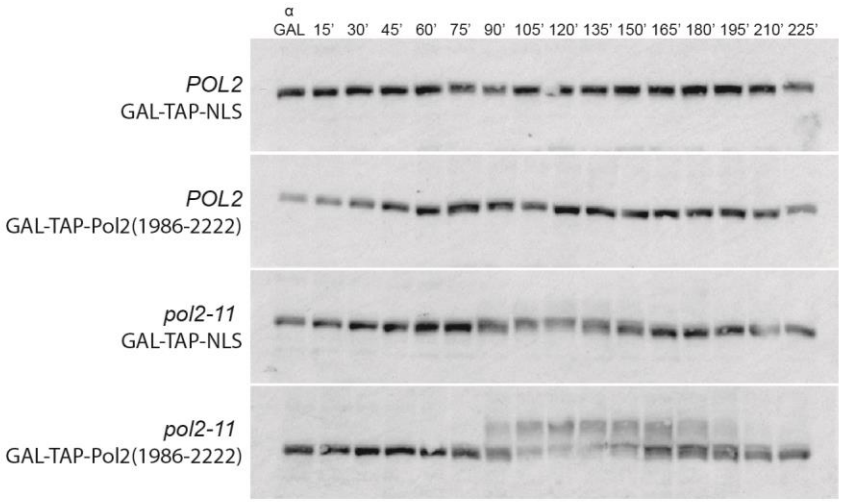
α
GAL 15' 30' 45' 60' 75' 90' 105' 120' 135' 150' 165' 180' 195' 210' 225'
POL2
GAL-TAP-NLS
POL2
GAL-TAP-Pol2(1986-2222)
pol2-11
GAL-TAP-NLS
pol2-11
GAL-TAP-Pol2(1986-2222)

B)

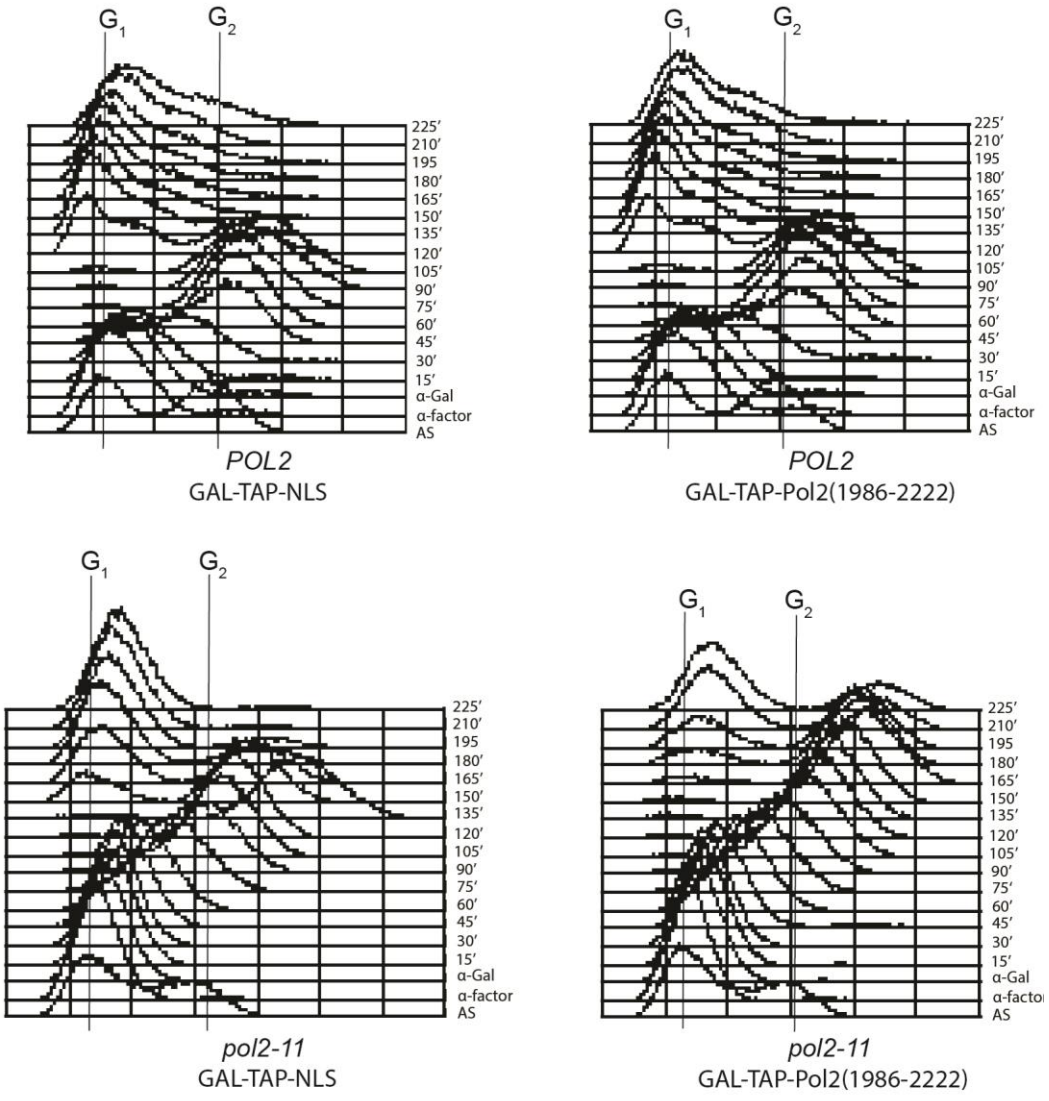
G1
G2
225′
210′
195
180′
165′
150′
135′
120′
105′
90′
75′
60′
45′
30′
15′
α-Gal
α-factor
AS
POL2
GAL-TAP-NLS
POL2
GAL-TAP-Pol2(1986-2222)
pol2-11
GAL-TAP-NLS
pol2-11
GAL-TAP-Pol2(1986-2222)

Figure 4.3: The activation of the checkpoint in G2/M in *pol2-11* expressing Pol2 C-terminal is not dependent on exposure to replication stress. A) Immunoblots of Rad53 from samples collected from a cell cycle experiment in order to check if the exposure to HU was required for the activation of the checkpoint later on in replication. For this experiment, the TAP control and TAP-tagged Pol2 C-terminus were expressed in *POL2* and *pol2-11* backgrounds (*POL2*: CS 699 and CS 700; *pol2-11*: CS 1463 and 1465, respectively). Cells were grown to the exponential phase in YP-Raf at 24°C, arrested in alpha factor and resuspended in YP-Gal for 35 minutes to express the TAP fragments. They were then released in YP-Gal to progress through the cell cycle for 225'. Expression of the Pol2 C-terminus produces a delay in *pol2-11* and causes the activation of Rad53 in G_2. α factor was added back to arrest cells in G1 after the progression in S phase. **B)** FACS replication profiles from the experiment in (A), where G_1 and G_2 peaks are labelled. The checkpoint reactivation appears to arrest the cells in G_2, shown by remnants of the peak remaining by the end of the experiment in the *pol2-11* strain with the Pol2 fragment. Data shown is representative of 2 independent experiments.

4.5 Checkpoint reactivation in *pol2-11* cells occurs in a Rad9-dependent manner.

Having seen the checkpoint reactivation occur in *pol2-11* cells in the presence of the Pol2 C-terminus possibly during G_2, I hypothesised that this could be due to signalling from the DNA damage checkpoint. In order to investigate this, I introduced the deletion of a key mediator of the DNA damage checkpoint, Rad9. Rad9 has a well-characterised role in assisting the DNA damage checkpoint in S phase/G_2, in which it binds to chromatin marked by phosphorylated histones including ɣ-H2A, which itself is mediated by Mec1 (Lee et al., 2014). After phosphorylations by Mec1, as detailed in section 1.4.4, it functions to further bind the Dpb11 as well as recruiting Rad53 for activation by Mec1 and its subsequent autophosphorylation, thus promoting its full activation and a robust checkpoint response (Pfander and Diffley, 2011, Sweeney et al., 2005). Now with a *rad9Δ* background, I carried out the same experiments as performed in Figure 4.2 and tested whether the checkpoint reactivation still occurred. As can be seen from the Rad53 immunoblots in Figure 4.4A, the reactivation phenotype characteristic of the Pol2 C-terminus now no longer occurs. Interestingly, the replication dynamics between the two *pol2-11* strains shown by the FACS profiles in Figure 4.4B remain different, as the cells expressing the C-terminus still slightly lag behind, although not as obviously as when Rad9 is present. These results would suggest that this checkpoint activation that occurs in G_2 in *pol2-11* cells appears to be due to the presence of DNA damage that arises over the course of a normal S phase. Whether damage is being caused in both *pol2-11* strains, but only the C-terminus can detect it or the Pol2 C-terminus is causing the damage in concert with *pol2-11*, is unclear.

4.6 The origin firing defect can be suppressed by overexpressing 6 ‘firing factors’.

While the temperature sensitivity observed *pol2-11* cells seems to be underpinned by its diminished ability to efficiently fire origins, its defect in responding to replication stress is less clear. Any efforts in assessing any role the Pol2 C-terminus could play in activating the S phase checkpoint is

hampered by the fact that this is inextricably linked to origin firing, as the greater numbers of forks present allow a greater response to replication stresses (Shimada et al., 2002). Considering the growth defect in the presence of HU is also suppressed by expressing the Pol2 C-terminus, and the increased firing efficiency that comes with this, it seems possible that the aforementioned loss of viability is solely down to the decreased level of origin licensing.

So, to study this, a method was required to normalise the firing efficiency of *pol2-11* with that of wild type *POL2* and then observe its behaviour during activation of the S phase checkpoint. To this end, it was checked whether the defects in origin firing in *pol2-11* could be bypassed by using a system developed in the Zegerman lab, which utilises a series of six 'firing factors' all of which have key roles in origin licensing (Sld2, Sld3, Sld7, Dbf4, Dpb11 and Cdc45, - known herein as GAL-SSSDDC -, shown in Figure 4.5A). These are placed under the control of a galactose-inducible promoter that greatly increases the level of origin firing in the cell (Mantiero et al., 2011). To understand the effect expressing these factors had upon the levels of origin firing in these strains, Mcm4 was FLAG-tagged and immunoprecipitated in both a *POL2* and *pol2-11* background. These samples were then immunoblotted for various components of the replisome in order to measure the number of forks present in the cell. FLAG was also immunoblotted to ensure that the amounts of immunoprecipitated material were consistent between samples.

These results, as shown in Figure 4.5B, showing the protein levels of other fork components illustrate that origin firing has been greatly increased when these 6 proteins have been expressed. As hoped, these results also show that the origin firing defect inherent to *pol2-11* was alleviated and the levels of licensing appear almost identical between it and the wild type strain in the presence of these firing factors. Consistent with the observation of this increased level of origin firing is the presence of hyper-phosphorylated Psf1 in these immunoprecipitations, a known marker of late origin firing in the presence of HU (De Piccoli et al., 2012).

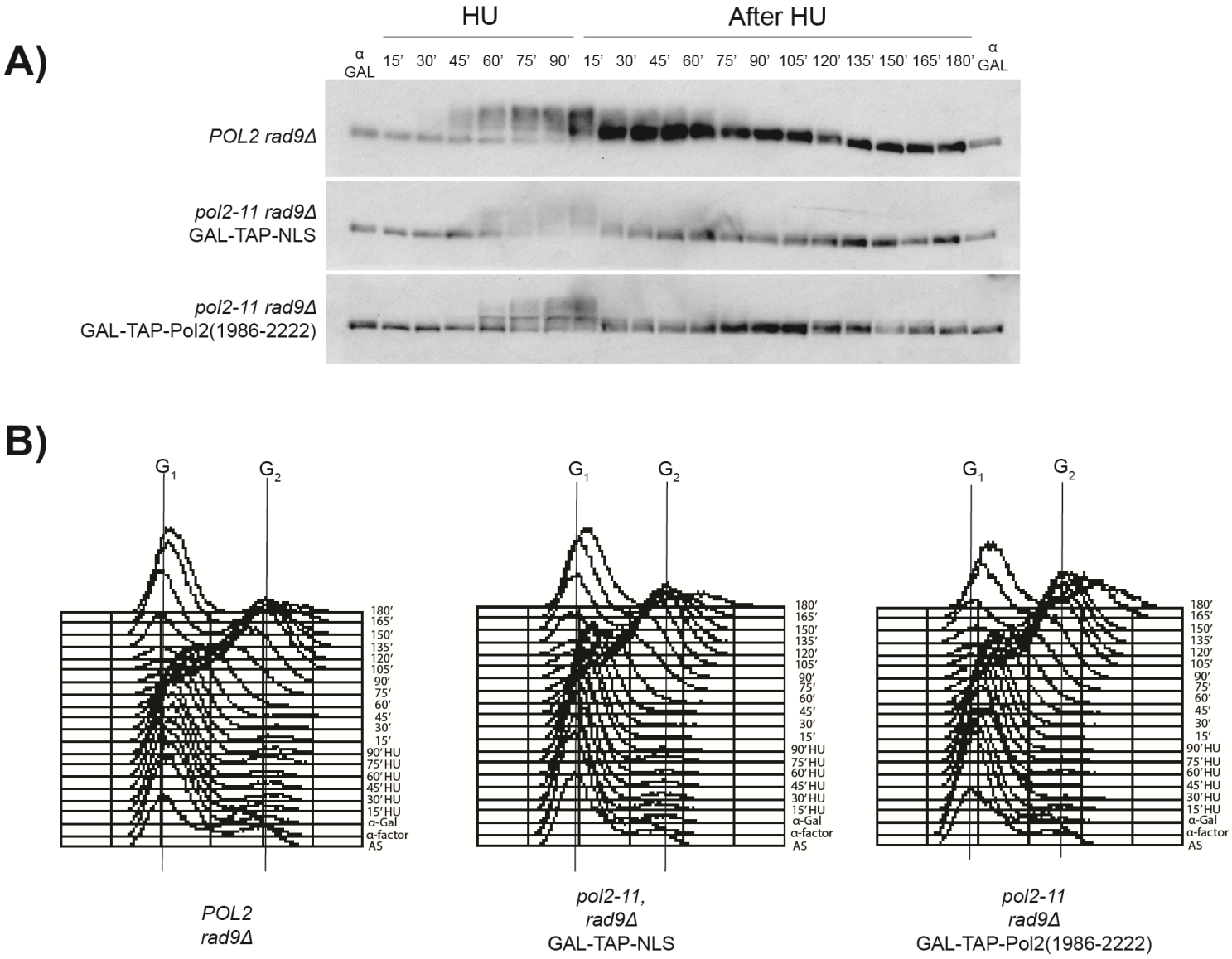
A)
HU
After HU
α GAL
15' 30' 45' 60' 75' 90' 15' 30' 45' 60' 75' 90' 105' 120' 135' 150' 165' 180'
α GAL
POL2 rad9Δ
pol2-11 rad9Δ
GAL-TAP-NLS
pol2-11 rad9Δ
GAL-TAP-Pol2(1986-2222)
B)
G1
G2
180'
165'
150'
135'
120'
105'
90'
75'
60'
45'
30'
15'
90' HU
75' HU
60' HU
45' HU
30' HU
15' HU
α-Gal
α-factor
AS
POL2
rad9Δ
pol2-11,
rad9Δ
GAL-TAP-NLS
pol2-11
rad9Δ
GAL-TAP-Pol2(1986-2222)

Figure 4.4: The reactivation of the checkpoint in *pol2-11* cells expressing the Pol2 C-terminus is dependent on Rad9. A) Immunoblots of Rad53 from samples collected from a cell cycle experiment to understand whether the reactivation of the checkpoint was the result of DNA damage signalling. To test this hypothesis, ***rad9Δ*** was introduced to all the strains previously (*POL2*: CS 1213, *pol2-11/*GAL-TAP-NLS: CS 2379, *pol2-11*/GAL-TAP-Pol2CT: CS 2381). Cells were grown to the exponential phase in YP-Raf at 24°C, arrested in alpha factor and resuspended in YP-Gal for 35 minutes to express the Pol2 C-terminal fragment. They were then released in YP-Gal 0.2M HU for 90 minutes, after which they were washed and resuspended in YP-Gal to progress through the cell cycle for 3 hours. With *RAD9* being deleted, there was no late-onset checkpoint reactivation, indicating that DNA damage endogenous to the strain in which the Pol2 C-terminus was expressed alongside *pol2-11* was causing activation of the DNA damage checkpoint. α factor was added back to arrest cells in G1 after the progression in S phase. **B)** FACS replication profiles from the experiment in (A), where G_1 and G_2 peaks are labelled. The replication profiles from the two *pol2-11* strains appear much more similar, although there still appears to be a slight delay when the C-terminal fragment is expressed.

A)

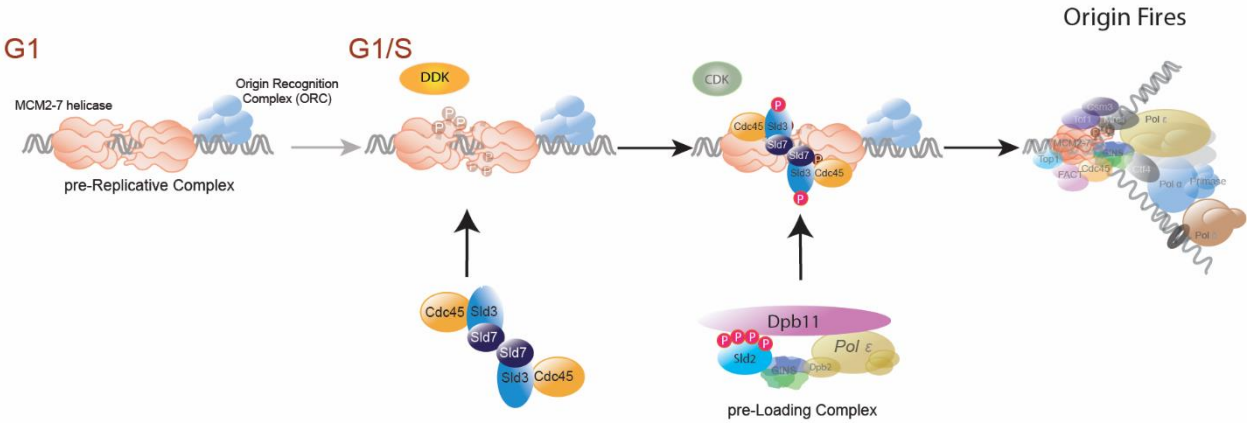

B)

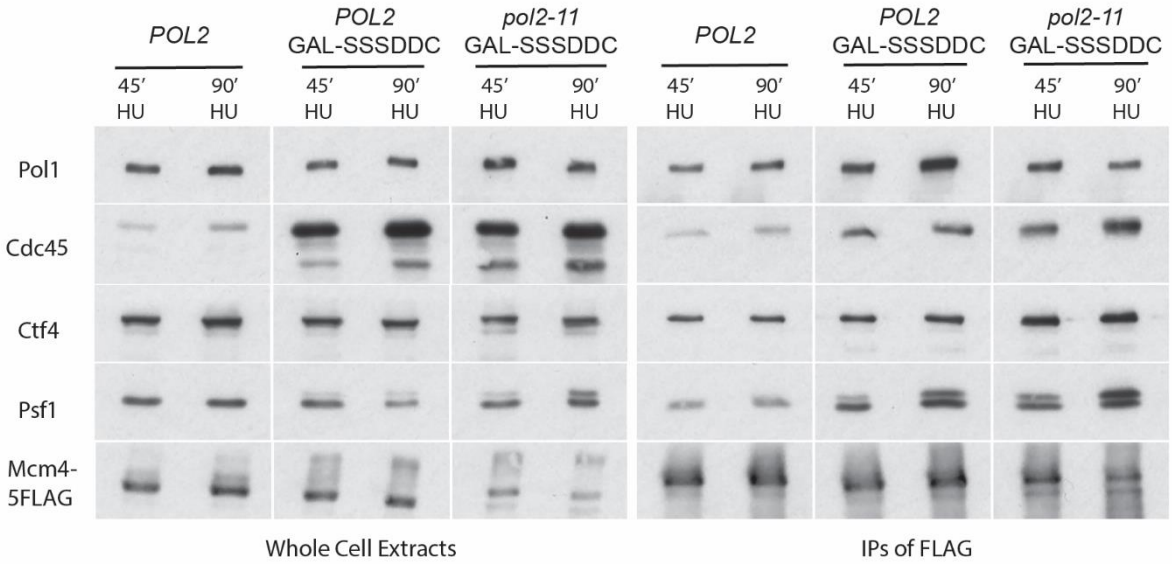

C)

	POL2		*POL2* GAL-SSSDDC		*pol2-11* GAL-SSSDDC	
	45' HU	**90' HU**	**45' HU**	**90' HU**	**45' HU**	**90' HU**
Pol1	0.291	0.349	0.653	0.986	0.545	0.404
Cdc45	0.123	0.206	0.461	0.497	0.623	0.890
Ctf4	0.502	0.433	0.564	0.624	0.805	0.819
Psf1	0.233	0.231	0.525	0.875	0.704	1.024

Figure 4.5: Through overexpression of Sld2, Sld3, Sld7, Dbf4, Dpb11 and Cdc45, origin firing levels between *POL2* and *pol2-11* cells are equalized. A) A cartoon showing the pathway of origin firing, with highlighted the factors that were overexpressed. These factors were identified by the Zegerman lab, and placed under the control of a galactose-inducible (Mantiero *et al.*). **B)** Samples from strains carrying a FLAG-tagged version of Mcm4 with the GAL-SSSDDC firing factor system in a *POL2* and *pol2-11* background (CS 2555 and CS2485, respectively) as well as a *POL2* strain without (CS 1166) were collected for immunoprecipitation. At 24°C, they were arrested in alpha factor, resuspended in YP-Gal for 35 minutes in α factor to express the firing factors and then released into YP-Gal 0.2M HU for 90'. Samples were collected and frozen at the indicated times. Following a single-step immunoprecipitation, samples were analysed by immunoblotting. By looking at the levels of co-immunoprecipitated replisome proteins, it is clear that the addition of the firing factors equalizes the origin firing efficiency of the two *POL2* alleles and increases them both from the wild type strain. **C)** Table of quantified band intensities of the immunoprecipitated samples from the immunoblot. All values have been normalized to the intensity of the Mcm4-5FLAG band.

4.7 After controlling for origin firing defects, *pol2-11* shows wild type checkpoint activation but defects in checkpoint maintenance.

The GAL-SSSDDC system allowed for normalising for the defects in origin firing observed in *pol2-11* and therefore directly tested whether the mutant played a direct role in checkpoint activation. Wild type and *pol2-11* strains were grown to the exponential phase in YP-Raf at 24°C, arrested in G_1, resuspended in YP-gal for 35 minutes, and then released into YP-Gal containing 0.2M HU for 90 minutes. This was washed out and cells were released from the block in early S phase to complete replication, after which they were re-arrested in G_1 by addition of alpha factor. Samples were taken every 15 minutes, the protein extracts were analysed by electrophoresis and immunoblotting for Rad53 and Mrc1, shown in Figure 4.6A, as a means of assessing the checkpoint activation. By observing the dynamics of the checkpoint response to the exposure to HU, it is clear that the much delayed activation that was characteristic of *pol2-11* is no longer present following the expression of GAL-SSSDDC, indicating that the defect that was initially observed was in fact a by-product of the mutant's decreased complement of replication forks. The Rad53 phosphorylation is mirrored by that of the checkpoint activator protein Mrc1 (Alcasabas et al., 2001). However, while the activation of the checkpoint has now been equalized between the two strains, there is a significant discrepancy in their maintenance of the response, and this has been quantified in Figure 4.6B. In the *POL2* wild type strain with GAL-SSSDDC, Rad53 remains hyperphosphorylated even 3 hours after the HU had been removed and this prolonged activation of the checkpoint causes a stalling in S phase, as can be seen by the FACS profiles from this experiment shown in Figure 4.6C. The prolonged checkpoint activation in the wild type *POL2* can be understood to be occurring due to the now greatly increased complement of forks all attempting to restart DNA synthesis simultaneously, while the pools of dNTPs that have been depleted by the exposure to HU are simply unable to recover and permit further replication. Alternatively, the unscheduled activation of the origin might cause damage that continues the checkpoint

activation even following the removal of HU. Meanwhile, the presence of *pol2-11* allele causes an attenuation of the checkpoint and allows a recovery from the HU, although not as quickly as the recovery shown without the firing factors, and cells are even beginning to finish the replication by the end of the time course, as can be seen with the re-emergence of a G1 peak in the FACS profiles. This indicates some form of checkpoint defect in *pol2-11* that is independent of its inability to fire origins efficiently, however, the reason underlying the attenuation observed in the experiment is not clear.

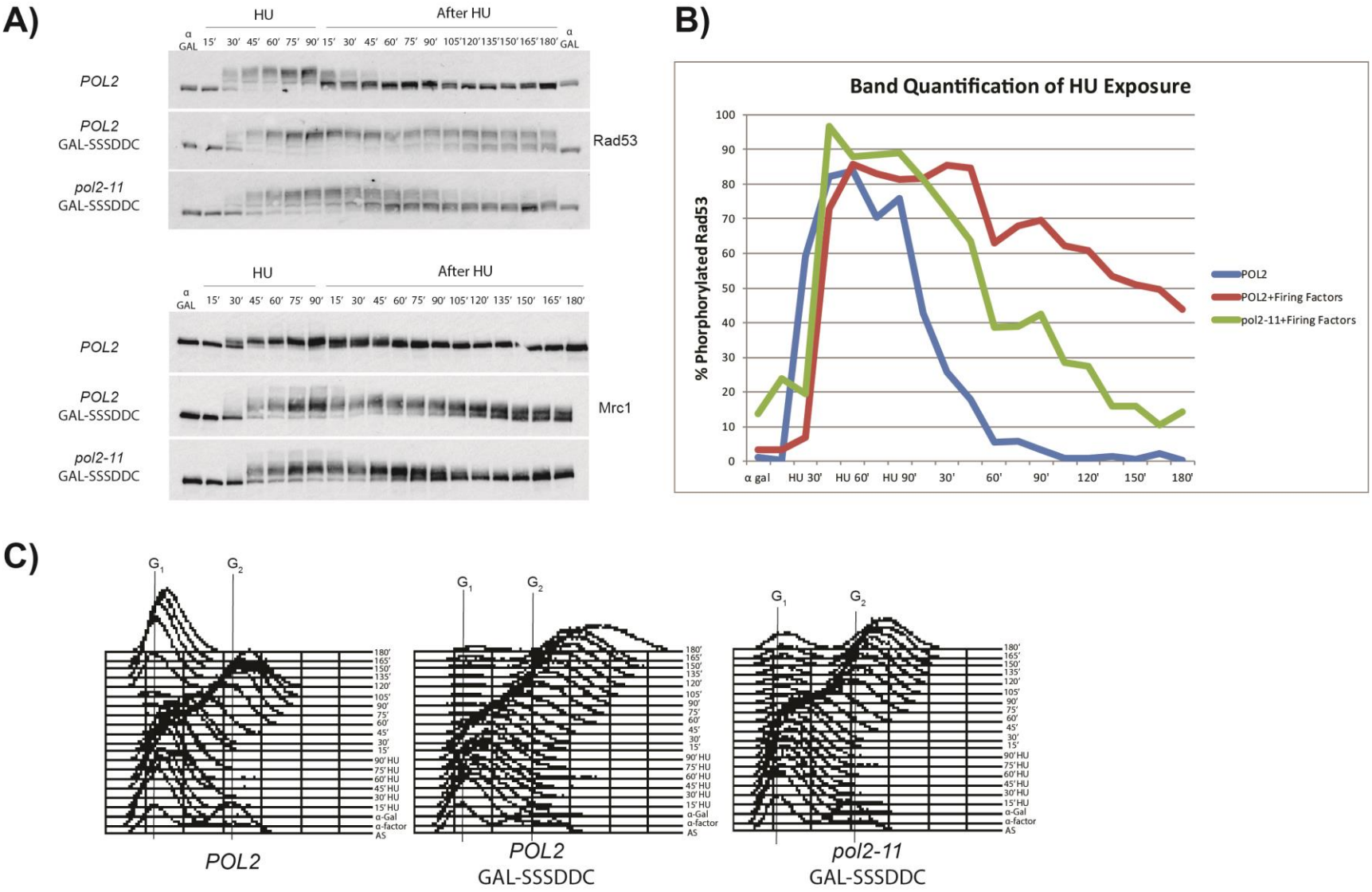
A)
HU
After HU
α GAL
15′ 30′ 45′ 60′ 75′ 90′ 15′ 30′ 45′ 60′ 75′ 90′ 105′ 120′ 135′ 150′ 165′ 180′
α GAL
POL2
POL2 GAL-SSSDDC
pol2-11 GAL-SSSDDC
Rad53
Mrc1
B)
Band Quantification of HU Exposure
% Phorphorylated Rad53
POL2
POL2+Firing Factors
pol2-11+Firing Factors
α gal
HU 30′
HU 60′
HU 90′
30′
60′
90′
120′
150′
180′
C)
G1
G2
POL2
POL2 GAL-SSSDDC
pol2-11 GAL-SSSDDC
α-Gal
α-factor
AS

Figure 4.6: After having controlled for origin firing, *pol2-11* still possesses a checkpoint signaling defect. A) Immunoblots of Rad53 and Mrc1 from samples collected from a cell cycle experiment checking the functioning of the S phase checkpoint in a wild type strain (CS 1), and strains with GAL-SSSDDC firing factor system with *POL2* and *pol2-11* backgrounds (CS 2126 and CS 2485, respectively). Cells were grown to the exponential phase in YP-Raf at 24°C, arrested in alpha factor and resuspended in YP-Gal for 35 minutes to express the firing factors. They were then released in YP-Gal 0.2M HU for 90 minutes, after which they were washed and resuspended in YP-Gal to progress through the cell cycle for 3 hours. α factor was added back to arrest cells in G1 after the progression in S phase. TCA samples were taken every 15 minutes starting from their arrest in G_1 in YP-Gal. The increased origin firing imparted by the firing factors has equalized the rate at which the checkpoint activates between *POL2* and *pol2-11* strains and causes a sustained activation in both of these compared to the strain without the firing factors. However, the checkpoint starts attenuating after 90 minutes in *pol2-11* cells, while it remains active in the wild type. The Rad53 activation profiles are representative of 6 independent experiments. **B)** A line graph plotting at each timepoint the intensity of the hyperphosphorylated Rad53 band as a percentage of the total signal of Rad53. This graph quantifies only the results shown in (A) and clearly illustrates in a quantitative manner the checkpoint attenuation that occurs in *pol2-11* strains after recovery from HU exposure. **C)** FACS replication profiles from the experiment in (A), where G_1 and G_2 peaks are labelled. The sustained activation of the checkpoint clearly prevents the *POL2* strain from finishing replication, stalling it in G_2, while the *pol2-11* cells are able to, albeit slowly, finish replication and begin forming a G_1 peak, tallying with the loss of checkpoint activation seen in the immunoblot after 120 minutes.

:

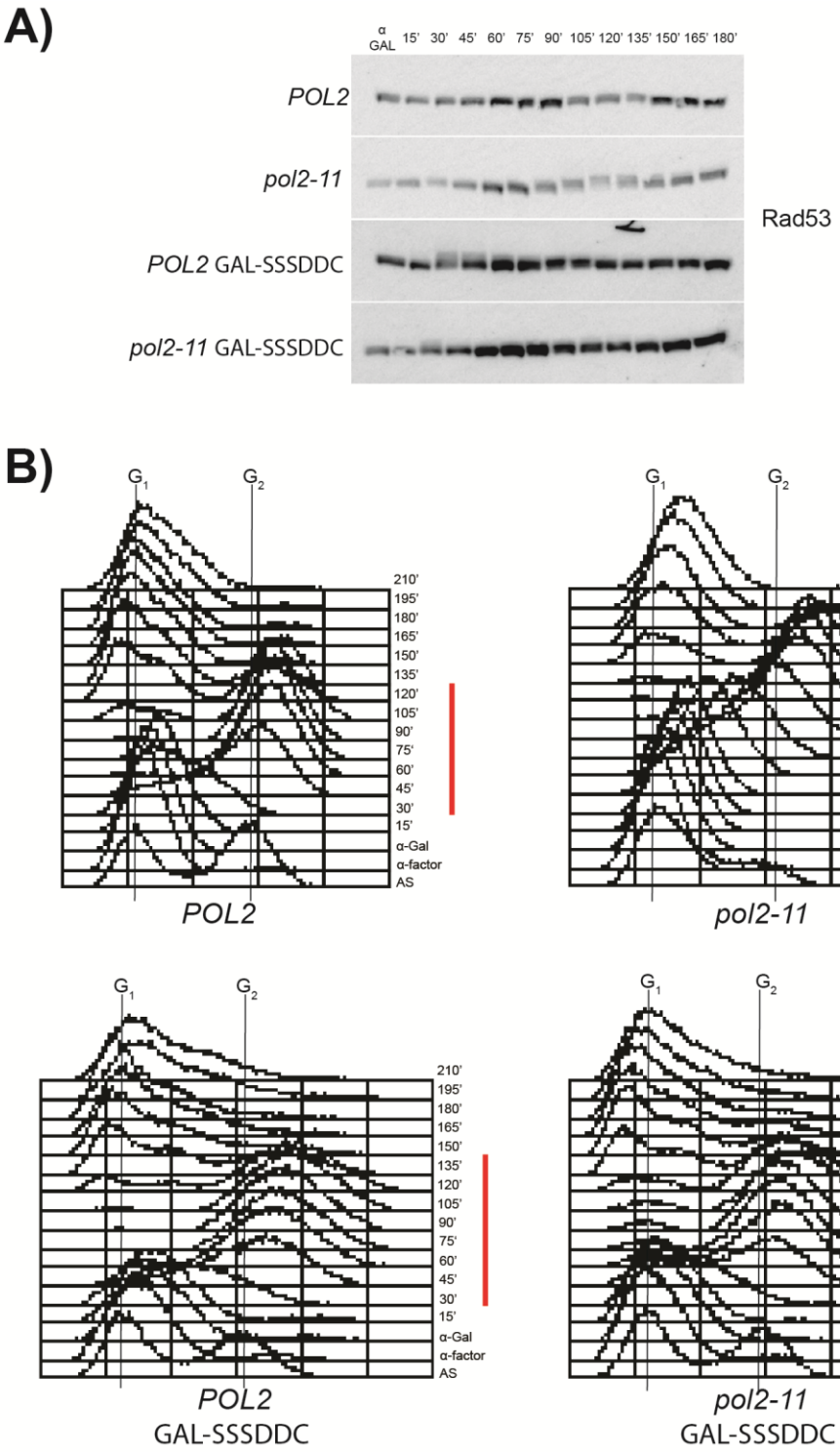
A)
α GAL
15' 30' 45' 60' 75' 90' 105' 120' 135' 150' 165' 180'
POL2
pol2-11
POL2 GAL-SSSDDC
pol2-11 GAL-SSSDDC
Rad53
B)
G1
G2
210' 195' 180' 165' 150' 135' 120' 105' 90' 75' 60' 45' 30' 15'
α-Gal
α-factor
AS
POL2
pol2-11
POL2
GAL-SSSDDC
pol2-11
GAL-SSSDDC

Figure 4.7: The checkpoint defect observed in *pol2-11* cells is dependent on the initial exposure to replication stress. A) An immunoblot for Rad53 from samples taken during an experiment observing a normal S phase in strains with *POL2* and *pol2-11* (CS 1 and CS 1463, respectively) and those with the GAL-SSSDDC firing factor system in the same backgrounds (CS 2126 and CS 2485, respectively). Cells were grown to the exponential phase in YP-Raf at 24°C, arrested in alpha factor and resuspended in YP-Gal for 35 minutes to express the firing factors. They were then released into YP-Gal to complete replication and α factor was added back to arrest cells in G1 after the progression in S phase. As can be seen, replication occurs uninhibited Rad53 activation does not occur, regardless of the *POL2* allele or the increased licensing, showing that the activation of the checkpoint only arises in the presence of replication stresses. **B)** FACS replication profiles from the experiment in (A), where G_1 and G_2 peaks are labelled and the time taken for replication to complete is represented by the red bar. As seen previously, *pol2-11* cells take longer to replicate than the wild type, however, when origin firing is increased, this difference is eliminated. Interestingly, this increase in origin licensing does not appear to quicken replication, as in the two *POL2* strains, those with the firing factors appear to take slightly longer to complete duplication.

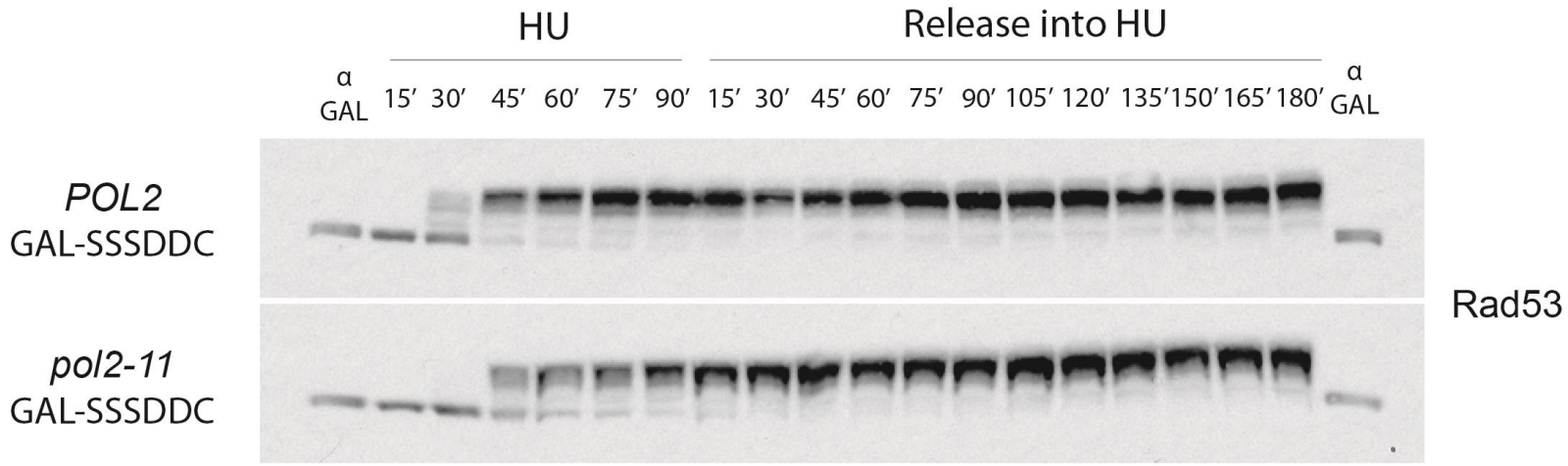

Figure 4.8: The checkpoint attenuation observed in *pol2-11* only occurs after the removal of replication stress. An immunoblot for Rad53 from samples taken during an experiment to explore the checkpoint dynamics in continued exposure to replication stress. The strains used in this experiment contained *POL2* and *pol2-11* alleles (CS 1 and CS 1463, respectively) and those with the GAL-SSSDDC firing factor system in the same backgrounds (CS 2126 and CS 2485, respectively). Cells were grown to the exponential phase in YP-Raf at 24°C, arrested in alpha factor and resuspended in YP-Gal for 35 minutes to express the firing factors. They were then released for an initial 90' in YP-Gal 0.2M HU exposure, followed by resuspension into fresh medium containing the drug for an additional 3 hours. α factor was added back to arrest cells in G1 after the progression in S phase. It can be seen that the checkpoint remains activated in all strains, indicating that the attenuation phenotype previously observed in *pol2-11* cells is dependent on the removal of replication stress.

4.8 The checkpoint defect of *pol2-11* requires both the exposure to and removal of replication stress.

Two control experiments were carried out to ensure what was being observed was only occurring when recovering from an exposure to replication stress. The first, shown in Figure 4.7A, was an unperturbed S phase, to ensure that wild type and *pol2-11* strains were able to replicate without impediment even with the greater complement of origins having fired and that this itself did not cause the same irreversible replication block seen when exposed to HU. Wild type and *pol2-11* strains were grown to the exponential phase in YP-Raf at 24°C, arrested in G_1, resuspended in YP-gal for 35 minutes to induce GAL-SSSDDC, and then released into YP-Gal carry out replication, before being re-arrested in G_1, by addition of alpha factor after 30 minutes. Samples were taken every 15 minutes, and the protein extracts were analysed by electrophoresis and immunoblotting for Rad53 to see if there was any activation of the checkpoint without the introduction of any replication stress. In agreement with what was shown in the literature, firing both early and late origins simultaneously induces a mild checkpoint response (Mantiero et al., 2011). In comparison with the strains with a wild type firing programme, a checkpoint response can be observed by the appearance of a faint upper band Rad53 30 minutes into the start of replication. This disappears quickly as replication progresses and the dynamics of this appear identical between the two alleles. Additionally, the FACS profiles from this experiment shown in Figure 4.7B shows that the time taken for replication to occur is equalised between *POL2* and *pol2-11* cells when origin firing is artificially increased. In agreement with the observation of a slight checkpoint activation, despite the increased number of replication forks, the S phase is slightly extended in these strains compared to the fully wild type strain. In Mantiero *et al.* (2011), the activation dynamics described were identical to those shown here, although the phosphorylation appeared somewhat more pronounced, and the immunoblots showed a greater background above the unphosphorylated Rad53 band even in the G_1 sample. It is conceivable that this would make any slight activation appear stronger.

The other control experiment was performed to examine whether the checkpoint attenuation observed in *pol2-11* was inherent to a recovery from the original stress, rather than an inability to maintain the signalling during extended periods of arrest. Here, wild type and *pol2-11* strains were grown to the exponential phase in YP-Raf at 24°C, arrested in G_1, resuspended in YP-gal for 35 minutes, and then released into YP-Gal containing 0.2M HU for 90 minutes. In this case, cells were re-suspended again in YP-Gal containing 0.2M HU for additional 3 hours. Samples were taken every 15 minutes, the protein extracts were analysed by electrophoresis and immunoblotting for Rad53. As can be seen in Figure 4.8, extending the exposure to the replication stress does not cause any premature attenuation of the checkpoint in *pol2-11*. This would indicate that the checkpoint defects observed in *pol2-11* are not due to a defect in the maintenance of the checkpoint activation.

4.9 The checkpoint defect observed in *pol2-11* is not shared among other mutants defective in origin firing.

Having observed the aberrant checkpoint recovery in *pol2-11,* I wanted to establish whether the defects in checkpoint maintenance were a consequence of a residual defect in origin firing. While the analysis of replisome formation in Fig 4.5B showed a similar profile for the *POL2* GAL-SSSDDC and *pol2-11* GAL-SSSDDC strains, we wanted to confirm this using other strains with known defects in origin firing. To this end, the same experiments were carried out with strains with known defects in their origin firing programme, in this case, *dpb2-1*, *psf1-1*, and the *pol2 mutant E* (E). If these strains were to show a similar pattern of checkpoint attenuation, the defect observed in *pol2-11* might be assumed to be a consequence in origin firing. All three of these alleles exhibit defective growth at temperatures beyond 33°C but not in the presence of drugs targeting either the S phase or DNA damage checkpoints, as can be seen in Figure 4.15. The first of these mutants, *dpb2-1*, is a four amino acid mutation of the Pol ε B subunit which has been characterised as having a much weakened interaction with Pol2, raising the possibility that this could be a mirror image of the defective Dpb2 interaction previously observed in *pol2-11* (Araki et al., 1991). The other

mutant, *psf1-1*, is a single point mutant that has been shown at restrictive temperatures to form a GINS complex without Psf3 and a severely depleted replisome and, through FACS analysis at this temperature, similar replication kinetics to *pol2-11* (Sengupta et al., 2013, Takayama et al., 2003). In order to analyse whether *pol2-11*'s checkpoint attenuation was caused by its origin firing defect, the GAL-SSSDDC system was introduced into cells containing the aforementioned alleles. The same cell cycle experiments were performed as above, in which cells released synchronously in YP-Gal 0.2M HU for 90 minutes, before being resuspended in YP-Gal and left to recover. The immunoblots analysis of Rad53 from the cell extracts samples from this experiment can be seen in Figure 4.9. Interestingly, I observe that none of these alleles are able to recapitulate neither the activation checkpoint nor the attenuation exhibited in the *pol2-11* cells. None of these other strains fully recapitulate the wild type checkpoint dynamics either though and all possess unique characteristics. Both *dpb2-1 and pol2 mutant E(E)* exhibit a slightly delayed activation of the checkpoint. The defect in checkpoint activation is quite surprising and further work is required to understand whether this indicates a defect in recognising checkpoint activation. In addition, *dpb2-1* strain does not exhibit the level of full activation shown by the wild type strain, as the unphosphorylated band remains visible throughout the experiment. This latter point can also be said for the *psf1-1* strain and, from what is understood about these strains, could indicate that the less stable initiation complexes/replisomes are inhibiting its ability to fully activate the checkpoint or cause a less synchronous progression in cell cycle. Although these all have varying degrees of checkpoint activation defects, these mutants did maintain the Rad53 activation following removal of HU, in sharp contrast with *pol2-11*. Taken together, these data show that the attenuation of Rad53 activation is not due to residual defects in origin firing.

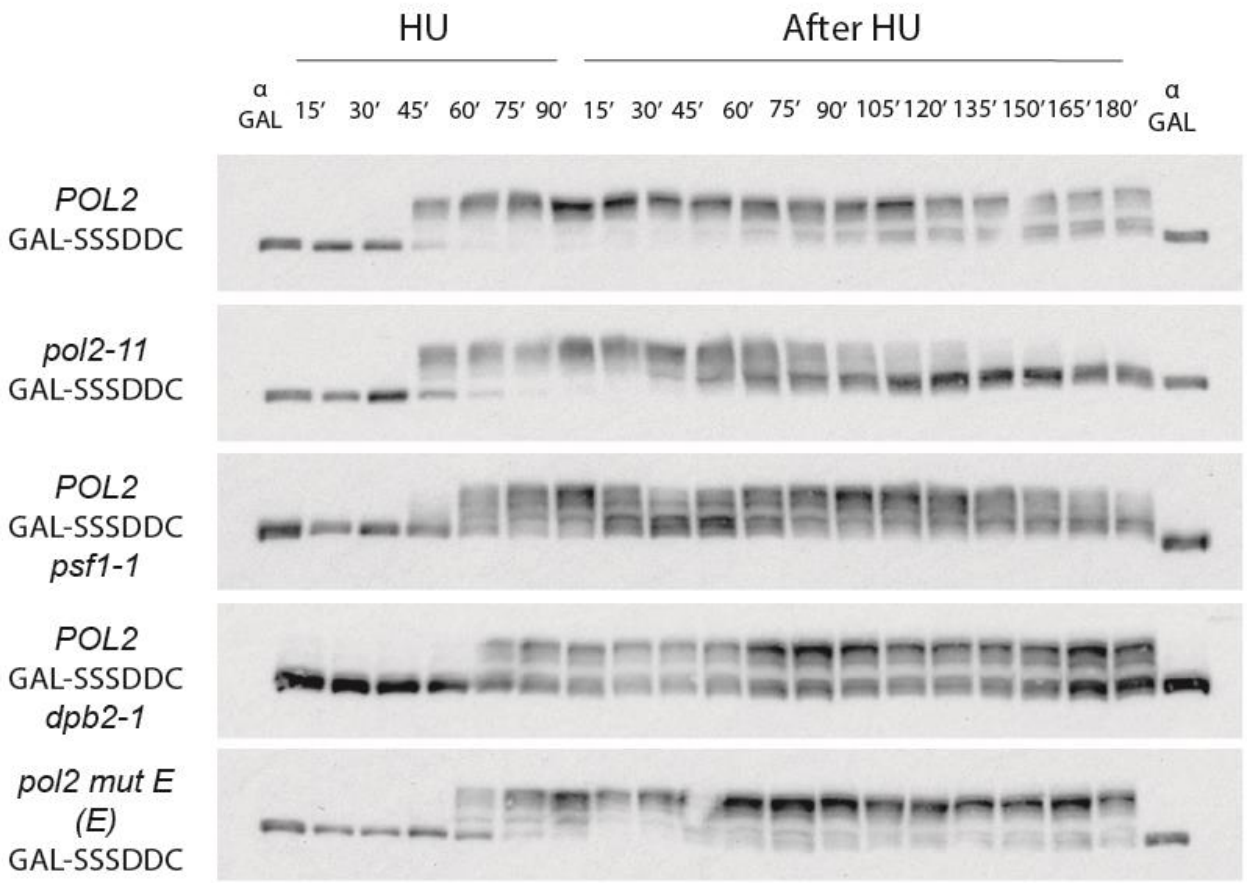
HU
After HU
α GAL
15′ 30′ 45′ 60′ 75′ 90′ 15′ 30′ 45′ 60′ 75′ 90′ 105′ 120′ 135′ 150′ 165′ 180′
α GAL
POL2 GAL-SSSDDC
pol2-11 GAL-SSSDDC
POL2 GAL-SSSDDC psf1-1
POL2 GAL-SSSDDC dpb2-1
pol2 mut E (E) GAL-SSSDDC
Rad53

Figure 4.9: The aberrant checkpoint signalling of *pol2-11* is not an artefact of its origin firing defect. Rad53 immunoblots on samples taken from experiments carried out on strains which contain alleles shown to possess origin firing defects, to ensure the checkpoint maintenance defect we have observed in *pol2-11* are not a consequence of lowered licensing efficiency. All strains contained the GAL-SSSDDC firing factor system, but in different backgrounds: *POL2* (CS 2126), *pol2-11* (CS 2485), *psf1-1* (CS 3624), *dpb2-1* (CS 3557) and *pol2 mutant E(E)* (CS 3559). Cells were grown to the exponential phase in YP-Raf at 24°C, arrested in alpha factor and resuspended in YP-Gal for 35 minutes to express the firing factors. They were then released in YP-Gal 0.2M HU for 90 minutes, after which they were washed and resuspended in YP-Gal to progress through the cell cycle for 3 hours. α factor was added back to arrest cells in G1 after the progression in S phase. These results show that these other strains that contain origin firing defects do not attenuate the checkpoint after the removal of replication stress in the manner of *pol2-11*. Data shown is representative of 2 independent experiments.

4.10 The premature attenuation of the checkpoint in *pol2-11* is not a result of an S phase checkpoint defect.

While Pol2 has long been associated with a function in the S phase checkpoint due to the high sensitivities that its mutants exhibit to genotoxic agents, it has also been found to bind several intermediaries of this signalling pathway. Mrc1, the Rad53 activator in the S phase checkpoint and Ctf18, a clamp-loader that acts downstream of Mec1, have both been shown to physically interact with Pol2 (Garcia-Rodriguez et al., 2015, Lou et al., 2008). In addition, Sgs1, a RecQ helicase that is able to bind Rad53, has also been found to bind to Pol2 through immunoprecipitation experiments (Hegnauer et al., 2012; De Piccoli, unpublished data). These data seem to strongly infer that Pol2 might play a direct or indirect role in the activation of the S phase checkpoint signalling. I therefore expected that the defect identified in *pol2-11* would be a consequence of a defect in this pathway. To check whether other mutants of the S phase checkpoint phenocopy that I have observed in *pol2-11*, experiments similar to the ones above were conducted using *mrc1*Δ*, ctf18*Δ and *sgs1*Δ backgrounds, all carrying the GAL-SSSDDC system. Mrc1 is a well conserved adapter protein that is understood to bind to the replisome through multiple sites of Pol2 and in conditions of replication stress is phosphorylated by both Mec1 and Rad53, which stabilises the replisome and provides a scaffold to provide prolonged checkpoint signalling; in addition it possesses a non-essential role in promoting fork progression (Naylor et al., 2009, Szyjka et al., 2005). Ctf18 is a clamp-loader which, through Dcc1 and Ctf8, is able to bind the Pol2 N-terminus and is believed to play some role in facilitating Rad53's phosphorylation by Mec1 at stalled forks (Grabarczyk et al., 2018, Crabbe et al., 2010). The RecQ DNA helicase Sgs1 is another target of Mec1 phosphorylation, which is believed to allow the recruitment of Rad53 to the fork and its deletion mutant's defects in recovering from the effects of HU appeared to be epistatic with *pol2-11* (Hegnauer et al., 2012, Frei and Gasser, 2000).

I examined the dynamics of Rad53 phosphorylation in wild type, *pol2-11*, *mrc1*Δ*, ctf18*Δ and *sgs1*Δ cells, all carrying the GAL-SSSDDC system. Cell cycle experiments and immunoblotting of the cell extracts were

conducted as described in 4.6, and the results are shown in Figure 4.10. Surprisingly, none of the deletions of these S phase checkpoint mediators exhibit the same phenotype shown by *pol2-11*, as they all resemble the wild type *POL2* in their recovery, or lack thereof, from the exposure to HU, with none even showing signs of reassertion of the non-phosphorylated form or Rad53. The only strain to show any different dynamics was Mrc1, which showed a heavily delayed activation in response to the replication stress, while it also appears that the level of this hyperphosphorylation of Rad53 is lower, showing the checkpoint to only be weakly activated. This phenotype is somewhat unsurprising as it has already been established that its phosphorylation is concomitant with Rad53 in these experiments and its importance in forming a robust checkpoint response at the fork is well known. Moreover, *ctf18*Δ cells showed a lower level of checkpoint activation throughout the experiment, with a greater fraction of unphosphorylated Rad53. Having said this, neither in *mrc1*Δ nor *ctf18*Δ did I observe an attenuation of the checkpoint signalling, and there is little sign that this would have happened if the recovery time had been longer. Perhaps most interesting is the *sgs1Δ* result, as the work by Frei and Gasser (2003) indicated that its role in recovering from activation of the S phase checkpoint, specifically after HU exposure, was in the same epistatic group as Pol2 and therefore appeared the best candidate to recapitulate phenomenon that has been exhibited by these experiments. Instead this indicates that the checkpoint attenuation is possibly not occurring through a defect in signalling the S phase checkpoint, but another pathway that Pol ε has yet to be properly implicated in.

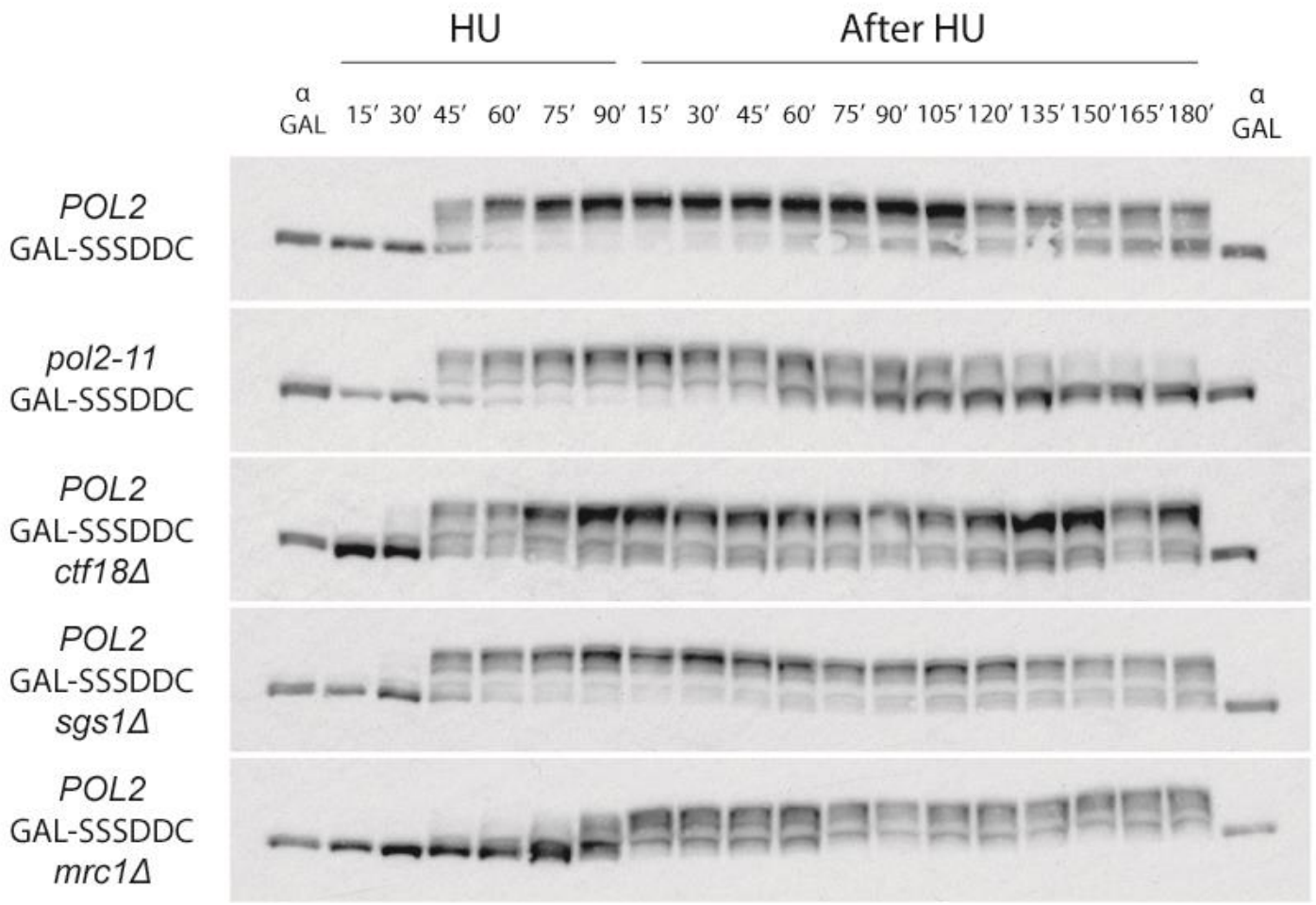
HU
After HU
α GAL
15′ 30′ 45′ 60′ 75′ 90′ 15′ 30′ 45′ 60′ 75′ 90′ 105′ 120′ 135′ 150′ 165′ 180′
α GAL
POL2 GAL-SSSDDC
pol2-11 GAL-SSSDDC
POL2 GAL-SSSDDC ctf18Δ
POL2 GAL-SSSDDC sgs1Δ
POL2 GAL-SSSDDC mrc1Δ
Rad53

Figure 4.10: The checkpoint maintenance defect observed in *pol2-11* cells in not due to an impairment in activating the S phase checkpoint. Rad53 immunoblot of samples taken from experiments performed on strains with S phase checkpoint mediators, known to physically interact with Pol2, deleted. All strains contained the GAL-SSSDDC firing factor system, but in different backgrounds: *POL2* (CS 2126), *pol2-11* (CS 2485), ***ctf18Δ*** (CS 3279), ***sgs1Δ*** (CS 3626) and ***mrc1Δ*** (CS 3630). Again, cells were grown to the exponential phase in YP-Raf at 24°C, arrested in alpha factor and resuspended in YP-Gal for 35 minutes to express the firing factors. They were then released in YP-Gal 0.2M HU for 90 minutes, after which they were washed and resuspended in YP-Gal to progress through the cell cycle for 3 hours. α factor was added back to arrest cells in G1 after the progression in S phase. Disrupting the S phase checkpoint by deleting its key mediators does not produce the same checkpoint attenuation phenotype observable in *pol2-11*. Data shown is representative of 2 independent experiments.

4.11 *pol2*-11's checkpoint defect appears to be due to impaired signalling of DNA damage.

Having been unsuccessful with recapitulating the *pol2-11* phenotype by disrupting the S phase checkpoint at the fork, it was decided to instead target the other signalling pathway operating behind them: the DNA damage checkpoint. This pathway recognises the accumulation of ssDNA behind forks and activates Rad53 to prevent cells entering mitosis with an incomplete genome. For this set of experiments, two genes were selected for deletion: *RAD24* and *RAD9*, which encode proteins that act as sensors and mediators of the DNA damage checkpoint, respectively. Similar to Ctf18, Rad24 is a clamp loader that is structurally related to replication factor C (RFC) subunits and functions to 'sense' DNA damage by loading the 9-1-1 complex at sites of RPA-bound ssDNA, either at the fork or behind it (Majka and Burgers, 2003). The presence of the 9-1-1 complex at sites of damage is able to activate Mec1 through its Ddc1 subunit which alone allows it to signal the checkpoint in G_1 (Navadgi-Patil and Burgers, 2009). However, in G_2 Mec1 is able to phosphorylate Ddc1, which recruits Dpb11 which can in turn activate Mec1, thus providing a parallel signalling branch for the checkpoint (Navadgi-Patil and Burgers, 2009). When recruited at forks in response to fork stalling, such as in response to HU, Mec1 can be activated by other components, like Dna2. However, when the damage occurs away or behind the replication fork, the process is fully dependent on the Rad24/ 9-1-1 complex (Wanrooij and Burgers, 2015). As previously detailed, Rad9 also has a key role in mediating the DNA damage response by transposing the DNA damage signals to the activation of Mec1.

As before, I examined the dynamics of Rad53 phosphorylation in wild type, *pol2-11*, *rad24*Δ and *rad9*Δ *cells*, all carrying the GAL-SSSDDC system. Cell cycle experiments and immunoblotting of the cell extracts were conducted as described in 4.6, the results are shown in Figure 4.11A. Remarkably, when the DNA damage checkpoint was disrupted through these mutations, a phenotype resembling that seen in *pol2-11* was observed. The deletions are not identical, however, as the two deletion mutants attenuate before the *pol2-11* strain and, out of these two mutants, the *rad9Δ* before the *rad24Δ*.

Neither of these mutants exhibited the lessened initial activation that could be seen in *ctf18Δ* or *mrc1Δ* strains from the previous experiment either, intimating that there appear to be two different 'types' of checkpoint activation over the course of this experiment: the initial activation, which appears to be dependent of the S phase checkpoint, and then the maintenance after the HU is removed, which, from these results appears dependent on the correct functioning of the DNA damage checkpoint. While none of the three strains where the checkpoint attenuated looked identical, it was the *rad24Δ* strain that appeared closest to the *pol2-11* dynamics and so it was decided to make a double mutant of these. If the pathways were epistatic, we would expect the double mutant to have similar kinetics of inactivation of Rad53; if *pol2-11* and *rad24*∆ were on different pathways, we would expect to see additive effect, with the inactivation of Rad53 faster than each single mutant. A cell-cycle experiment with cells wild type, *pol2-11, rad24Δ* and *pol2-11 rad24Δ,* all carrying the GAL-SSSDDC system, was carried out as described in 4.6, cell extracts were immunoblotted for Rad53, with the results shown in Figure 4.11B. Here, it appears that the double mutant exhibits the checkpoint activation dynamics of *pol2-11*, where the last time-point containing a significant hyperphosphorylated band is at 135 minutes after removal of the HU, whereas this appears to occur almost 30 minutes before in the single *rad24Δ* mutant, and this is further confirmed by band quantification shown in Figure 14.11C. This result would suggest that *POL2* and *RAD24* lie in the same epistatic group.

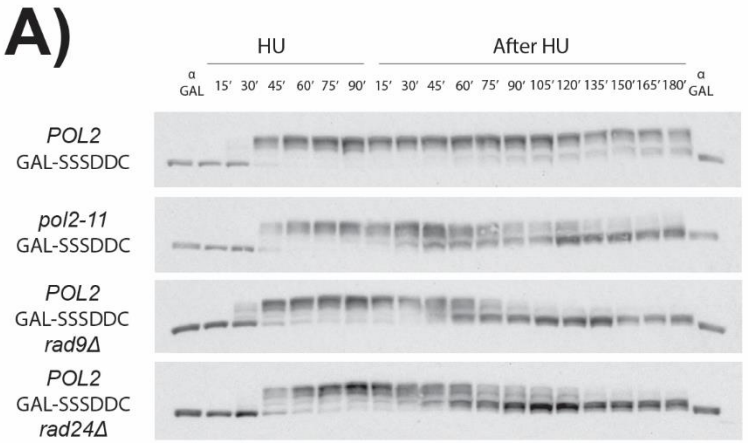
A)
HU
After HU
α GAL
15′ 30′ 45′ 60′ 75′ 90′ 15′ 30′ 45′ 60′ 75′ 90′ 105′ 120′ 135′ 150′ 165′ 180′
α GAL
POL2 GAL-SSSDDC
pol2-11 GAL-SSSDDC
POL2 GAL-SSSDDC rad9Δ
POL2 GAL-SSSDDC rad24Δ
Rad53

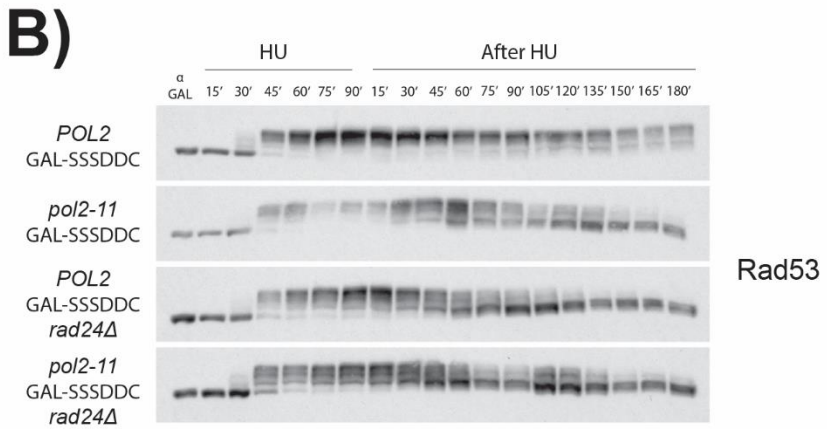
B)
HU
After HU
α GAL
15′ 30′ 45′ 60′ 75′ 90′ 15′ 30′ 45′ 60′ 75′ 90′ 105′ 120′ 135′ 150′ 165′ 180′
POL2 GAL-SSSDDC
pol2-11 GAL-SSSDDC
POL2 GAL-SSSDDC rad24Δ
pol2-11 GAL-SSSDDC rad24Δ
Rad53

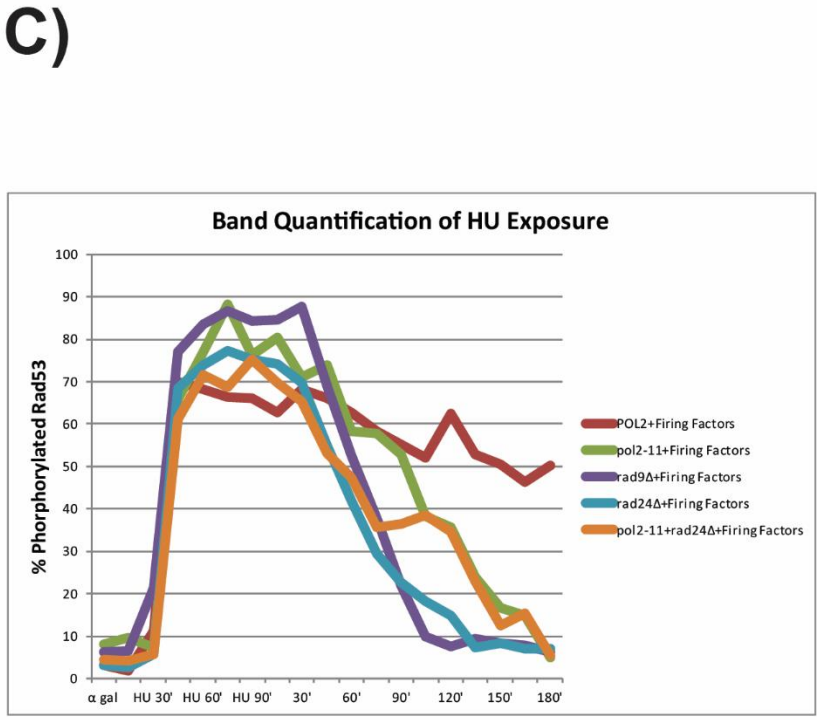
C)
Band Quantification of HU Exposure
% Phorphorylated Rad53
100
90
80
70
60
50
40
30
20
10
0
α gal
HU 30'
HU 60'
HU 90'
30'
60'
90'
120'
150'
180'
POL2+Firing Factors
pol2-11+Firing Factors
rad9Δ+Firing Factors
rad24Δ+Firing Factors
pol2-11+rad24Δ+Firing Factors

Figure 4.11: *pol2-11* cells are defective in signaling the DNA damage checkpoint. A) Rad53 immunoblots to of samples taken from experiments performed on strains with DNA damage checkpoint mediators deleted. All strains contained the GAL-SSSDDC firing factor system, but in different backgrounds: *POL2* (CS 2126), *pol2-11* (CS 2485), *rad9Δ* (CS 3696) and *rad24Δ* (CS 3468). These cells were grown to the exponential phase in YP-Raf at 24°C, arrested in alpha factor and resuspended in YP-Gal for 35 minutes to express the firing factors. They were then released in YP-Gal 0.2M HU for 90 minutes, after which they were washed and resuspended in YP-Gal to progress through the cell cycle for 3 hours. α factor was added back to arrest cells in G1 after the progression in S phase. In the cells in which the DNA damage checkpoint was disrupted, both exhibited similar, but not identical, dynamics of checkpoint attenuation to *pol2-11* after the removal of HU. **B)** Immunoblots of Rad53 from an identical experiment to that shown in (A) except with the *pol2-11/rad24Δ* strain (CS 3777) present. The double mutant indicates the epistatic nature of these defects, as its dynamics appear very similar to the *pol2-11* single mutant. **C)** A graph is shown plotting at each timepoint the intensity of the hyperphosphorylated Rad53 band as a percentage of the combined intensities of the top and bottom bands. This graph quantifies the results shown in (A) and (B) only and illustrates the similarity, although not identicality, in checkpoint attenuation dynamic between *pol2-11* and the deletions of the DNA damage checkpoint proteins. Data shown is representative of 2 independent experiments.

4.12 *pol2-11* is defective in DNA damage signalling.

Having seen that a defective DNA damage checkpoint appears to be responsible for the *pol2-11* phenotype, this was further probed by mainly targeting this pathway. Here, the cell cycle experiments were repeated with strains containing wild type *POL2* or *pol2-11*, all carrying the GAL-SSSDDC system, as well as a fully wild type strain, however instead, the exogenous replication stress that was exerted upon the cells was switched from HU to 0.033% alkylating agent MMS, a drug that preferentially activates the DNA damage checkpoint (Balint et al., 2015). Cells were grown to the exponential phase in YP-Raf at 24°C, arrested in G_1, resuspended in YP-gal for 35 minutes, and then released into YP-Gal containing 0.033% alkylating agent MMS for 90 minutes. This was washed out and cells were left to recover and complete replication, after which they were re-arrested in G_1 by addition of alpha factor. Samples were taken every 15 minutes, the protein extract were analysed by electrophoresis and immunoblotting for Rad53 and Mrc1. The results from the immunoblots are shown in Figure 4.12A and the quantification of the band intensities in 4.12B.

From these results, it is noticeable in wild type cells that the activation dynamics of the checkpoint are very similar to those seen with the HU, indicating that different replication stresses produce a sustained checkpoint response observed in the wild type cells with increased origin firing. Further strengthening the conclusion that it is the DNA damage checkpoint defective in *pol2-11* cells is the observation that the level of activation of Rad53 is also markedly decreased, as the lower phosphorylated band remains visible throughout the time-course, indicating an inability to fully activate the checkpoint. This is very much unlike the HU experiments, in which the activation dynamics during the initial exposures were nearly identical. The levels of Mrc1 phosphorylation in all of these strains are much decreased compared to those seen with HU, but still appear to roughly mirror what is seen in the Rad53 activation levels. This observation is to be expected though, as Mrc1 is not the main mediator of signalling the checkpoint, since this is mostly overseen by Rad9.

A)

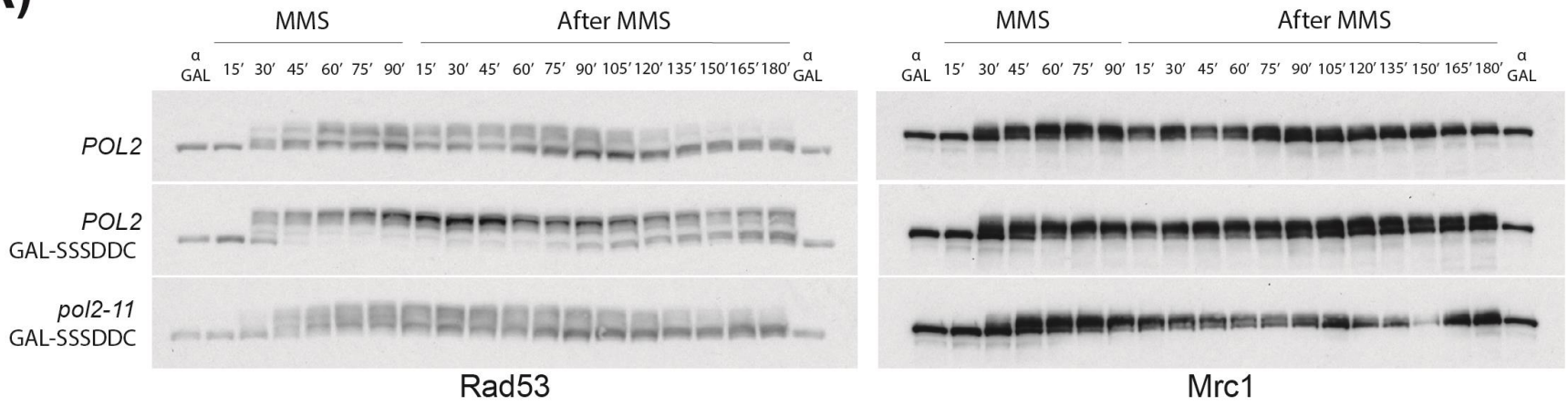
MMS
After MMS
α GAL
15′ 30′ 45′ 60′ 75′ 90′ 15′ 30′ 45′ 60′ 75′ 90′ 105′ 120′ 135′ 150′ 165′ 180′
α GAL
POL2
POL2 GAL-SSSDDC
pol2-11 GAL-SSSDDC
Rad53
Mrc1

B)

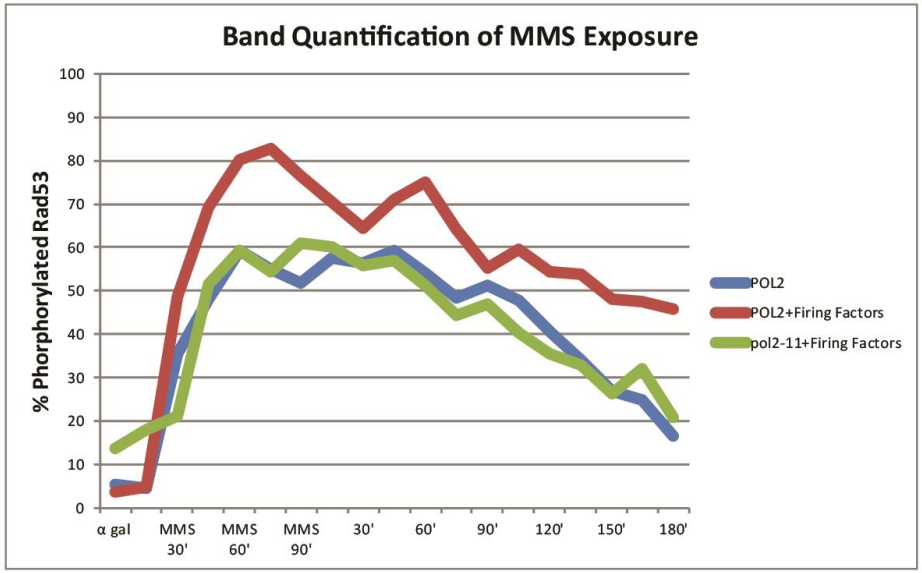
Band Quantification of MMS Exposure
% Phorphorylated Rad53
100
90
80
70
60
50
40
30
20
10
0
α gal
MMS 30'
MMS 60'
MMS 90'
30'
60'
90'
120'
150'
180'
POL2
POL2+Firing Factors
pol2-11+Firing Factors

Figure 4.12: When exposed to DNA damage, *pol2-11* cells show a defective checkpoint response. A) Rad53 and Mrc1 immunoblotting of samples taken from experiments observing the checkpoint response of cells to MMS treatment are shown. A wild type strain (CS 1), and strains with GAL-SSSDDC firing factor system with *POL2* and *pol2-11* backgrounds (CS 2126 and CS 2485, respectively) were used in this experiment. Cells were grown to the exponential phase in YP-Raf at 24°C, arrested in alpha factor and resuspended in YP-Gal for 35 minutes to express the firing factors. They were then released in YP-Gal 0.033% MMS for 90 minutes, after which they were washed and resuspended in YP-Gal to progress through the cell cycle for 3 hours. α factor was added back to arrest cells in G1 after the progression in S phase. In response to the DNA damage inflicted on the genome by MMS, *pol2-11* cells, even with the increased origin licensing show a decreased level of Rad53 hyperphosphorylation compared to the wild type. The checkpoint attenuates similarly to before and this is not observed in the *POL2* cells with increased origin firing. Data shown is representative of 2 independent experiments.. **B)** A graph is shown plotting at each timepoint the intensity of the hyperphosphorylated Rad53 band as a percentage of the combined intensities of the top and bottom bands. This graph quantifies the results shown only in (A) and clearly shows the decreased level of Rad53 activation in *pol2-11* cells as well as its subsequent attenuation.

4.13 The checkpoint defect of *pol2-11* is not defective in Mec1 signalling DNA damage.

The defects in the activation of the DNA damage checkpoint observed in *pol2-11* cells in the previous experiments raise the possibility that Pol2 is required for the activation of Rad53, working as an accessory mediator of the DNA damage signal. Alternatively, Pol2 might work in the activation or recruitment of the sensor kinase Mec1, the most upstream step required for checkpoint activation. I therefore decided to test whether Mec1 was activated in timely manner in *pol2-11* strains. To explore this, the levels of ɣ-H2AX were used as a downstream indicator of the activation of Mec1 in response to DNA damage. In this experiment, samples from the wild type and *pol2-11* strains with the firing factors acquired from the experiment shown in Figure 4.12, were immunoblotted for ɣ-H2AX and PCNA, which was used as a loading control. The results are shown in Figure 4.13 and, as can be seen, the timing of phosphorylation by Mec1 seems very comparable between strains, indicating this initial detection of replication stress is not the catalyst for the checkpoint attenuating and that it lies in its downstream signalling.

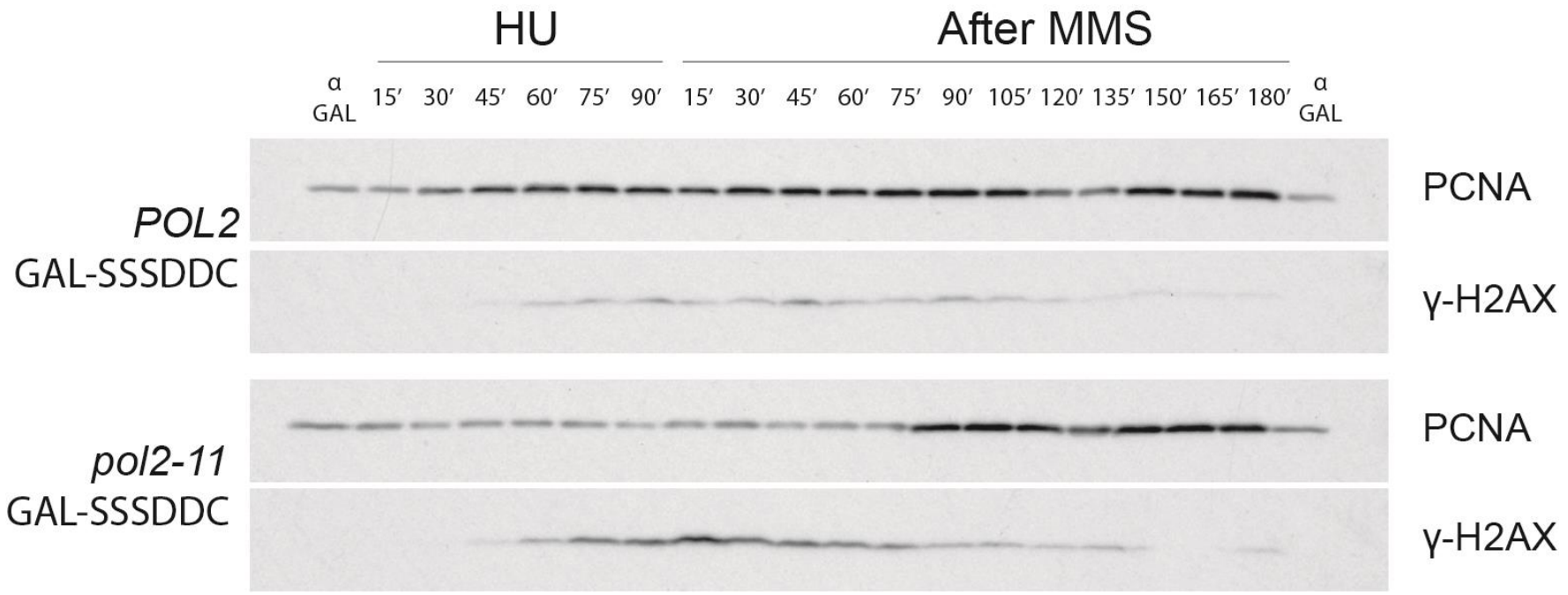

Figure 4.13: Mec1 activation is not affected in *pol2-11* cells. An immunoblot of γ-H2AX and PCNA in samples taken from wild type and *pol2-11* cells in the presence of MMS. These two strains contained the GAL-SSSDDC firing factor system in *POL2* and *pol2-11* backgrounds (CS 2126 and CS 2485, respectively). Cells were grown to the exponential phase in YP-Raf at 24°C, arrested in alpha factor and resuspended in YP-Gal for 35 minutes to express the firing factors. They were then released in YP-Gal 0.033% MMS for 90 minutes, after which they were washed and resuspended in YP-Gal to progress through the cell cycle for 3 hours. α factor was added back to arrest cells in G1 after the progression in S phase. These results illustrate the similar kinetic of H2A phosphorylation in the two strains, which is used as a marker for Mec1 activation in response to DNA damage, indicating that the presence of either *POL2* allele has no effect on Mec1 activation. Immunoblots for PCNA from samples of the same experiment used as a loading control.

4.14 The checkpoint attenuation phenotype in *pol2-11* can be suppressed by inhibiting translation.

As the replication fork is a highly dynamic complex, many of the factors that associate do so with much less stable interactions, resulting in many of them binding and rebinding in a dynamic manner depending each specific binding ability (Gambus et al., 2009). Moreover, protein degradation is believed to play an important role in the switching off of the checkpoint response (Chaudhury and Koepp, 2017). I hypothesized that in *pol2-11* there might be an increased turnover of these factors at forks and this might promote the shutdown of the checkpoint arrest. In this case, activated forms of proteins might be diluted more quickly with inactivated forms of the same factors and this could be prevented by disrupting protein synthesis. In order to inhibit translation, the glutarimide antibiotic cycloheximide (CHX) was used, which functions in preventing translational elongation possibly through binding the 60S ribosome subunit (Schneider-Poetsch et al., 2010). In these experiments, cells were grown to exponential phase, upon which they were arrested in G_1 by adding α factor. Cells were resuspended in YP-Gal to express the firing factors and then released into YP-Gal 0.2M HU for 90'. 60' into this HU exposure, CHX was added at a concentration of 200µg/mL to inhibit translation. Following the HU exposure, cells were washed, supplemented further with CHX and released into S phase for 3 hours to complete replication. The immunoblots for Rad53 and Mrc1 from this experiment are shown in Figure 4.14. Remarkably, the inhibition or translation suppressed the checkpoint attenuation phenotype of *pol2-11*, as Rad53 remained phosphorylated for the remainder of the experiment. Despite this, the checkpoint dynamics between the two Gal-SSSDCC strains are not identical. It appears that the addition of CHX may only temporarily maintain the checkpoint activation, as following its release from HU, the levels of hyperphosphorylated Rad53 appear to decrease and by the end the unphosphorylated band predominates. As translation is such a fundamental, constitutive process in the cell, it is not immediately clear how this could be preventing the checkpoint attenuation in *pol2-11*, especially as it is unclear what causes this in the first place. However, it is possible that the answer lies

in the deregulation of the more dynamic aspects of checkpoint maintenance, such as protein degradation or the phosphatase-mediated deactivation.

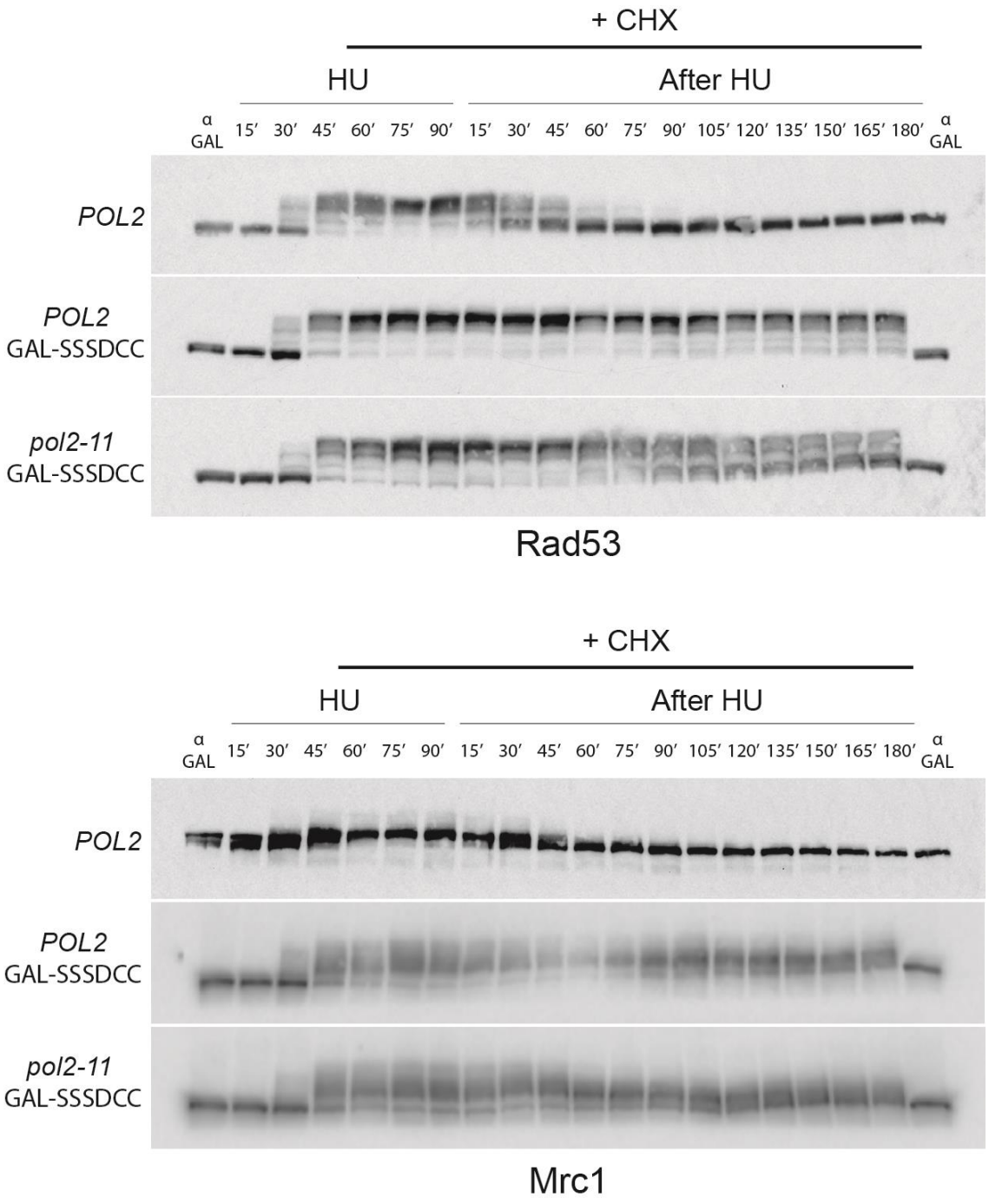

Figure 4.14: Inhibition of translation suppresses the checkpoint attenuation in *pol2-11* cells. Immunoblotting of Rad53 and Mrc1 from an experiment to observe how inhibiting translation affected the checkpoint maintenance in wild type cells (CS 1) and strains with the GAL-SSSDCC firing factor system in *POL2* and *pol2-11* backgrounds (CS 2126 and CS 2485, respectively). Cells were grown to the exponential phase in YP-Raf at 24°C, arrested in alpha factor and resuspended in YP-Gal for 35 minutes to express the firing factors. They were then released in YP-Gal 0.2M HU for 90 minutes, during which 200µg/mL cycloheximide (CHX) was added after 1 hour. Cells were then washed and resuspended in YP-Gal with supplementation of CHX to progress through the cell cycle for 3 hours. α factor was added back to arrest cells in G1 after the progression in S phase. The inhibition of protein synthesis by CHX addition maintains the Rad53 hyperphosphorylation after recovery from HU in *pol2-11* cells, while the checkpoint dynamics remain identical in both wild type *POL2* strains.

4.15 The checkpoint activation in G_2/M in response to double strand breaks is not affected in *pol2-11* cells.

The previous experiment suggests a role for Pol2 in the activation of the DNA damage checkpoint during S phase. In this context, rather than double strand breaks, Pol2 would most likely act at the single strand gaps occurring behind the forks. Whether this function in checkpoint activation is extended outside S phase, however, was not clear. To this aim, I tested whether *pol2-11* cells could activate the DNA damage checkpoint in response to a double strand break. For this experiment, wild type, *pol2-11* and *rad24Δ* cells were grown to exponential phase at 24°C, arrested in G_2 by the use of 10μg/ml Benomyl and 15μg/ml Nocodazole and then, once more than 85% of the cells were arrested as large budded cells, they were incubated with 100μg/mL Zeocin for 90 minutes. Zeocin is a member of the bleomycin family of antibiotics and functions by intercalating into DNA and causing cleavage, giving rise to numerous double strand breaks across the genome (Ehrenfeld et al., 1987). Samples were taken every 15 minutes, and cell extracts were analysed by electrophoresis and immunoblotting for Rad53. The results from this experiment, (Figure 4.15), show that both wild type and *pol2-11* alleles activate Rad53 in response to the onset of double strand break formation with similar dynamics. This suggests that the role of Pol2 in checkpoint activation is restricted to S phase. Moreover, this suggests that *pol2-11* cells might have no defect in sensing double strand breaks, promoting the idea that Pol2 might help the checkpoint activation mainly behind the fork, probably at sites of interrupted replication. The *rad24Δ* strain was included as a negative control, as this protein is key in recruiting Mec1 to double strand break sites and thereby promoting the activation of Rad53 (Dubrana et al., 2007). Together, these results suggest a novel role for DNA polymerase ε in signalling the DNA damage checkpoint away from forks.

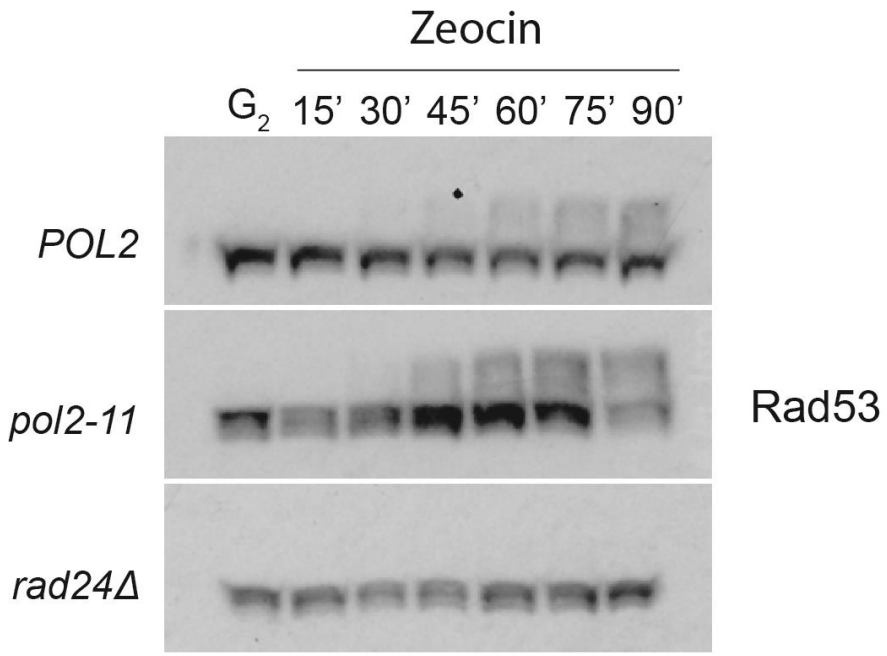

Figure 4.15: *pol2-11* does not possess a defect in signaling the G_2/M checkpoint in response to double strand breaks. Immunoblotting of Rad53 from an experiment in which the ability of *pol2-11* to sense double strand breaks was assessed. For this experiment, wild type*, pol2-11 and rad24Δ* (CS 1, CS 1159 and CS 722, respectively) strains were used. Cells were grown to the exponential phase in YPD at 24°C and arrested in G_2 by the use of benomyl and nocodazole. While arrested, 100µg/mL Zeocin was added to induce double strand breaks and samples were collected for 90'. The similar phosphorylation dynamics observed between the two *POL2* alleles indicates that there is no deficiency in the monitoring of double strand breaks between *pol2-11* and *POL2*. The *rad24Δ* strain was used as a control for cells defective in this checkpoint.

4.16 Increasing origin firing increases DNA damage sensitivity and loss of viability.

Having seen the alleviation of the origin firing defects in *pol2-11* through this firing factor system, the viability of these strains, as well as those containing numerous other mutants of origin firing- and checkpoint-related genes were checked by a dilution spotting experiment shown in Figure 4.16. The strains were grown in conditions of restrictive temperatures, HU and MMS with and without expression of the firing factors by using galactose and glucose-based media, respectively. In these experiments, growth in lower concentrations of hydroxyurea was observed due to the additional strain exerted on the checkpoint signalling by the firing factors. The deleterious effect the constitutive expression of these firing factors had upon the growth of cells is consistent with what has been shown in the literature, and has been hypothesised to be due to the overexpression of Dbf4 disrupting the strict temporal program of the cell cycle and causing initiation to occur in G_1 or even re-replication (Mantiero et al., 2011). Interestingly, the slight decrease in viability of *pol2-11* compared to the wild type in HU conditions is mirrored when the firing factors are expressed, and although this difference is very slight it permits a tentative conclusion that this checkpoint defect could in fact be independent from its origin licensing deficiency. Also noteworthy is the fact that the temperature sensitivity of *pol2-11*, is not suppressed by the firing factors considering that high copy number levels of either *DPB11* or *SLD2* have been shown to have this effect (Araki et al., 1995). This could be explained by the fact that the suppressive effects of the increased levels of Dpb11 or Sld2 are being masked by the negative effects of the other firing factors outside of just the forming of the pre-loading complex, although most likely only Dbf4. In addition, the loss of the suppressive effect of *DPB11* overexpression is not exclusive to *pol2-11,* as the same paper also showed this to occur with *dpb2-1* and another in *psf1-1*, whose viabilities can be seen to be clearly still exhibiting the temperature sensitivity even with the presence of the firing factors (Araki et al., 1995, Takayama et al., 2003). With the deletions of any of the checkpoint proteins, the increased sensitivities of these strains to the alkylating agent MMS were

immediately noticeable and understandable, as was the increased sensitivity to HU which, interestingly, only occurred when the firing factors were expressed.

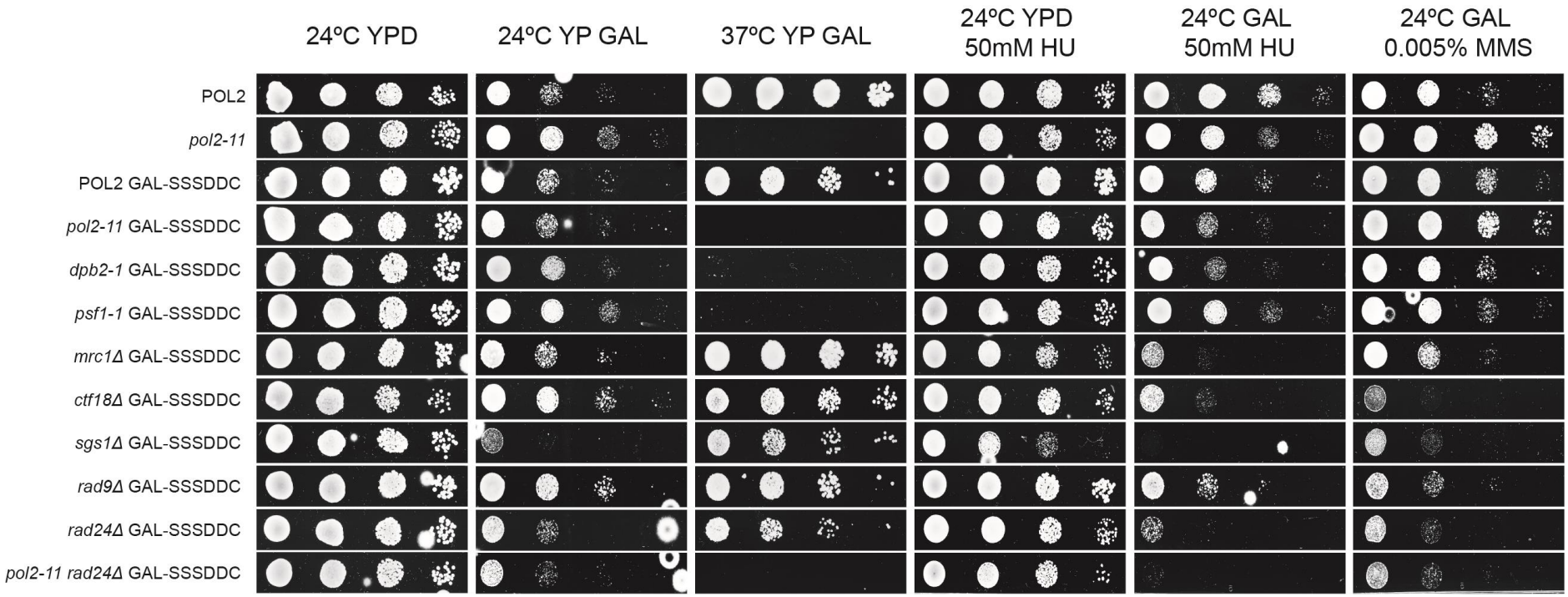

Figure 4.16 Artificially raising origin firing levels in *POL2* and *pol2-11* cells produces an enhanced sensitivity to replication stresses. A dilution spotting experiment in which the SSSDDC firing factor system was expressed in a range of different genetic backgrounds. Strains used in order of the order of their appearance from top to bottom: CS 1, CS 1159, CS 2126, CS 3775, CS 3557, CS 3624, CS 3630, CS 3279, CS 3626, CS 3696, CS 3648, CS 3777 and plate scans were taken 96 hours after spotting. Images of the colonies were taken after 72 hours of incubation at both permissive and restrictive temperatures, with and without expression of the firing factors as well as the presence of genotoxic drugs like HU and MMS. As can be seen, expressing the firing factors severely impacts the long-term viability of cells, although the presence of replication stress does not appear to specifically target the growth of *pol2-11* strains. Data shown is representative of 2 independent experiments.

Chapter 5: Discussion

5.1 The role of the Pol2 C-terminus at forks

It is well established that the C-terminus of Pol ε's catalytic subunit, Pol2, is essential for its function. Despite it being non-catalytic, its expression has been shown to suppress the deletion of its polymerase and exonuclease domains in a manner conserved through to higher eukaryotes (Kesti et al., 1999, Suyari et al., 2012). Additionally, C-terminal mutants exhibit severe growth defects, as well as temperature and genotoxic stress sensitivity phenotypes (Navas et al., 1995). One recently characterised function of this Pol2 C-terminus is to bind its B subunit, Dpb2, physically linking it to the helicase component, GINS, and thereby being instrumental in the formation of the pre-LC during origin firing (Dua et al., 1999, Sun et al., 2015). Beyond this, Pol ε has also been described *in vitro* to stimulate the activity of the helicase, to which it binds not just through its intermediate Dpb2 to GINS, but also directly through several C-terminal sites to the Mcm2-7 hexamer (Kang et al., 2012, Sun et al., 2015). However, it is yet to be established to what extent these interactions explain some of the defects observed in Pol2 C-terminal mutants. The work I have described in Chapter 3 sought to further our understanding of the diverse roles the Pol2 C-terminus might play during DNA replication.

In this work, I used a C-terminal mutant, *pol2-11*, coupled with a short C-terminal fragment of Pol2 in order to probe its functions in the cell cycle. I showed that *pol2-11* is in possession of a mild growth defect at permissive temperature and lethality at restrictive temperatures, as well as a sensitivity to HU. Furthermore, I characterised *pol2-11* as being defective in origin firing as well as having a much-weakened interaction with Dpb2. I coupled with this a construct containing the last 236 residues of Pol2 under the control of a galactose-inducible promoter and found that expression of this suppressed many of the abnormal phenotypes observed in the *pol2-11* allele. Here, I will contextualise my findings with the current understanding of the literature as well as hypothesise what these results might mean at a functional level. Finally, I will critically examine the work performed and explore how I intend to further this work to gain solid conclusions about the observed results.

My first experiments showed that *pol2-11* has an origin firing defect that is only partially suppressed by expression of the small Pol2 C-terminal fragment. Additionally, at restrictive temperatures *pol2-11* appears unable to initiate replication, while the Pol2 C-terminus permits progression through the cell cycle, albeit at a much slower rate than the wild type. Furthermore, the nature of this suppression by the Pol2 C-terminal fragment is not just restricted to assisting in the origin firing programme, as when a subset of origins were licensed and fired, it also appeared to aid the progression of the replication forks (Fig. 3.6). The results also illustrated that *pol2-11* had a weakened interaction with Dpb2, and this potentially provides a mechanistic understanding for the origin firing defect. In these cells, it can be conceived that the presence of *pol2-11* would destabilise Pol ε's presence in the pre-LC during origin firing, and thereby reduce efficiency of origin firing in these strains. Moreover, at restrictive temperatures these interactions would be destabilised further and possibly totally abolish the recruitment of Pol ε and GINS to forks. The importance of binding Dpb2 in the function of the C-terminal fragment can be seen in figure 3.8, as when this interaction is broken through mutation of the second zinc finger, this suppressive phenotype is lost. However, whether this is entirely due to its defective Dpb2 binding is not clear, as in the literature, the temperature sensitivity of *pol2-11* can be suppressed through the overexpression of two other pre-LC components, Dpb11 and Sld2, which were also shown to bind this C-terminus through Y2H assays (Kamimura et al., 1998). Unfortunately, our mass spectrometric analysis experiment didn't provide me with any information of the binding partners of the Pol2-C terminus, so this makes understanding the mechanism of its function difficult.

While it has been shown that the C-terminal half of Pol2 is sufficient to suppress its full deletion, I was unable to prove that this could be recapitulated with the smaller fragment (Kesti et al., 1999). I performed a plasmid shuffling experiment, in which I attempted to suppress progressively larger deletions, from full length, to the C-terminal half as well as just the last 236 residues, with the fragment (Data not shown). Unfortunately, these experiments were beset with problems as we were unable to replicate results from deletions observed

elsewhere, although they appeared to show that the C-terminal fragment was only sufficient to suppress a deletion of the same region. While it is unclear whether this observation is valid, it would appear that the entirety of the C-terminal half is required for its essential function. Therefore, we predict some essential role for the poorly conserved region of the Pol2 C-terminus. Unfortunately, little is known about this intervening sequence between the catalytic N-terminus and the zinc finger at the C-terminus, and structural analyses of the binding of Dpb2 and Pol2 have only focused on the very extreme C-terminus of the latter, even in human cells (Baranovskiy et al., 2017). This could indicate a region within that could assist in Pol2's essential origin firing function, and this is the role being fulfilled by *pol2-11* in the context of these experiments. Therefore, we believe that in our experiments the suppression of *pol2-11* temperature sensitivity occurs by two factors co-operating: the extreme C-terminal expressed and another unidentified region within the C-terminal half of *pol2-11*.

Although *pol2-11* cells survived at 37°C following the expression of the last 236 residue fragment, cells showed severe defects in DNA replication in these conditions. I reasoned that the partial suppression observed in *pol2-11* expressing the Pol2 fragment was due to a disconnection between the polymerase motor (Pol2) and the rest of the replisome, thus causing a slow progression of the replication fork. Interestingly, *in vitro* work shows that the Pol ε greatly increases the speed of DNA unwinding (Kang et al., 2012). Therefore, I attempted to fully suppress the temperature sensitivity of *pol2-11* by fusing the Pol2 C-terminus to the catalytic domain of Pol3. This chimera, however, appeared to bear little improvement in suppressing the defects of *pol2-11* over the Pol2 C-terminus. It should also be noted that this fusion protein was also unable to suppress a *POL2* deletion in the plasmid shuffling experiment detailed earlier, although these results are obviously not entirely reliable (data not shown). Owing to the similarity in phenotypes regardless of the presence of a catalytic domain, these results did show that the presence of the Pol3 region was not inhibiting the origin firing function of the fragment, although it was unclear as to whether any DNA synthesis was being carried out by the chimera. It is possible that the synthesis might be negligible because of the weak

recruitment of the chimera to the DNA and the lack of PCNA binding on the leading strand (the PCNA-Pol3 interaction motif was disrupted in the chimera), thus giving it a low processivity due to the absence of the clamp, as has been observed in the literature (Acharya et al., 2011). In this case, even in the presence of the chimera, the endogenous Pol δ complex performs DNA synthesis on the leading strand, and the chimera does not participate with the process, unlike in catalytic dead *POL2* mutants.

Collectively, these results suggest different possible mechanisms by which the Pol2 fragment could be involved in suppressing the *pol2-11* allele at restrictive temperatures. In one scenario, the Pol2-C-terminal fragment interacts only weakly and transiently with the relevant target, thus promoting origin firing. Following this, DNA replication occurs fully independently from Pol2 C-terminal and this might explain why we never managed to observe Pol2 C-terminal at forks, even after crosslinking (data not shown). Nevertheless, this does not explain the improvement we observed in fork progression in the *sld3-7/pol2-11* strains following HU release at non-permissive temperatures. Alternatively, we could imagine a transient but continuous recruitment at forks of Pol2 C-terminal fragment, thus playing a role at the replisome.

Moreover, the Pol2 fragment could work either *in cis* or *in trans* with the *pol2-11* allele at restrictive temperatures. In the case of the former, the fragment might work by binding to *pol2-11* and compensate for its less functional C-terminus by virtue of the presence of its last 26 residues. This could therefore assist in somewhat stabilising its binding to Dpb2 and promote pre-LC formation during origin firing, resulting in increased numbers of forks present during replication, particularly at non-permissive temperatures. This would, however, suggest a dimerization of Pol2 for which little evidence exists. Alternatively, it is possible the small fragment could operate largely independently of *pol2-11*, in which it would bind Dpb2 alone and in that manner promote the formation of the pre-LC during origin firing. At the fork, the C-terminus would remain associated with the CMG through Dpb2, as well as other theoretical binding sites like Mcm2 and -6 (Sun et al., 2015).

In non-permissive conditions, it is unclear whether *pol2-11* is actually synthesising DNA at forks in cells expressing the Pol2 C-terminus. While we know that *pol2-11* can still bind to the replisome, although with reduced affinity (Fig 3.16), it is reasonable to speculate that at higher temperatures, this interaction might be weakened further and this suggests that Pol δ might take over replication on the leading strand. However, in the presence of the Pol2 C-terminal domain, its direct contact with the helicase enables it to stimulate its function and aid fork progression. While inconclusive, the plasmid shuffling experiments would suggest *pol2-11* is playing a role in replication in some capacity, although whether this occurs only during origin firing or also in DNA synthesis at forks is unclear.

In order to understand the possible mechanism of suppression by this C-terminal fragment, I would suggest carrying out further experiments that could answer outstanding questions. In order to understand the mechanisms underlying the function of the C-terminus in a *pol2-11* background, it must first be addressed how DNA synthesis is being performed at the fork. Initially, it would be prudent to see if there is a difference in recruitment of *pol2-11* to forks at restrictive temperatures with or without expressing the Pol2 C-terminus. This could be performed by an immunoprecipitation of the replisome, possibly in the presence of cross-linking, followed by analysis of protein content. Furthermore, similar to experiments which established the theory of division of labour at the fork between the Pol ε and δ, the presence or absence of *pol2-11* at the leading strand could be tested by introducing a mutational bias individually to each polymerase, including the chimera, followed by sequencing analysis in conditions of restrictive and permissive temperatures in the presence of the C-terminal fragment (Pursell et al., 2007).

Following on from the experiments utilising the chimeric Pol3/Pol2 protein, I would also seek to find a method of fully suppressing the temperature sensitivity phenotype of *pol2-11*. By fusing a fully functional polymerase that is able to competently perform leading strand synthesis to the Pol2 C-terminus, any suppression of *pol2-11* defects could give an indication of what function the fragment performs in DNA replication. If this results in a full suppression of *pol2-11*, this would heavily indicate that not only is the essential function of Pol2

localised within its last 236 residues, it also dictates its leading strand synthesis activity. While the results were unclear as to whether the fused polymerase domain was in fact carrying out DNA synthesis, it is interesting to note that the Pol3 fragment fused to the C-terminus had its PIP box disrupted (Acharya et al., 2011). If this domain was in fact carrying out DNA synthesis, the chimera's partial suppression could be explained by its inability to bind PCNA, leaving it incapable of achieving the rates of processivity required for the leading strand polymerase. Therefore, if the catalytic domain was replaced with a single subunit, processive polymerase from a bacterial or viral system that can operate without the need for a sliding clamp, it is conceivable that maximal rates of processivity could be achieved. The Burgers lab have already shown a chimera containing the PCNA-interacting C-terminus of Pol3 fused to a bacteriophage polymerase to be functional and able to achieve comparable rates of processivity to the full length protein (Stodola et al., 2016). If these experiments were unsuccessful, it could indicate that there is a defining property of the N-terminus of Pol2 outside of its catalytic activity that enables it to efficiently synthesise DNA on the leading strand.

The suppressive effect the Pol2 C-terminus has on *pol2-11* in response to HU is also a matter of great interest. The expression of the C-terminal fragment confers a significant improvement in viability when *pol2-11* cells are grown in the presence of HU. However, when observing the dynamics of checkpoint activation in response to the same stress, it is not immediately clear how this suppression arises. In these cells, it appears that DNA damage occurs in *pol2-11* cells only when the C-terminus was expressed, as Rad53 activation is observed late in replication in a Rad9-dependent manner. I have formulated two hypotheses that could explain this phenotype: one possibility is that the Pol2 C-terminal causes damage to the genome during replication with *pol2-11* and this activates the DNA damage checkpoint. This, however, seems incongruous with the improved viability the expression of the C-terminus confers on *pol2-11* cells when grown in the presence of HU. Alternatively, it is worth considering that *pol2-11* perhaps inherently causes gaps behind forks. Through some mechanism, possibly away from forks, the C-terminus can assist in

recognising these and signals the DNA damage checkpoint and further work will be required to distinguish between these two hypotheses

Finally, the inability to purify the C-terminal fragment and analyse its binding partners had also significantly impacted my ability to assess its function in replication. Despite having attempted to express and purify this fragment by the use of a wide range of tags, conditions and organisms, I was simply unable to extract enough protein for a reliable MS screen. After having consulted others who had performed protein purifications on a larger portion of the Pol2 C-terminus, it appears that the expression of this region is not amenable to protein purification (Costa, personal communication) and therefore this method of detecting interactions is perhaps not the best way to proceed. In the future, it might be interesting to instead use an *in vivo* approach like the Biotin Identification (BioID) system, by which I would fuse a biotin ligase to the C-terminal fragment and then analyse which proteins have been proximally biotinylated (Roux et al., 2018). While initially developed in mammalian cells, this has been shown to also function in yeast systems as well as in analysing protein-protein interactions in DNA replication (Opitz et al., 2017, Dubois et al., 2016).

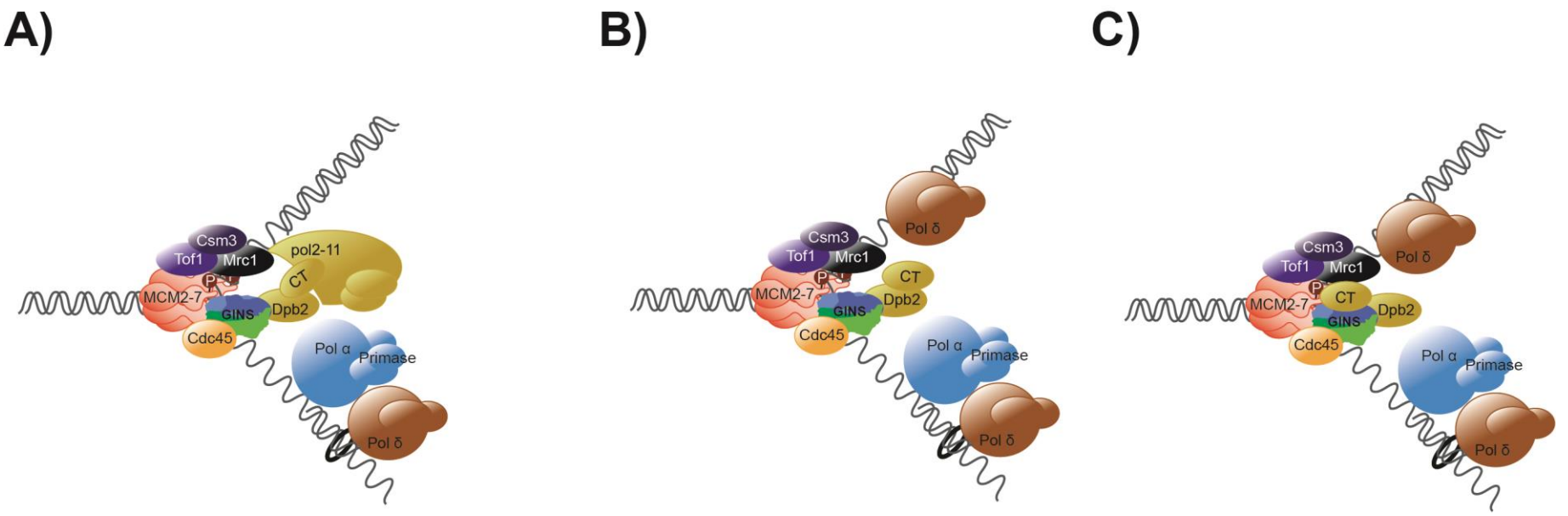

Figure 5.1: Figure 5.1: Three possible mechanisms by which the Pol2 C-terminus operates at the fork. From the work performed with *pol2-11* and the 236 residue Pol2 C-terminus, I have hypothesised three mechanisms through which this functions at the replication fork. **A)** The C-terminal fragment dimerises with the C-terminus of *pol2-11*, thereby somewhat repairing its interaction with Dpb2. This allows *pol2-11* to be integrated into the replisome and carry out leading strand synthesis. **B)** The Pol2 C-terminus binds Dpb2 alone, stabilising it in its interaction with Psf1 and allowing it to carry out its essential role in origin firing. The lack of *pol2-11* at the fork results in Pol δ carrying out leading strand synthesis. **C)** The Pol2 fragment binds at the Mcm2-5 gate in an interaction that has been identified by electron microscopy. This allows it to bind the CMG during the pre-LC and stabilise it during origin firing. This interaction would be rooted in the conserved hydrophobic domains of the fragment. Additionally, the lack of *pol2-11* means Pol δ takes over leading strand synthesis.

5.2 The function of the hydrophobic residues at the Pol2 C-terminus

Structurally, very little is understood about the Pol2 C-terminus, with the exception of the presence of its two highly conserved zinc fingers, the second of which has been shown to be integral in binding Dpb2 (Dua et al., 1998). In the rest of the work presented in Chapter 3, I focused on understanding the function of another conserved feature of this C-terminus: 5 hydrophobic residues beyond the zinc finger region. I found that mutating these residues to alanine in the C-terminal fragment abolished its suppressive effects, while introducing these same mutations in a genomic copy of *POL2* produced no independent phenotype. However, these mutants did exhibit defective and beneficial genetic interactions with two temperature sensitive alleles of origin firing-associated proteins: *sld2-6* and *mcm10-1*, respectively. Furthermore, mutating these same residues to glutamate radically altered the phenotype exhibited by the mutant, which made it temperature sensitive and synthetically lethal in the presence of *sld2-6*. Further functional analysis of this mutant revealed that this protein exhibited a defective interaction with Dpb2 coupled with a minor origin firing defect, reminiscent of a milder *pol2-11* phenotype. In this section I will contextualise these findings in order to make an assessment of the function these hydrophobic residues play in Pol2's role in DNA replication.

Perhaps the most interesting phenotype exhibited by the *pol2 mut E* mutant was its genetic interaction with *mcm10-1,* which improved its viability at restrictive temperatures and also appeared to allow it to initiate replication quicker. Previous studies have illustrated that *mcm10-1* has various replication defects, including replisomes remaining at the origins due to defective elongation at restrictive temperatures (van Deursen et al., 2012). Our assay of measuring replisome formation at similar temperatures did not show any kind of origin firing defect. Additionally, we observed no differences in replisome formation between the wild type and *pol2 mut E* allele. I hypothesise that this method of measuring origin firing is unsuitable in assessing the phenotypes of an *MCM10* mutant, as it can be assumed that the defect would arise after the components have been recruited to the fork (van Deursen et al., 2012).

Therefore, in order to further understand the how DNA initiation and fork progression is being affected, a method like DNA combing or two-dimensional gel electrophoresis would be best placed to assess any differences. With this, the levels of forks that are delayed during the initial elongation phase could be identified and the rates of progression could be quantified in the single and double mutants. What we see could be analogous to the suppressive effects of other Mcm mutants that have been observed in the literature. In studies involving Mcm10 and its binding partner, Mcm7, it was shown that both *mcm10-1* and *mcm7-1* alleles exhibited reduced levels of interaction with its wild type interactor, resulting in temperature sensitivity and DNA synthesis defects. However, the double mutant suppressed these defects and this was hypothesised to be due to the mutations within each of these proteins producing compensatory effects on their binding interface, thus restoring their wild type function (Homesley et al., 2000).

This could mean that the C-terminus plays some role in the remodelling of the helicase complex that occurs as elongation begins. Perhaps most significant in the implication of a direct interaction between these two proteins are two recent studies which have independently mapped essential interactions for Mcm10's helicase activation with the N-termini of Mcm2 and -6 subunits of CMG, which coincidentally have also been identified as interactors of the Pol2 C-terminus through cross-linking mass spectrometry, although through their C-terminal regions (Quan et al., 2015, Douglas and Diffley, 2016, Sun et al., 2015). Furthermore, these interactions have been shown to be weakened in the *mcm10-1* single mutant (Looke et al., 2017). While the nature of the binding of Pol2 to Mcm2 and -6 is yet to be established mechanistically, it is possible the hydrophobic domains being mutated to alanine could cause a small level of disruption in their interactions with Mcm2 and -6, and this could be transduced to the Mcm10 binding interface, which could ameliorate the unstable interaction in *mcm10-1*. This could indicate a somewhat indirect role of Pol ε in regulating the remodelling of the helicase complex prior to DNA elongation.

The severe temperature sensitivity phenotype exhibited by the glutamate mutant, *pol2 mutE(E),* very much resembled *pol2-11*, however its lack of a sensitivity to HU appeared to dictate that this was in fact a separation of

function between these two observed defects. Through analysis of its Dpb2 binding, it appeared to be extremely defective and only marginally better than *pol2-11*. Working under the hypothesis that it is this faulty interaction that underlies the origin firing deficiencies of *pol2-11*, this appears to be somewhat corroborated in *pol2 mut E(E)*, although this is by no means obvious and therefore it would be ideal to utilise a method through which these levels could be accurately quantified. One such method would be DNA combing which, by measuring track lengths emerging from origins, can quantify the levels of initiation events and has previously been used to study Mcm10 in human cells (Nieminuszczy et al., 2016, Kliszczak et al., 2015). However, fibre analysis is not always reliable in budding yeast systems, so other avenues of quantifying origin firing may be necessary, and 2D gels analysing replication intermediates from specific origins may be the best alternative. Further to this Dpb2 binding, in the alanine mutant this interaction was shown to be unaffected and this was corroborated by Y2H assays performed on the fragment (De Piccoli, unpublished data), yet in spite of this, it was still unable to suppress *pol2-11*'s defects when expressed ectopically as a C-terminal fragment. This could indicate that these hydrophobic residues play some role in stabilising or positioning the Zn finger to promote Dpb2 binding, whereas in the mutant, this interaction could be impacted to a significant degree that suppression cannot occur, though still enough that it's detectable by Y2H analysis. Alternatively, this could indicate that suppression occurs through mechanisms outside of simply binding Dpb2. It is possible to speculate that, by binding the Mcm2-7 complex, the Pol2 C-terminal hydrophobic amino acids might tether the fragment to the rest of the pre-LC complex, thus helping origin firing.

The defective nature of this mutant fragment would be best answered through a thorough analysis of its binding interactors by the method, as outlined for the wild type in the previous section, and then comparing how mutating these hydrophobic residues affects its binding profile. Furthering the notion that these hydrophobic residues have an independent function to Dpb2 binding, the presence of *sld2-6* in a *pol2 mut E* background created a synthetic defect which further exacerbated the former's temperature sensitivity. In this context, we know that the strength of Dpb2 is unaffected, and yet the presence of alanine

residues is able to cause an observable growth defect. Unfortunately, I was unable to elucidate the nature of this defect, but considering it is an *SLD2* allele and has previously been shown to be defective in Dpb11 binding, it can be speculated that its defect is localised to the formation of the pre-LC and possibly renders it unstable (Kamimura et al., 1998). Therefore, it is possible that these residues contribute in a minor way to the overall stability of the pre-LC, or by helping the anchoring of the pre-LC to the Mcm complex on the DNA. In a small fragment, it could be imagined that the lack of the entirety of the Pol2 protein could introduce an extra level of instability and mutating these residues simply crosses a threshold that prevents pre-LC formation. This could be corroborated by the synthetic lethalities noted with *pol2-11* and *pol2 mut E(E)*, two alleles which in concert with *sld2-6* could destabilise the binding of the pre-LC subunits past their threshold.

5.3 How does Pol ε function in the DNA damage checkpoint?

Pol ε has long been associated with a function in signalling the S phase checkpoint in response to replication stress. This has been inferred from its multiple interactions with checkpoint mediators, like Sgs1 and Mrc1, as well as the severe sensitivities to a range of genotoxic agents observed in its C-terminal mutants (Lou et al., 2008, Navas et al., 1995). However, the well characterised active role the C-terminus of Pol2 plays in origin firing complicates the notion of it having an independent checkpoint function. This is because it has been shown that a robust checkpoint response is predicated on a required threshold of forks to signal the presence of replication stress (Shimada et al., 2002). I have already shown that *pol2-11* exhibits origin firing defects as well as decreased viability in the presence of hydroxyurea, making it impossible to delineate whether these are independent functions of Pol2.

In my work in Chapter 4, I used the *pol2-11* allele alongside a characterised system of artificially increasing origin firing in order to explore whether Pol2 does possess an independent checkpoint signalling function (Mantiero et al., 2011). The firing factor system was sufficient to equalise origin firing levels between wild type and *pol2-11* strains and when probed for a

checkpoint defect, the C-terminal mutant exhibited a rapid attenuation of the checkpoint signal following exposure to HU. Through further analysis of mutants deficient in diverse aspects of the checkpoint, I illustrated that this defect was fully independent from those in origin firing, while also specifically identifying the DNA damage pathway as the means through which *pol2-11* is defective in checkpoint signalling. Finally, I showed that this attenuation exhibited by *pol2-11* can be suppressed by inhibiting protein translation.

From the results I have presented in this chapter, I believe that during the exposure to and release from HU in cells with expanded origin firing programmes, we are seeing an interplay of both the S phase and DNA damage signalling pathways. During the initial activation in response to HU, the dynamics of the hyperphosphorylation of Rad53 is delayed in *pol2-11* strains compared to the wild type. However, when origin firing is equalised between these two strains, the activation dynamics become indistinguishable. This is broadly true for the many other genetic backgrounds tested, except for the *mrc1Δ* strain, in which the hyperphosphorylation of Rad53 was extremely delayed. I concluded, therefore, that this initial response to HU was an activation of the S phase checkpoint and, in the case of *pol2-11* its defect in signalling this was fully suppressed by raising origin firing.

However, following from this, the dynamics of the checkpoint signal radically diverge from what we see in cells with an ordinary origin firing programme, in which, after the removal of stress, the checkpoint gradually turns off and replication proceeds. With increased levels of origin firing though, the checkpoint instead remains active following removal of the stress and replication appears to stall in G_2, characteristic of DNA damage signalling. In *pol2-11* cells, however, the levels of phosphorylated Rad53 slowly decrease after the removal of HU and the checkpoint is switched off, allowing replication to finish. Furthermore, this was not a phenotype present in the similarly temperature sensitive, but HU insensitive, *pol2 mut E(E)*, indicating that this does appear to be a separation of function mutant. Interestingly, the recapitulation of the attenuation phenotype was achieved by deleting mediators specifically of the DNA damage checkpoint, Rad24 and Rad9. This allows the conclusion that this second phase of checkpoint activation, after the removal of

stress, is in fact dependent on the DNA damage checkpoint and this is clearly defective in *pol2-11* cells. This defective nature of *pol2-11* in signalling the DNA damage checkpoint was further strengthened when the replication stress was MMS, which is predominantly signalled by this pathway. In these cells, the activation resembled strains without the increased levels of forks, as it appeared that the hyperphosphorylation of Rad53 was not only delayed but also reduced and again followed by the characteristic attenuation. Furthermore, translating what was observed previously in the activation of the checkpoint in *pol2-11* cells to the strains in which origin firing is increased, we can hypothesise the underpinning of this mutant's DNA damage signalling defect. What is being observed could be the widespread emergence of gaps behind forks as they undergo HU-mediated stalling. In a normal cell, these are detected with the assistance of the full-length Pol2 and the checkpoint remains active, whereas in *pol2-11* cells, these remain undetected and the cell cycle progresses.

From these results, I propose a model shown in figure 5.2 by which Pol ε forms an active part of the signalling network in the DNA damage checkpoint. I hypothesise that as cells encounter damage at the fork, the replisome moves forward and then leaves a gap to be resolved in late S phase, and Pol ε is loaded behind the fork at the site of the formation of the gap, either *de novo* or by disengaging itself from the replisome, and stays behind at these sites following their bypass by the replisome (Karras and Jentsch, 2010). Then, presumably through the C-terminus of Pol2, this is able to form a scaffold through which it is able to maybe generate a stable complex with other checkpoint components from which the checkpoint can be signalled and these stretches of DNA be repaired. In the context of this model, it is impossible to say whether Pol ε is functioning through Rad24, Rad9, Dpb11 or any other component of the DNA damage checkpoint, as the dynamics observed in the *po2-11/rad24Δ* double mutant, while they appeared epistatic, were inconclusive as to which one was upstream, although it appeared to be *pol2-11*. Ideally, this would be best achieved through the quantification of band intensity, however currently all of the data are n=1 and therefore several more repeats would be required before anything definitive in this area could be stated. Additionally, I will seek to test for the localisation of Pol ε with the DNA damage checkpoint

machinery by performing immunoprecipitations in the presence and absence of crosslinking.

Furthermore, it is also unclear how the inhibition of translation suppresses the *pol2-11* defect. It has previously been shown that addition of cycloheximide in the manner performed in this experiment does not impact at all on checkpoint recovery after HU exposure, so it is correct to conclude that this is something specific to *pol2-11* cells and this leads to two hypotheses (Tercero et al., 2003). In the first, I believe that the replication forks of *pol2-11*, possibly owing to its differing Pol ε complex stability, is prone to far more dynamic interactions, involving much more recycling of factors binding to the replisome. Additionally, activated forms of these factors that are dynamically binding could be responsible for maintaining the checkpoint, therefore, if they are recycled more they could be replaced by inactive forms causing a premature exit from the block. This theory would explain why, when protein synthesis is inhibited, the checkpoint remained active and replication was unable to restart. The other theory presupposes that the cycloheximide causes the depletion of proteins that are unstable. A subset of these unstable proteins could be acting through a pathway that would cause a release from the checkpoint to which *pol2-11* is inherently more sensitive. However, when cycloheximide is present these unstable proteins would be degraded and not replaced, resulting in the checkpoint remaining active. Types of protein that could be central in both of these hypotheses are phosphatases or ubiquitin ligases; therefore in order to further study this, I will attempt to disrupt the pathways these could be working through. Although there is the possibility of off-site effects, in the case of disrupting the proteasome system, we might also gain an understanding of whether the root of the cycloheximide result is due to the degradation of proteins or the synthesis of new ones.

From my current hypothesis of the checkpoint role of Pol2 I have identified, there is little existing evidence that would corroborate a system of Pol ε being left behind at forks. Furthermore, most work focusing on Pol ε's role in signalling the checkpoint has focused on the S phase checkpoint, for which numerous interactions have been identified with specific mediators of this pathway (Lou et al., 2008, Garcia-Rodriguez et al., 2015). Clearly more work

will be needed to fully prove and understand this function. Nevertheless, it is very tempting to speculate why Pol ε would be required for recognising DNA damage at the fork. As the leading strand polymerase, Pol ε replicates DNA continuously and therefore does not encounter gaps like Pol δ or Pol α would. Furthermore, it is tightly coupled with the helicase, as shown by the interaction of the Pol2 C-terminus buried within the Mcm5-2 'gate' recently identified by EM structures. It is possible that upon the DNA polymerase encountering a damaged DNA template, the CMG and the rest of the replisome moves forward, disengaging Pol ε and thus exposing Pol2 C-terminus. This could either cause a remodelling of the Pol ε complex or just present a surface that is usually covered during DNA replication. As such, this would be an ideal signal for the cell of defects in DNA replication. There are obviously a lot of gaps in our understanding of this, but there are several ways in which we could experimentally test the notion of Pol ε's presence at damage sites. Ideally, I would want to show that Pol ε can be localised away from forks and with other components of the DNA damage machinery, like Rad9, Rad24 or 9-1-1. Following on from this, I would like to understand the feature of *pol2-11* that is causing this checkpoint defect, and whether its C-terminal truncation is causing defective interactions with other components of the replisome, rather than just Dpb2. Future work will address these possibilities.

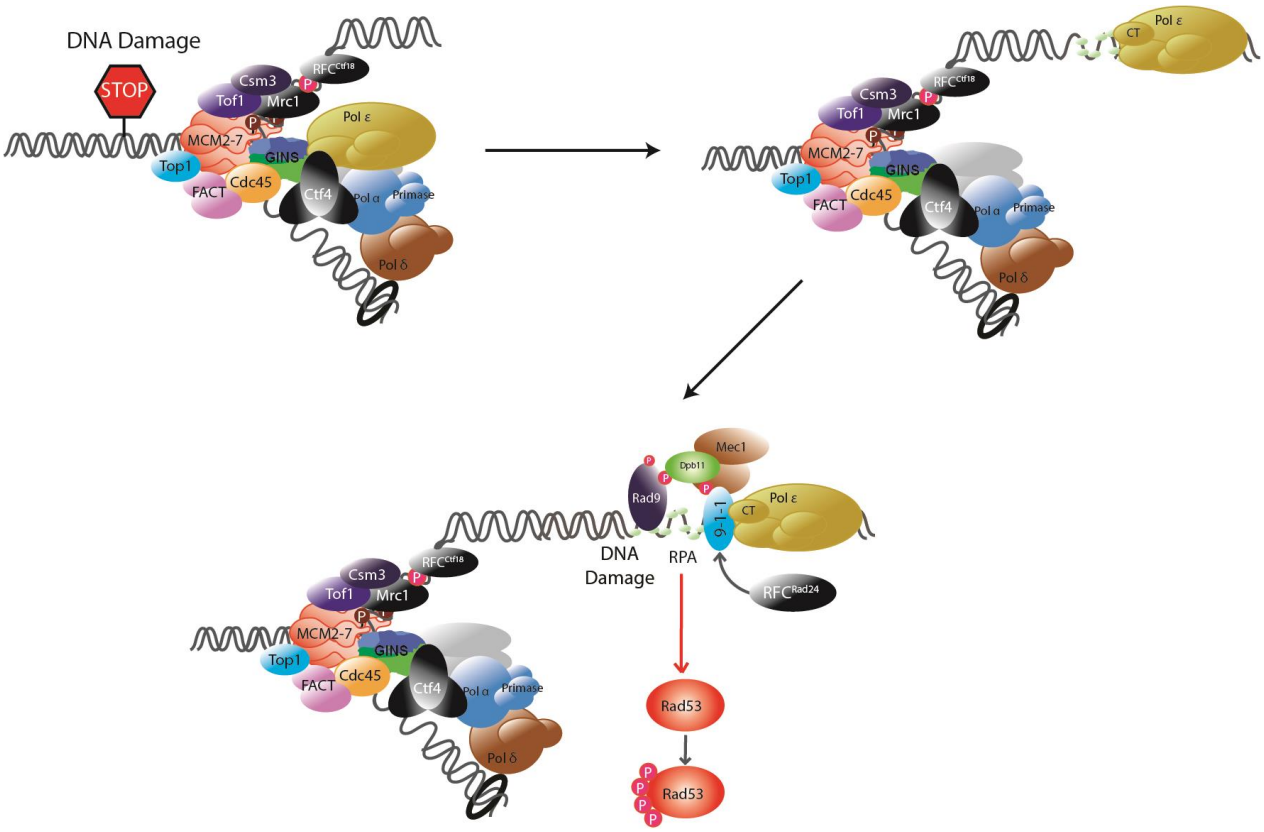

Figure 5.2: A possible mechanism of Pol ε's functioning in the DNA damage checkpoint. Here, I have presented a model in which Pol ε assists in signalling the DNA damage. I believe that upon encountering damage, Pol ε somehow remains associated with the site of damage after its bypass by the replisome. Whether this occurs by it being deposited by other factors or disengaging itself from the replisome is unclear. As it remains associated with these areas of DNA damage, this could provide a scaffold through which Rad9 and 9-1-1 could be recruited, possibly binding through its C-terminus, to activate Rad53 and signal the DNA damage checkpoint.

Abbreviations

APC/C: Anaphase promoting complex/ cyclosome

ARS: Autonomously replicating sequence

BRCT: BRCA1 C-Terminus

BSA: Bovine serum albumin

CDK: Cyclin-dependent protein kinase

CMG: Cdc45-Mcm2-7-GINS

DDK: Dbf4-dependent protein kinase

DMSO: Dimethyl sulfoxide

DNA: Deoxyribonucleic acid

dNTP: Deoxyribonucleotide triphosphate

EDTA: Ethylenediaminetetraacetic acid

EM: Electron microscopy

FACS: Fluorescence activated cell sorting

FILS: Facial dysmorphism, immunodeficiency, livedo, and short stature

Gal: Galactose

GINS: Sld5 (Go), Psf1 (Ichi), Psf2 (Ni), Psf3 (San)

GST: Glutathione-S-transferase

HU: Hydroxyurea

IP: Immunoprecipitation

MMS: Methyl methanesulfonate

ORC: Origin recognition complex

PBS: Phosphate-buffered saline

PCNA: Proliferating cell nuclear antigen

PEG: Polyethylene glycol

PIKK: Phosphoinositide 3-kinase-related kinases

PIP: PCNA interacting peptide

pre-LC: Pre-loading complex

Raff: Raffinose

RFC: Replication factor C

RPA: Replication protein A

RSM: Rapid sporulation medium

SDS-PAGE: Sodium dodecyl sulfate polyacrylamide gel electrophoresis

SOC: Super Optimal broth with Catabolite repression

TAD: Topologically associated domains

TBS-T: Tris buffered saline-TWEEN (0.1%)

TCS: Trichloroacetic acid

TD (or td): Temperature degron

Y2H: Yeast-2-hybrid

YP(D/Gal/Raf): Yeast peptone (dextrose/galactose/raffinose)

References

ACHARYA, N., KLASSEN, R., JOHNSON, R. E., PRAKASH, L. & PRAKASH, S. 2011. PCNA binding domains in all three subunits of yeast DNA polymerase delta modulate its function in DNA replication. *Proc Natl Acad Sci U S A,* 108**,** 17927-32.

AGARWAL, R., TANG, Z., YU, H. & COHEN-FIX, O. 2003. Two distinct pathways for inhibiting pds1 ubiquitination in response to DNA damage. *J Biol Chem,* 278**,** 45027-33.

AKSENOVA, A., VOLKOV, K., MACELUCH, J., PURSELL, Z. F., ROGOZIN, I. B., KUNKEL, T. A., PAVLOV, Y. I. & JOHANSSON, E. 2010. Mismatch repair-independent increase in spontaneous mutagenesis in yeast lacking non-essential subunits of DNA polymerase epsilon. *PLoS genetics,* 6**,** e1001209.

ALADJEM, M. I., RODEWALD, L. W., KOLMAN, J. L. & WAHL, G. M. 1998. Genetic dissection of a mammalian replicator in the human beta-globin locus [see comments]. *Science,* 281**,** 1005-9.

ALCASABAS, A. A., OSBORN, A. J., BACHANT, J., HU, F., WERLER, P. J., BOUSSET, K., FURUYA, K., DIFFLEY, J. F., CARR, A. M. & ELLEDGE, S. J. 2001. Mrc1 transduces signals of DNA replication stress to activate Rad53. *Nat Cell Biol,* 3**,** 958-65.

ANDREWS, B. & MEASDAY, V. 1998. The cyclin family of budding yeast: abundant use of a good idea. *Trends Genet,* 14**,** 66-72.

ARAKI, H., HAMATAKE, R. K., JOHNSTON, L. H. & SUGINO, A. 1991. DPB2, the gene encoding DNA polymerase II subunit B, is required for chromosome replication in Saccharomyces cerevisiae. *Proc Natl Acad Sci U S A,* 88**,** 4601-5.

ARAKI, H., LEEM, S. H., PHONGDARA, A. & SUGINO, A. 1995. Dpb11, which interacts with DNApolymerase II(epsilon) in *Saccharomyces cerevisiae*, has a dual role in S-phase progression and at a cell-cycle checkpoint. *Proc. Natl Acad. Sci. U S A,* 92**,** 11791-11795.

ASAHARA, H., LI, Y., FUSS, J., HAINES, D. S., VLATKOVIC, N., BOYD, M. T. & LINN, S. 2003. Stimulation of human DNA polymerase epsilon by MDM2. *Nucleic Acids Res,* 31**,** 2451-9.

BAE, S. H., BAE, K. H., KIM, J. A. & SEO, Y. S. 2001. RPA governs endonuclease switching during processing of Okazaki fragments in eukaryotes. *Nature,* 412**,** 456-61.

BALINT, A., KIM, T., GALLO, D., CUSSIOL, J. R., BASTOS DE OLIVEIRA, F. M., YIMIT, A., OU, J., NAKATO, R., GUREVICH, A., SHIRAHIGE, K., SMOLKA, M. B., ZHANG, Z. & BROWN, G. W. 2015. Assembly of Slx4 signaling complexes behind DNA replication forks. *Embo j,* 34**,** 2182-97.

BANDO, M., KATOU, Y., KOMATA, M., TANAKA, H., ITOH, T., SUTANI, T. & SHIRAHIGE, K. 2009. Csm3, Tof1, and Mrc1 form a heterotrimeric mediator complex that associates with DNA replication forks. *J Biol Chem,* 284**,** 34355-65.

BARANOVSKIY, A. G., GU, J., BABAYEVA, N. D., KURINOV, I., PAVLOV, Y. I. & TAHIROV, T. H. 2017. Crystal structure of the human Pol B-subunit in complex with the C-terminal domain of the catalytic subunit. *J Biol Chem,* 292**,** 15717-15730.

BARBARI, S. R., KANE, D. P., MOORE, E. A. & SHCHERBAKOVA, P. V. 2018. Functional Analysis of Cancer-Associated DNA Polymerase epsilon Variants in Saccharomyces cerevisiae. *G3 (Bethesda),* 8**,** 1019-1029.

BARNUM, K. J. & O'CONNELL, M. J. 2014. Cell cycle regulation by checkpoints. *Methods Mol Biol,* 1170**,** 29-40.

BASTIA, D., SRIVASTAVA, P., ZAMAN, S., CHOUDHURY, M., MOHANTY, B. K., BACAL, J., LANGSTON, L. D., PASERO, P. & O'DONNELL, M. E. 2016. Phosphorylation of CMG helicase and Tof1 is required for programmed fork arrest. *Proc Natl Acad Sci U S A,* 113**,** E3639-48.

BASTOS DE OLIVEIRA, F. M., KIM, D., CUSSIOL, J. R., DAS, J., JEONG, M. C., DOERFLER, L., SCHMIDT, K. H., YU, H. & SMOLKA, M. B. 2015. Phosphoproteomics reveals distinct modes of Mec1/ATR signaling during DNA replication. *Mol Cell,* 57**,** 1124-1132.

BAZZI, M., MANTIERO, D., TROVESI, C., LUCCHINI, G. & LONGHESE, M. P. 2010. Dephosphorylation of gamma H2A by Glc7/protein phosphatase 1 promotes recovery from inhibition of DNA replication. *Mol Cell Biol,* 30**,** 131-45.

BELLELLI, R., BOREL, V., LOGAN, C., SVENDSEN, J., COX, D. E., NYE, E., METCALFE, K., O'CONNELL, S. M., STAMP, G., FLYNN, H. R., SNIJDERS, A. P., LASSAILLY, F., JACKSON, A. & BOULTON, S. J. 2018. Polepsilon Instability Drives Replication Stress, Abnormal Development, and Tumorigenesis. *Mol Cell,* 70**,** 707-721.e7.

BERMUDEZ, V. P., FARINA, A., RAGHAVAN, V., TAPPIN, I. & HURWITZ, J. 2011. Studies on human DNA polymerase epsilon and GINS complex and their role in DNA replication. *The Journal of biological chemistry,* 286**,** 28963-77.

BERMUDEZ-LOPEZ, M., VILLORIA, M. T., ESTERAS, M., JARMUZ, A., TORRES-ROSELL, J., CLEMENTE-BLANCO, A. & ARAGON, L. 2016. Sgs1's roles in DNA end resection, HJ dissolution, and crossover suppression require a two-step SUMO regulation dependent on Smc5/6. *Genes Dev,* 30**,** 1339-56.

BERTOLI, C., HERLIHY, A. E., PENNYCOOK, B. R., KRISTON-VIZI, J. & DE BRUIN, R. A. M. 2016. Sustained E2F-Dependent Transcription Is a Key Mechanism to Prevent Replication-Stress-Induced DNA Damage. *Cell Rep,* 15**,** 1412-1422.

BERTOLI, C., KLIER, S., MCGOWAN, C., WITTENBERG, C. & DE BRUIN, R. A. 2013. Chk1 inhibits E2F6 repressor function in response to replication stress to maintain cell-cycle transcription. *Curr Biol,* 23**,** 1629-37.

BJERGBAEK, L., COBB, J. A., TSAI-PFLUGFELDER, M. & GASSER, S. M. 2005. Mechanistically distinct roles for Sgs1p in checkpoint activation and replication fork maintenance. *Embo J,* 24**,** 405-17.

BRUIN, D. 2009. All eukaryotes: Before turning off G1-S transcription, please check your DNA. *Cell Cycle,* 8**,** 214-217.

BURGERS, P. M. & GERIK, K. J. 1998. Structure and processivity of two forms of Saccharomyces cerevisiae DNA polymerase delta. *J Biol Chem,* 273**,** 19756-62.

BYLUND, G. O. & BURGERS, P. M. 2005. Replication protein A-directed unloading of PCNA by the Ctf18 cohesion establishment complex. *Mol Cell Biol,* 25**,** 5445-55.

CARETTI, G., MOTTA, M. C. & MANTOVANI, R. 1999. NF-Y associates with H3-H4 tetramers and octamers by multiple mechanisms. *Mol Cell Biol,* 19**,** 8591-603.

CAYROU, C., COULOMBE, P., VIGNERON, A., STANOJCIC, S., GANIER, O., PEIFFER, I., RIVALS, E., PUY, A., LAURENT-CHABALIER, S., DESPRAT, R. & MECHALI, M. 2011. Genome-scale analysis of metazoan replication origins reveals their organization in specific but flexible sites defined by conserved features. *Genome Res,* 21**,** 1438-49.

CHAUDHURY, I. & KOEPP, D. M. 2017. Degradation of Mrc1 promotes recombination-mediated restart of stalled replication forks. *Nucleic Acids Res,* 45**,** 2558-2570.

CHEN, E. S., HOCH, N. C., WANG, S. C., PELLICIOLI, A., HEIERHORST, J. & TSAI, M. D. 2014. Use of quantitative mass spectrometric analysis to elucidate the mechanisms of phospho-priming and auto-activation of the checkpoint kinase Rad53 in vivo. *Mol Cell Proteomics,* 13**,** 551-65.

CHEN, S. H., ALBUQUERQUE, C. P., LIANG, J., SUHANDYNATA, R. T. & ZHOU, H. 2010. A proteome-wide analysis of kinase-substrate network in the DNA damage response. *The Journal of biological chemistry,* 285**,** 12803-12.

CHEN, Y., CALDWELL, J. M., PEREIRA, E., BAKER, R. W. & SANCHEZ, Y. 2009. ATRMec1 phosphorylation-independent activation of Chk1 in vivo. *J Biol Chem,* 284**,** 182-90.

CHILKOVA, O., STENLUND, P., ISOZ, I., STITH, C. M., GRABOWSKI, P., LUNDSTROM, E. B., BURGERS, P. M. & JOHANSSON, E. 2007. The eukaryotic leading and lagging strand DNA polymerases are loaded onto primer-ends via separate mechanisms but have comparable processivity in the presence of PCNA. *Nucleic Acids Res,* 35**,** 6588-97.

CIMBORA, D. M., SCHUBELER, D., REIK, A., HAMILTON, J., FRANCASTEL, C., EPNER, E. M. & GROUDINE, M. 2000. Long-distance control of origin choice and replication timing in the human beta-globin locus are independent of the locus control region. *Mol Cell Biol,* 20**,** 5581-91.

COBB, J. A., BJERGBAEK, L., SHIMADA, K., FREI, C. & GASSER, S. M. 2003. DNA polymerase stabilization at stalled replication forks requires Mec1 and the RecQ helicase Sgs1. *Embo J,* 22**,** 4325-36.

COBB, J. A., SCHLEKER, T., ROJAS, V., BJERGBAEK, L., TERCERO, J. A. & GASSER, S. M. 2005. Replisome instability, fork collapse, and gross chromosomal rearrangements arise synergistically from Mec1 kinase and RecQ helicase mutations. *Genes Dev,* 19**,** 3055-69.

COMPTON, J. L., ZAMIR, A. & SZALAY, A. A. 1982. Insertion of nonhomologous DNA into the yeast genome mediated by homologous recombination with a cotransforming plasmid. *Mol Gen Genet,* 188**,** 44-50.

CORTEZ, D. 2015. Preventing replication fork collapse to maintain genome integrity. *DNA Repair (Amst),* 32**,** 149-57.
CRABBE, L., THOMAS, A., PANTESCO, V., DE VOS, J., PASERO, P. & LENGRONNE, A. 2010. Analysis of replication profiles reveals key role of RFC-Ctf18 in yeast replication stress response. *Nature structural & molecular biology,* 17**,** 1391-7.
D'URSO, G., GRALLERT, B. & NURSE, P. 1995. DNA polymerase alpha, a component of the replication initiation complex, is essential for the checkpoint coupling S phase to mitosis in fission yeast. *J Cell Sci,* 108**,** 3109-18.
D'URSO, G. & NURSE, P. 1997. Schizosaccharomyces pombe cdc20+ encodes DNA polymerase epsilon and is required for chromosomal replication but not for the S phase checkpoint. *Proc Natl Acad Sci U S A,* 94**,** 12491-6.
DAIGAKU, Y., KESZTHELYI, A., MULLER, C. A., MIYABE, I., BROOKS, T., RETKUTE, R., HUBANK, M., NIEDUSZYNSKI, C. A. & CARR, A. M. 2015. A global profile of replicative polymerase usage. *Nat Struct Mol Biol,* 22**,** 192-198.
DE BRUIN, R. A., MCDONALD, W. H., KALASHNIKOVA, T. I., YATES, J., 3RD & WITTENBERG, C. 2004. Cln3 activates G1-specific transcription via phosphorylation of the SBF bound repressor Whi5. *Cell,* 117**,** 887-98.
DE LA TORRE-RUIZ, M. A., GREEN, C. M. & LOWNDES, N. F. 1998. RAD9 and RAD24 define two additive, interacting branches of the DNA damage checkpoint pathway in budding yeast normally required for Rad53 modification and activation. *Embo J,* 17**,** 2687-98.
DE PICCOLI, G., KATOU, Y., ITOH, T., NAKATO, R., SHIRAHIGE, K. & LABIB, K. 2012. Replisome stability at defective DNA replication forks is independent of S phase checkpoint kinases. *Molecular cell,* 45**,** 696-704.
DEEGAN, T. D., YEELES, J. T. & DIFFLEY, J. F. 2016. Phosphopeptide binding by Sld3 links Dbf4-dependent kinase to MCM replicative helicase activation. *Embo j,* 35**,** 961-73.
DESHPANDE, I., SEEBER, A., SHIMADA, K., KEUSCH, J. J., GUT, H. & GASSER, S. M. 2017. Structural Basis of Mec1-Ddc2-RPA Assembly and Activation on Single-Stranded DNA at Sites of Damage. *Mol Cell,* 68**,** 431-445.e5.
DEVBHANDARI, S., JIANG, J., KUMAR, C., WHITEHOUSE, I. & REMUS, D. 2017. Chromatin Constrains the Initiation and Elongation of DNA Replication. *Mol Cell,* 65**,** 131-141.
DIBITETTO, D., FERRARI, M., RAWAL, C. C., BALINT, A., KIM, T., ZHANG, Z., SMOLKA, M. B., BROWN, G. W., MARINI, F. & PELLICIOLI, A. 2016. Slx4 and Rtt107 control checkpoint signalling and DNA resection at double-strand breaks. *Nucleic Acids Res,* 44**,** 669-82.
DMOWSKI, M. & FIJALKOWSKA, I. J. 2017. Diverse roles of Dpb2, the non-catalytic subunit of DNA polymerase epsilon. *Curr Genet,* 63**,** 983-987.
DMOWSKI, M., RUDZKA, J., CAMPBELL, J. L., JONCZYK, P. & FIJALKOWSKA, I. J. 2017. Mutations in the Non-Catalytic Subunit

Dpb2 of DNA Polymerase Epsilon Affect the Nrm1 Branch of the DNA Replication Checkpoint. *PLoS Genet,* 13**,** e1006572.
DOHMEN, R. J., WU, P. & VARSHAVSKY, A. 1994. Heat-inducible degron: a method for constructing temperature-sensitive mutants. *Science,* 263**,** 1273-6.
DONALDSON, A. D. 2000. The yeast mitotic cyclin Clb2 cannot substitute for S phase cyclins in replication origin firing. *EMBO Rep,* 1**,** 507-12.
DOUGLAS, M. E., ALI, F. A., COSTA, A. & DIFFLEY, J. F. X. 2018. The mechanism of eukaryotic CMG helicase activation. *Nature,* 555**,** 265-268.
DOUGLAS, M. E. & DIFFLEY, J. F. 2016. Recruitment of Mcm10 to Sites of Replication Initiation Requires Direct Binding to the Minichromosome Maintenance (MCM) Complex. *J Biol Chem,* 291**,** 5879-88.
DOWNS, J. A., LOWNDES, N. F. & JACKSON, S. P. 2000. A role for Saccharomyces cerevisiae histone H2A in DNA repair. *Nature,* 408**,** 1001-4.
DUA, R., EDWARDS, S., LEVY, D. L. & CAMPBELL, J. L. 2000. Subunit interactions within the Saccharomyces cerevisiae DNA polymerase epsilon (pol epsilon) complex. Demonstration of a dimeric pol epsilon. *J Biol Chem,* 275**,** 28816-25.
DUA, R., LEVY, D. L. & CAMPBELL, J. L. 1998. Role of the putative zinc finger domain of Saccharomyces cerevisiae DNA polymerase epsilon in DNA replication and the S/M checkpoint pathway. *J Biol Chem,* 273**,** 30046-55.
DUA, R., LEVY, D. L. & CAMPBELL, J. L. 1999. Analysis of the essential functions of the C-terminal protein/protein interaction domain of Saccharomyces cerevisiae pol epsilon and its unexpected ability to support growth in the absence of the DNA polymerase domain. *J Biol Chem,* 274**,** 22283-8.
DUBOIS, M. L., BASTIN, C., LEVESQUE, D. & BOISVERT, F. M. 2016. Comprehensive Characterization of Minichromosome Maintenance Complex (MCM) Protein Interactions Using Affinity and Proximity Purifications Coupled to Mass Spectrometry. *J Proteome Res,* 15**,** 2924-34.
DUBRANA, K., VAN ATTIKUM, H., HEDIGER, F. & GASSER, S. M. 2007. The processing of double-strand breaks and binding of single-strand-binding proteins RPA and Rad51 modulate the formation of ATR-kinase foci in yeast. *J Cell Sci,* 120**,** 4209-20.
DUROCHER, D., HENCKEL, J., FERSHT, A. R. & JACKSON, S. P. 1999. The FHA domain is a modular phosphopeptide recognition motif. *Mol Cell,* 4**,** 387-94.
EHRENFELD, G. M., SHIPLEY, J. B., HEIMBROOK, D. C., SUGIYAMA, H., LONG, E. C., VAN BOOM, J. H., VAN DER MAREL, G. A., OPPENHEIMER, N. J. & HECHT, S. M. 1987. Copper-dependent cleavage of DNA by bleomycin. *Biochemistry,* 26**,** 931-42.
ESER, U., CHANDLER-BROWN, D., AY, F., STRAIGHT, A. F., DUAN, Z., NOBLE, W. S. & SKOTHEIM, J. M. 2017. Form and function of topologically associating genomic domains in budding yeast. *Proc Natl Acad Sci U S A,* 114**,** E3061-e3070.

EVRIN, C., CLARKE, P., ZECH, J., LURZ, R., SUN, J., UHLE, S., LI, H., STILLMAN, B. & SPECK, C. 2009. A double-hexameric MCM2-7 complex is loaded onto origin DNA during licensing of eukaryotic DNA replication. *Proc Natl Acad Sci U S A,* 106**,** 20240-5.

FANG, D., LENGRONNE, A., SHI, D., FOREY, R., SKRZYPCZAK, M., GINALSKI, K., YAN, C., WANG, X., CAO, Q., PASERO, P. & LOU, H. 2017. Dbf4 recruitment by forkhead transcription factors defines an upstream rate-limiting step in determining origin firing timing. *Genes Dev,* 31**,** 2405-2415.

FENG, W. & D'URSO, G. 2001. Schizosaccharomyces pombe cells lacking the amino-terminal catalytic domains of DNA polymerase epsilon are viable but require the DNA damage checkpoint control. *Mol Cell Biol,* 21**,** 4495-504.

FOLTMAN, M., EVRIN, C., DE PICCOLI, G., JONES, R. C., EDMONDSON, R. D., KATOU, Y., NAKATO, R., SHIRAHIGE, K. & LABIB, K. 2013. Eukaryotic replisome components cooperate to process histones during chromosome replication. *Cell reports,* 3**,** 892-904.

FREI, C. & GASSER, S. M. 2000. The yeast Sgs1p helicase acts upstream of Rad53p in the DNA replication checkpoint and colocalizes with Rad53p in S-phase-specific foci. *Genes Dev,* 14**,** 81-96.

FRIGOLA, J., HE, J., KINKELIN, K., PYE, V. E., RENAULT, L., DOUGLAS, M. E., REMUS, D., CHEREPANOV, P., COSTA, A. & DIFFLEY, J. F. X. 2017. Cdt1 stabilizes an open MCM ring for helicase loading. *Nat Commun,* 8**,** 15720.

FU, Y. V., YARDIMCI, H., LONG, D. T., HO, T. V., GUAINAZZI, A., BERMUDEZ, V. P., HURWITZ, J., VAN OIJEN, A., SCHARER, O. D. & WALTER, J. C. 2011. Selective bypass of a lagging strand roadblock by the eukaryotic replicative DNA helicase. *Cell,* 146**,** 931-41.

FUCHS, S. Y., CHEN, A., XIONG, Y., PAN, Z. Q. & RONAI, Z. 1999. HOS, a human homolog of Slimb, forms an SCF complex with Skp1 and Cullin1 and targets the phosphorylation-dependent degradation of IkappaB and beta-catenin. *Oncogene,* 18**,** 2039-46.

FUKUI, T., YAMAUCHI, K., MUROYA, T., AKIYAMA, M., MAKI, H., SUGINO, A. & WAGA, S. 2004. Distinct roles of DNA polymerases delta and epsilon at the replication fork in Xenopus egg extracts. *Genes Cells,* 9**,** 179-91.

FURNARI, B., RHIND, N. & RUSSELL, P. 1997. Cdc25 mitotic inducer targeted by chk1 DNA damage checkpoint kinase. *Science,* 277**,** 1495-7.

GAMBUS, A., VAN DEURSEN, F., POLYCHRONOPOULOS, D., FOLTMAN, M., JONES, R. C., EDMONDSON, R. D., CALZADA, A. & LABIB, K. 2009. A key role for Ctf4 in coupling the MCM2-7 helicase to DNA polymerase alpha within the eukaryotic replisome. *EMBO J,* 28**,** 2992-3004.

GANAI, R. A., OSTERMAN, P. & JOHANSSON, E. 2015. Yeast DNA polymerase catalytic core and holoenzyme have comparable catalytic rates. *J Biol Chem,* 290**,** 3825-35.

GARBACZ, M. A., LUJAN, S. A., BURKHOLDER, A. B., COX, P. B., WU, Q., ZHOU, Z. X., HABER, J. E. & KUNKEL, T. A. 2018. Evidence that

DNA polymerase delta contributes to initiating leading strand DNA replication in Saccharomyces cerevisiae. *Nat Commun,* 9**,** 858.
GARCIA-RODRIGUEZ, L. J., DE PICCOLI, G., MARCHESI, V., JONES, R. C., EDMONDSON, R. D. & LABIB, K. 2015. A conserved Pol binding module in Ctf18-RFC is required for S-phase checkpoint activation downstream of Mec1. *Nucleic Acids Res,* 43**,** 8830-8.
GARG, P., STITH, C. M., SABOURI, N., JOHANSSON, E. & BURGERS, P. M. 2004. Idling by DNA polymerase delta maintains a ligatable nick during lagging-strand DNA replication. *Genes Dev,* 18**,** 2764-73.
GEORGESCU, R. E., LANGSTON, L., YAO, N. Y., YURIEVA, O., ZHANG, D., FINKELSTEIN, J., AGARWAL, T. & O'DONNELL, M. E. 2014. Mechanism of asymmetric polymerase assembly at the eukaryotic replication fork. *Nat Struct Mol Biol,* 21**,** 664-70.
GIANNATTASIO, M. & BRANZEI, D. 2017. S-phase checkpoint regulations that preserve replication and chromosome integrity upon dNTP depletion. *Cell Mol Life Sci,* 74**,** 2361-2380.
GOFFEAU, A., BARRELL, B. G., BUSSEY, H., DAVIS, R. W., DUJON, B., FELDMANN, H., GALIBERT, F., HOHEISEL, J. D., JACQ, C., JOHNSTON, M., LOUIS, E. J., MEWES, H. W., MURAKAMI, Y., PHILIPPSEN, P., TETTELIN, H. & OLIVER, S. G. 1996. Life with 6000 genes. *Science,* 274**,** 546, 563-7.
GRABARCZYK, D. B., SILKENAT, S. & KISKER, C. 2018. Structural Basis for the Recruitment of Ctf18-RFC to the Replisome. *Structure,* 26**,** 137-144.e3.
GRANDIN, N. & REED, S. I. 1993. Differential function and expression of Saccharomyces cerevisiae B-type cyclins in mitosis and meiosis. *Mol Cell Biol,* 13**,** 2113-25.
GRENON, M., COSTELLOE, T., JIMENO, S., O'SHAUGHNESSY, A., FITZGERALD, J., ZGHEIB, O., DEGERTH, L. & LOWNDES, N. F. 2007. Docking onto chromatin via the Saccharomyces cerevisiae Rad9 Tudor domain. *Yeast,* 24**,** 105-19.
GROSSI, S., PUGLISI, A., DMITRIEV, P. V., LOPES, M. & SHORE, D. 2004. Pol12, the B subunit of DNA polymerase alpha, functions in both telomere capping and length regulation. *Genes Dev,* 18**,** 992-1006.
GUO, C., KUMAGAI, A., SCHLACHER, K., SHEVCHENKO, A., SHEVCHENKO, A. & DUNPHY, W. G. 2015. Interaction of Chk1 with Treslin negatively regulates the initiation of chromosomal DNA replication. *Mol Cell,* 57**,** 492-505.
HAMMET, A., MAGILL, C., HEIERHORST, J. & JACKSON, S. P. 2007. Rad9 BRCT domain interaction with phosphorylated H2AX regulates the G1 checkpoint in budding yeast. *EMBO Rep,* 8**,** 851-7.
HANDA, T., KANKE, M., TAKAHASHI, T. S., NAKAGAWA, T. & MASUKATA, H. 2012. DNA polymerization-independent functions of DNA polymerase epsilon in assembly and progression of the replisome in fission yeast. *Molecular biology of the cell,* 23**,** 3240-53.
HATANO, Y., NAOKI, K., SUZUKI, A. & USHIMARU, T. 2016. Positive feedback promotes mitotic exit via the APC/C-Cdh1-separase-Cdc14 axis in budding yeast. *Cell Signal,* 28**,** 1545-54.
HE, H., LI, Y., DONG, Q., CHANG, A. Y., GAO, F., CHI, Z., SU, M., ZHANG, F., BAN, H., MARTIENSSEN, R., CHEN, Y. H. & LI, F. 2017.

Coordinated regulation of heterochromatin inheritance by Dpb3-Dpb4 complex. *Proc Natl Acad Sci U S A,* 114**,** 12524-12529.
HEGNAUER, A. M., HUSTEDT, N., SHIMADA, K., PIKE, B. L., VOGEL, M., AMSLER, P., RUBIN, S. M., VAN LEEUWEN, F., GUENOLE, A., VAN ATTIKUM, H., THOMA, N. H. & GASSER, S. M. 2012. An N-terminal acidic region of Sgs1 interacts with Rpa70 and recruits Rad53 kinase to stalled forks. *Embo j,* 31**,** 3768-83.
HERSKOWITZ, I. 1988. Life cycle of the budding yeast Saccharomyces cerevisiae. *Microbiol Rev,* 52**,** 536-53.
HOGG, M., OSTERMAN, P., BYLUND, G. O., GANAI, R. A., LUNDSTROM, E. B., SAUER-ERIKSSON, A. E. & JOHANSSON, E. 2014. Structural basis for processive DNA synthesis by yeast DNA polymerase varepsilon. *Nat Struct Mol Biol,* 21**,** 49-55.
HOMESLEY, L., LEI, M., KAWASAKI, Y., SAWYER, S., CHRISTENSEN, T. & TYE, B. K. 2000. Mcm10 and the MCM2-7 complex interact to initiate DNA synthesis and to release replication factors from origins. *Genes Dev,* 14**,** 913-26.
HU, J., SUN, L., SHEN, F., CHEN, Y., HUA, Y., LIU, Y., ZHANG, M., HU, Y., WANG, Q., XU, W., SUN, F., JI, J., MURRAY, J. M., CARR, A. M. & KONG, D. 2012. The intra-S phase checkpoint targets Dna2 to prevent stalled replication forks from reversing. *Cell,* 149**,** 1221-32.
HUANG, M., ZHOU, Z. & ELLEDGE, S. J. 1998. The DNA replication and damage checkpoint pathways induce transcription by inhibition of the Crt1 repressor. *Cell,* 94**,** 595-605.
HUSTEDT, N., SEEBER, A., SACK, R., TSAI-PFLUGFELDER, M., BHULLAR, B., VLAMING, H., VAN LEEUWEN, F., GUENOLE, A., VAN ATTIKUM, H., SRIVAS, R., IDEKER, T., SHIMADA, K. & GASSER, S. M. 2015. Yeast PP4 interacts with ATR homolog Ddc2-Mec1 and regulates checkpoint signaling. *Mol Cell,* 57**,** 273-89.
IIDA, T. & ARAKI, H. 2004. Noncompetitive counteractions of DNA polymerase epsilon and ISW2/yCHRAC for epigenetic inheritance of telomere position effect in Saccharomyces cerevisiae. *Molecular and cellular biology,* 24**,** 217-27.
IRNIGER, S. & NASMYTH, K. 1997. The anaphase-promoting complex is required in G1 arrested yeast cells to inhibit B-type cyclin accumulation and to prevent uncontrolled entry into S-phase. *J Cell Sci,* 110 (Pt 13)**,** 1523-31.
ISOZ, I., PERSSON, U., VOLKOV, K. & JOHANSSON, E. 2012. The C-terminus of Dpb2 is required for interaction with Pol2 and for cell viability. *Nucleic acids research,* 40**,** 11545-53.
JABLONOWSKI, C. M., CUSSIOL, J. R., OBERLY, S., YIMIT, A., BALINT, A., KIM, T., ZHANG, Z., BROWN, G. W. & SMOLKA, M. B. 2015. Termination of Replication Stress Signaling via Concerted Action of the Slx4 Scaffold and the PP4 Phosphatase. *Genetics,* 201**,** 937-49.
JAQUENOUD, M., VAN DROGEN, F. & PETER, M. 2002. Cell cycle-dependent nuclear export of Cdh1p may contribute to the inactivation of APC/C(Cdh1). *Embo j,* 21**,** 6515-26.
JASZCZUR, M., RUDZKA, J., KRASZEWSKA, J., FLIS, K., POLACZEK, P., CAMPBELL, J. L., FIJALKOWSKA, I. J. & JONCZYK, P. 2009. Defective interaction between Pol2p and Dpb2p, subunits of DNA

polymerase epsilon, contributes to a mutator phenotype in Saccharomyces cerevisiae. *Mutat Res,* 669**,** 27-35.
JESSBERGER, R., PODUST, V., HUBSCHER, U. & BERG, P. 1993. A mammalian protein complex that repairs double-strand breaks and deletions by recombination. *J Biol Chem,* 268**,** 15070-9.
JOHNSON, R. E., KLASSEN, R., PRAKASH, L. & PRAKASH, S. 2015. A major role of DNA polymerase δ in replication of both the leading and lagging DNA strands. *Molecular cell,* 59**,** 163-175.
JOHNSON, R. E., PRAKASH, L. & PRAKASH, S. 2012. Pol31 and Pol32 subunits of yeast DNA polymerase delta are also essential subunits of DNA polymerase zeta. *Proc Natl Acad Sci U S A,* 109**,** 12455-60.
KAMIMURA, Y., MASUMOTO, H., SUGINO, A. & ARAKI, H. 1998. Sld2, which interacts with Dpb11 in *Saccharomyces cerevisiae*, is required for chromosomal DNA replication. *Mol. Cell. Biol.,* 18**,** 6102-6109.
KANEMAKI, M. & LABIB, K. 2006. Distinct roles for Sld3 and GINS during establishment and progression of eukaryotic DNA replication forks. *Embo J,* 25**,** 1753-63.
KANG, Y. H., GALAL, W. C., FARINA, A., TAPPIN, I. & HURWITZ, J. 2012. Properties of the human Cdc45/Mcm2-7/GINS helicase complex and its action with DNA polymerase epsilon in rolling circle DNA synthesis. *Proceedings of the National Academy of Sciences of the United States of America,* 109**,** 6042-7.
KARANJA, K. K. & LIVINGSTON, D. M. 2009. C-terminal flap endonuclease (rad27) mutations: lethal interactions with a DNA ligase I mutation (cdc9-p) and suppression by proliferating cell nuclear antigen (POL30) in Saccharomyces cerevisiae. *Genetics,* 183**,** 63-78.
KARRAS, G. I. & JENTSCH, S. 2010. The RAD6 DNA damage tolerance pathway operates uncoupled from the replication fork and is functional beyond S phase. *Cell,* 141**,** 255-67.
KATOU, Y., KANOH, Y., BANDO, M., NOGUCHI, H., TANAKA, H., ASHIKARI, T., SUGIMOTO, K. & SHIRAHIGE, K. 2003. S-phase checkpoint proteins Tof1 and Mrc1 form a stable replication-pausing complex. *Nature,* 424**,** 1078-83.
KERMI, C., LO FURNO, E. & MAIORANO, D. 2017. Regulation of DNA Replication in Early Embryonic Cleavages. *Genes (Basel),* 8.
KESTI, T., FLICK, K., KERANEN, S., SYVAOJA, J. E. & WITTENBERG, C. 1999. DNA polymerase epsilon catalytic domains are dispensable for DNA replication, DNA repair, and cell viability. *Mol Cell,* 3**,** 679-85.
KESTI, T., MCDONALD, W. H., YATES, J. R., 3RD & WITTENBERG, C. 2004. Cell cycle-dependent phosphorylation of the DNA polymerase epsilon subunit, Dpb2, by the Cdc28 cyclin-dependent protein kinase. *J Biol Chem,* 279**,** 14245-55.
KLISZCZAK, M., SEDLACKOVA, H., PITCHAI, G. P., STREICHER, W. W., KREJCI, L. & HICKSON, I. D. 2015. Interaction of RECQ4 and MCM10 is important for efficient DNA replication origin firing in human cells. *Oncotarget,* 6**,** 40464-79.
KNOTT, S. R., PEACE, J. M., OSTROW, A. Z., GAN, Y., REX, A. E., VIGGIANI, C. J., TAVARE, S. & APARICIO, O. M. 2012. Forkhead transcription factors establish origin timing and long-range clustering in S. cerevisiae. *Cell,* 148**,** 99-111.

KNOTT, S. R., VIGGIANI, C. J., TAVARE, S. & APARICIO, O. M. 2009. Genome-wide replication profiles indicate an expansive role for Rpd3L in regulating replication initiation timing or efficiency, and reveal genomic loci of Rpd3 function in Saccharomyces cerevisiae. *Genes Dev,* 23**,** 1077-90.

KOIVOMAGI, M., VALK, E., VENTA, R., IOFIK, A., LEPIKU, M., BALOG, E. R., RUBIN, S. M., MORGAN, D. O. & LOOG, M. 2011. Cascades of multisite phosphorylation control Sic1 destruction at the onset of S phase. *Nature,* 480**,** 128-31.

KOMATA, M., BANDO, M., ARAKI, H. & SHIRAHIGE, K. 2009. The direct binding of Mrc1, a checkpoint mediator, to Mcm6, a replication helicase, is essential for the replication checkpoint against methyl methanesulfonate-induced stress. *Mol Cell Biol,* 29**,** 5008-19.

KONDO, T., WAKAYAMA, T., NAIKI, T., MATSUMOTO, K. & SUGIMOTO, K. 2001. Recruitment of Mec1 and Ddc1 checkpoint proteins to double-strand breaks through distinct mechanisms. *Science,* 294**,** 867-70.

KUCZERA, T., BAYRAM, O., SARI, F., BRAUS, G. H. & IRNIGER, S. 2010. Dissection of mitotic functions of the yeast cyclin Clb2. *Cell Cycle,* 9**,** 2611-9.

KUNKEL, T. A. 2004. DNA replication fidelity. *J Biol Chem,* 279**,** 16895-8.

LANGSTON, L. D. & O'DONNELL, M. 2008. DNA polymerase delta is highly processive with proliferating cell nuclear antigen and undergoes collision release upon completing DNA. *J Biol Chem,* 283**,** 29522-31.

LANGSTON, L. D., ZHANG, D., YURIEVA, O., GEORGESCU, R. E., FINKELSTEIN, J., YAO, N. Y., INDIANI, C. & O'DONNELL, M. E. 2014. CMG helicase and DNA polymerase epsilon form a functional 15-subunit holoenzyme for eukaryotic leading-strand DNA replication. *Proc Natl Acad Sci U S A,* 111**,** 15390-5.

LANZ, M. C., OBERLY, S., SANFORD, E. J., SHARMA, S., CHABES, A. & SMOLKA, M. B. 2018. Separable roles for Mec1/ATR in genome maintenance, DNA replication, and checkpoint signaling. *Genes Dev,* 32**,** 822-835.

LEE, C. S., LEE, K., LEGUBE, G. & HABER, J. E. 2014. Dynamics of yeast histone H2A and H2B phosphorylation in response to a double-strand break. *Nat Struct Mol Biol,* 21**,** 103-9.

LEE, Y. D., WANG, J., STUBBE, J. & ELLEDGE, S. J. 2008. Dif1 is a DNA-damage-regulated facilitator of nuclear import for ribonucleotide reductase. *Molecular cell,* 32**,** 70-80.

LENGRONNE, A., MCINTYRE, J., KATOU, Y., KANOH, Y., HOPFNER, K. P., SHIRAHIGE, K. & UHLMANN, F. 2006. Establishment of sister chromatid cohesion at the S. cerevisiae replication fork. *Mol Cell,* 23**,** 787-99.

LEROY, C., LEE, S. E., VAZE, M. B., OCHSENBEIN, F., GUEROIS, R., HABER, J. E. & MARSOLIER-KERGOAT, M. C. 2003. PP2C phosphatases Ptc2 and Ptc3 are required for DNA checkpoint inactivation after a double-strand break. *Mol Cell,* 11**,** 827-35.

LI, F., MARTIENSSEN, R. & CANDE, W. Z. 2011. Coordination of DNA replication and histone modification by the Rik1-Dos2 complex. *Nature,* 475**,** 244-8.

LIU, Q., GUNTUKU, S., CUI, X. S., MATSUOKA, S., CORTEZ, D., TAMAI, K., LUO, G., CARATTINI-RIVERA, S., DEMAYO, F., BRADLEY, A., DONEHOWER, L. A. & ELLEDGE, S. J. 2000. Chk1 is an essential kinase that is regulated by Atr and required for the G(2)/M DNA damage checkpoint. *Genes Dev,* 14**,** 1448-59.

LIU, Y., KAO, H. I. & BAMBARA, R. A. 2004. Flap endonuclease 1: a central component of DNA metabolism. *Annu Rev Biochem,* 73**,** 589-615.

LOOKE, M., MALONEY, M. F. & BELL, S. P. 2017. Mcm10 regulates DNA replication elongation by stimulating the CMG replicative helicase. *Genes Dev,* 31**,** 291-305.

LOPEZ-MOSQUEDA, J., MAAS, N. L., JONSSON, Z. O., DEFAZIO-ELI, L. G., WOHLSCHLEGEL, J. & TOCZYSKI, D. P. 2010. Damage-induced phosphorylation of Sld3 is important to block late origin firing. *Nature,* 467**,** 479-83.

LOU, H., KOMATA, M., KATOU, Y., GUAN, Z., REIS, C. C., BUDD, M., SHIRAHIGE, K. & CAMPBELL, J. L. 2008. Mrc1 and DNA polymerase epsilon function together in linking DNA replication and the S phase checkpoint. *Mol Cell,* 32**,** 106-17.

LUCCA, C., VANOLI, F., COTTA-RAMUSINO, C., PELLICIOLI, A., LIBERI, G., HABER, J. & FOIANI, M. 2004. Checkpoint-mediated control of replisome-fork association and signalling in response to replication pausing. *Oncogene,* 23**,** 1206-13.

LUCIANO, P., DEHE, P. M., AUDEBERT, S., GELI, V. & CORDA, Y. 2015. Replisome function during replicative stress is modulated by histone h3 lysine 56 acetylation through Ctf4. *Genetics,* 199**,** 1047-63.

MAILAND, N., BEKKER-JENSEN, S., BARTEK, J. & LUKAS, J. 2006. Destruction of Claspin by SCFbetaTrCP restrains Chk1 activation and facilitates recovery from genotoxic stress. *Mol Cell,* 23**,** 307-18.

MAJKA, J., BINZ, S. K., WOLD, M. S. & BURGERS, P. M. 2006. Replication protein A directs loading of the DNA damage checkpoint clamp to 5'-DNA junctions. *J Biol Chem,* 281**,** 27855-61.

MAJKA, J. & BURGERS, P. M. 2003. Yeast Rad17/Mec3/Ddc1: a sliding clamp for the DNA damage checkpoint. *Proc Natl Acad Sci U S A,* 100**,** 2249-54.

MAJKA, J. & BURGERS, P. M. 2004. The PCNA-RFC families of DNA clamps and clamp loaders. *Progress in nucleic acid research and molecular biology,* 78**,** 227-60.

MANTIERO, D., MACKENZIE, A., DONALDSON, A. & ZEGERMAN, P. 2011. Limiting replication initiation factors execute the temporal programme of origin firing in budding yeast. *Embo j,* 30**,** 4805-14.

MARIC, M., MACULINS, T., DE PICCOLI, G. & LABIB, K. 2014. Cdc48 and a ubiquitin ligase drive disassembly of the CMG helicase at the end of DNA replication. *Science,* 346**,** 1253596.

MARIC, M., MUKHERJEE, P., TATHAM, M. H., HAY, R. & LABIB, K. 2017. Ufd1-Npl4 Recruit Cdc48 for Disassembly of Ubiquitylated CMG Helicase at the End of Chromosome Replication. *Cell Rep,* 18**,** 3033-3042.

MARKOVITZ, A. 2005. A new in vivo termination function for DNA polymerase I of Escherichia coli K12. *Mol Microbiol,* 55**,** 1867-82.

MAYER, M. L., GYGI, S. P., AEBERSOLD, R. & HIETER, P. 2001. Identification of RFC(Ctf18p, Ctf8p, Dcc1p): an alternative RFC complex required for sister chromatid cohesion in S. cerevisiae. *Mol Cell,* 7**,** 959-70.

MCGUFFEE, S. R., SMITH, D. J. & WHITEHOUSE, I. 2013. Quantitative, genome-wide analysis of eukaryotic replication initiation and termination. *Mol Cell,* 50**,** 123-35.

MCINERNY, C. J., PARTRIDGE, J. F., MIKESELL, G. E., CREEMER, D. P. & BREEDEN, L. L. 1997. A novel Mcm1-dependent element in the SWI4, CLN3, CDC6, and CDC47 promoters activates M/G1-specific transcription. *Genes Dev,* 11**,** 1277-88.

MOISEEVA, T. N., GAMPER, A. M., HOOD, B. L., CONRADS, T. P. & BAKKENIST, C. J. 2016. Human DNA polymerase epsilon is phosphorylated at serine-1940 after DNA damage and interacts with the iron-sulfur complex chaperones CIAO1 and MMS19. *DNA Repair (Amst),* 43**,** 9-17.

MORENO, S. P., BAILEY, R., CAMPION, N., HERRON, S. & GAMBUS, A. 2014. Polyubiquitylation drives replisome disassembly at the termination of DNA replication. *Science,* 346**,** 477-481.

MORIN, I., NGO, H. P., GREENALL, A., ZUBKO, M. K., MORRICE, N. & LYDALL, D. 2008. Checkpoint-dependent phosphorylation of Exo1 modulates the DNA damage response. *The EMBO journal,* 27**,** 2400-10.

MORRISON, A. & SUGINO, A. 1993. DNA polymerase II, the epsilon polymerase of Saccharomyces cerevisiae. *Prog Nucleic Acid Res Mol Biol,* 46**,** 93-120.

MURAMATSU, S., HIRAI, K., TAK, Y. S., KAMIMURA, Y. & ARAKI, H. 2010. CDK-dependent complex formation between replication proteins Dpb11, Sld2, Pol epsilon, and GINS in budding yeast. *Genes Dev,* 24**,** 602-12.

NAKADA, D., MATSUMOTO, K. & SUGIMOTO, K. 2003. ATM-related Tel1 associates with double-strand breaks through an Xrs2-dependent mechanism. *Genes Dev,* 17**,** 1957-62.

NAVADGI-PATIL, V. M. & BURGERS, P. M. 2008. Yeast DNA replication protein Dpb11 activates the Mec1/ATR checkpoint kinase. *J Biol Chem,* 283**,** 35853-9.

NAVADGI-PATIL, V. M. & BURGERS, P. M. 2009. The unstructured C-terminal tail of the 9-1-1 clamp subunit Ddc1 activates Mec1/ATR via two distinct mechanisms. *Mol Cell,* 36**,** 743-53.

NAVAS, T. A., ZHOU, Z. & ELLEDGE, S. J. 1995. DNA polymerase epsilon links the DNA replication machinery to the S phase checkpoint. *Cell,* 80**,** 29-39.

NAYLOR, M. L., LI, J. M., OSBORN, A. J. & ELLEDGE, S. J. 2009. Mrc1 phosphorylation in response to DNA replication stress is required for Mec1 accumulation at the stalled fork. *Proceedings of the National Academy of Sciences of the United States of America,* 106**,** 12765-70.

NGUYEN, T. A., TAK, Y. S., LEE, C. H., KANG, Y. H., CHO, I. T. & SEO, Y. S. 2011. Analysis of subunit assembly and function of the Saccharomyces cerevisiae RNase H2 complex. *Febs j,* 278**,** 4927-42.

NGUYEN, V. Q., CO, C. & LI, J. J. 2001. Cyclin-dependent kinases prevent DNA re-replication through multiple mechanisms. *Nature,* 411**,** 1068-73.
NICK MCELHINNY, S. A., GORDENIN, D. A., STITH, C. M., BURGERS, P. M. & KUNKEL, T. A. 2008. Division of labor at the eukaryotic replication fork. *Mol Cell,* 30**,** 137-44.
NIEMINUSZCZY, J., SCHWAB, R. A. & NIEDZWIEDZ, W. 2016. The DNA fibre technique - tracking helicases at work. *Methods,* 108**,** 92-8.
NISHIZAWA, M., KAWASUMI, M., FUJINO, M. & TOH-E, A. 1998. Phosphorylation of sic1, a cyclin-dependent kinase (Cdk) inhibitor, by Cdk including Pho85 kinase is required for its prompt degradation. *Mol Biol Cell,* 9**,** 2393-405.
OHOUO, P. Y., BASTOS DE OLIVEIRA, F. M., LIU, Y., MA, C. J. & SMOLKA, M. B. 2013. DNA-repair scaffolds dampen checkpoint signalling by counteracting the adaptor Rad9. *Nature,* 493**,** 120-4.
OHYA, T., MAKI, S., KAWASAKI, Y. & SUGINO, A. 2000. Structure and function of the fourth subunit (Dpb4p) of DNA polymerase epsilon in Saccharomyces cerevisiae. *Nucleic Acids Res,* 28**,** 3846-52.
OPITZ, N., SCHMITT, K., HOFER-PRETZ, V., NEUMANN, B., KREBBER, H., BRAUS, G. H. & VALERIUS, O. 2017. Capturing the Asc1p/Receptor for Activated C Kinase 1 (RACK1) Microenvironment at the Head Region of the 40S Ribosome with Quantitative BioID in Yeast. *Mol Cell Proteomics,* 16**,** 2199-2218.
OSBORN, A. J. & ELLEDGE, S. J. 2003. Mrc1 is a replication fork component whose phosphorylation in response to DNA replication stress activates Rad53. *Genes Dev,* 17**,** 1755-67.
PACHLOPNIK SCHMID, J., LEMOINE, R., NEHME, N., CORMIER-DAIRE, V., REVY, P., DEBEURME, F., DEBRE, M., NITSCHKE, P., BOLE-FEYSOT, C., LEGEAI-MALLET, L., LIM, A., DE VILLARTAY, J. P., PICARD, C., DURANDY, A., FISCHER, A. & DE SAINT BASILE, G. 2012. Polymerase epsilon1 mutation in a human syndrome with facial dysmorphism, immunodeficiency, livedo, and short stature ("FILS syndrome"). *J Exp Med,* 209**,** 2323-30.
PACIOTTI, V., CLERICI, M., LUCCHINI, G. & LONGHESE, M. P. 2000. The checkpoint protein Ddc2, functionally related to S. pombe Rad26, interacts with Mec1 and is regulated by Mec1-dependent phosphorylation in budding yeast. *Genes Dev,* 14**,** 2046-59.
PALLES, C., CAZIER, J. B., HOWARTH, K. M., DOMINGO, E., JONES, A. M., BRODERICK, P., KEMP, Z., SPAIN, S. L., GUARINO, E., SALGUERO, I., SHERBORNE, A., CHUBB, D., CARVAJAL-CARMONA, L. G., MA, Y., KAUR, K., DOBBINS, S., BARCLAY, E., GORMAN, M., MARTIN, L., KOVAC, M. B., HUMPHRAY, S., CONSORTIUM, C., CONSORTIUM, W. G. S., LUCASSEN, A., HOLMES, C. C., BENTLEY, D., DONNELLY, P., TAYLOR, J., PETRIDIS, C., ROYLANCE, R., SAWYER, E. J., KERR, D. J., CLARK, S., GRIMES, J., KEARSEY, S. E., THOMAS, H. J., MCVEAN, G., HOULSTON, R. S. & TOMLINSON, I. 2013. Germline mutations affecting the proofreading domains of POLE and POLD1 predispose to colorectal adenomas and carcinomas. *Nat Genet,* 45**,** 136-44.

PARK, H. & STERNGLANZ, R. 1999. Identification and characterization of the genes for two topoisomerase I-interacting proteins from Saccharomyces cerevisiae. *Yeast,* 15**,** 35-41.
PARVIZ, F. & HEIDEMAN, W. 1998. Growth-independent regulation of CLN3 mRNA levels by nutrients in Saccharomyces cerevisiae. *J Bacteriol,* 180**,** 225-30.
PAVLOV, Y. I., FRAHM, C., NICK MCELHINNY, S. A., NIIMI, A., SUZUKI, M. & KUNKEL, T. A. 2006. Evidence that errors made by DNA polymerase alpha are corrected by DNA polymerase delta. *Curr Biol,* 16**,** 202-7.
PELLEGRINI, L. & COSTA, A. 2016. New Insights into the Mechanism of DNA Duplication by the Eukaryotic Replisome. *Trends Biochem Sci,* 41**,** 859-871.
PERERA, R. L., TORELLA, R., KLINGE, S., KILKENNY, M. L., MAMAN, J. D. & PELLEGRINI, L. 2013. Mechanism for priming DNA synthesis by yeast DNA Polymerase alpha. *eLife,* 2**,** e00482.
PETERS, J. M. 1998. SCF and APC: the yin and yang of cell cycle regulated proteolysis. *Curr Opin Cell Biol,* 10**,** 759-68.
PETERS, J. M. 2002. The anaphase-promoting complex: proteolysis in mitosis and beyond. *Mol Cell,* 9**,** 931-43.
PETRYK, N., KAHLI, M., D'AUBENTON-CARAFA, Y., JASZCZYSZYN, Y., SHEN, Y., SILVAIN, M., THERMES, C., CHEN, C. L. & HYRIEN, O. 2016. Replication landscape of the human genome. *Nat Commun,* 7**,** 10208.
PFANDER, B. & DIFFLEY, J. F. 2011. Dpb11 coordinates Mec1 kinase activation with cell cycle-regulated Rad9 recruitment. *Embo j,* 30**,** 4897-907.
POPE, B. D., RYBA, T., DILEEP, V., YUE, F., WU, W., DENAS, O., VERA, D. L., WANG, Y., HANSEN, R. S., CANFIELD, T. K., THURMAN, R. E., CHENG, Y., GULSOY, G., DENNIS, J. H., SNYDER, M. P., STAMATOYANNOPOULOS, J. A., TAYLOR, J., HARDISON, R. C., KAHVECI, T., REN, B. & GILBERT, D. M. 2014. Topologically associating domains are stable units of replication-timing regulation. *Nature,* 515**,** 402-5.
POWERS, B. L. & HALL, M. C. 2017. Re-examining the role of Cdc14 phosphatase in reversal of Cdk phosphorylation during mitotic exit. *J Cell Sci,* 130**,** 2673-2681.
PRADO, F. & MAYA, D. 2017. Regulation of Replication Fork Advance and Stability by Nucleosome Assembly. *Genes (Basel),* 8.
PUDDU, F., GRANATA, M., DI NOLA, L., BALESTRINI, A., PIERGIOVANNI, G., LAZZARO, F., GIANNATTASIO, M., PLEVANI, P. & MUZI-FALCONI, M. 2008. Phosphorylation of the budding yeast 9-1-1 complex is required for Dpb11 function in the full activation of the UV-induced DNA damage checkpoint. *Mol Cell Biol,* 28**,** 4782-93.
PUDDU, F., PIERGIOVANNI, G., PLEVANI, P. & MUZI-FALCONI, M. 2011. Sensing of replication stress and Mec1 activation act through two independent pathways involving the 9-1-1 complex and DNA polymerase epsilon. *PLoS genetics,* 7**,** e1002022.

PURSELL, Z. F., ISOZ, I., LUNDSTROM, E. B., JOHANSSON, E. & KUNKEL, T. A. 2007. Yeast DNA polymerase epsilon participates in leading-strand DNA replication. *Science,* 317**,** 127-30.

QUAN, Y., XIA, Y., LIU, L., CUI, J., LI, Z., CAO, Q., CHEN, X. S., CAMPBELL, J. L. & LOU, H. 2015. Cell-Cycle-Regulated Interaction between Mcm10 and Double Hexameric Mcm2-7 Is Required for Helicase Splitting and Activation during S Phase. *Cell Rep,* 13**,** 2576-2586.

QUILIS, I. & IGUAL, J. C. 2017. A comparative study of the degradation of yeast cyclins Cln1 and Cln2. *FEBS Open Bio,* 7**,** 74-87.

RAHAL, R. & AMON, A. 2008. Mitotic CDKs control the metaphase-anaphase transition and trigger spindle elongation. *Genes Dev,* 22**,** 1534-48.

RANDELL, J. C., BOWERS, J. L., RODRIGUEZ, H. K. & BELL, S. P. 2006. Sequential ATP hydrolysis by Cdc6 and ORC directs loading of the Mcm2-7 helicase. *Mol Cell,* 21**,** 29-39.

REMUS, D., BEURON, F., TOLUN, G., GRIFFITH, J. D., MORRIS, E. P. & DIFFLEY, J. F. 2009. Concerted loading of Mcm2-7 double hexamers around DNA during DNA replication origin licensing. *Cell,* 139**,** 719-30.

RHIND, N., YANG, S. C. & BECHHOEFER, J. 2010. Reconciling stochastic origin firing with defined replication timing. *Chromosome Res,* 18**,** 35-43.

ROSSI, S. E., AJAZI, A., CAROTENUTO, W., FOIANI, M. & GIANNATTASIO, M. 2015. Rad53-Mediated Regulation of Rrm3 and Pif1 DNA Helicases Contributes to Prevention of Aberrant Fork Transitions under Replication Stress. *Cell Rep,* 13**,** 80-92.

ROUX, K. J., KIM, D. I., BURKE, B. & MAY, D. G. 2018. BioID: A Screen for Protein-Protein Interactions. *Curr Protoc Protein Sci,* 91**,** 19.23.1-19.23.15.

SAHASHI, R., MATSUDA, R., SUYARI, O., KAWAI, M., YOSHIDA, H., COTTERILL, S. & YAMAGUCHI, M. 2013. Functional analysis of Drosophila DNA polymerase epsilon p58 subunit. *Am J Cancer Res,* 3**,** 478-89.

SANCHEZ GARCIA, J., CIUFO, L. F., YANG, X., KEARSEY, S. E. & MACNEILL, S. A. 2004. The C-terminal zinc finger of the catalytic subunit of DNA polymerase delta is responsible for direct interaction with the B-subunit. *Nucleic Acids Res,* 32**,** 3005-16.

SANCHEZ, Y., BACHANT, J., WANG, H., HU, F., LIU, D., TETZLAFF, M. & ELLEDGE, S. J. 1999. Control of the DNA damage checkpoint by chk1 and rad53 protein kinases through distinct mechanisms. *Science,* 286**,** 1166-71.

SANCHEZ, Y., WONG, C., THOMA, R. S., RICHMAN, R., WU, Z., PIWNICA-WORMS, H. & ELLEDGE, S. J. 1997. Conservation of the Chk1 checkpoint pathway in mammals: linkage of DNA damage to Cdk regulation through Cdc25. *Science,* 277**,** 1497-501.

SANCHEZ-DIAZ, A., KANEMAKI, M., MARCHESI, V. & LABIB, K. 2004. Rapid depletion of budding yeast proteins by fusion to a heat-inducible degron. *Sci STKE,* 2004**,** PL8.

SCHNEIDER-POETSCH, T., JU, J., EYLER, D. E., DANG, Y., BHAT, S., MERRICK, W. C., GREEN, R., SHEN, B. & LIU, J. O. 2010. Inhibition

of eukaryotic translation elongation by cycloheximide and lactimidomycin. *Nat Chem Biol,* 6**,** 209-217.
SCHWARTZ, M. F., DUONG, J. K., SUN, Z., MORROW, J. S., PRADHAN, D. & STERN, D. F. 2002. Rad9 phosphorylation sites couple Rad53 to the Saccharomyces cerevisiae DNA damage checkpoint. *Mol Cell,* 9**,** 1055-65.
SCHWOB, E., BOHM, T., MENDENHALL, M. D. & NASMYTH, K. 1994. The B-type cyclin kinase inhibitor p40^{SIC1} controls the G1 to S transition in *S. cerevisiae*. *Cell,* 79**,** 233-244.
SEGAL, M., CLARKE, D. J., MADDOX, P., SALMON, E. D., BLOOM, K. & REED, S. I. 2000. Coordinated spindle assembly and orientation requires Clb5p-dependent kinase in budding yeast. *J Cell Biol,* 148**,** 441-52.
SEGURADO, M. & DIFFLEY, J. F. 2008. Separate roles for the DNA damage checkpoint protein kinases in stabilizing DNA replication forks. *Genes Dev,* 22**,** 1816-27.
SEKI, M., TADA, S. & ENOMOTO, T. 2006. Function of recQ family helicase in genome stability. *Subcell Biochem,* 40**,** 49-73.
SENGUPTA, S., VAN DEURSEN, F., DE PICCOLI, G. & LABIB, K. 2013. Dpb2 integrates the leading-strand DNA polymerase into the eukaryotic replisome. *Current biology : CB,* 23**,** 543-52.
SHACKLETON, N. & PELTIER, W. 1992. ATP-dependent recognition of eukaryotic origins of DNA replication by a multiprotein complex. *Nature,* 357.
SHIKATA, K., SASA-MASUDA, T., OKUNO, Y., WAGA, S. & SUGINO, A. 2006. The DNA polymerase activity of Pol epsilon holoenzyme is required for rapid and efficient chromosomal DNA replication in Xenopus egg extracts. *BMC Biochem,* 7**,** 21.
SHIMADA, K., PASERO, P. & GASSER, S. M. 2002. ORC and the intra-S-phase checkpoint: a threshold regulates Rad53p activation in S phase. *Genes Dev,* 16**,** 3236-52.
SHIRAHIGE, K., HORI, Y., SHIRAISHI, K., YAMASHITA, M., TAKAHASHI, K., OBUSE, C., TSURIMOTO, T. & YOSHIKAWA, H. 1998. Regulation of DNA-replication origins during cell-cycle progression. *Nature,* 395**,** 618-21.
SHIVJI, M. K. K., PODUST, V. N., HUBSCHER, U. & WOOD, R. D. 1995. Nucleotide excision-repair DNA-synthesis by DNA polymerase-epsilon in the presence of pcna, rfc, and rpa. *Biochemistry,* 34**,** 5011-5017.
SINGH, A. & XU, Y. J. 2016. The Cell Killing Mechanisms of Hydroxyurea. *Genes (Basel),* 7.
SLATER, M. L. 1973. Effect of reversible inhibition of deoxyribonucleic acid synthesis on the yeast cell cycle. *J. Bacteriol.,* 113**,** 267-270.
SMITH, D. J. & WHITEHOUSE, I. 2012. Intrinsic coupling of lagging-strand synthesis to chromatin assembly. *Nature,* 483**,** 434-8.
SMOLKA, M. B., ALBUQUERQUE, C. P., CHEN, S. H. & ZHOU, H. 2007. Proteome-wide identification of in vivo targets of DNA damage checkpoint kinases. *Proceedings of the National Academy of Sciences of the United States of America,* 104**,** 10364-9.

SMOLKA, M. B., BASTOS DE OLIVEIRA, F. M., HARRIS, M. R. & DE BRUIN, R. A. 2012. The checkpoint transcriptional response: make sure to turn it off once you are satisfied. *Cell Cycle,* 11**,** 3166-74.

SMOLKA, M. B., CHEN, S. H., MADDOX, P. S., ENSERINK, J. M., ALBUQUERQUE, C. P., WEI, X. X., DESAI, A., KOLODNER, R. D. & ZHOU, H. 2006. An FHA domain-mediated protein interaction network of Rad53 reveals its role in polarized cell growth. *J Cell Biol,* 175**,** 743-53.

SONNEVILLE, R., MORENO, S. P., KNEBEL, A., JOHNSON, C., HASTIE, C. J., GARTNER, A., GAMBUS, A. & LABIB, K. 2017. CUL-2(LRR-1) and UBXN-3 drive replisome disassembly during DNA replication termination and mitosis. *Nat Cell Biol,* 19**,** 468-479.

SOWD, G. A. & FANNING, E. 2012. A wolf in sheep's clothing: SV40 co-opts host genome maintenance proteins to replicate viral DNA. *PLoS Pathog,* 8**,** e1002994.

SPIGA, M. G. & D'URSO, G. 2004. Identification and cloning of two putative subunits of DNA polymerase epsilon in fission yeast. *Nucleic Acids Res,* 32**,** 4945-53.

ST-PIERRE, J., DOUZIECH, M., BAZILE, F., PASCARIU, M., BONNEIL, E., SAUVE, V., RATSIMA, H. & D'AMOURS, D. 2009. Polo kinase regulates mitotic chromosome condensation by hyperactivation of condensin DNA supercoiling activity. *Mol Cell,* 34**,** 416-26.

STODOLA, J. L., STITH, C. M. & BURGERS, P. M. 2016. Proficient Replication of the Yeast Genome by a Viral DNA Polymerase. *J Biol Chem,* 291**,** 11698-705.

SUN, J., SHI, Y., GEORGESCU, R. E., YUAN, Z., CHAIT, B. T., LI, H. & O'DONNELL, M. E. 2015. The architecture of a eukaryotic replisome. *Nat Struct Mol Biol,* 22**,** 976-82.

SUYARI, O., KAWAI, M., IDA, H., YOSHIDA, H., SAKAGUCHI, K. & YAMAGUCHI, M. 2012. Differential requirement for the N-terminal catalytic domain of the DNA polymerase epsilon p255 subunit in the mitotic cell cycle and the endocycle. *Gene,* 495**,** 104-14.

SWEENEY, F. D., YANG, F., CHI, A., SHABANOWITZ, J., HUNT, D. F. & DUROCHER, D. 2005. Saccharomyces cerevisiae Rad9 acts as a Mec1 adaptor to allow Rad53 activation. *Curr Biol,* 15**,** 1364-75.

SZYJKA, S. J., APARICIO, J. G., VIGGIANI, C. J., KNOTT, S., XU, W., TAVARE, S. & APARICIO, O. M. 2008. Rad53 regulates replication fork restart after DNA damage in Saccharomyces cerevisiae. *Genes & development,* 22**,** 1906-20.

SZYJKA, S. J., VIGGIANI, C. J. & APARICIO, O. M. 2005. Mrc1 is required for normal progression of replication forks throughout chromatin in S. cerevisiae. *Mol Cell,* 19**,** 691-7.

TABANCAY, A. P., JR. & FORSBURG, S. L. 2006. Eukaryotic DNA replication in a chromatin context. *Curr Top Dev Biol,* 76**,** 129-84.

TAHIROV, T. H., MAKAROVA, K. S., ROGOZIN, I. B., PAVLOV, Y. I. & KOONIN, E. V. 2009. Evolution of DNA polymerases: an inactivated polymerase-exonuclease module in Pol epsilon and a chimeric origin of eukaryotic polymerases from two classes of archaeal ancestors. *Biol Direct,* 4**,** 11.

TAKARA, T. J. & BELL, S. P. 2011. Multiple Cdt1 molecules act at each origin to load replication-competent Mcm2-7 helicases. *The EMBO journal*.

TAKAYAMA, Y., KAMIMURA, Y., OKAWA, M., MURAMATSU, S., SUGINO, A. & ARAKI, H. 2003. GINS, a novel multiprotein complex required for chromosomal DNA replication in budding yeast. *Genes Dev,* 17**,** 1153-65.

TANAKA, S., UMEMORI, T., HIRAI, K., MURAMATSU, S., KAMIMURA, Y. & ARAKI, H. 2007. CDK-dependent phosphorylation of Sld2 and Sld3 initiates DNA replication in budding yeast. *Nature,* 445**,** 328-32.

TANAKA, T., UMEMORI, T., ENDO, S., MURAMATSU, S., KANEMAKI, M., KAMIMURA, Y., OBUSE, C. & ARAKI, H. 2011. Sld7, an Sld3-associated protein required for efficient chromosomal DNA replication in budding yeast. *The EMBO journal,* 30**,** 2019-30.

TEMKO, D., VAN GOOL, I. C., RAYNER, E., GLAIRE, M., MAKINO, S., BROWN, M., CHEGWIDDEN, L., PALLES, C., DEPREEUW, J., BEGGS, A., STATHOPOULOU, C., MASON, J., BAKER, A. M., WILLIAMS, M., CERUNDOLO, V., REI, M., TAYLOR, J. C., SCHUH, A., AHMED, A., AMANT, F., LAMBRECHTS, D., SMIT, V. T., BOSSE, T., GRAHAM, T. A., CHURCH, D. N. & TOMLINSON, I. 2018. Somatic POLE exonuclease domain mutations are early events in sporadic endometrial and colorectal carcinogenesis, determining driver mutational landscape, clonal neoantigen burden and immune response. *J Pathol,* 245**,** 283-296.

TERCERO, J. A. & DIFFLEY, J. F. 2001. Regulation of DNA replication fork progression through damaged DNA by the Mec1/Rad53 checkpoint. *Nature,* 412**,** 553-7.

TERCERO, J. A., LONGHESE, M. P. & DIFFLEY, J. F. 2003. A central role for DNA replication forks in checkpoint activation and response. *Mol Cell,* 11**,** 1323-36.

THIFFAULT, I., SAUNDERS, C., JENKINS, J., RAJE, N., CANTY, K., SHARMA, M., GROTE, L., WELSH, H. I., FARROW, E., TWIST, G., MILLER, N., ZWICK, D., ZELLMER, L., KINGSMORE, S. F. & SAFINA, N. P. 2015. A patient with polymerase E1 deficiency (POLE1): clinical features and overlap with DNA breakage/instability syndromes. *BMC Med Genet,* 16**,** 31.

THORNTON, B. R. & TOCZYSKI, D. P. 2003. Securin and B-cyclin/CDK are the only essential targets of the APC. *Nat Cell Biol,* 5**,** 1090-4.

TICAU, S., FRIEDMAN, L. J., IVICA, N. A., GELLES, J. & BELL, S. P. 2015. Single-molecule studies of origin licensing reveal mechanisms ensuring bidirectional helicase loading. *Cell,* 161**,** 513-525.

TOLEDO, L. I., ALTMEYER, M., RASK, M. B., LUKAS, C., LARSEN, D. H., POVLSEN, L. K., BEKKER-JENSEN, S., MAILAND, N., BARTEK, J. & LUKAS, J. 2013. ATR prohibits replication catastrophe by preventing global exhaustion of RPA. *Cell,* 155**,** 1088-103.

TRAVESA, A., KALASHNIKOVA, T. I., DE BRUIN, R. A., CASS, S. R., CHAHWAN, C., LEE, D. E., LOWNDES, N. F. & WITTENBERG, C. 2013. Repression of G1/S transcription is mediated via interaction of the GTB motifs of Nrm1 and Whi5 with Swi6. *Mol Cell Biol,* 33**,** 1476-86.

TSAI, F. L., VIJAYRAGHAVAN, S., PRINZ, J., MACALPINE, H. K., MACALPINE, D. M. & SCHWACHA, A. 2015. Mcm2-7 Is an Active Player in the DNA Replication Checkpoint Signaling Cascade via Proposed Modulation of Its DNA Gate. *Mol Cell Biol,* 35**,** 2131-43.

TSAPONINA, O., BARSOUM, E., ASTROM, S. U. & CHABES, A. 2011. Ixr1 is required for the expression of the ribonucleotide reductase Rnr1 and maintenance of dNTP pools. *PLoS Genet,* 7**,** e1002061.

TURCHI, J. J., HUANG, L., MURANTE, R. S., KIM, Y. & BAMBARA, R. A. 1994. Enzymatic completion of mammalian lagging-strand DNA replication. *Proc Natl Acad Sci U S A,* 91**,** 9803-7.

TYERS, M., TOKIWA, G. & FUTCHER, B. 1993. Comparison of the Saccharomyces cerevisiae G1 cyclins: Cln3 may be an upstream activator of Cln1, Cln2 and other cyclins. *Embo J,* 12**,** 1955-68.

VAN DEURSEN, F., SENGUPTA, S., DE PICCOLI, G., SANCHEZ-DIAZ, A. & LABIB, K. 2012. Mcm10 associates with the loaded DNA helicase at replication origins and defines a novel step in its activation. *The EMBO journal,* 31**,** 2195-206.

VERMA, R., ANNAN, R. S., HUDDLESTON, M. J., CARR, S. A., REYNARD, G. & DESHAIES, R. J. 1997. Phosphorylation of Sic1p by G1 Cdk Required for Its Degradation and Entry into S Phase. *Science,* 278**,** 455-460.

VILLA, F., SIMON, A. C., ORTIZ BAZAN, M. A., KILKENNY, M. L., WIRTHENSOHN, D., WIGHTMAN, M., MATAK-VINKOVIC, D., PELLEGRINI, L. & LABIB, K. 2016. Ctf4 Is a Hub in the Eukaryotic Replisome that Links Multiple CIP-Box Proteins to the CMG Helicase. *Mol Cell,* 63**,** 385-96.

VISINTIN, R., CRAIG, K., HWANG, E. S., PRINZ, S., TYERS, M. & AMON, A. 1998. The phosphatase Cdc14 triggers mitotic exit by reversal of Cdk- dependent phosphorylation. *Mol Cell,* 2**,** 709-18.

VODERMAIER, H. C. 2004. APC/C and SCF: controlling each other and the cell cycle. *Curr Biol,* 14**,** R787-96.

WAGA, S., MASUDA, T., TAKISAWA, H. & SUGINO, A. 2001. DNA polymerase epsilon is required for coordinated and efficient chromosomal DNA replication in Xenopus egg extracts. *Proc Natl Acad Sci U S A,* 98**,** 4978-83.

WANROOIJ, P. H. & BURGERS, P. M. 2015. Yet another job for Dna2: Checkpoint activation. *DNA Repair (Amst),* 32**,** 17-23.

WEAVER, D. T., FIELDS BERRY, S. C. & DEPAMPHILIS, M. L. 1985. The termination region for SV40 DNA replication directs the mode of separation for the two sibling molecules. *Cell,* 41**,** 565-75 Issn: 0092-8674.

WEINBERGER, M., TRABOLD, P. A., LU, M., SHARMA, K., HUBERMAN, J. A. & BURHANS, W. C. 1999. Induction by adozelesin and hydroxyurea of origin recognition complex- dependent DNA damage and DNA replication checkpoints in Saccharomyces cerevisiae. *J. Biol. Chem.,* 274**,** 35975-84.

WENDEL, B. M., COURCELLE, C. T. & COURCELLE, J. 2014. Completion of DNA replication in Escherichia coli. *Proc Natl Acad Sci U S A,* 111**,** 16454-9.

WYBENGA-GROOT, L. E., HO, C. S., SWEENEY, F. D., CECCARELLI, D. F., MCGLADE, C. J., DUROCHER, D. & SICHERI, F. 2014. Structural basis of Rad53 kinase activation by dimerization and activation segment exchange. *Cell Signal,* 26**,** 1825-36.

WYSOCKI, R., JAVAHERI, A., ALLARD, S., SHA, F., COTE, J. & KRON, S. J. 2005. Role of Dot1-dependent histone H3 methylation in G1 and S phase DNA damage checkpoint functions of Rad9. *Mol Cell Biol,* 25**,** 8430-43.

XIAO, W., CHOW, B. L., HANNA, M. & DOETSCH, P. W. 2001. Deletion of the MAG1 DNA glycosylase gene suppresses alkylation-induced killing and mutagenesis in yeast cells lacking AP endonucleases. *Mutat Res,* 487**,** 137-47.

YAO, N. Y., JOHNSON, A., BOWMAN, G. D., KURIYAN, J. & O'DONNELL, M. 2006. Mechanism of proliferating cell nuclear antigen clamp opening by replication factor C. *J Biol Chem,* 281**,** 17528-39.

YEELES, J. T., DEEGAN, T. D., JANSKA, A., EARLY, A. & DIFFLEY, J. F. 2015. Regulated eukaryotic DNA replication origin firing with purified proteins. *Nature,* 519**,** 431-5.

YEELES, J. T. P., JANSKA, A., EARLY, A. & DIFFLEY, J. F. X. 2017. How the Eukaryotic Replisome Achieves Rapid and Efficient DNA Replication. *Mol Cell,* 65**,** 105-116.

YOSHIDA, R., MIYASHITA, K., INOUE, M., SHIMAMOTO, A., YAN, Z., EGASHIRA, A., OKI, E., KAKEJI, Y., ODA, S. & MAEHARA, Y. 2011. Concurrent genetic alterations in DNA polymerase proofreading and mismatch repair in human colorectal cancer. *Eur J Hum Genet,* 19**,** 320-5.

YU, C., GAN, H., SERRA-CARDONA, A., ZHANG, L., GAN, S., SHARMA, S., JOHANSSON, E., CHABES, A., XU, R. M. & ZHANG, Z. 2018. A mechanism for preventing asymmetric histone segregation onto replicating DNA strands. *Science*.

ZEGERMAN, P. & DIFFLEY, J. F. 2010. Checkpoint-dependent inhibition of DNA replication initiation by Sld3 and Dbf4 phosphorylation. *Nature,* 467**,** 474-8.

ZHAO, X. & ROTHSTEIN, R. 2002. The Dun1 checkpoint kinase phosphorylates and regulates the ribonucleotide reductase inhibitor Sml1. *Proc Natl Acad Sci U S A,* 99**,** 3746-51.

ZHOU, C., ELIA, A. E., NAYLOR, M. L., DEPHOURE, N., BALLIF, B. A., GOEL, G., XU, Q., NG, A., CHOU, D. M., XAVIER, R. J., GYGI, S. P. & ELLEDGE, S. J. 2016. Profiling DNA damage-induced phosphorylation in budding yeast reveals diverse signaling networks. *Proc Natl Acad Sci U S A,* 113**,** E3667-75.

ZHOU, J. C., JANSKA, A., GOSWAMI, P., RENAULT, L., ABID ALI, F., KOTECHA, A., DIFFLEY, J. F. X. & COSTA, A. 2017. CMG-Pol epsilon dynamics suggests a mechanism for the establishment of leading-strand synthesis in the eukaryotic replisome. *Proc Natl Acad Sci U S A,* 114**,** 4141-4146.

ZHU, W., UKOMADU, C., JHA, S., SENGA, T., DHAR, S. K., WOHLSCHLEGEL, J. A., NUTT, L. K., KORNBLUTH, S. & DUTTA, A. 2007. Mcm10 and And-1/CTF4 recruit DNA polymerase alpha to chromatin for initiation of DNA replication. *Genes Dev,* 21**,** 2288-99.

ZOU, L. & ELLEDGE, S. J. 2003. Sensing DNA damage through ATRIP recognition of RPA-ssDNA complexes. *Science,* 300**,** 1542-8.